7922606

LENHART, ROBERT JAMES
NEARSHORE MARINE BEDFORMS FORMATIVE PROCESSES, DISTRIBUTION, AND INTERNAL STRUCTURES.

UNIVERSITY OF CINCINNATI, PH.D., 1979

University Microfilms International 300 N. ZEEB ROAD, ANN ARBOR, MI 48106

PLEASE NOTE:

In all cases this material has been filmed in the best possible way from the available copy. Problems encountered with this document have been identified here with a check mark ✓.

1. Glossy photographs _______
2. Colored illustrations ✓
3. Photographs with dark background ✓
4. Illustrations are poor copy _______
5. Print shows through as there is text on both sides of page _______
6. Indistinct, broken or small print on several pages _______ throughout _______
7. Tightly bound copy with print lost in spine _______
8. Computer printout pages with indistinct print _______
9. Page(s) _______ lacking when material received, and not available from school or author _______
10. Page(s) _______ seem to be missing in numbering only as text follows _______
11. Poor carbon copy _______
12. Not original copy, several pages with blurred type _______
13. Appendix pages are poor copy _______
14. Original copy with light type _______
15. Curling and wrinkled pages _______
16. Other _______

University Microfilms International

300 N. ZEEB RD., ANN ARBOR, MI 48106 (313) 761-4700

NEARSHORE MARINE BEDFORMS
FORMATIVE PROCESSES,
DISTRIBUTION,
AND INTERNAL STRUCTURES

A thesis submitted to the

Division of Graduate Education and Research
of the University of Cincinnati

in partial fulfillment of the
requirements for the degree of

DOCTOR OF PHILOSOPHY

in the Department of Geology
of the College of Arts and Sciences

1979

by

Robert J Lenhart

B.S., Pennsylvania State University, 1972
M.S., University of Cincinnati, 1974

UNIVERSITY OF CINCINNATI

November 29 *19* 78

I hereby recommend that the thesis prepared under my supervision by Robert J. Lenhart

entitled Nearshore Marine Bedforms: Formative Processes, Distribution and Internal Structures

be accepted as fulfilling this part of the requirements for the degree of Doctor of Philosophy

Approved by:

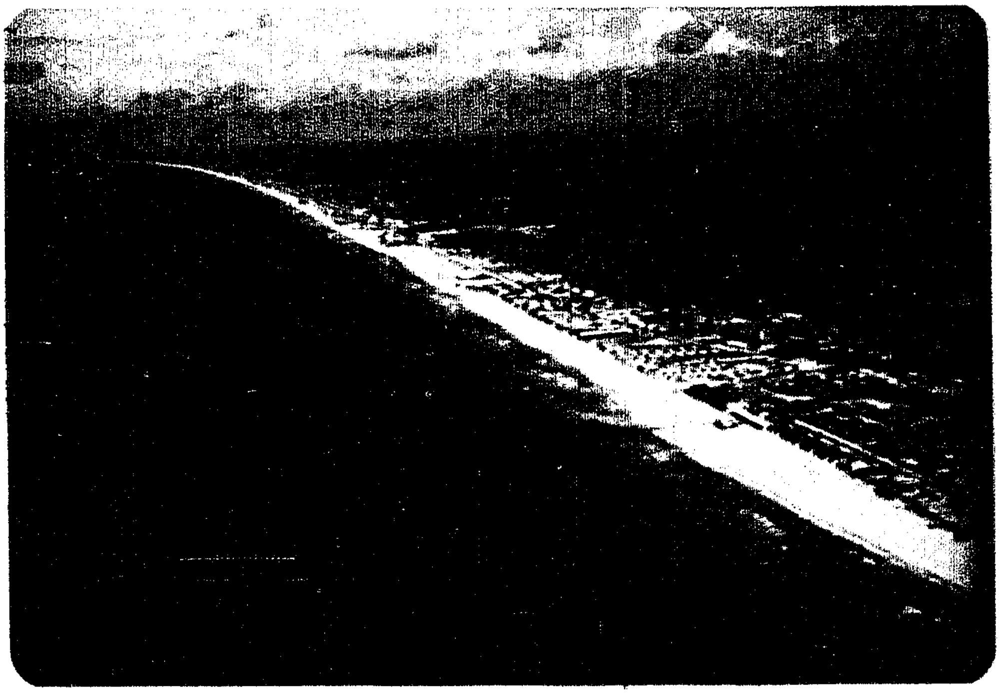

ACKNOWLEDGMENTS

The author gratefully acknowledges the assistance of the following people and organizations who helped make this study possible. The three field assistants who aided in the data collection were Dana Gilbert, Elaine Feldman, and Richard Fluegeman. Thanks go to them for risking life and limb in the ocean and for helping me through some difficult situations.

Valuable environmental data was supplied by the Naval Coastal Research Laboratory at Panama City. The cooperation of the Army Corps of Engineers is also greatly appreciated. Dennis Wilson of the Corps' Mobile office and Chris Schneider and Bob Schwartz of the Fort Belvoir, Virginia office were all very helpful. Eugene Nakamura, of the NOAA facility in Panama City, provided information about the biota and was a constant source of enthusiasm. Dr. James Howard of the Skidaway Institute of Oceanography was instrumental in getting the box coring operation started. His experience with this technique was invaluable.

Financial support from the U. C. Sedimentation Fund was provided for some of the field work and some of the equipment. Dr. Warren Huff and Dr. David Nash were kind enough to read and constructively criticize the first draft. Dr. Wayne Pryor was the ultimate source of inspiration, patience, and support throughout this project and special thanks are reserved for him. Finally I would like to thank my parents for their unrelenting support.

TABLE OF CONTENTS

LIST OF FIGURES

TABLES

ABSTRACT

Data from a three-summer monitoring program of nearshore marine bedforms are presented. Bedform type, orientation, dimensions, and water depth and bottom velocities were measured along profiles which were perpendicular to shore. Beaches with rhythmic submarine bar topography exhibit distinctive patterns of bedform types which vary with water depth and wave energy. The sequence of bedforms observed with decreasing depth on the seaward slope of the inner bar is: symmetric ripples → asymmetric ripples → ladderback ripples → lunate megaripples → plane bed (rare). The orientation of the seaward slope bedforms responds to changes in wave direction. Landward of the inner bar crest, the bedform type and orientation responds to a complex blend of waves, topography, and nearshore currents.

When the inner bar is welded to shore at regularly spaced intervals it restricts the type of longshore circulation which can occur. When shore-welded bars are present, closed circulation cells and unidirectional longshore flow (consistent with the grain of the bar topography) can occur but bidirectional longshore flow is prevented by the topography. Storm conditions produce a straight-crested bar, parallel to shore, which is not stable under normal wave conditions and is soon modified to a cuspate bar.

There is a strong relationship between bedforms, topography, and measured bottom velocities. A plot of depth and water velocity similar

to that used for fluvial bedforms permits discrimination of the various types of marine bedforms on the bar's seaward slope. Another plot of velocity and velocity asymmetry also allows discrimination of bedform types. This plot reveals that the plane bed observed in the swash zone exhibits near-symmetric velocities unlike the near-unidirectional currents which form plane beds in the breaker zone (Clifton, 1976).

The internal structures of nearshore sands were examined by box coring. Sedimentary structures are poorly preserved because of the depth of daily scour, the uniform nature of the sediment, and bioturbation. Parallel, horizontal or slightly seaward-inclined, fine laminae are the most common structures. Other sedimentary structures in the nearshore include medium-scale cross-bedding which is shoreward-inclined and small scale cross-bedding which is both landward and seaward-inclined. The degree of bioturbation increases in the offshore direction and is primarily attributed to polychaete worms and Callianassa shrimp.

Key Words

nearshore marine bedforms
rhythmic topography
bedform-related velocities
combined flow hydraulics
nearshore sedimentary structures
ladderback ripples.

INTRODUCTION

There is a large amount of geologic, engineering, and oceanographic literature on beach and nearshore environments. Perhaps reflecting the complexity of processes and the pleasures of working along the shoreline. The interaction of the atmosphere with the ocean and the coexistence of oscillatory and unidirectional flow in the nearshore complicate the investigation of nearshore sedimentary processes.

Nearshore bedforms had been largely neglected in the literature until recently when Clifton, et al. (1971) studied them. The importance of modern bedform studies lies in their use for interpretation of ancient sedimentary environments. Observation of the bedforms provides a key to the hydraulics of the overlying fluid medium. In addition, information on the behavior of marine bedforms related to controlling processes fills a gap in geologic knowledge.

Previous Work

Previous work on bedforms has been mostly restricted to fluvial bedforms. These forms are primarily a product of unidirectional current flow and their dynamics have been studied extensively in flumes and in the field. Simons, Richardson, and Nordin (1965) presented one of the most complete descriptions of the fluvial bedform sequence which develops with increasing flow strength. Harms and Fahnestock (1965) described the distribution of bedforms in the modern deposits of the Rio Grande.

Walker (1965) extended the work done on fluvial bedforms to interpret turbidite bedform sequences.

Clifton, et al. (1971) was the first serious attempt to analyze and classify the nearshore marine bedforms. A classification scheme was devised based on the shoreward increase in velocity asymmetry. In theory the bottom velocities below wave base are symmetric in magnitude in both the onshore and offshore directions. Above wave base the bottom velocities become progressively more asymmetric in shallower water. Clifton was the first to describe the sequence of marine bedforms which develops under shoaling ocean waves. He noted the similarity between the fluvial and the marine bedform sequence as they correspond to increasing flow strength. This model was developed from observations of three different non-barred coasts with three different levels of wave energy. A more complete consideration of Clifton's model will follow in the discussion section of this report.

Clifton's work was done on plane-sloping beaches without sand bars. A subsequent paper by Davidson-Arnott and Greenwood (1974) applied Clifton's ideas to the nearshore bedforms on a barred beach in Canada. My study also deals with a barred beach but it is on the Gulf of Mexico on the Florida Panhandle (Fig. 1). This coast is characterized by a double bar system (Fig. 2) with an inner bar of variable form and a passive outer bar which is continuous and is only modified during periods of high waves. This double bar system extends as a stable configuration for 100 miles between Panama City beach and Santa Rosa Island near Pensacola.

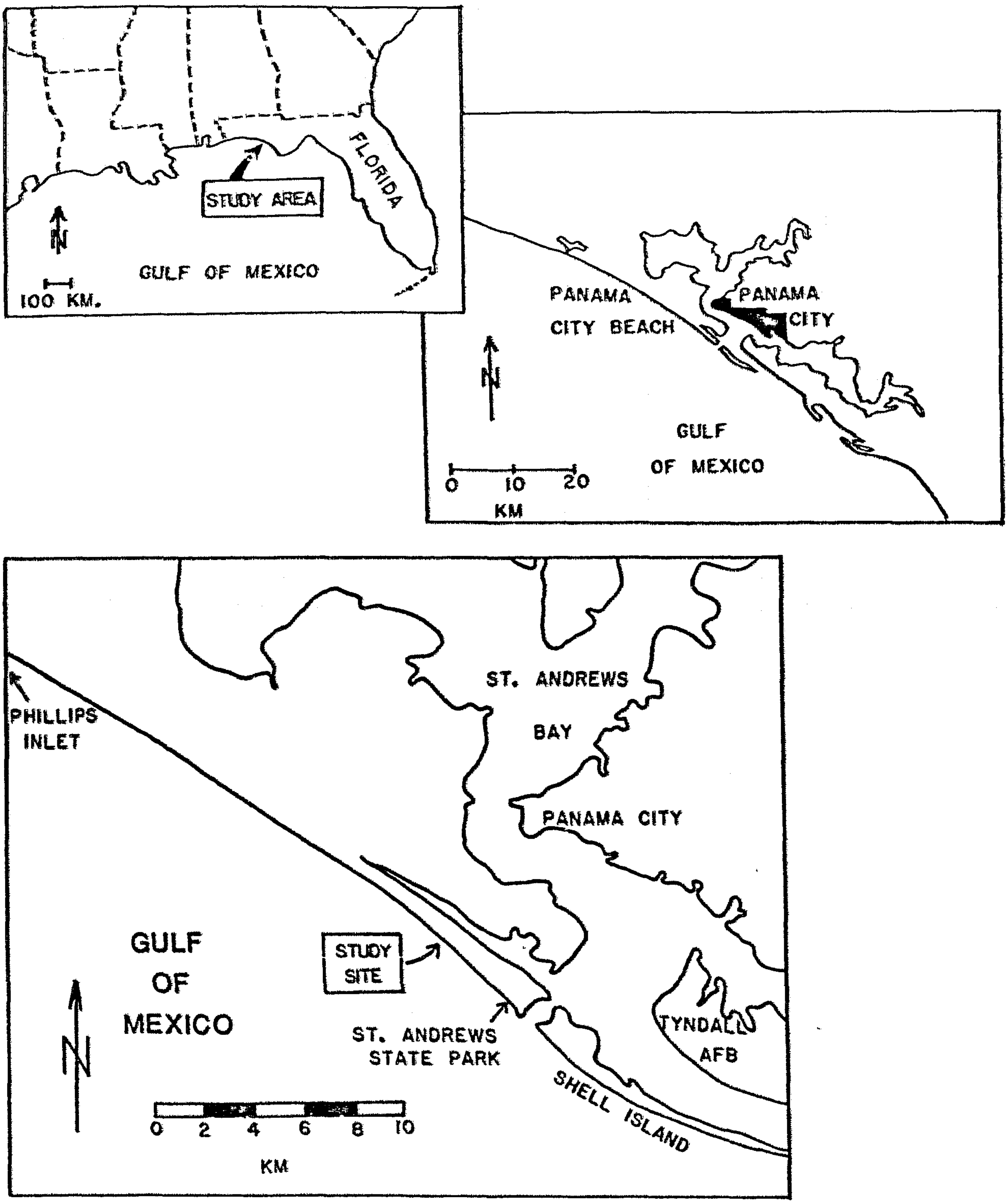

Figure 1: Location map.

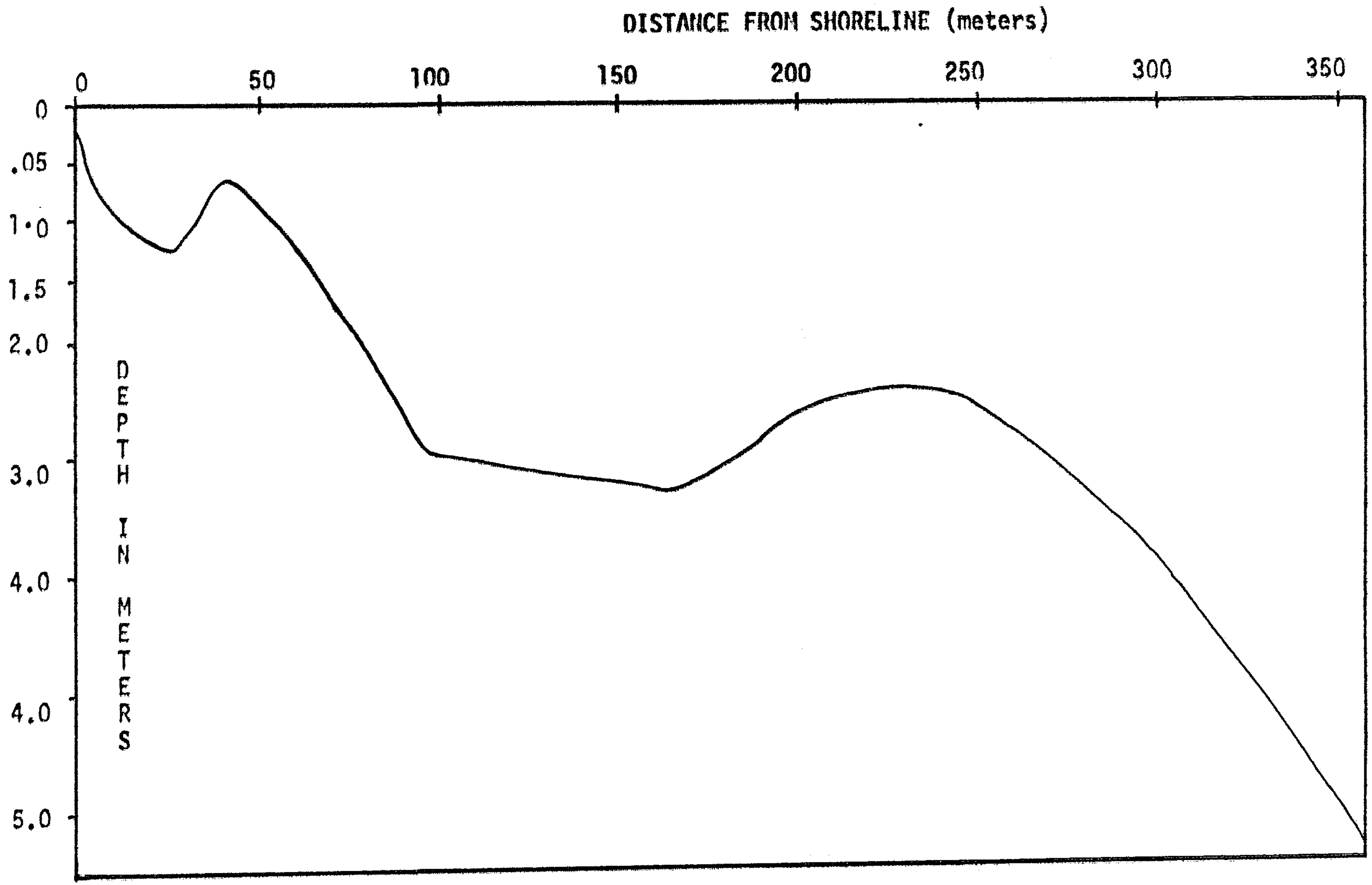

Figure 2: Nearshore profile across both sand bars at Panama City Beach; courtesy of Panama City Naval Coastal Research Lab.

Purpose

The purpose of this paper is to report my investigation of the factors that control nearshore marine bedforms associated with barred submarine topography. The currents and wave oscillation occurring around barred topography are not as simple as those occurring on a plane-sloping beach. This is especially true of the inner bar whose form varies almost daily. Therefore a monitoring program of the significant factors in the nearshore was begun in the summer of 1975. The Panama City Beach area was selected in an attempt to minimize the variability of some of the processes effecting bedforms. There is a small tidal range ($\leq$ 60 cm) and the area has only one tidal cycle per day. Variations of sediment grain size also influence bedforms, but Panama City beaches are composed of a well-sorted, uniform quartz sand (Balsillie, 1975; Saloman, 1976).

Because field descriptions of the development of nearshore bedforms are scarce in the literature, my study was organized around a few simple questions:

1. What is the effect of the winds and waves on the nearshore bottom topography?
2. What is the nature of the velocity field associated with nearshore bedforms and can velocity be used to predict bedform type?
3. What types of bedforms exist in the nearshore of a barred coastline and how do they relate to the submarine topography?

4. Do nearshore marine bedforms conform to Clifton's (1976) model of increasing shoreward velocity asymmetry and are they comparable to fluvial bedforms?

5. What types of sedimentary structures are produced by nearshore bedforms and what is the likelihood of their preservation?

METHODS

Bedform-Velocity Profiles

Topographic profiles were measured perpendicular to shore by using two poles with meter sticks mounted on them. By sighting over the top of the seaward stick and aligning its top with the horizon, one can read the elevation difference in centimeters on the shoreward stick. Profiles were begun landward of the berm from a standard position and were extended across the crest of the first bar. The seaward limit of these profiles was governed by water depth and wave conditions and ranged from 1.5 to 2.0 meters in depth.

Four adjacent profile localities were established 25 meters apart on Panama City beach. One of the localities, hereafter referred to as the standard profile, was measured almost daily. The other three localities were measured every week or two.

Bedforms were mapped along the standard profile on days when water clarity and wave conditions permitted such work. A 75 meter length of washline was staked on the bottom along the profile with knots at 5 meter intervals. For each interval the following information was recorded by a diver: bedform type, height, wavelength, crest orientation, sinuousity, and symmetry or asymmetry. Bedform dimensions were measured with a meter stick, crest orientations with an underwater compass, and sinuousity was visually judged as being either straight, sinuous, catenary, or lunate (Fig. 3).

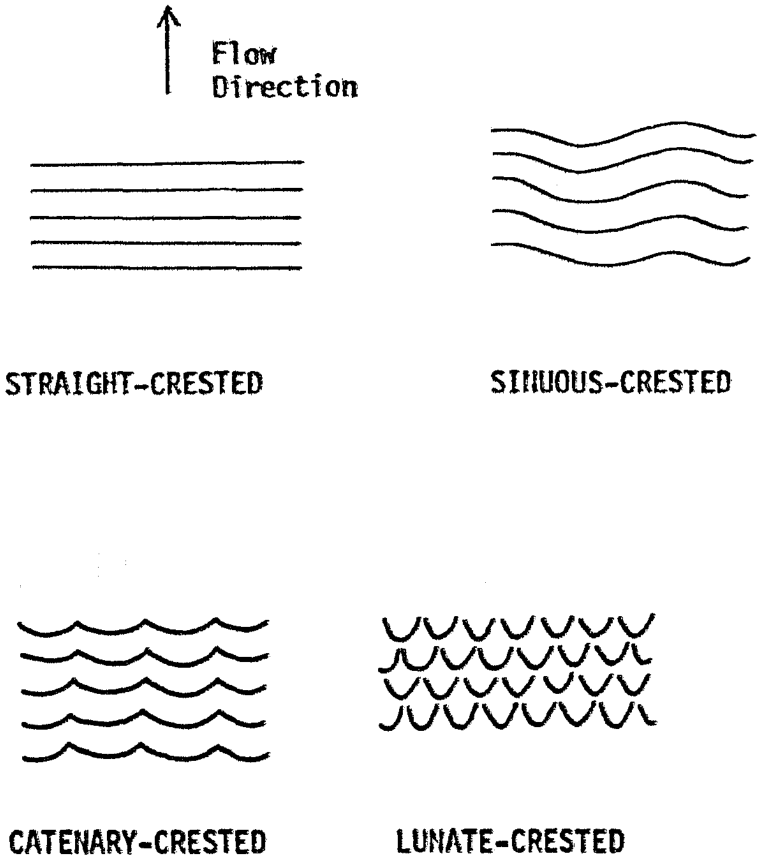

Figure 3: Bedform crestline geometry examples.

Velocity data recorded for each interval included horizontal bottom velocities perpendicular to shore, longshore bottom velocities and some vertical velocities. Horizontal bottom velocities and longshore bottom velocities were measured with a simple "swing-type" device (Fig. 4A). The swing meter was constructed from plexiglass, copper wire and a lead tire weight used to limit the deflection of the paddle. The advantages of using this device were its immediate response to short-lived currents, simplicity of operation underwater, and cost. The scale of the swing meter acted as a vane in the water and therefore the maximum component of the velocity could be measured. Measurements were made just a few centimeters above the bedform crests by a heavily weighted diver, hand-holding the device. For landward and seaward oscillations the velocity range, maximum, and relative durations were noted. Calibration of the swing meter was done in a flume with a Gurley Pygmy Current Meter. For more details please see Appendix C.

Longshore bottom current measurement was done in a similar manner along the profile. Some surface measurements of longshore current were made with a timed wooden float over a measured reach between the four topographic profile localities.

Vertical velocities were measured with a commercial flowmeter designed for laboratory use (Fig. 4B). It consists of a tapered, tubular, glass scale containing a nylon sphere. Apertures in the top and the bottom of the tube allow liquid to flow through the device. Measurements were made near the surface and along the bottom at each 5 meter interval.

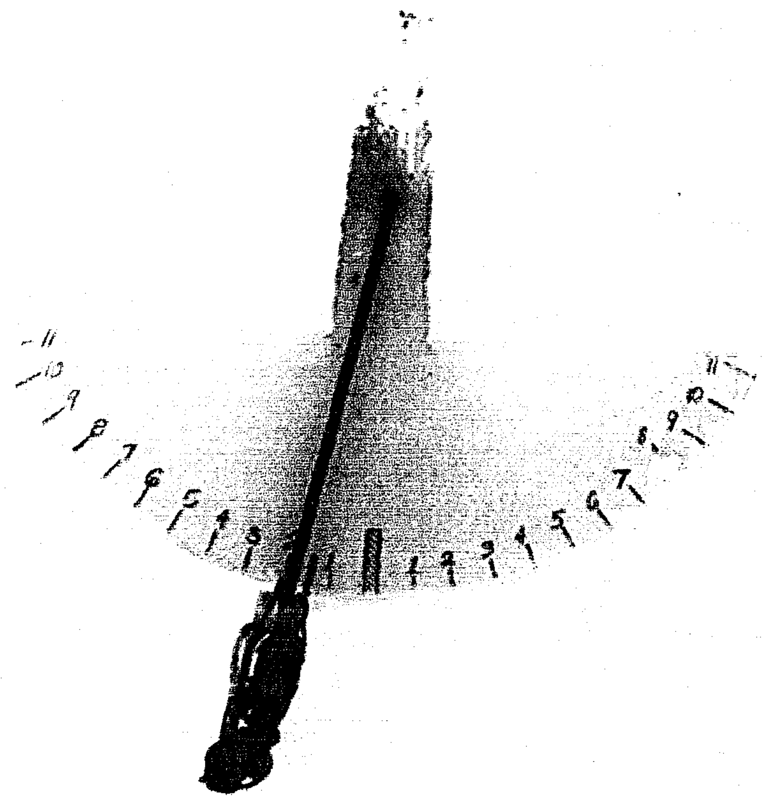

A: Swing-Surge Meter

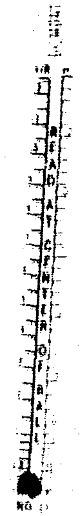

B: Vertical Velocity Meter

Figure 4: Velocity meters used in this study.

Plan View Observations

To gain some insight into the distribution of bedforms and currents along shore, several plan view sketch maps were made of the area covered by the four profile locations. No attempt was made to preserve the exact geometry of the topography. Mapping was done by diving and surface observation of bedform types and current directions. Emphasis was placed on the overall pattern, not the details. The original sketches were made on a plexiglass tablet with a grease pencil. Aerial photographs were obtained to survey the extent of variability of the nearshore topography. Photography for four dates ranging from 1942 to 1975 was purchased from the U.S. Department of Agriculture. The Florida Department of Natural Resources provided three sets of photography from the period of 1970 to 1975 including photos taken the day after Hurricane Eloise (September 23, 1975). Five sets of aerial photos were obtained by the author from a rental aircraft during the course of the study (1975-1977). The latter are high oblique photographs taken from an altitude of 1000 feet with a 35 mm camera. All of the government airphotos were vertical in aspect and the altitude varied from 1000 to 20,000 feet.

Most of the coverage was for a five-mile length of beach between St. Andrews State Park and Panama City Beach. The area of intensive study, Biltmore Beach, was centered between these two points. There was also some photography available for Shell Island to the southeast of the study area.

Photo-mosaics were constructed from the oblique photographs to provide a continuous map of the bar topography. Because of the scale variation across an oblique photograph match points were located on the inner sand bar in the center of the photograph.

Navy Wave Records

The Naval Coastal Research Lab (NCRL) in Panama City provided data on waves, winds, and tides for the study area. Continuous information was collected from two offshore stages. Stage I is located 17.7 km offshore in 31.7 m of water and Stage II is located 3.2 km offshore in 19.2 m of water (Breeding, 1972). Both platforms record significant wave height, tidal fluctuations, and wind speed and direction. Significant wave height is defined as the average of the one-third highest waves in a sequence of waves observed at a point (Newmann and Pierson, 1966). All of the environmental information was plotted against time on a single chart to allow comparison.

The significant wave height data are most useful as a measure of the amount of energy being expended at the shoreline. Wave heights were measured by several wave staffs which sense relative changes in water level by the variation of the impedence through a nichrome wire. Wave staffs of varying length are located on the north, south, east, and west sides of both stages, allowing directional resolution. Wind speed and direction were measured with a 3-cup anemometer and a vane. The instrumentation was originally designed by Texas A and M University (Kirst and Gaul, 1964) and has been in use since 1962.

The significantwave height data were computed from continuous water level records which showed the complete sequence of waves passing the staff. Portions of these original wave records were obtained for eleven dates in July of 1977 and were used to determine the periods of the waves impinging on Panama City Beach. Wave period was determined for a 600 second record by counting the number of times the curve crossed the mean water level line. Only upward crossing (positive-slopes) were counted and this number was divided into 600 to yield the mean zero-crossing period (Draper, 1966).

NOAA Wind Data:

Data on wind speed and direction were purchased from the National Oceanic and Atmospheric Administration (NOAA). The wind data were collected at Tyndall Air Force Base, eight miles southeast of the study area. Observations were made every hour or more frequently when conditions varied significantly. This information was used to supplement and confirm the accuracy of the NCRL data. Daily wind direction and speed were plotted on polar coordinate graph paper for the dates for which bedform profiles were available. Summary plots of weekly wind patterns were also made to evaluate long term effects on nearshore topography.

Box Coring

Box coring devices were contructed from a design used by Dr. J. D. Howard of the Skidaway Oceanographic Institute. The boxes were made of stainless steel, each with dimensions of 12" x 8" x 4". All cores were obtained underwater by a diver. This required considerable effort, especially in the surf zone. Cores were allowed to drain briefly and were then extruded on the beach.

The object of coring was to obtain epoxy-impregnated peels of longitudinal slices through the cores. The freshly extruded core was carefully laid down on a plexiglass tray. Then a long spatula was used to whittle the core down to 12" x 8" x 3/4" slice. Later, the core slice was sandwiched against a piece of fiberboard, coated with epoxy, and allowed to cure for a few days. At this point the specimens were placed outside in a vertical position to allow the excess sediment to fall off and reveal internal structures.

Several techniques were employed to maximize information on the sedimentary and biogenic structures in the cores. Core slices were sketched and photographed while still wet and then X-rayed. Peels were photographed with low-angle illumination and X-rayed again.

Cylindrical cores were obtained with a two-inch diameter plexiglass tube. The average depth of penetration of these cores was about 25 centimeters. Tube cores were taken by hand all along the bedform traverses. Most of this coring was done in 1976 before the box coring devices were constructed. Sediment samples were removed from the tops and bottoms of the cores for grain size analysis.

RESULTS

Wind Data

Winds are ultimately responsible for water motion and the resultant bedforms, so their patterns are important to this study. The wind data which are summarized here pertain only to the summer months during which bedform data were collected.

1975

During the 13-day period of August 6-19, 1975 the following wind patterns were recorded as summarized in Table 1 (original data are in Appendix A). The wind was fairly constant from the Southwest except for August 8-10 when it came from the Southeast to East. On days dominated by Southwest winds the direction shifted to the West around mid-day and then returned to the Southwest. Wind speed was less than or equal to ten knots for most of the record. Winds of 20 to 30 knots occurred at the beginning of the record as a result of a three-day storm.

1976

Data for 1976 were collected from June 12 to July 22. The record was dominated by daily cycles of wind direction change which began in the North in the early morning and rotated clockwise during the day, ending at north again around midnight. Wind velocity was also controlled by this cycle. It rose from zero in the morning to a maximum

BAR PATTERN	Crescent Bar	Cuspate Bar	Skewed Cuspate--Horn--Shore-Parallel
	1975	1976	1977
WIND & WAVE VARIABILITY & DIRECTION	Primarily from the SW (perpendicular to shore).	Alternating between periods of cyclic, variable winds (dominant) and constant SW winds.	Alternating between periods of constant SW winds (dominant) and periods of variable (cyclic) winds; constant S-SE winds during the storm.
WAVE HEIGHT RANGE	0.3 - 2.0 m	0.3 - 1.3 m	0.2 - 2.0 m
AVERAGE WAVE HEIGHT	0.5 m	0.6 m	0.5 m
WIND SPEED	≤10 Knots except for 10-20 knots during a storm.	average is 10-20 knots; 20 knots is maximum	average is 10 knots; 25 knots is maximum
STORMS	July 29-30,1975 August 5-7,1975	none	July 17-20,1977
WAVE PERIOD	no data	no data	$\bar{x}$ = 3.4 seconds range = 2.3-8.0 seconds

Table 1: Summary of wind and wave data for the three field seasons at Panama City Beach.

of about 15 knots at 1 to 2 P.M. and then dropped back to zero at night. There were a few intervals during which the winds were constant from the Southwest to West and these were June 16, June 29-July 4, and July 11-18. During these intervals of constant direction, wind velocities remained relatively constant (15-20 knots) and higher than those recorded for days dominated by the clockwise cycle of wind direction change.

Weekly summaries of the wind direction and speed were plotted on rose diagrams to better display the dominant winds (Appendix A). This wind data comes from observations at Tyndall AFB between June 15 and July 15, 1976. Direction was plotted in forty-degree sectors of the compass and velocities were classed as 1-8 knots, 9-16 knots, or 16-24 knots. The plots display consistent winds from the southwest quarter which is essentially perpendicular to the shoreline at Panama City.

1977

NCRL wind information from 1977 spans the longest time period: June 11 through July 28. As in 1975 and 1976 the wind direction alternated between daily cycles of clockwise change and periods of constant southwest winds which persisted for several days. The daily cycles did not always involve a 360 degree directional shift. Sometimes the wind direction rotated from East in the morning through South to the West in the afternoon as the velocity increased. On other days the directional changes were erratic but generally conformed to the 360° directional cycle with maximum wind velocities in the afternoon.

During periods of constant wind direction winds were from the

Southwest with the exception of the interval from July 17-20 when they originated from the Southeast. Southeast winds coincided with the passage of a small low pressure air mass through the area and produced the highest wind velocities (25 knots) recorded for this summer. A look at the NOAA weekly wind data summaries (Appendix A) shows that most of June, 1977 was characterized by west to southwest winds with a shift towards the Southwest in early July. The wind source changed to the East-Northeast during mid-July when the storm arrived and returned to the Southwest at the end of the month.

Wave Conditions

NCRL significant wave height records are summarized in Table 1 for the three summers of bedform observation. The following is a qualitative summary of the wave conditions for these periods in terms of significant wave height, direction of approach, and occasional measurements of wave period.

Wave direction is assumed to be the same as wind direction based on data from Tolbert and Austin (1956). Information on wind and wave directions was gathered from an anchored vessel near Stage II from April 12 to December 28, 1955. A comparison of wind and wave directions revealed that 92.4 percent of the time they were the same and 7.6 percent of the time they differed by 20 degrees or less. Between April and September the agreement was 100 percent.

1975

During the three week period in August of 1975 there were two periods of large waves at the beginning of the month. Two consecutive storms produced waves in the 1.7-2.0 m and 1.4-1.7 m range. The remainder of the time the significant wave height varied from 0.3 to 0.6 m.

Wind wave direction during August of 1975 was primarily from the Southwest and West. There were two days when southeast and east waves dominated. During periods of constant wind direction the significant wave height increased continually from day to day. Variable winds produced the lowest wave heights. All of these trends can be seen in the NCRL significant wave height plots in Appendix A.

1976

The significant wave height data for 1976 were collected from June 12 to July 22. From June 12 to July 11 the wave height oscillated between 1 meter events and 0.3-0.6 m events which lasted for approximately three days each. During July 12 through July 17 the significant wave height increased to the 1-1.3 m range and then dropped back down to 0.3-0.6 m. Again the highest waves coincided with times of constant wind direction and the lowest waves with variable winds. Although there was a tidal effect at work here too, its influence upon the wave height was not as obvious as that of the wind.

The average direction of wave approach for the summer of 1976 is best summarized on the NOAA weekly summaries of wind direction (Appendix A). From June 15-29 the wind waves were from the Southwest and the

South, from June 29 to July 13 the waves originated from the Southwest and the West, and from July 13 to July 15 they came from the West and Northwest. Therefore the 1976 study period was dominated by waves arriving with their crests parallel to shore. Towards the end of the field season the wave source became more westerly causing oblique wave incidence at Panama City Beach. There was no wave period data available for 1976.

1977

Table 1 shows the significant wave height range for the interval from June 11 to July 28, 1977. This time period was characterized by comparatively small waves except for a three-day storm in mid-July. Most of the waves remained in the 0.3-0.6 m range with an occasional 1.0 m event (June 12 and June 25-27). The largest wave heights coincided with high velocity winds and winds of constant direction. The largest waves recorded for all three summers occurred during a storm which lasted from late July 16 through July 19, 1977. The significant wave heights for this storm peaked in the 1.5-2.0 m range and averaged 1 to 1.5 m in height.

Wind wave direction exhibited a strong component from the West and Southwest for June 1 to June 22, 1977. During the week of June 22-29 the west and southwest wave components attained equal strength and then the southwest waves dominated until July 13. The storm in mid-July brought waves from the Southeast during the week of July 13-20. After the storm waves subsided the wave source swung around to the

South and then the Southwest.

Wave period was sampled in the afternoon on several dates in June and July of 1977 (Appendix A). The data indicate an average of two to four seconds for waves arriving at Panama City Beach. Slightly longer period waves arrived during the storm.

Breaker type is a qualitative observation which classes the wave breakage as plunging or spilling. Plunging breakers dissipate their energy rapidly as the wave form collapses instantaneously upon over-steepening. This situation occurs for steep wind waves (wave steepness = wave height/wave length) on beaches with a steep slope. Spilling breakers distribute their energy over a broad area as they break gradually, maintaining their wave form with progressively decreasing wave height as they shoal on the beach. Spilling breakers were the most common type observed on Panama City Beach except during storms when plunging breakers also occurred. Waves usually broke twice, once on the inner bar and then again in the swash zone. During storms the larger waves broke on the outer bar, then the inner bar and then again in the swash.

Horizontal Bottom Velocity Measurements

1976

Figures 12-23 display the horizontal bottom velocity measurements associated with topographic profiles measured in 1976. Velocity components were measured perpendicular to shore. The topographic variation during this period involved changes in the width of the inner trough, in the shape of the bar, and in the steepness of the swash zone. Bottom velocity patterns are described here in terms of the submarine topography.

In general the horizontal bottom velocities indicate symmetric oscillation in the deeper areas and asymmetric oscillation in the shallows. The highest velocities also coincide with the two shallowest points along the profile, the bar crest and the swash zone. The highest velocities occur during times of large waves and often exceed 92 cm/sec, the upper limit of the swing-surge meter. Figure 19 shows a good example of large waves and high landward velocities. In figure 16 the highest landward velocities are found on the seaward side of the bar crest and they are opposed by seaward velocities on the bar crest!

In the swash zone, bottom velocities are large and either symmetric or slightly asymmetric landward in relative intensity. There are two surveys (Figs. 12 and 39) in which seaward swash velocities dominate.

The horizontal bottom velocities in the inner trough are quite variable. Symmetric oscillation is the most common situation observed. Landward asymmetry is the second most common velocity configuration. Seaward asymmetry of water motion sometimes occurs at the base of the swash and at the base of the bar's avalanche face (Figs. 16, 17 and 22). The direction of longshore water movement in the trough is indicated by an arrow perpendicular to the profile. Eight surveys exhibit westward longshore flow, four exhibit eastward flow.

1977

The horizontal bottom velocity data from 1977 is shown in Figures 27-39. The changes in nearshore bottom topography for this year are known more completely than those of 1976. Therefore the velocities are described here in terms of the general bar patterns observed during the summer of 1977.

Profiles in Figures 27, 28, and 29 show a broad inner trough with a subtle bar crest, a great distance from shore. In the first two profiles, seaward and symmetric velocities dominate the inner trough. Landward and symmetric bottom velocities are found in the inner trough in the third profile. The longshore current flow in the trough is eastward for all three dates. The profile in Figure 28 is the only one which shows longshore velocity components along the entire traverse. The longshore bottom velocity is fairly uniform across the inner trough but diminishes seaward of the bar crest. The onshore-offshore velocities on the bar crest are landward in Figures 27 and 29 but seaward in Figure 28. Therefore, in Figure 28 (June 23, 1977), the velocity asymmetry is seaward along the entire profile.

The three profiles of July 3, 5, and 7 (Figures 30-33) are all characterized by steep-faced bars close to shore. The longshore current flow in the constricted inner trough is still eastward. Onshore-offshore water motion in the trough is seaward in Figure 30, landward in Figures 30-31, and mostly symmetric in Figure 32. On the bar crest the asymmetry is landward for all three dates. Symmetric and some slightly seaward velocities exist on the back of the bar.

In Figures 34 and 37 (July 9th and 15th) the bar profiles are rounded but still relatively close to shore. Both profiles have seaward velocity asymmetry over the bar crest. In fact the seaward velocities dominate the entire profile in Figure 37. In Figure 34 the velocities are landward in the swash, symmetric in the trough, seaward over the bar crest, and on the seaward slope they vary from symmetric to asymmetric in both directions. The longshore current measurements in Figure 34 demonstrate a unique situation; flow is eastward in the inner trough and westward in the outer trough! In Figure 37 the longshore flow is eastward in the inner trough.

Vertical velocities measured on July 15th are shown in Figure 5. Measurements made on the bottom are essentially zero. Vertical velocities near the surface range from 0.3 to 3.3 cm/sec. The maximum readings are located above the bar crest in the breaker zone. Abundant quantities of suspended sand were observed in the water column above the bar crest on the day these measurements were made.

The last two profiles (Figs. 38 and 39) were measured following the three-day storm previously mentioned in the wind and wave results. The bar form is very steep-faced and farther offshore than the preceding forms. These two profiles exhibit westward longshore drift in the inner trough. The water motion perpendicular to shore is seaward over the bar crest on July 21 (Fig. 38) and landward on July 27 (Fig. 39). Velocities in the trough are mostly symmetrical. Vertical velocities measured on the 21st are insignificant relative to horizontal bottom velocities. The largest values are near the water surface and measure-

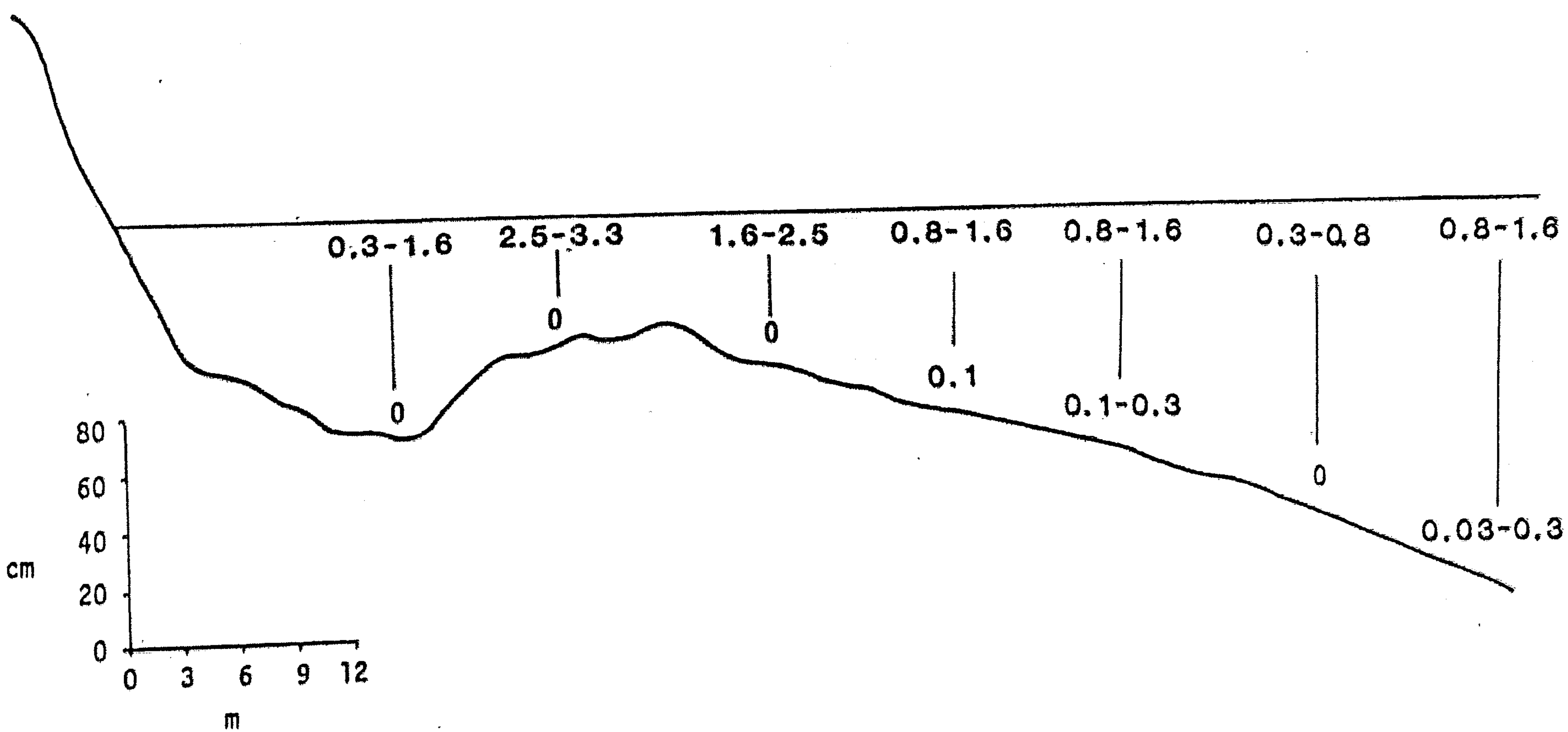

Figure 5: Vertical velocity profile from July 15,1977. All readings are in cm/sec.

ments near the bottom are essentially zero.

Bar Patterns

Figures 6, 7 and 8 display sketches made from aerial photographs of various configurations of nearshore sand bar topography along Panama City Beach. The inner sand bar assumes a few basic bar patterns with intermediate forms. The cuspate bar is the form most frequently observed on the aerial photographs (Fig. 6). The cuspate bar occurs as a continuous, near-perfect, sine wave pattern (Fig. 6a), sometimes it is skewed alongshore (Fig. 6b), and sometimes it is partially or completely welded onto the shoreline (Fig. 6c).

Another basic bar pattern is the "horn", which is composed of discontinuous shoals, welded onto the shoreline at regular intervals (Fig. 7a). These shoals are often associated with a cuspate shoreline. The shoals can assume a skewed pattern alongshore producing the horn-like appearance (Fig. 7b).

The third basic bar pattern observed in the nearshore is the shore-parallel bar (Fig. 8a). The shore-parallel bar is a straight-line shape in plan view and the topographic profiles show the uniformity of its cross section alongshore. This is the simplest configuration that was observed but it also has variants. Photography from January 22, 1953 (Fig. 8b) shows a shore-parallel bar with occasional cusps on the shoreward side.

The form of the offshore bar is straight to cuspate with a very long wavelength. The outer bar showed very little change during the three summers of observation. The passage of Hurricane Eloise on

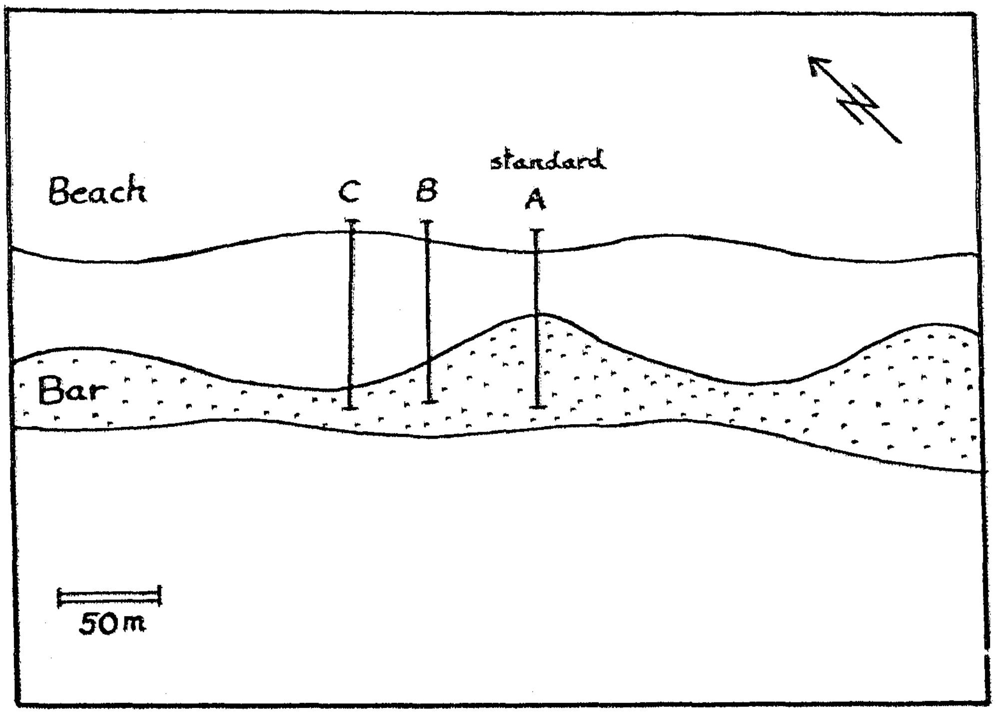

Figure 6a: Cuspate bar (symmetric) with profile localities; June 19,1976.

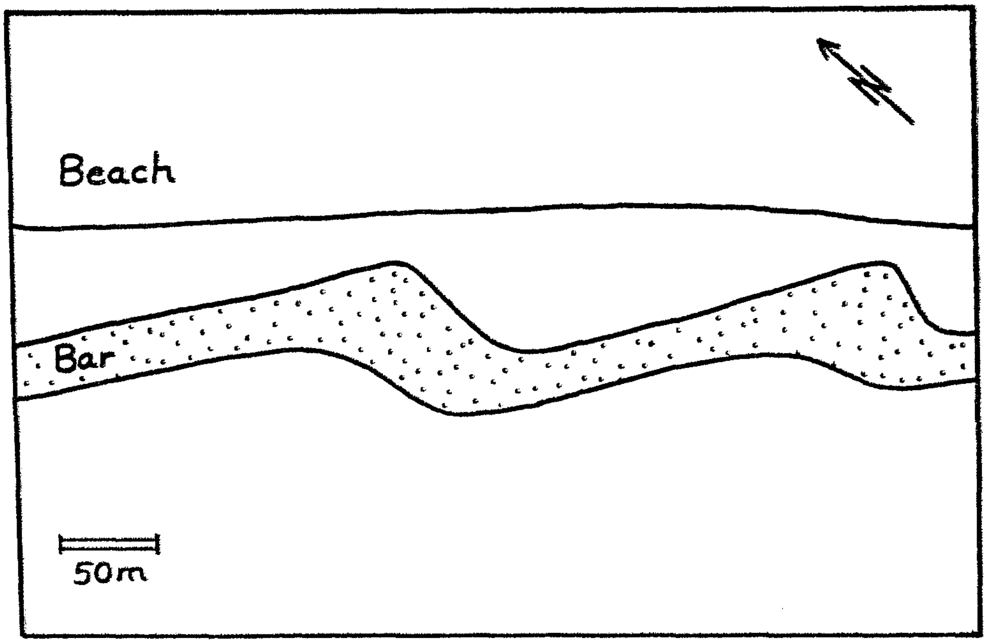

Figure 6b: Cuspate bar (skewed); September 10,1942.

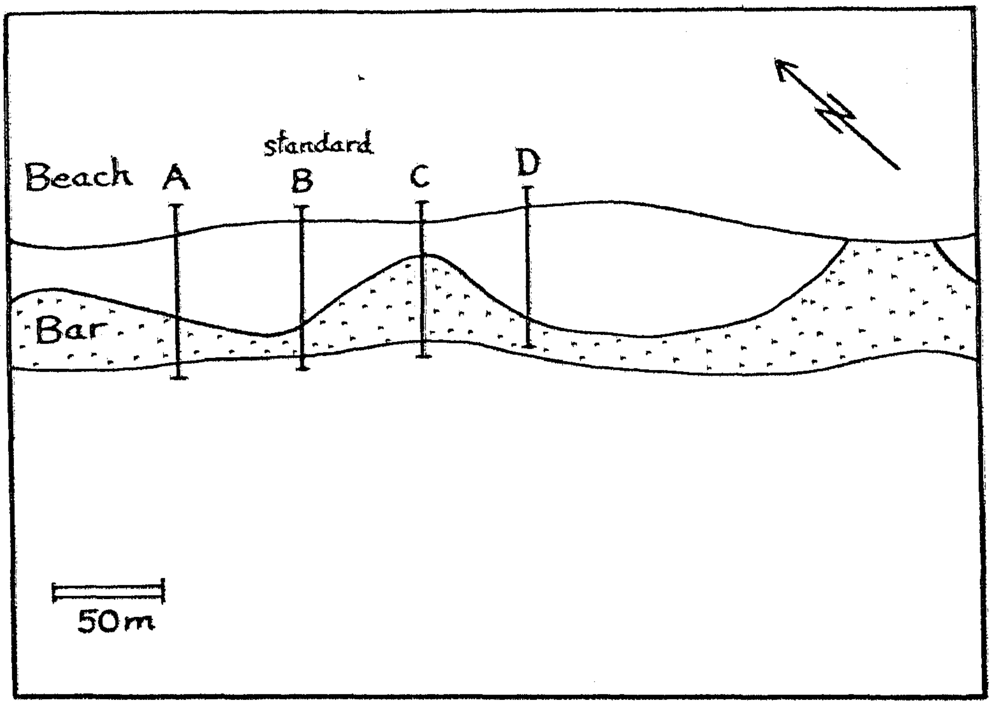

Figure 6c: Cuspate bar (partially welded to the beach); June 22,1977.

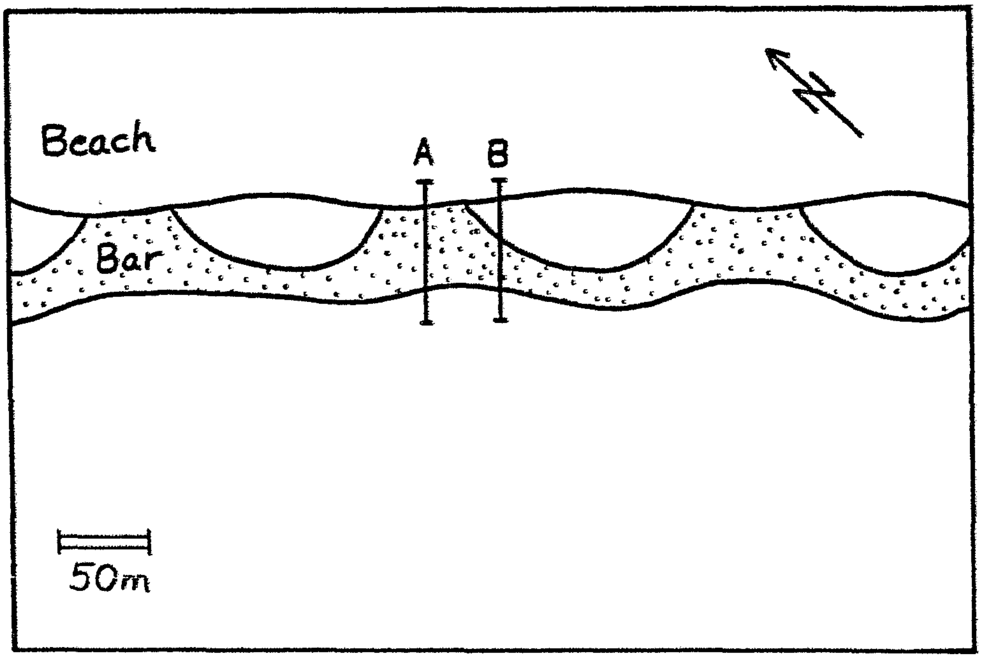

Figure 6d: Cuspate bar (welded to the beach) with profile localities; August 16, 1975.

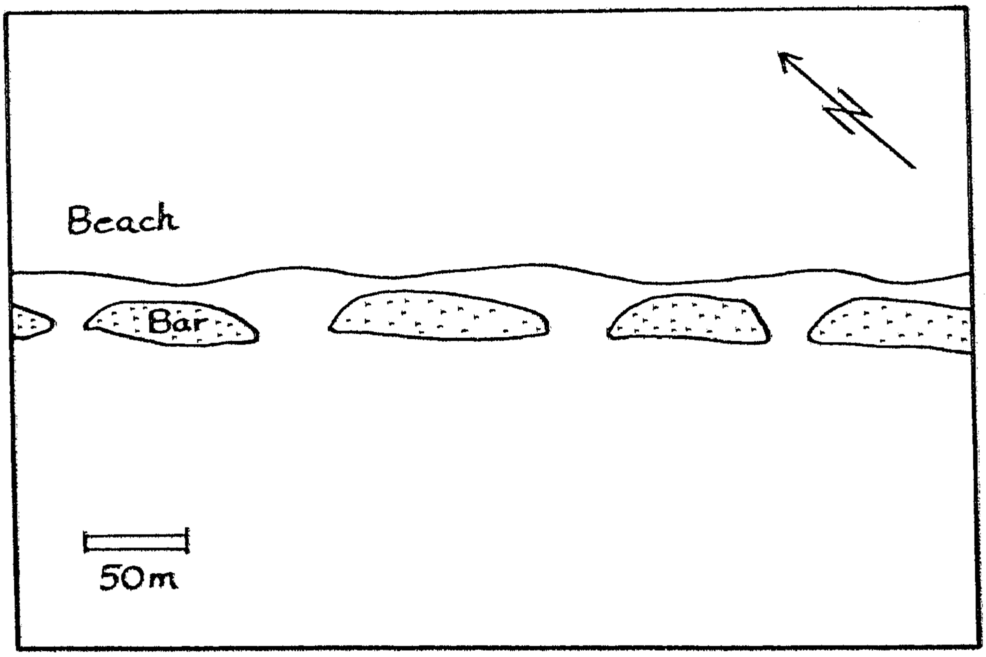

Figure 7a: Horn bar (discontinuous shoals); January 7,1972

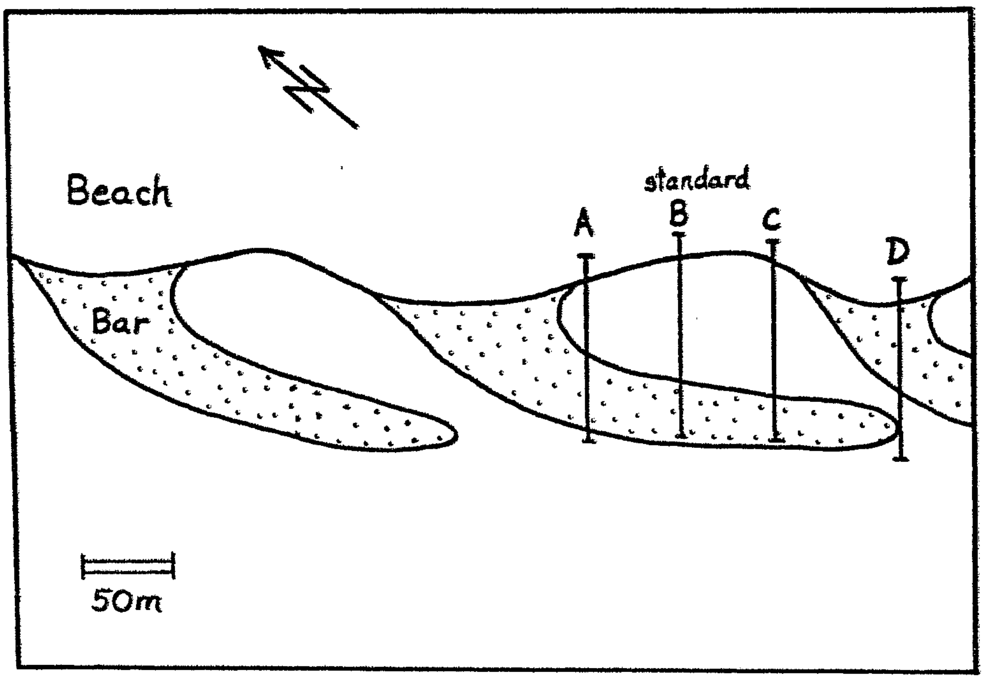

Figure 7b: Horn bar (skewed) with profile localities;
June 29,1977.

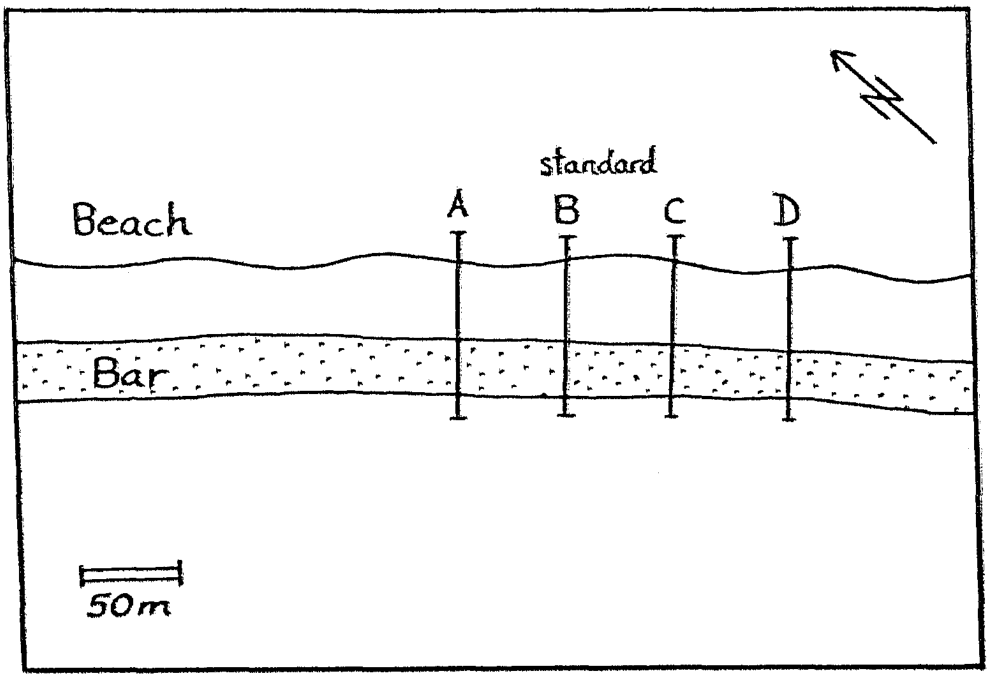

Figure 8a: Shore-parallel bar; July 27,1977.

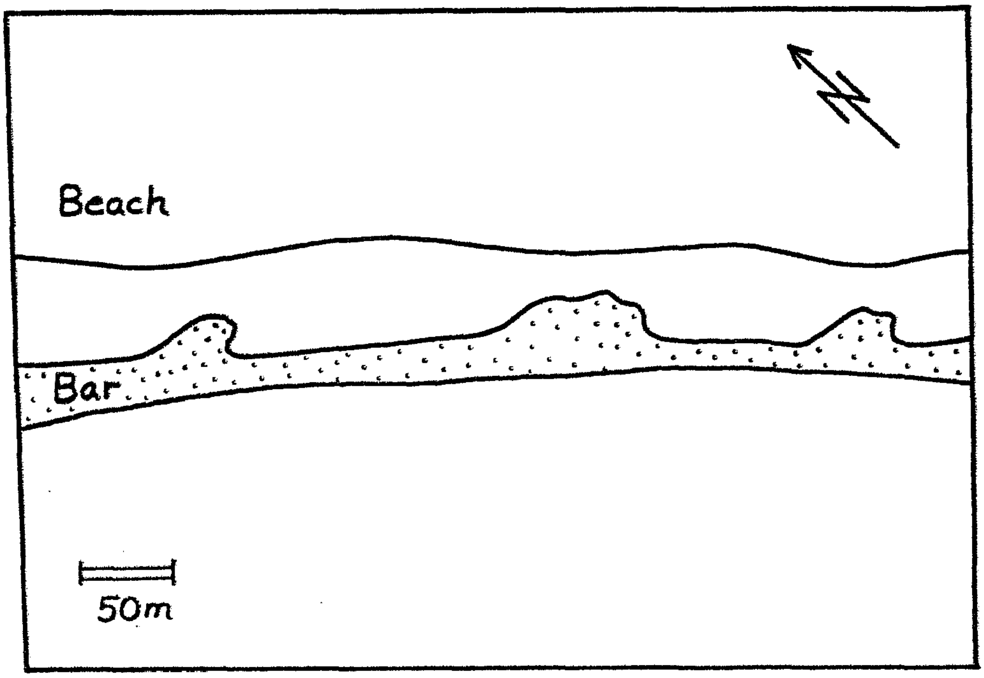

Figure 8b: Shore-parallel bar with cusps; January 22,1953.

September 23, 1975 increased the depth over the outer bar crest from about two meters to over three meters and increased the width of the bar. Between 1976 and 1977 the outer bar shallowed to about 2.5 meters. Breaking waves were only observed on the outer bar during storms and periods of high waves.

Topographic Profiles

1975

Only two profile localities were surveyed in 1975 and they were 25 m apart. The nearshore topographic profiles can be found in Appendix B. The two localities used in 1975 were not far enough apart to show the complete variation in topography alongshore but profiles measured by Sonu, et al. (1973) on shore-welded cuspate bars complement the Panama City Beach data. In Figure 9 one can see the difference between a cusp and an intercusp profile. The former is a smooth, convex-up profile with no sand bar and the latter shows a bar, close to shore.

1976

Many of the 1976 profiles were only partial traverses because of high waves and deeper water in the inner trough during this period. Therefore the first seven profiles only record changes in the configuration of the swash. A distinctive feature of the swash zone is the break in slope which occurs just below the water line. On June 18, 24, and July 1, 1976 the break in slope is very pronounced and almost looks like a small sand bar. On all of these dates the significant wave

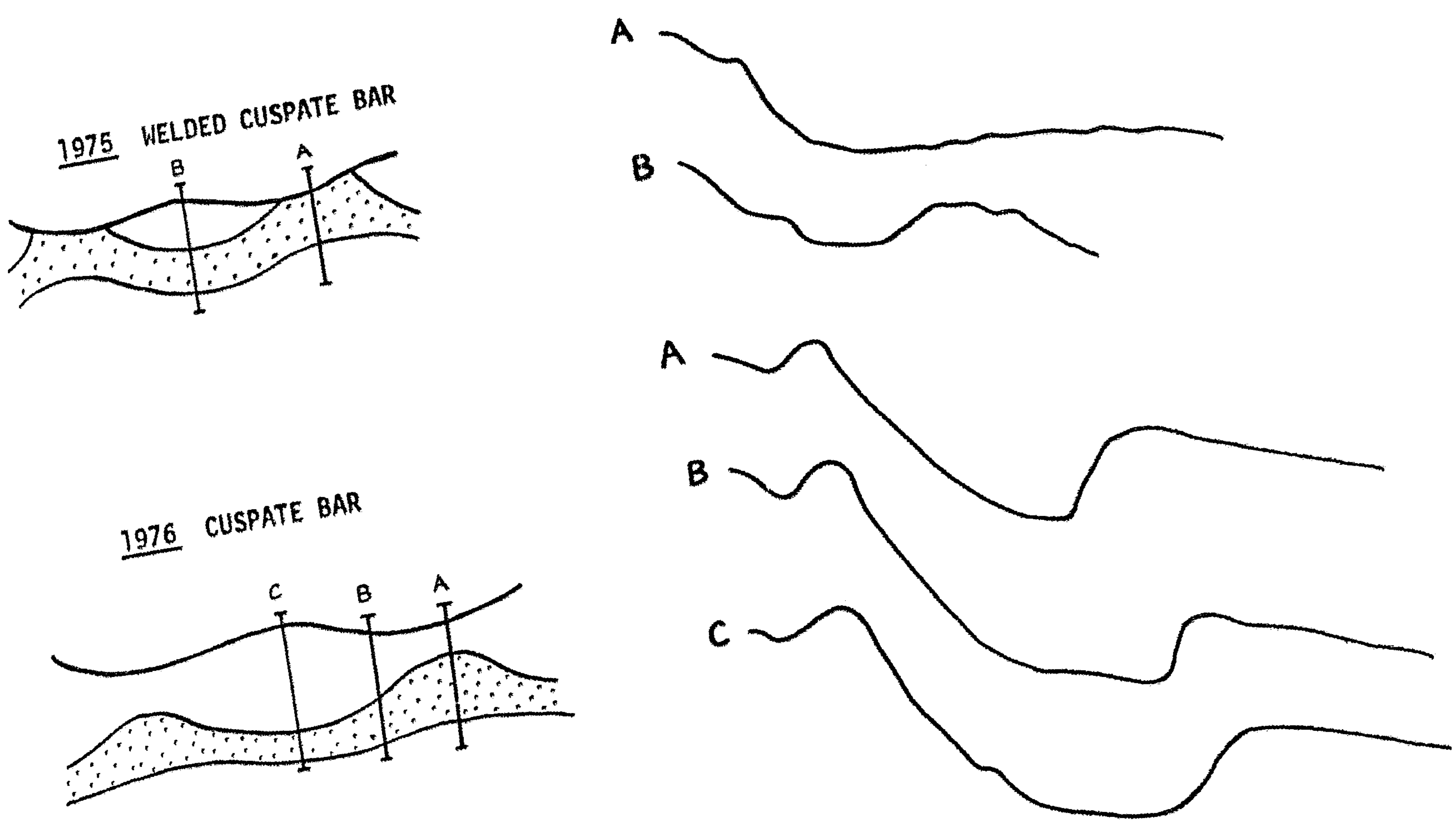

Figure 9: Summary of topographic profiles from 1975-76.

height is larger than usual.

On July 14th there is a most pronounced break in slope in the swash zone and a ridge and runnel system has formed in the trough. Ridge and runnel systems are small, very regular bar forms which are common on some beaches but were only observed on Panama City Beach once. This unusual profile and the two which precede it (July 13A, 13C, and 14 in Appendix B) were measured during a dredging and replenishment program carried out by the Army Corps of Engineers. Sand was dredged from offshore and pumped into the longshore current system along the reach between Phillip's Inlet and St. Andrew's Bay entrance channel. The large waves which occurred on July 14th combined with the abundant suspended sediment from the dredging to produce the unusual bedforms.

Before the dredging began the bar pattern was a very regular cuspate form as seen in Figure 9. The accompanying profiles show the variation in nearshore topography within one wavelength of the cuspate bar. On the cusp the profile shows a massive bar, located close to shore, with a steep, active avalanche face. In the intercusp, bay area the profiles indicate a progressively smaller bar, farther from shore with a less active avalanche face. In the bay the overall slope of the profile is steeper.

The amount of profile variation observed in the above-described cusp unit during one month in 1976 is relatively small except for the changes seen during dredging. Most of the minor changes involved onshore-offshore movements of the bar which are only apparent changes caused by the alongshore migration of the bar form.

1977

During the 1977 field season, two distinct bar patterns were observed in the nearshore of Panama City Beach. Fifty topographic profiles were measured and they can be found in Appendix B in chronological order. This group of profiles includes one from Shell Island and several sets of four profiles taken on individual days at 25 meter spacings alongshore.

The first bar pattern observed in mid-June was a skewed version of the cuspate form with some portions welded onto the beach (Fig. 6c). The aerial view of this topography resembles a series of elongate pools, arranged along the coastline. However this bar pattern was only an intermediate form which gradually evolved into a horn bar on June 29, 1977.

The topographic profiles associated with a single horn bar are shown in Figure 10. The alongshore variation in profile shape is similar to that observed for the cuspate bar. The difference is that the horn bar profiles show a flatter bar which is not continuous alongshore and ends farther offshore than the cuspate variety. There is a marked decrease in bar size, height, and slip face steepness in the seaward direction. The profile across the seaward most portion of the horn bar portrays a broad, almost level, nearshore sand platform which drops off rapidly into the outer trough.

Following the storm of July 17-19 the bar was found to have a shore-parallel form as seen in Figure 10. The four profiles show no significant variation in the topography alongshore. There is some difference in bar height alongshore but no difference in distance from shore. The cross sectional shape of this post-storm bar is unusually steep and narrow. During subsequent days the shore-parallel bar profiles became less steep and acquired a cuspate nature. At regular intervals alongshore, portions of the bar migrated shoreward and became larger in size. The last network, measured on July 26, 1977 shows these modifications (Appendix B).

A miscellaneous profile was obtained near the eastern end of Shell Island on July 24, 1977 (Appendix B). This profile was quite different than any of the Panama City Beach profiles. It depicts a broad, shallow nearshore region with a wide, rounded trough whose thalweg is in the center of the trough. Panama City Beach profiles show the thalweg of the trough to be at the base of the bar avalanche face. The bar on the Shell Island profile was low relief but massive, with a gentle seaward slope. Aerial photographs of Shell Island indicate the presence of only one longshore bar. The bar patterns observed on photography from 1953, 1964, 1975, 1976, and 1977 are primarily cuspate with variable wavelengths.

Bedforms

Figures 12-23 and 27-39 detail the daily bedform distribution along the standard profiles. Figure 11 is the key to the symbols used in these two sets of diagrams. There were twelve bedform traverses

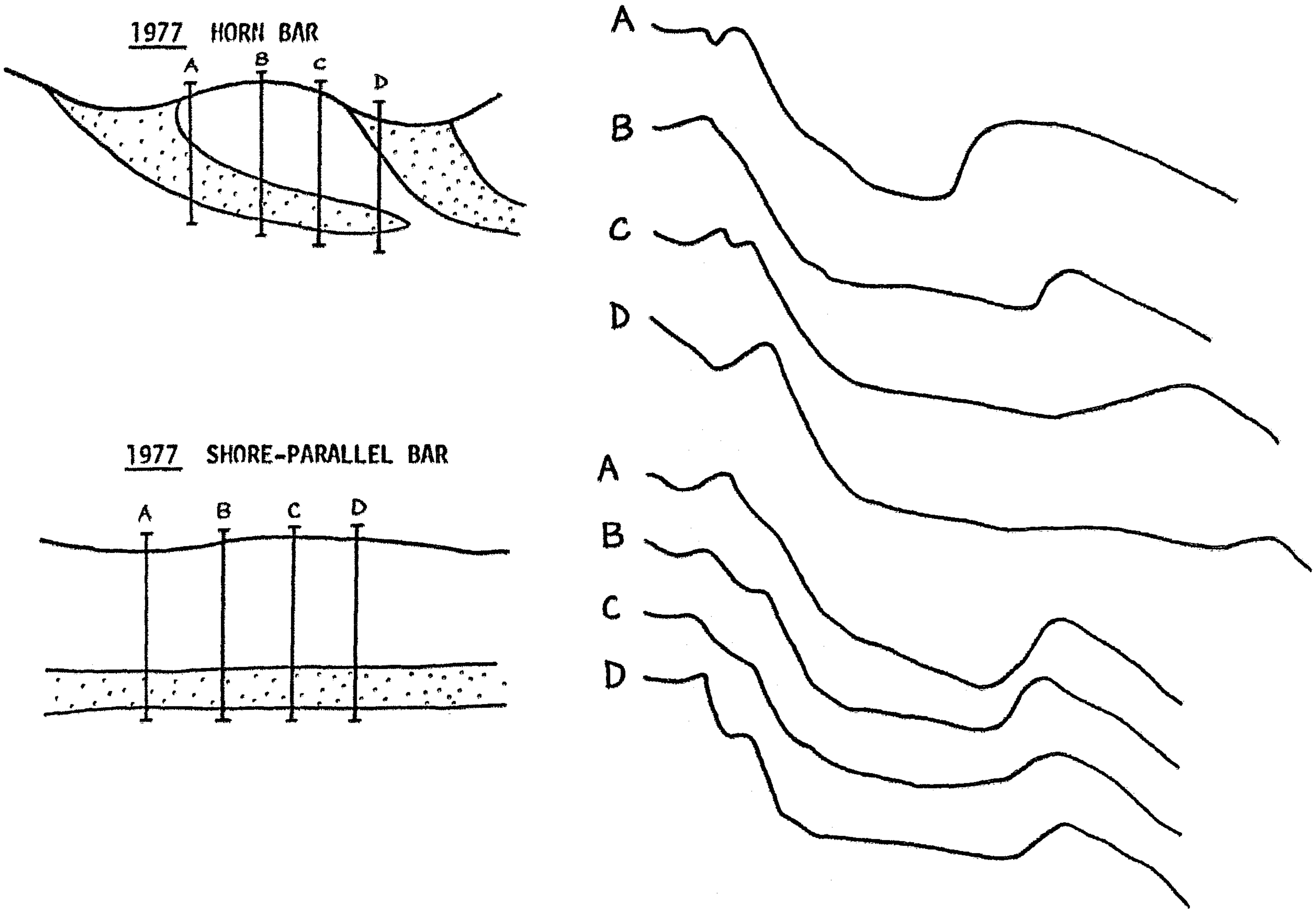

Figure 10: Summary of 1977 topographic profiles.

from 1976, fourteen from 1977, and none from 1975. The figures have two parts, a plan view of the bedforms and a cross sectional view. The plan view displays bedform type and orientation. The cross sectional view details the bedform amplitude, wavelength, sinuousity and relation to topography. The dominant wave approach direction and the longshore drift direction are also indicated on the plan view maps. The numbered intervals along each profile are mapping units of five meter width.

1976

The traverses of Figures 12 through 23 represent bedform data gathered in 1976. Several general relationships can be seen in these plots and will be noted in this section. These profiles are characterized by an abundance of large bedforms in the form of lunate megaripples and as ladderbacks, a type of interference ripple. The ladderbacks have been variously referred to in the literature as cross-ripples, composite ripples, and compound ripples. They consist of two sets of ripples which are commonly oriented perpendicular to each other. One set has straight crests and is nearly symmetrical in cross section, the other ripple set is asymmetrical in cross section and has a catenary crestline. Therefore the straight-crested forms resemble oscillation ripples and the catenary-crested forms appear to be current ripples migrating down the troughs of the oscillation ripples (Fig. 24). The lunate megaripples are discontinuous dunes with crescent-shaped depressions in front of their avalanche faces (Fig. 25).

Daily observation of the ripple types on the seaward slope of the bar revealed a sequence of forms which occurred with marked regularity.

As one progressed shoreward the forms changed from long-crested, symmetrical oscillation ripples to sinuous, asymmetrical ripples to ladderbacks to lunate megaripples and sometimes to a plane bed. This marine bedform sequence was first reported by Clifton et al. (1971) from his studies of the Oregon coast. The entire sequence of forms did not appear every day but when it did, the waves were larger than usual. The profile of June 28, 1976 (Fig. 15) illustrates a complete bedform sequence and also exhibits an irregularity in the pattern. A set of lunate-crested, asymmetrical ripples intervenes between the ladderbacks and the lunate megaripples on this date.

On some dates the sequence progresses only to ladderbacks (Fig. 13, June 24, 1976) or it consists entirely of asymmetrical ripples (Fig. 21, July 9, 1976) but the order of the forms is constant.

A progressive increase in bedform amplitude and wavelength can be seen in a shoreward direction along most of the bedform profiles. The two parameters increase in magnitude with decreasing depth on the seaward slope of the bar and then repeat this trend in the trough. Therefore the largest bedforms should be located on the bar crest and the landward edge of the inner trough. This is not always true of the bar crest as seen on July 5, 1976 (Fig. 19). In this case the bedform amplitude and wavelength increase up the back of the bar but are diminished at the crest. Ladderback ripple sets present a unique situation with regards to trends in amplitude and wavelength. Using the June 28, 1976 profile (Fig. 15) as an example it can be seen in interval four that the lunate-crested ripple set of these ladderbacks conforms with

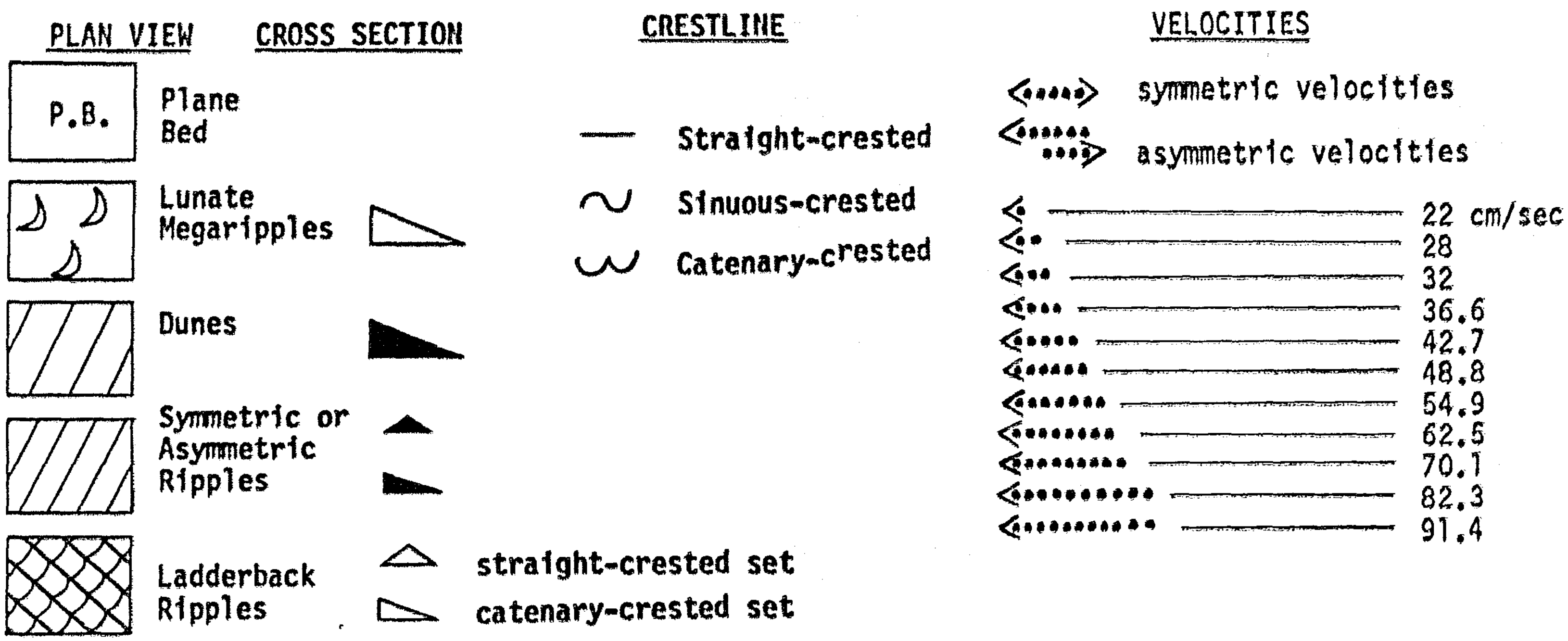

Miscellaneous Notes: 1. "a"= bedform amplitude in cm "λ"= bedform wavelength in cm

2. Numbered sections of the plan view map are 5 meter intervals.

3. Bedforms which are labeled "transition" are irregular in form, orientation, and dimensions.

4. Dashed line bottom profiles were constructed from point source depth measurements because surveying was not possible.

Figure 11: Key to Bedform-Velocity Profile Diagrams in figures 12 through 23 and figures 27 through 39.

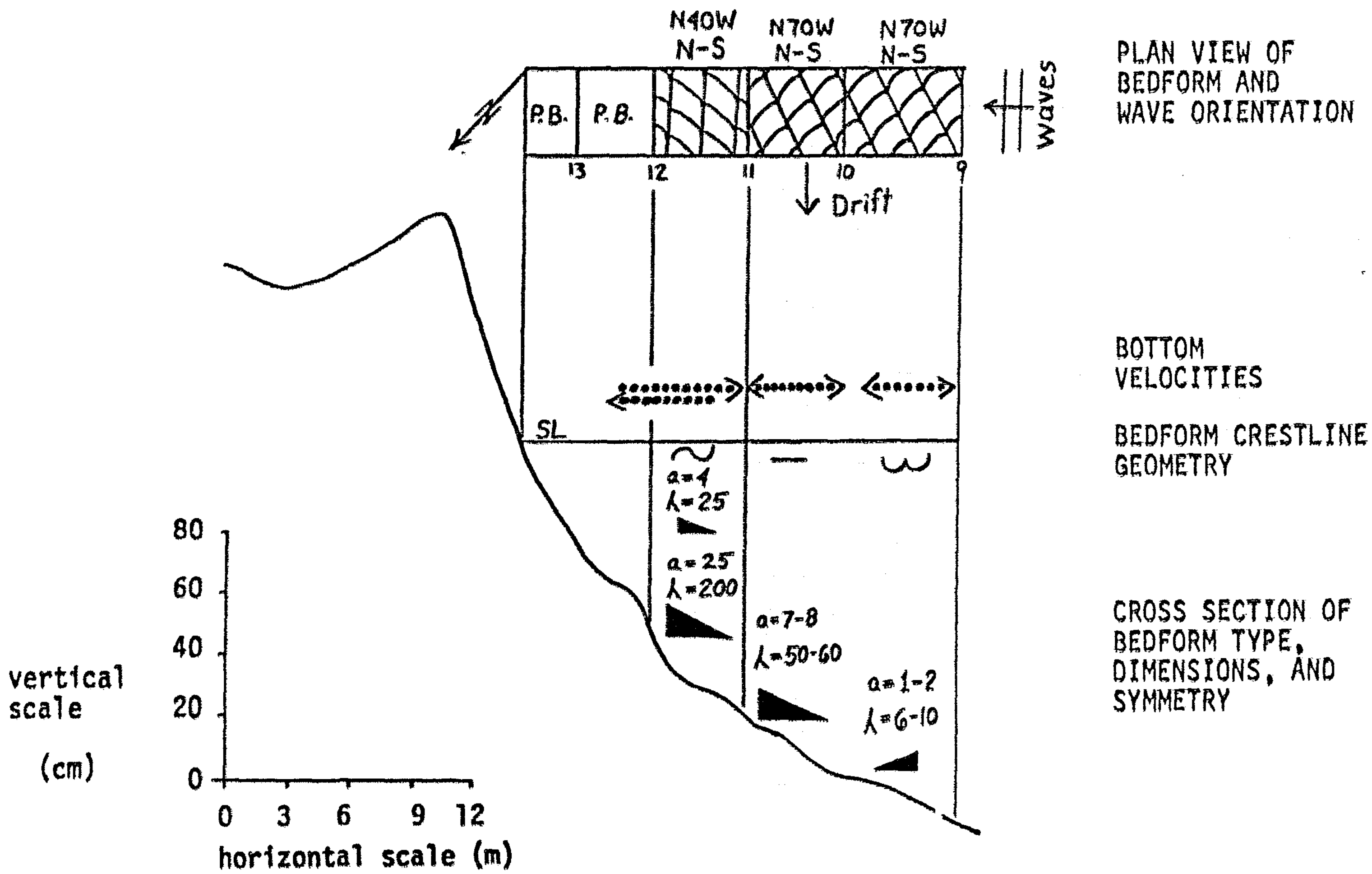

Figure 12: Bedform-Velocity Profile; June 21,1976

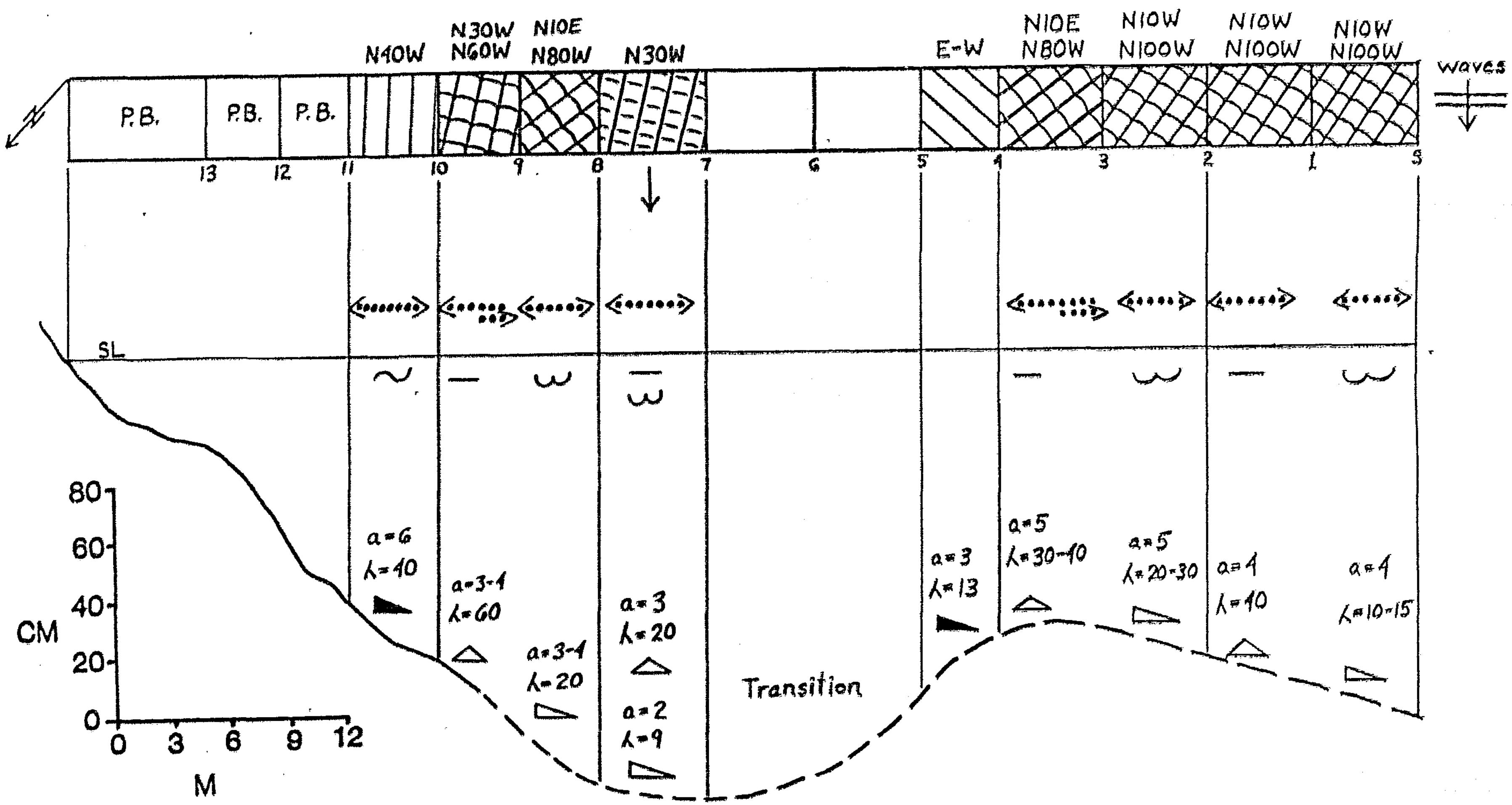

Figure 13: Bedform-Velocity Profile; June24,1976

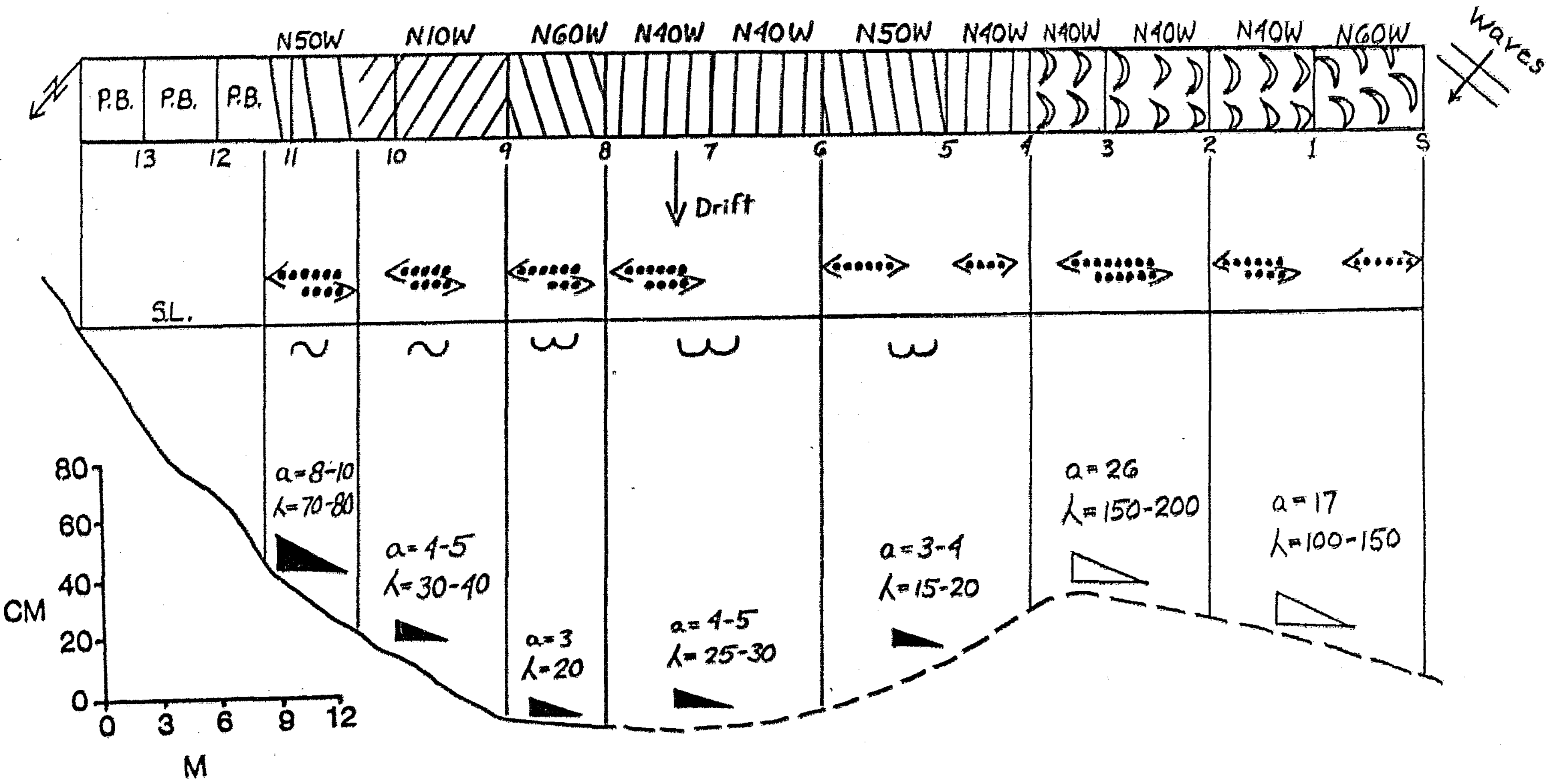

Figure 14: Bedform-Velocity Profile; June 26,1976

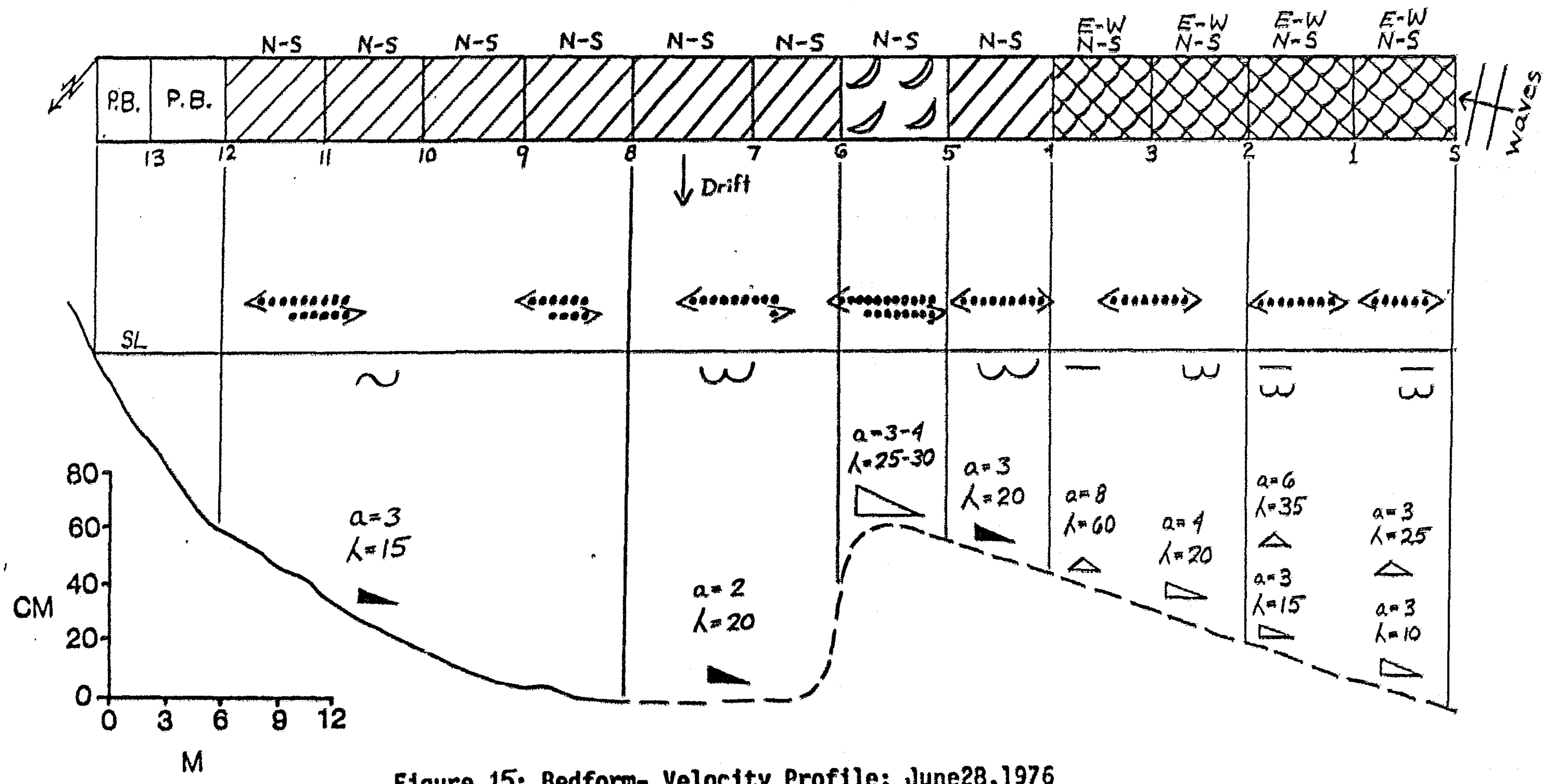

Figure 15: Bedform- Velocity Profile; June28,1976

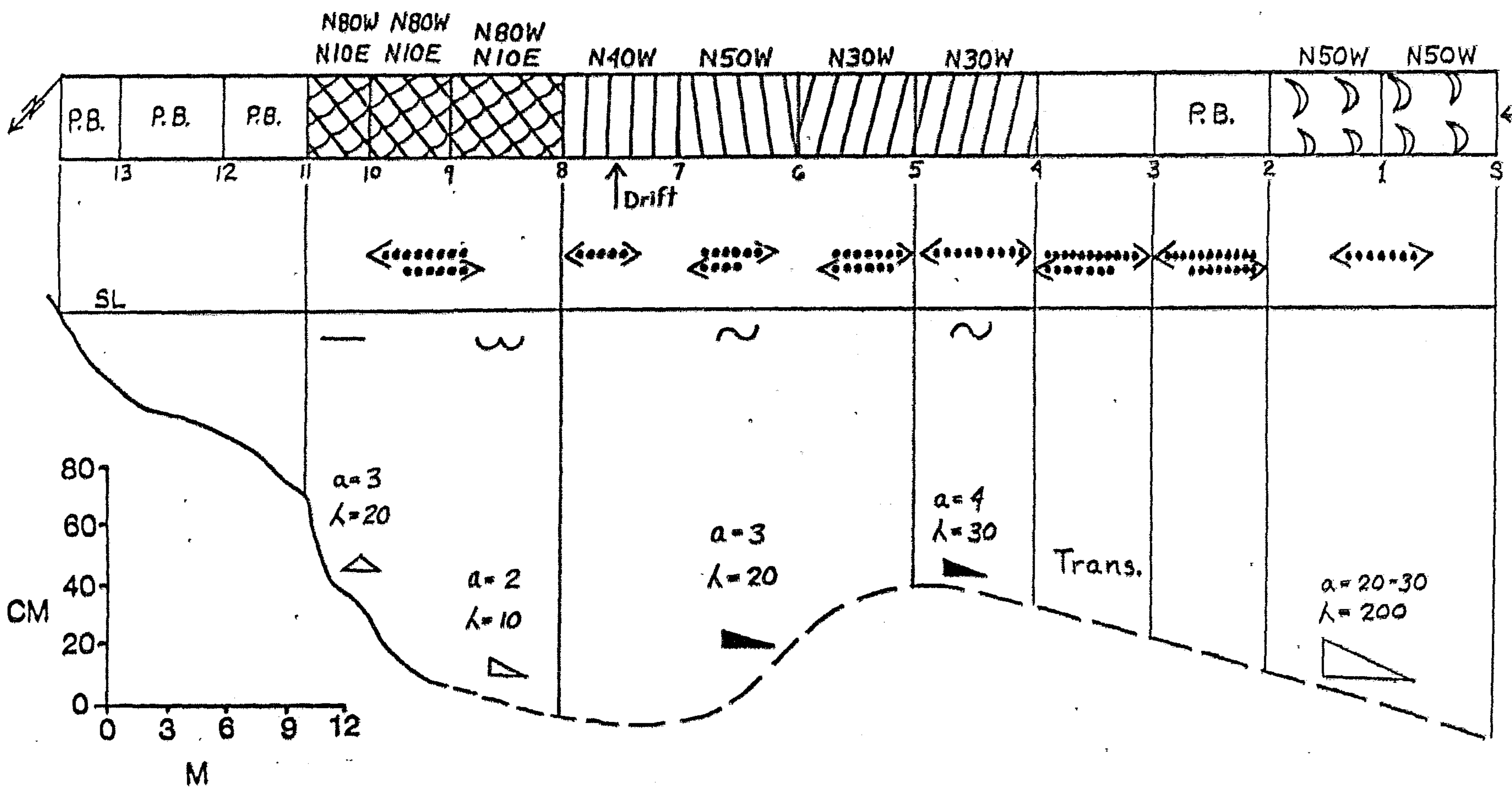

Figure 16: Bedform-Velocity Profile; July 1,1976

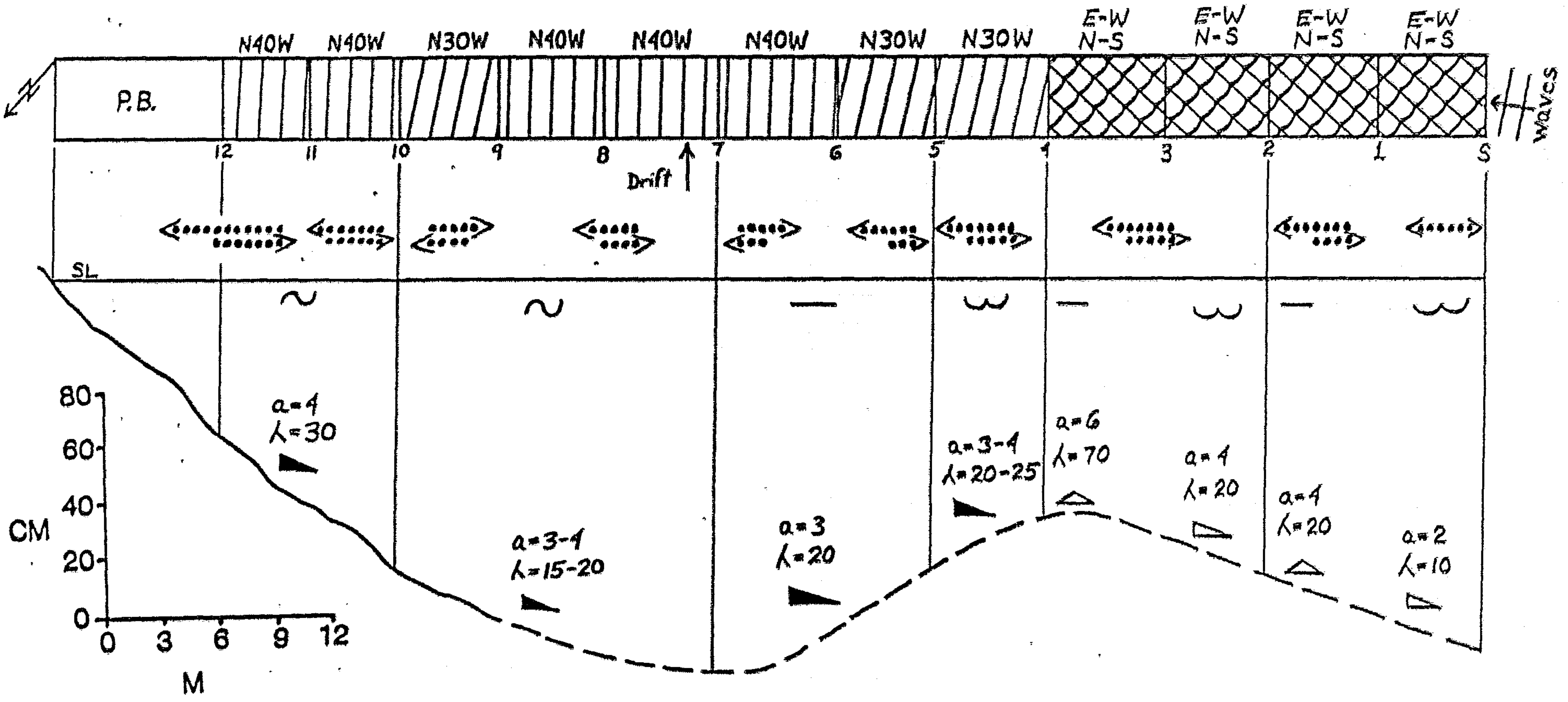

Figure 17: Bedform-Velocity Profile; July 2,1976

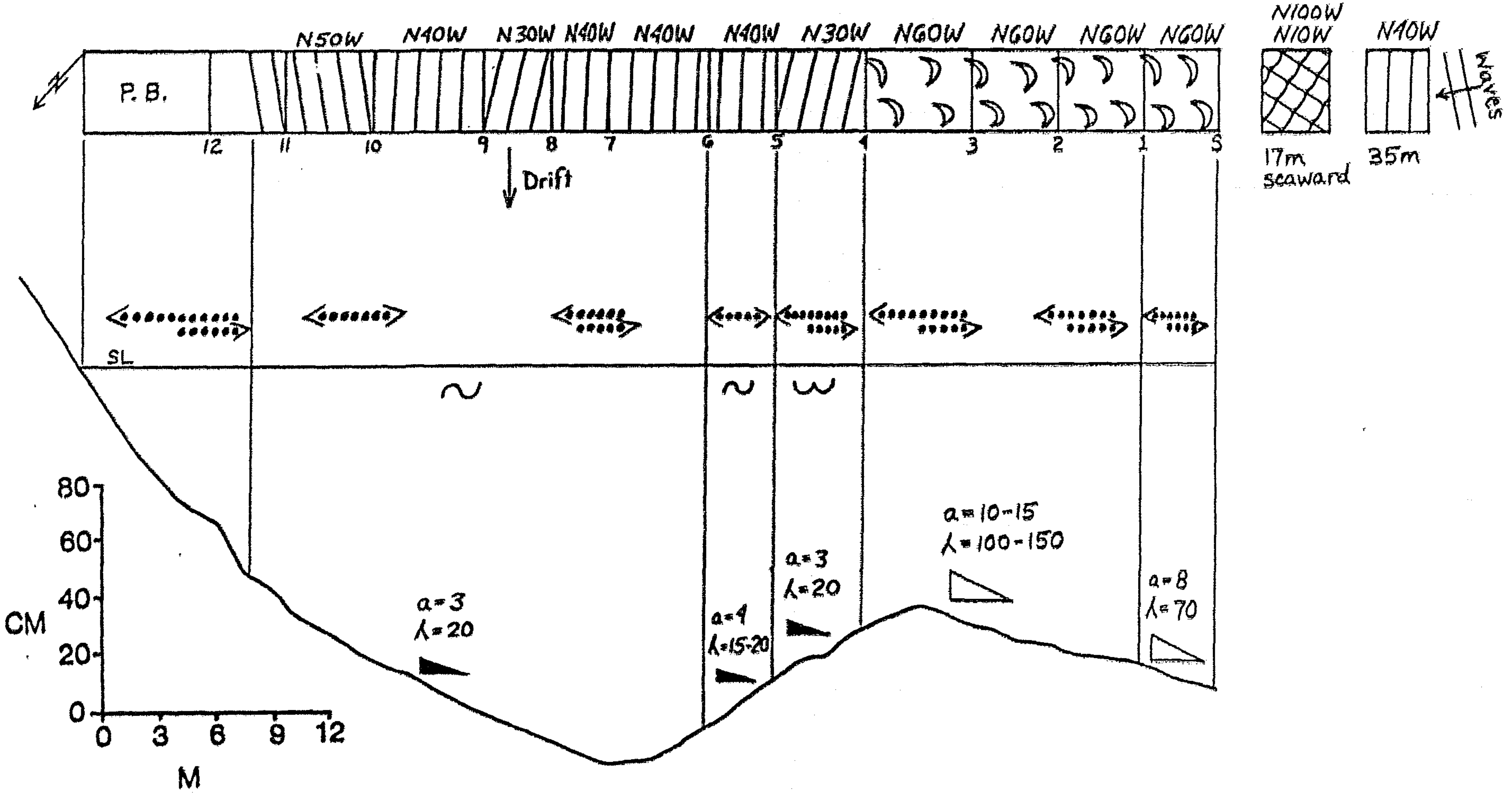

Figure 18: Bedform-Velocity Profile; July 3,1976

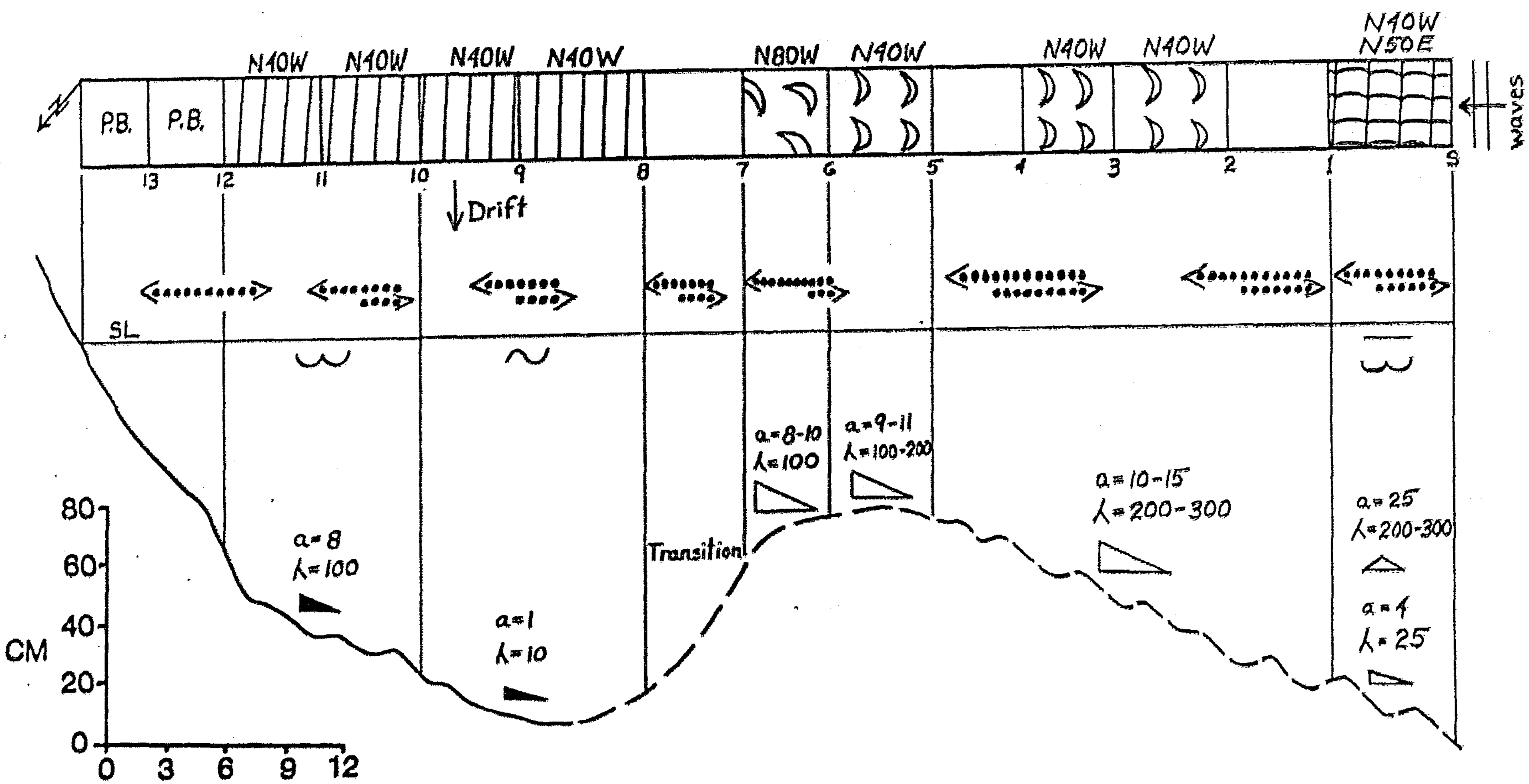

M

Figure 19: Bedform-Velocity Profile; July 5,1976

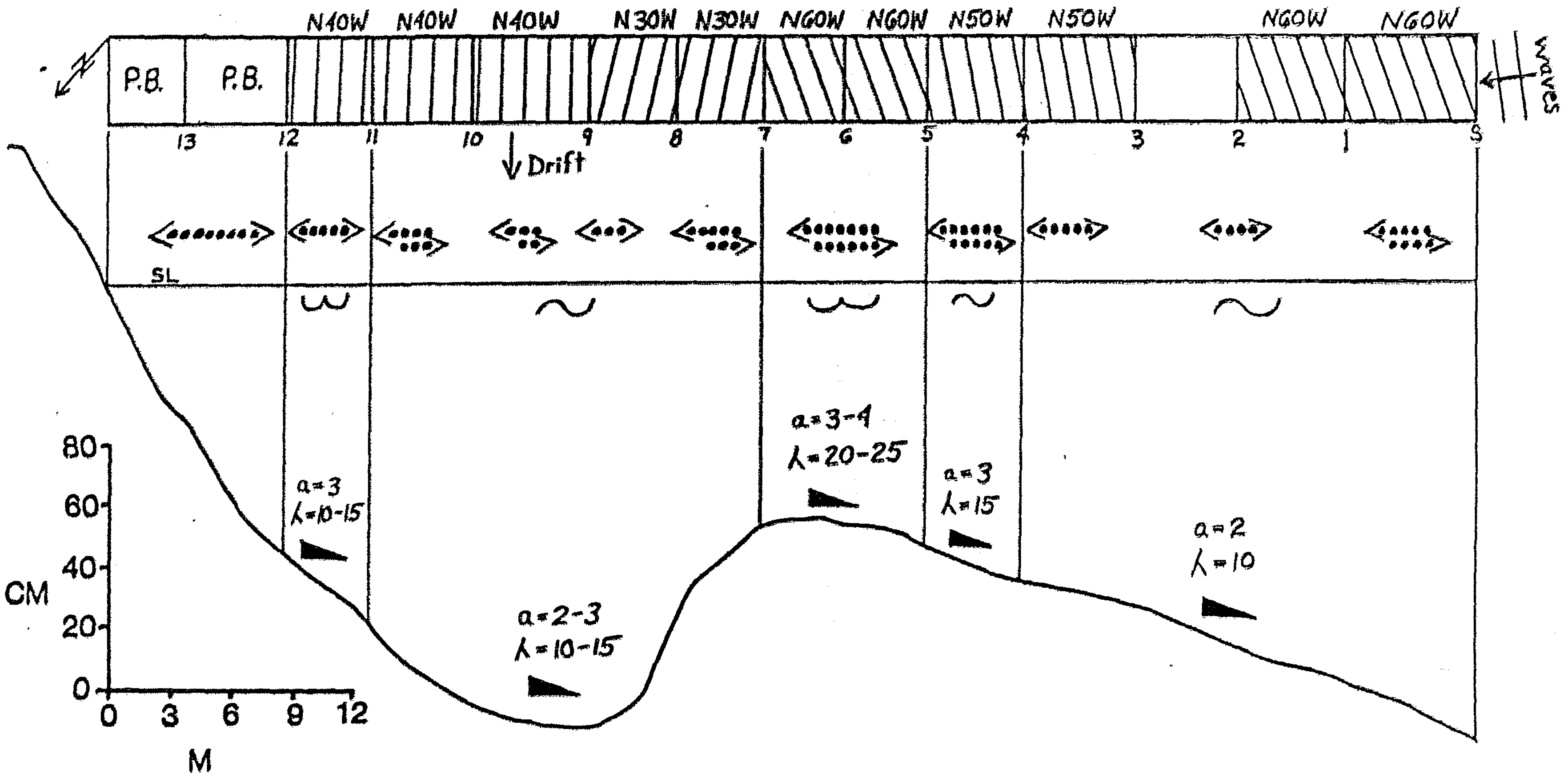

Figure 20: Bedform-Velocity Profile; July 8,1976

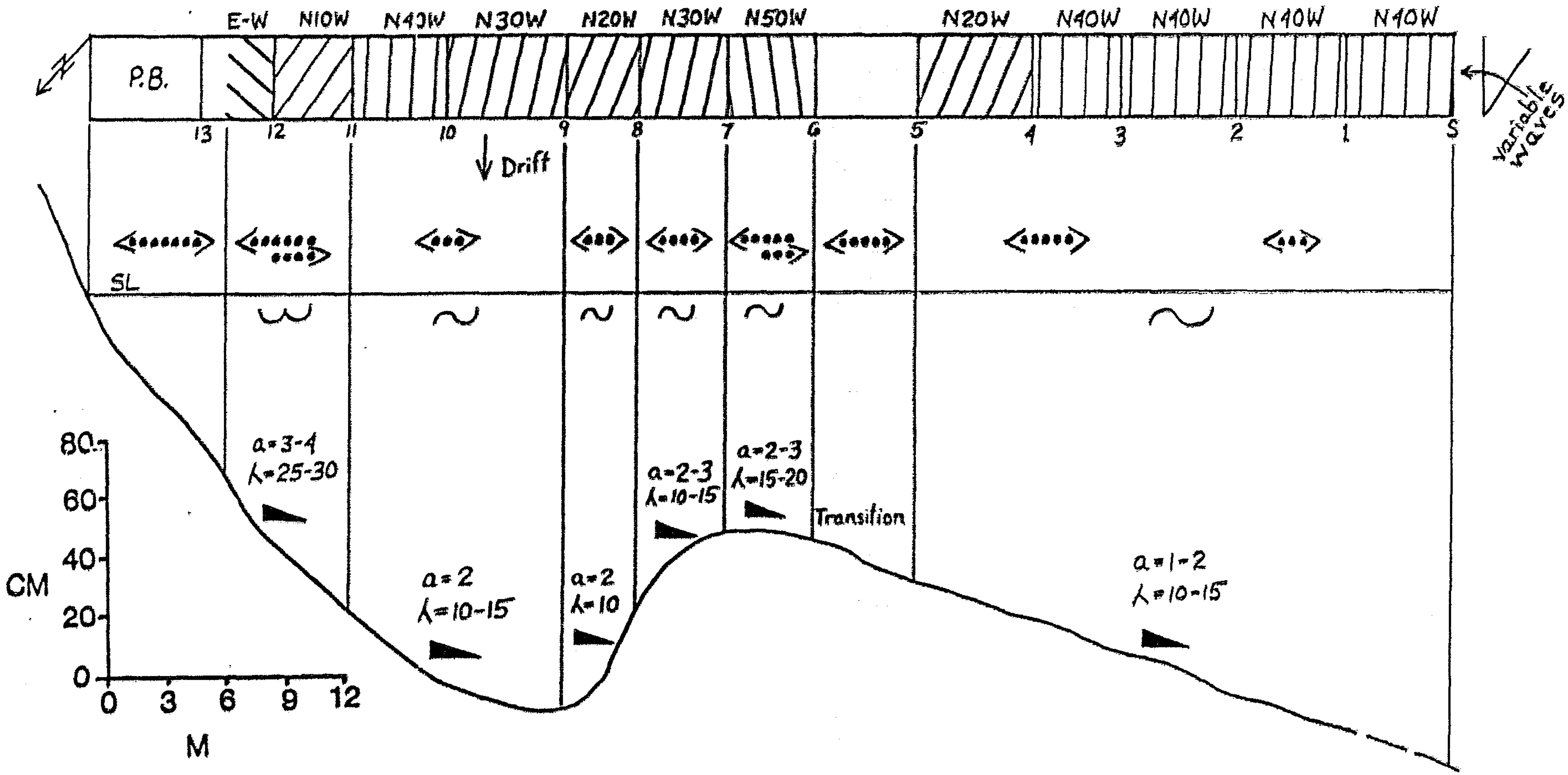

Figure 21: Bedform-Velocity Profile; July 9,1976

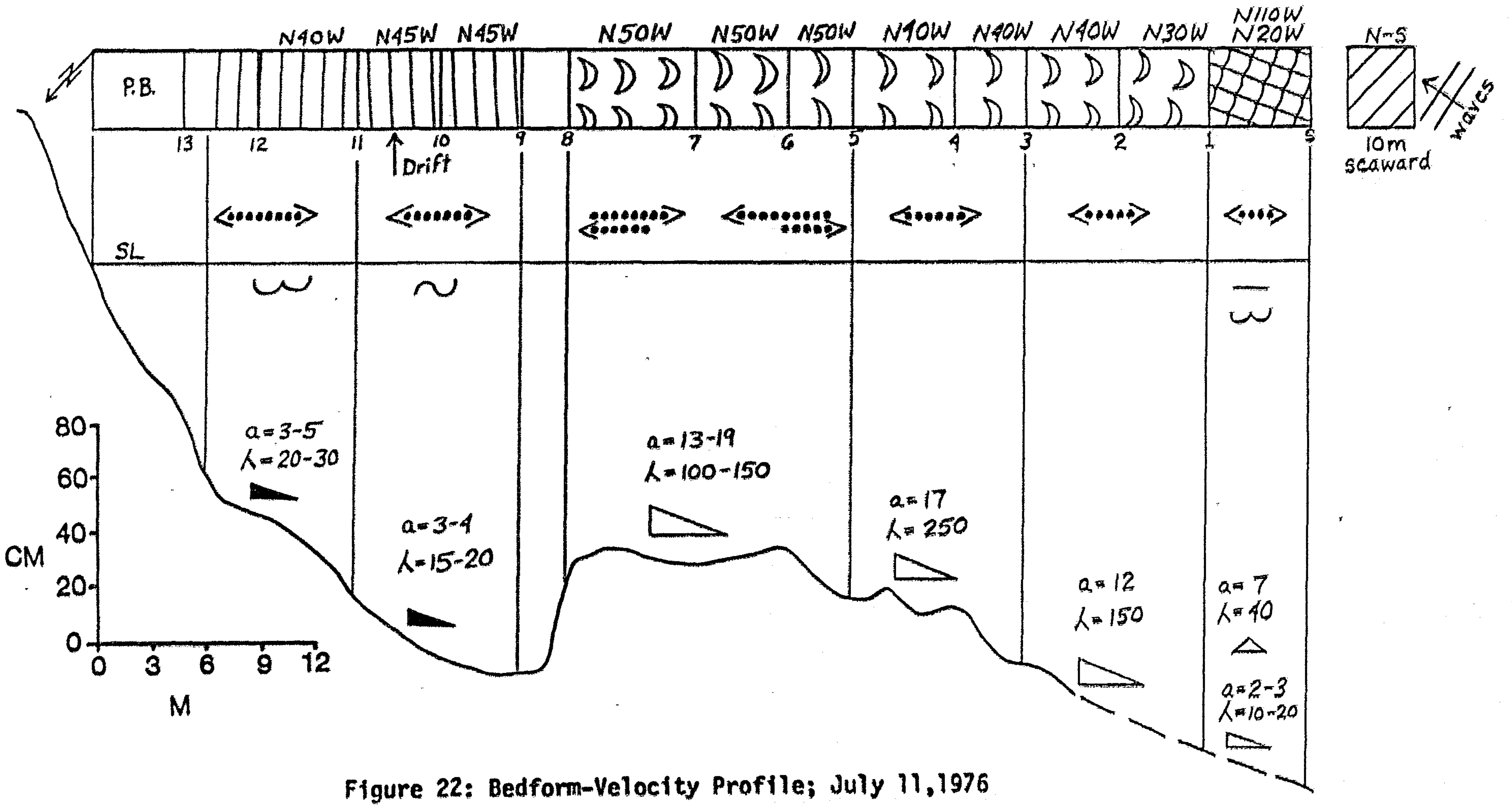

Figure 22: Bedform-Velocity Profile; July 11,1976

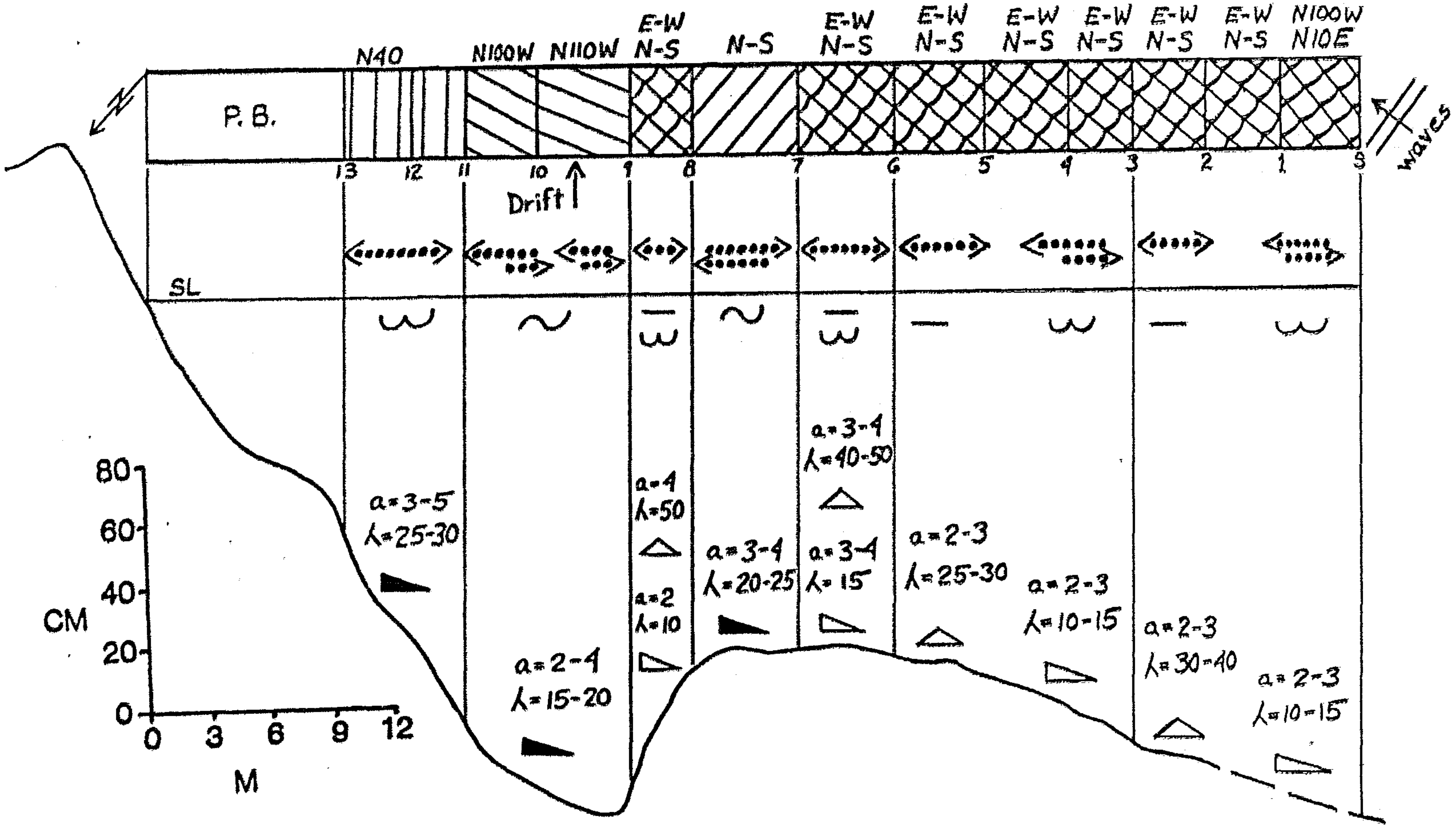

Figure 23: Bedform-Velocity Profile; July 12,1976

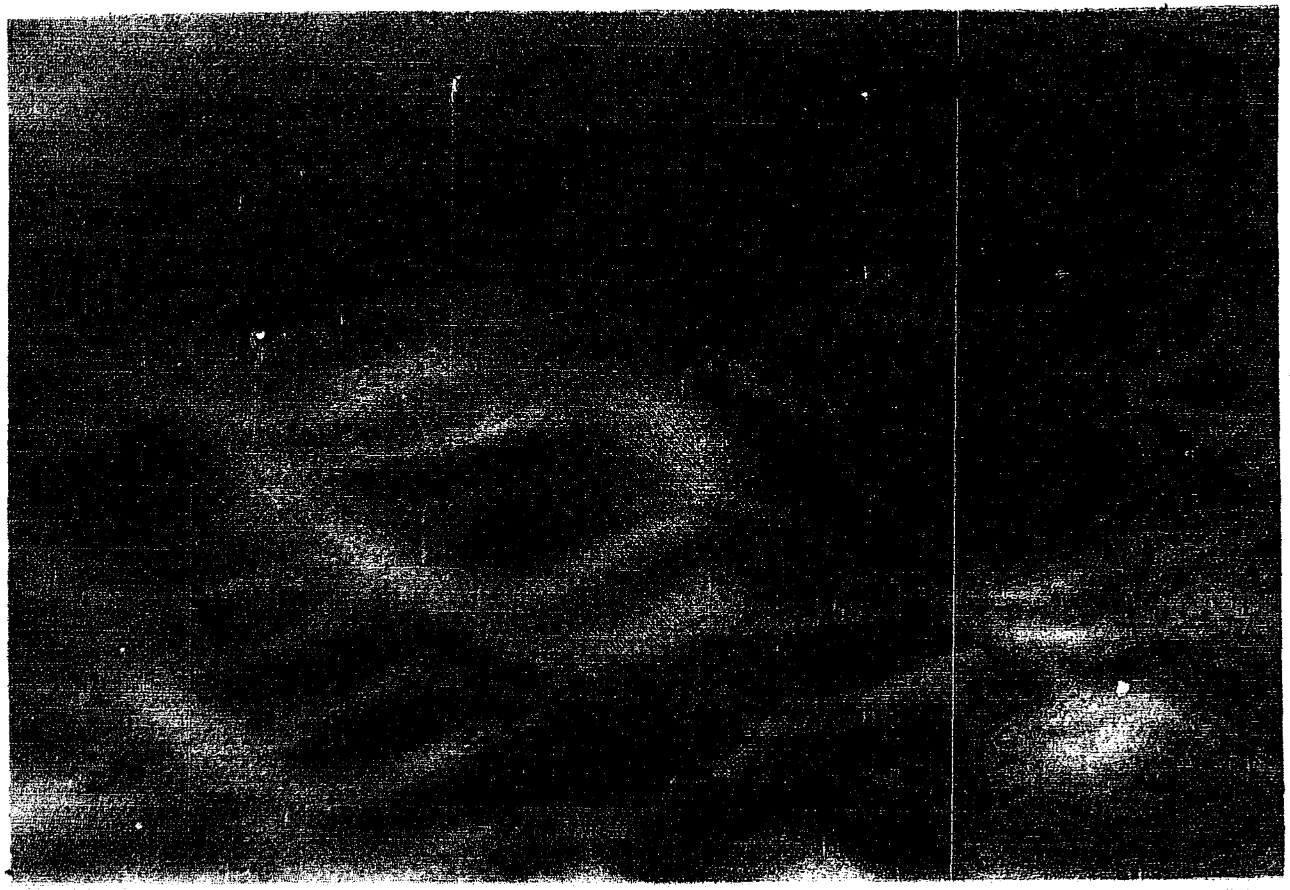

Figure 24: Underwater photograph of ladderback ripples. Trough ripples are migrating towards the camera. Wooden scale is parallel to the straight-crested, symmetric ripples and is 36 cm long.

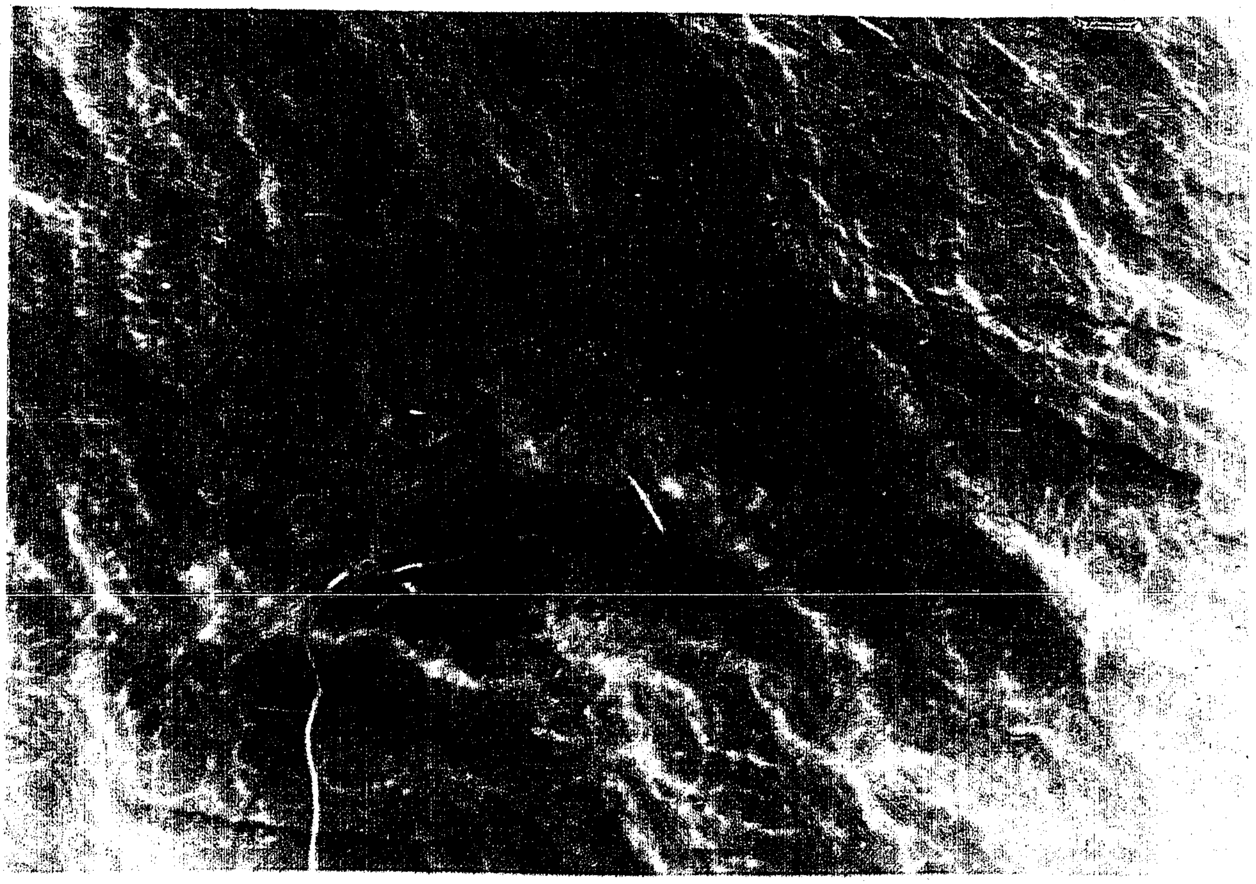

Figure 25A: Photograph of a lunate megaripple avalanche face in shallow water on the inner bar crest. Lead diving weight is 8 cm square.

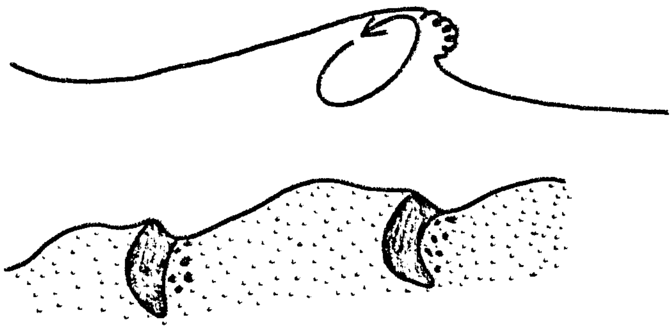

Figure 25B: Sketch of lunate megaripples forming under breaking waves.

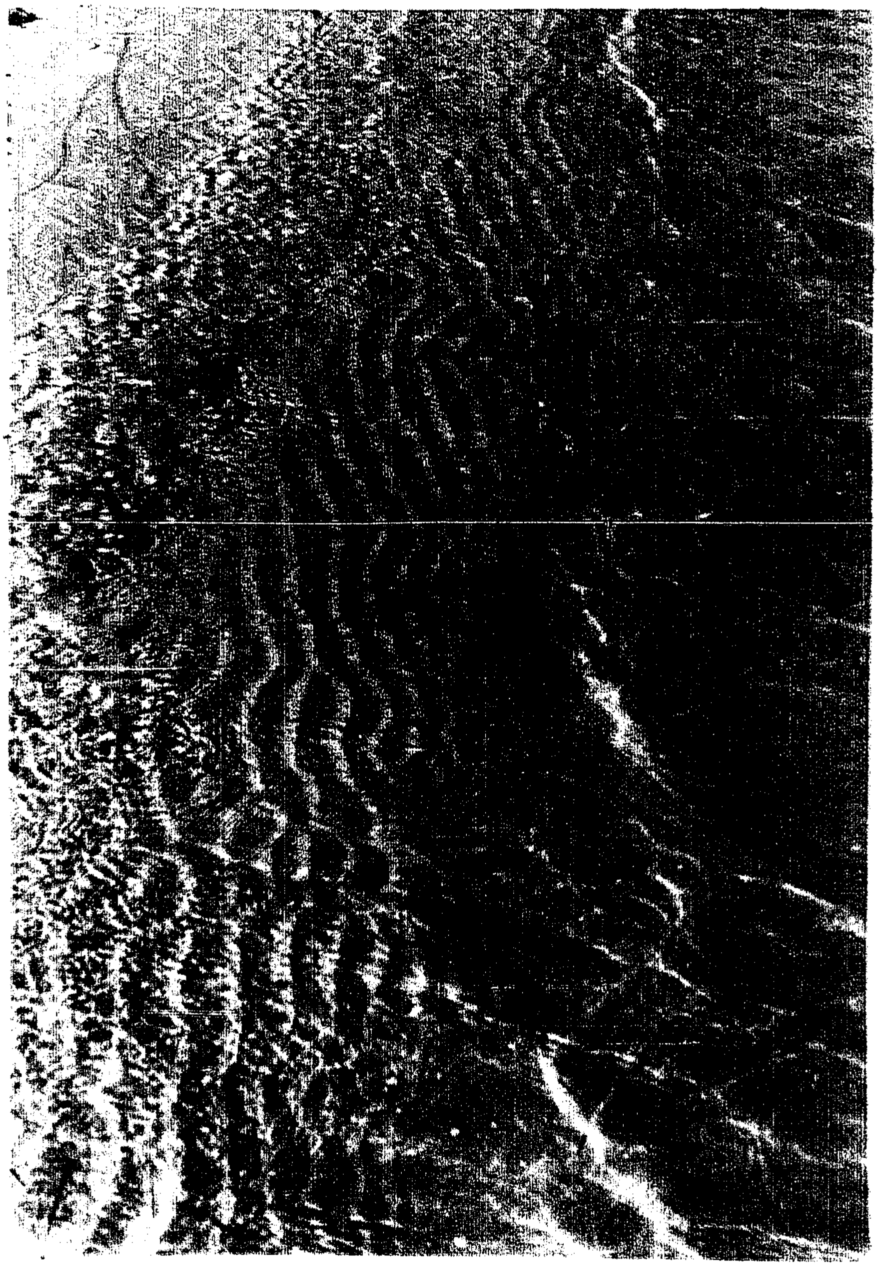

Figure 26: Photograph of the abrupt transition from inner trough ripples to the swash plane bed in the upper left corner.

the aforementioned trend in bedform dimensions. However the straight-crested ripple set is invariably larger in amplitude and wavelength than the lunate-crested set.

Another important relationship is the agreement between ripple crest orientation and wind-wave crest orientation. Except for ladder-backs, the bedforms are oriented nearly parallel to shore in most cases. However submarine topography and wave approach direction exhibit a great deal of influence upon the ripple orientations. On the seaward slope of the innerbar the ripples became increasingly parallel to shore with the decrease in depth in a shoreward direction (Fig. 20, July 8, 1976).

The relationship between ladderback ripple orientations and wave orientation is not clear. The two ripple sets which compose the ladder-backs are almost invariably oriented North-South and East-West. The approaching wave crests are sometimes parallel to the lunate-crested ripple set (Fig. 23, July 12, 1976) but more often they display a bi-secting relationship such that the wave crest orientation bisects the angle between the two ripple sets (Fig. 18, July 3, 1976). The rela-tionship between ladderback ripple orientations and other ripples in the bedform sequence is also noteworthy. The ladderback ripples' catenary-crested ripple set is oriented at 45 degrees to the forms which precede it in the bedform sequence (Fig. 22, July 11, 1976). The lunate megaripples, landward of the ladderbacks are oriented parallel to the catenary ladderback ripples. The catenary-crested ripples are always asymmetric in a shoreward direction regardless of their orientation.

The transition bedforms referred to on several of the profiles are irregular ripples of variable form and orientation. These fields of confused ripples are commonly found on the landward and seaward edges of ladderback ripple fields.

Inner trough bedforms are variable in orientation and do not always conform with wave crest orientation. The ripples in the shallow, shoreward edge of the trough often parallel the wave crest orientation as shown in interval 11 and 12 of the June 26, 1976 profile (Fig. 14). However the other ripples in the trough on this same date exhibit varied orientations. On July 12, 1976 (Fig. 23) the ripple crests in interval 10 and 11 are almost perpendicular to the shoreline. This relationship occurs on a day when the inner trough was constricted by shoreward bar migration. The ripple crests in the inner trough are nearly shore-parallel for the most of the 1976 profile dates.

Ladderbacks and dunes occur in the inner trough on occasion. The dunes are comparable to lunate megaripples in size but exhibit a continuous crestline. Lunate dunes observed on June 21, 1976 (Fig. 12) have smaller ripples oriented at 70 degrees to them. Ladderbacks are more common and occur in various states of development. On June 24, 1976 (Fig. 13) one can see a ripple set in interval 8 with poorly developed trough forms oriented perpendicular to the longshore current. Right next to these bedforms is a well-developed set of ladderbacks in interval 9 with a slightly different orientation. However the catenary-crested ripple subset of the ladderbacks is always asymmetrical in the direction of the longshore current.

The swash zone is characterized by an upper regime flow plane bed. The beginning of this zone can be seen on the topographic profile as an abrupt slope change which will be called the swash ramp (Fig. 16, July 1, 1976). The inner trough ripples end abruptly against the seaward edge of this swash ramp as shown in Figure 26. The width of the plane bed is quite variable. On dates when the plane bed is extensive (Fig. 13, June 24, 1976 and Fig. 23, July 12, 1976) the topography of the swash zone exhibits a pronounced break in slope.

1977

The bedform information for the summer of 1977 is more complete than that of 1976 because of better topographic control. In addition to the abundance of topographic profiles for 1977 there are also several plan view, sketch maps of the bedform distribution alongshore. On July 5, 1977 the bedforms were surveyed at mid-day and then again in the late afternoon to ascertain the change in the course of a day. The uniform wave conditions for this period provided an excellent opportunity to observe bedform behavior under nearly constant conditions.

In general the bedforms mapped during the summer of 1977 had smaller dimensions than those mapped in 1976. Lunate megaripples occurred infrequently but ladderback ripple sets were abundant. The most frequently observed bedforms were asymmetric, sinuous ripples with an average amplitude of 2-3 cm and a wavelength of 10-20 cm.

The first three bedform profiles (Figs. 27, 28, 29) are linked to a nearshore topography dominated by a broad, flat inner trough and a distant, subtle bar. The trough is covered with sinuous to lunate-crested asymmetric ripples whose orientations parallel those of the incoming waves from the southwest. The bar's seaward slope is covered with straight to sinuous-crested, symmetric ripples which pass into ladderback ripples near the bar crest.

Figures 31 and 32 show the two July 5th traverses which demonstrate the evolution of the bedforms between 1:30 PM and 6 PM. In the later traverse only alternate intervals were mapped. The two surveys were made on a topographic profile showing a sand bar at an intermediate distance from shore. The early traverse displays an almost uniform field of asymmetric ripples with wavelengths of 10-20 cm and amplitudes of 2 to 4 cm. Bedforms in the deeper water (intervals 1-4 and 11-12) are oriented parallel to the southerly waves of the previous day, July 4th. All other bedforms in the trough are parallel to shore and bar crest bedforms are parallel to the southwesterly waves which occurred on July 5th.

Under the influence of the southwesterly waves the late traverse on July 5th shows changes in bedform type and orientation. The bedforms at the seaward end of the profile become parallel to shore. Ladderback ripples develop over most of the bar crest and seaward slope. The catenary-crested ripple subset of these ladderbacks is approximately parallel to the orientation of the asymmetric ripples found here earlier in the day. The sinuous, asymmetric ripples in interval 11 maintain their southerly orientation and develop minor trough bedforms whose asymmetry corresponds with the eastward longshore current. The ripples in interval 13 reorient themselves with respect to the southwesterly waves and also developed trough forms. There are no significant changes in overall bedform dimensions during this afternoon except for the appearance of the straight-crested subset of the ladderback ripples whose dimensions are two to three times larger than those of the other ripples.

During the period from June 22 through July 13, 1977 (Figs. 27-36) the ladderback ripple orientations remain relatively constant under the influence of westerly to southwesterly waves. The straight-crested ripple subset is oriented approximately East-West and the catenary-crested set is North-South. On July 15th (Fig. 37) the straight-crested ripples are oriented North-South and the lunate-crested ripples are East-West. On subsequent dates the ripple orientations return to their original values.

Lunate megaripples first appear on the July 15th bedform traverse (Fig. 37). They occur on the bar crest but are asymmetric in the seaward direction as are the ripples in the inner trough and on the bar avalanche face. The velocity data for this date indicate a strong seaward asymmetry all along the profile. Ladderback ripples on the back of the bar are asymmetric in the landward direction as are other ripples in deeper water. The wind waves show a strong southeastern component on this day as the three-day storm was about to begin.

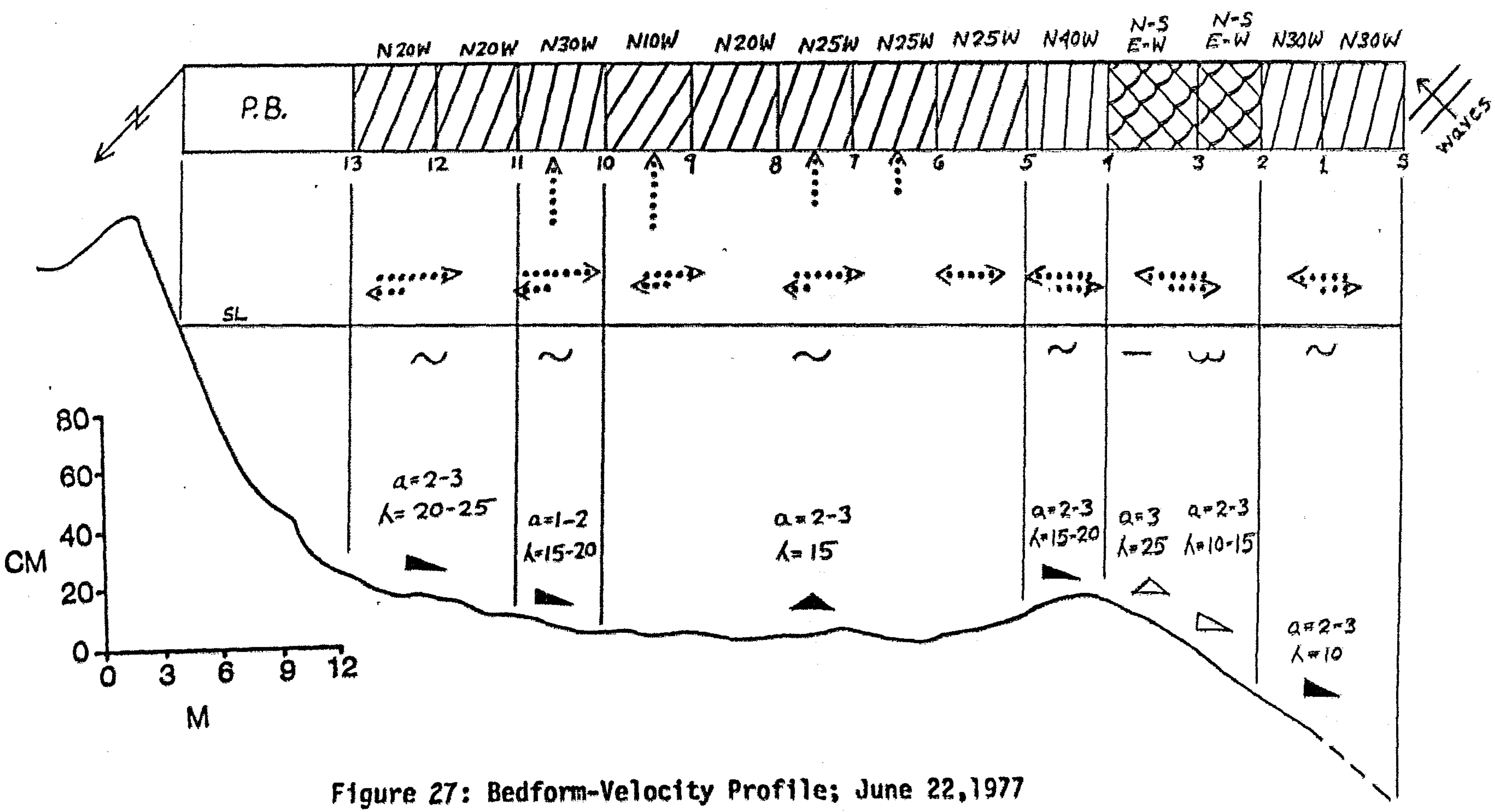

Figure 27: Bedform-Velocity Profile; June 22,1977

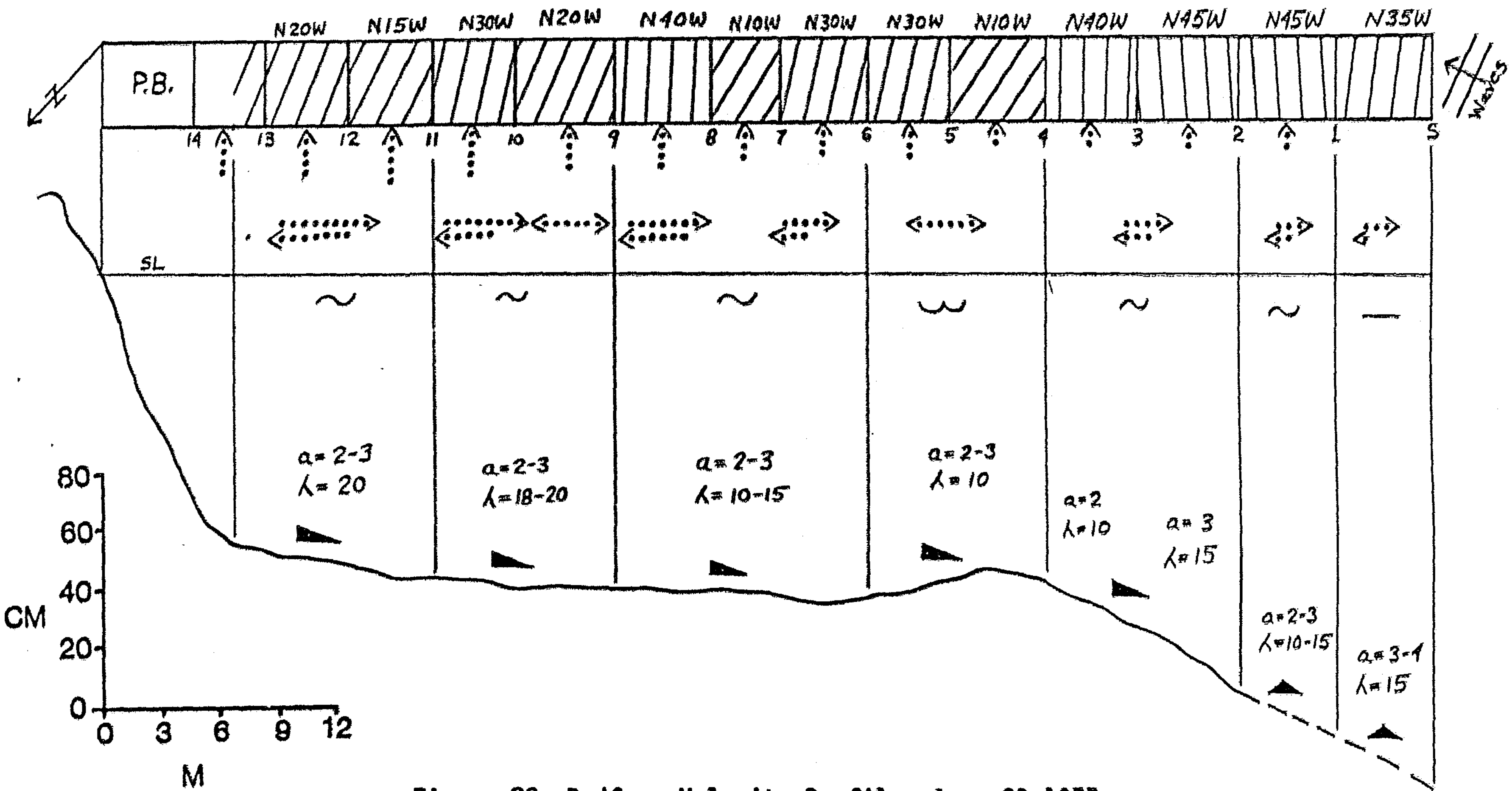

Figure 28: Bedform-Velocity Profile; June 23,1977

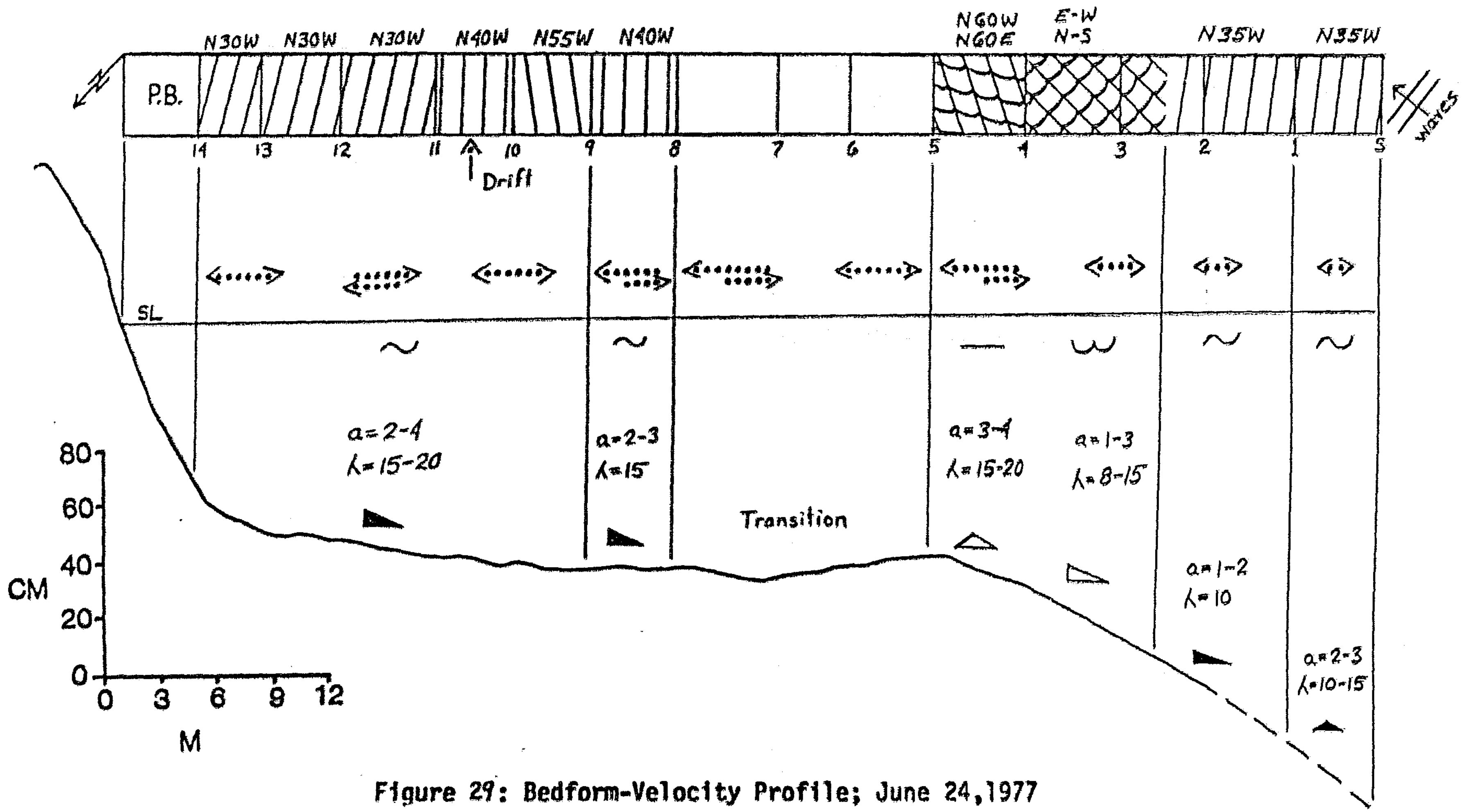

Figure 29: Bedform-Velocity Profile; June 24,1977

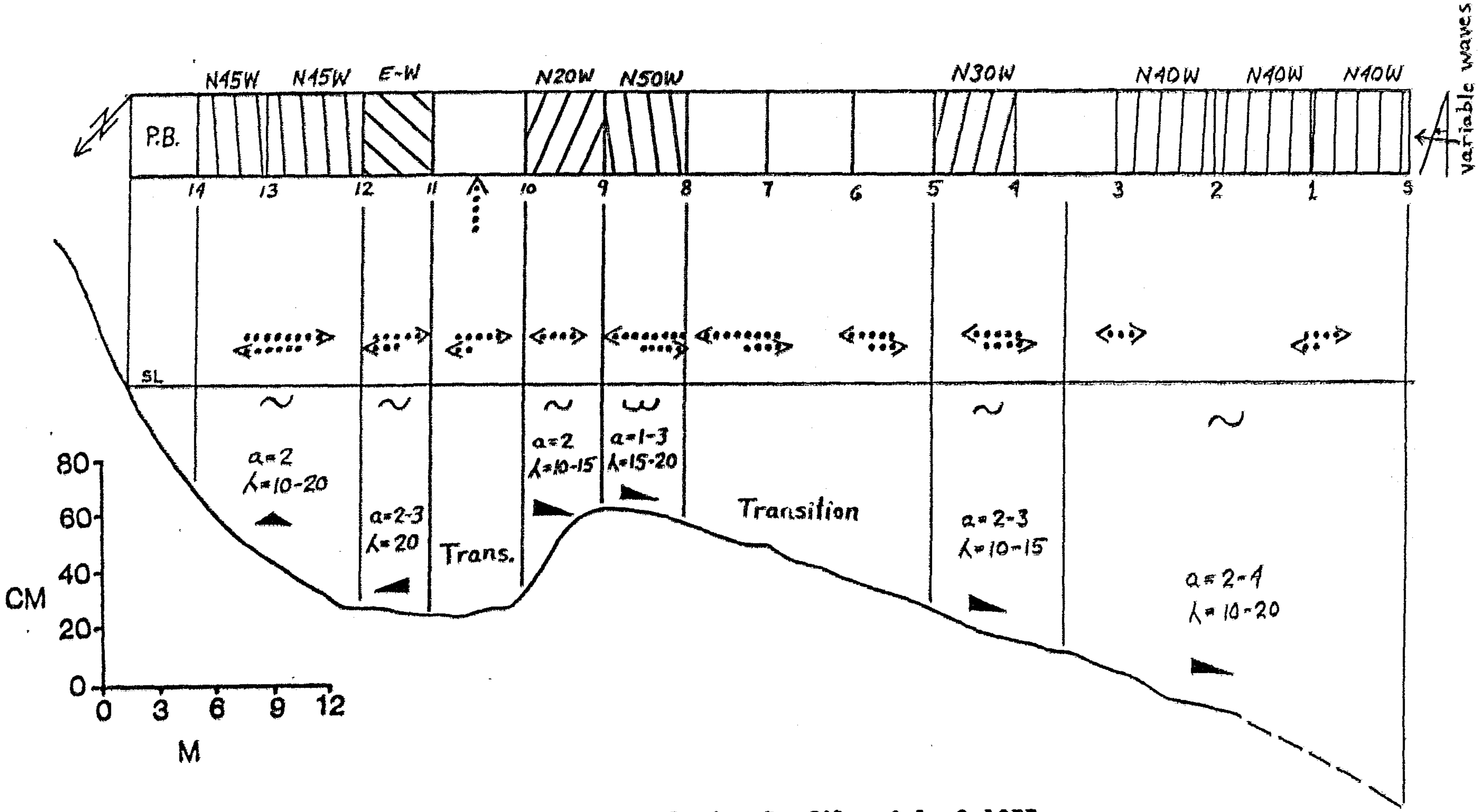

Figure 30: Bedform-Velocity Profile; July 3,1977

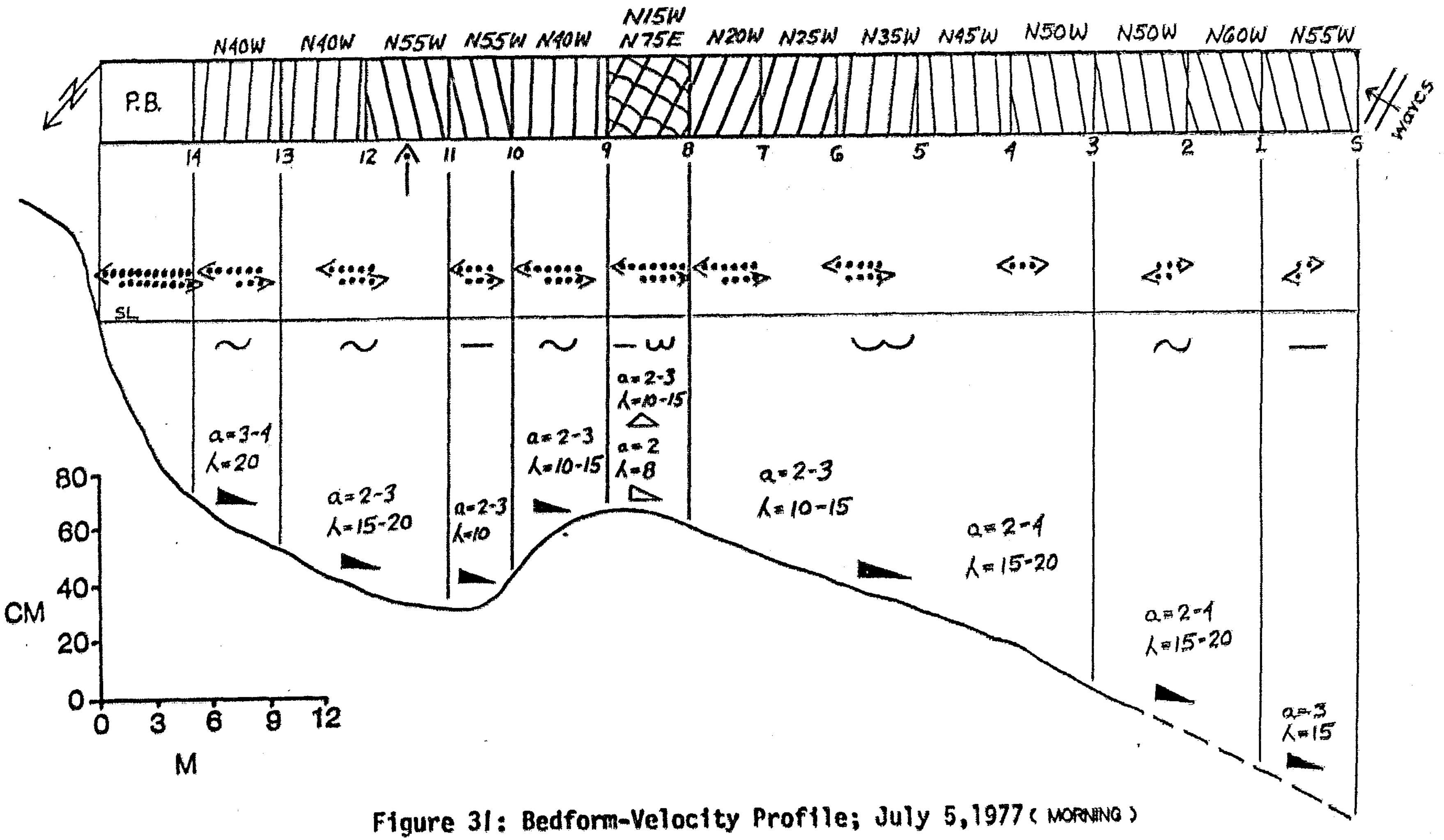

Figure 31: Bedform-Velocity Profile; July 5,1977 (MORNING)

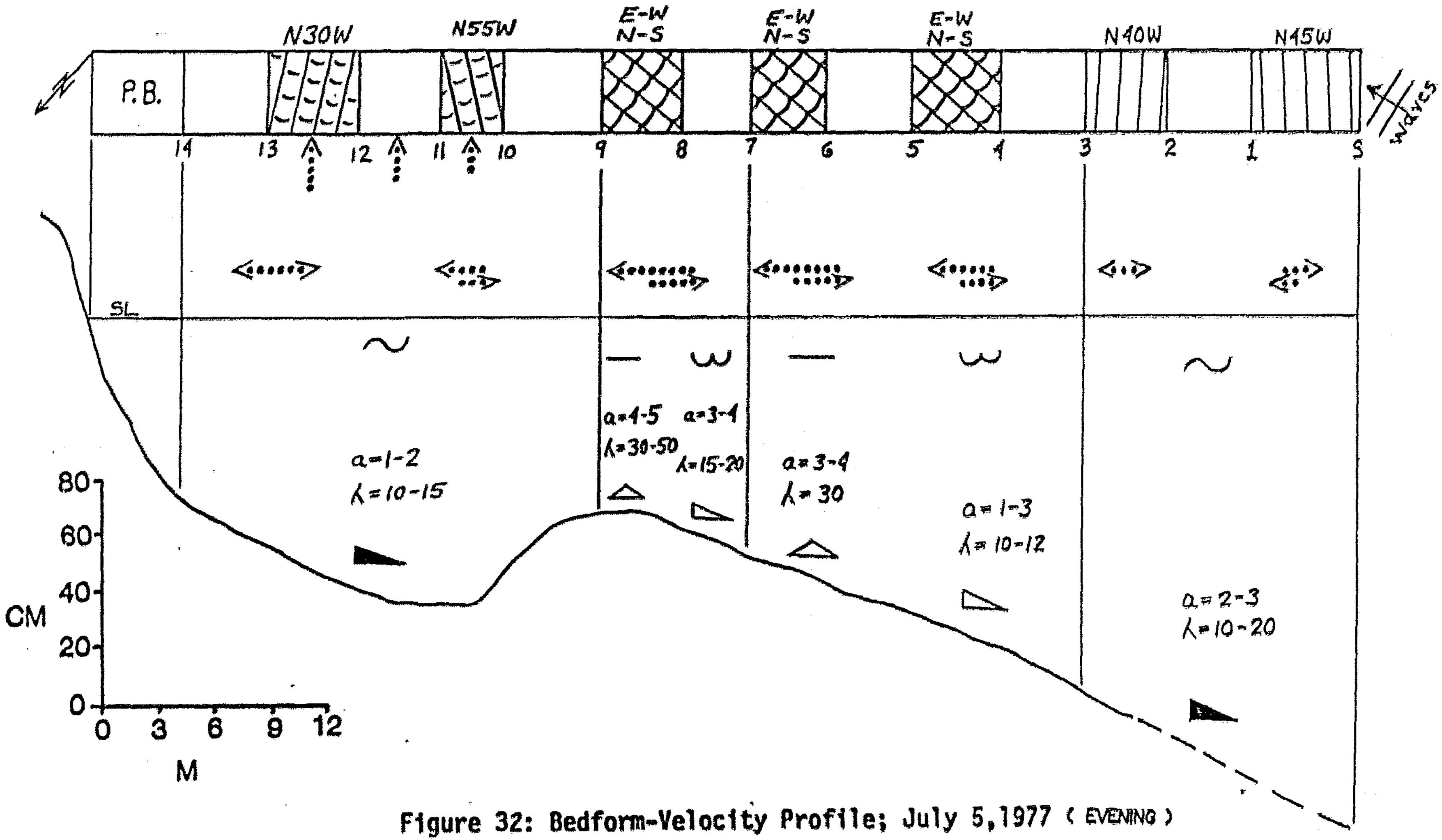

Figure 32: Bedform-Velocity Profile; July 5,1977 (EVENING)

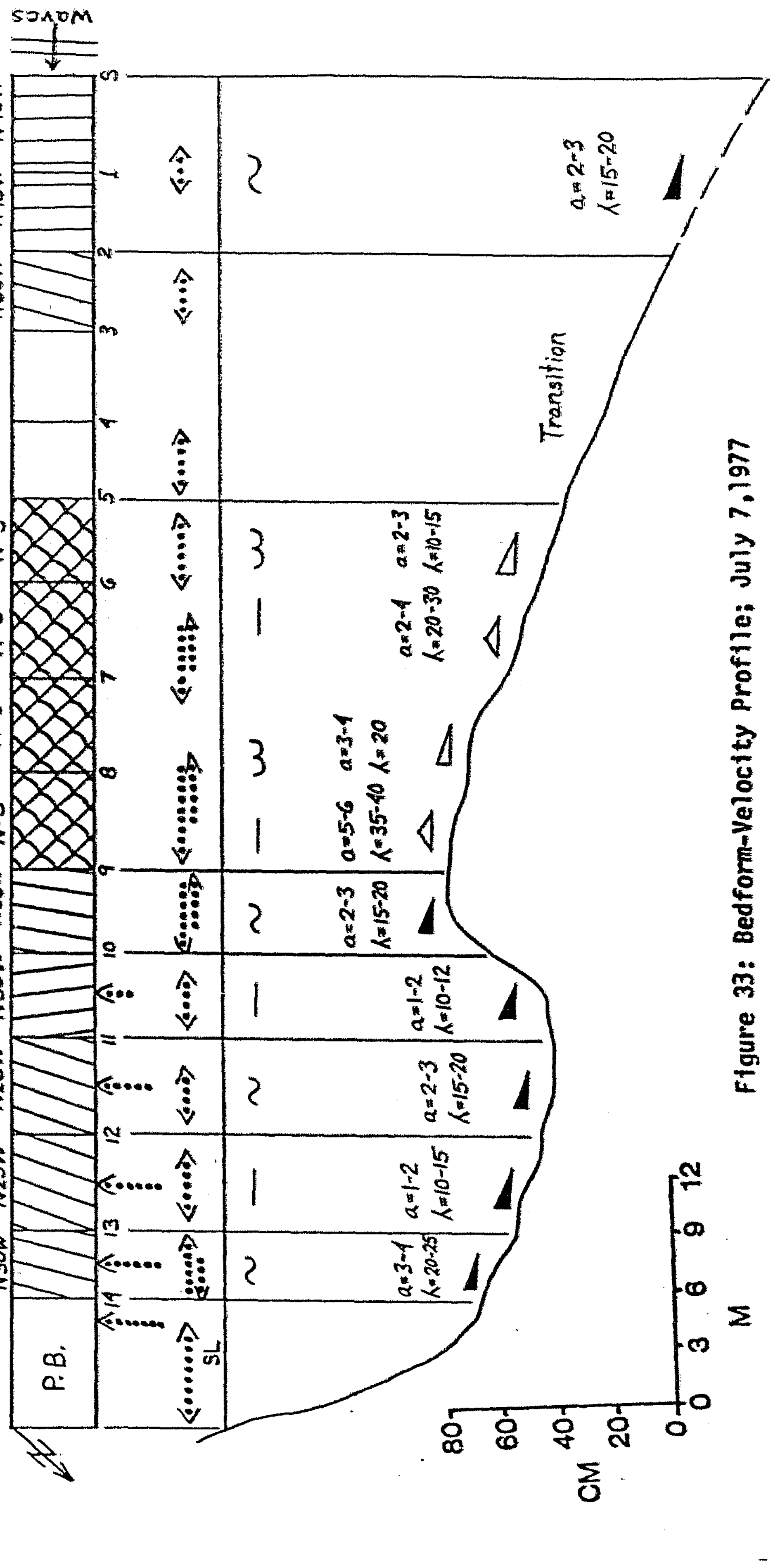

Figure 33: Bedform-Velocity Profile; July 7,1977

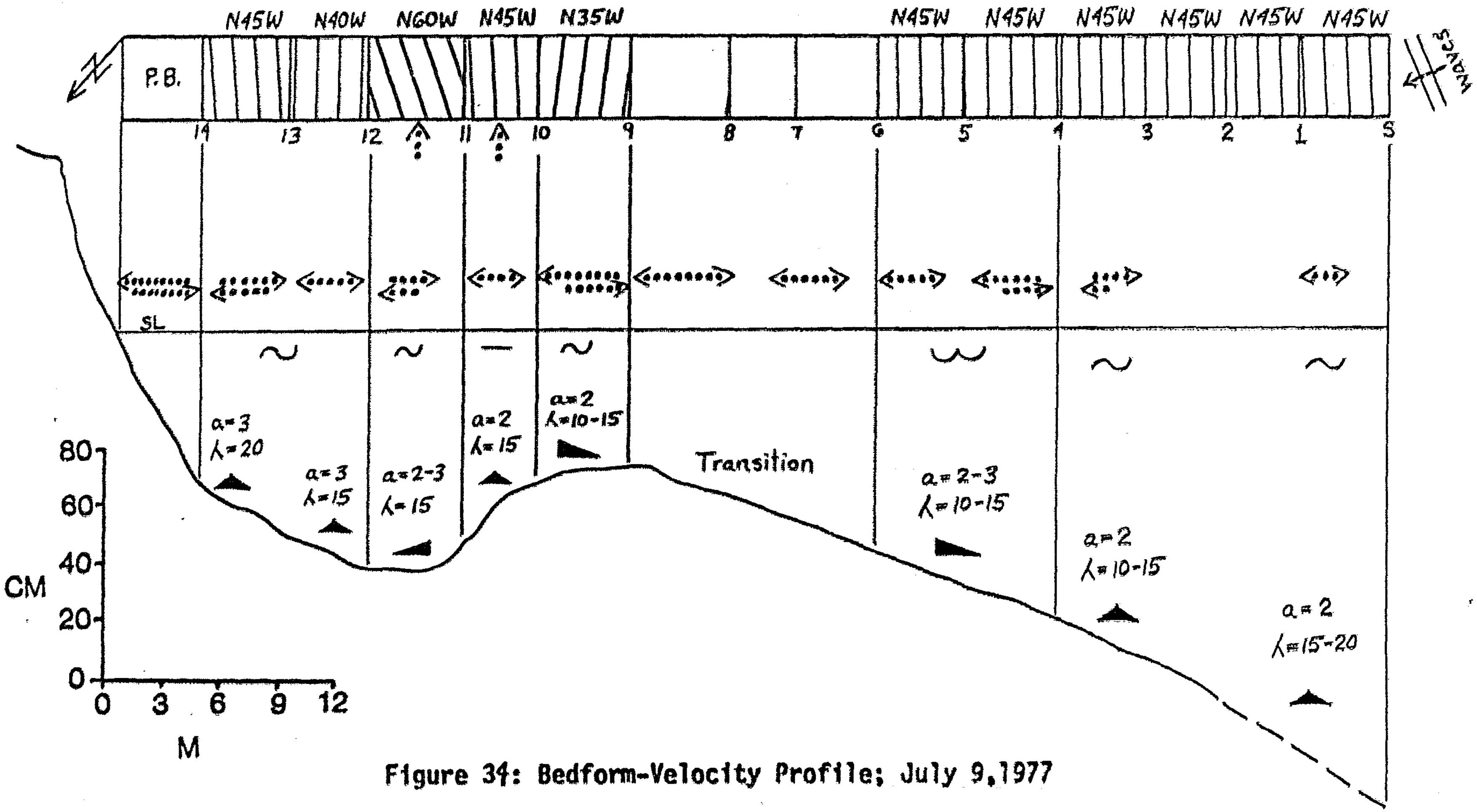

Figure 34: Bedform-Velocity Profile; July 9,1977

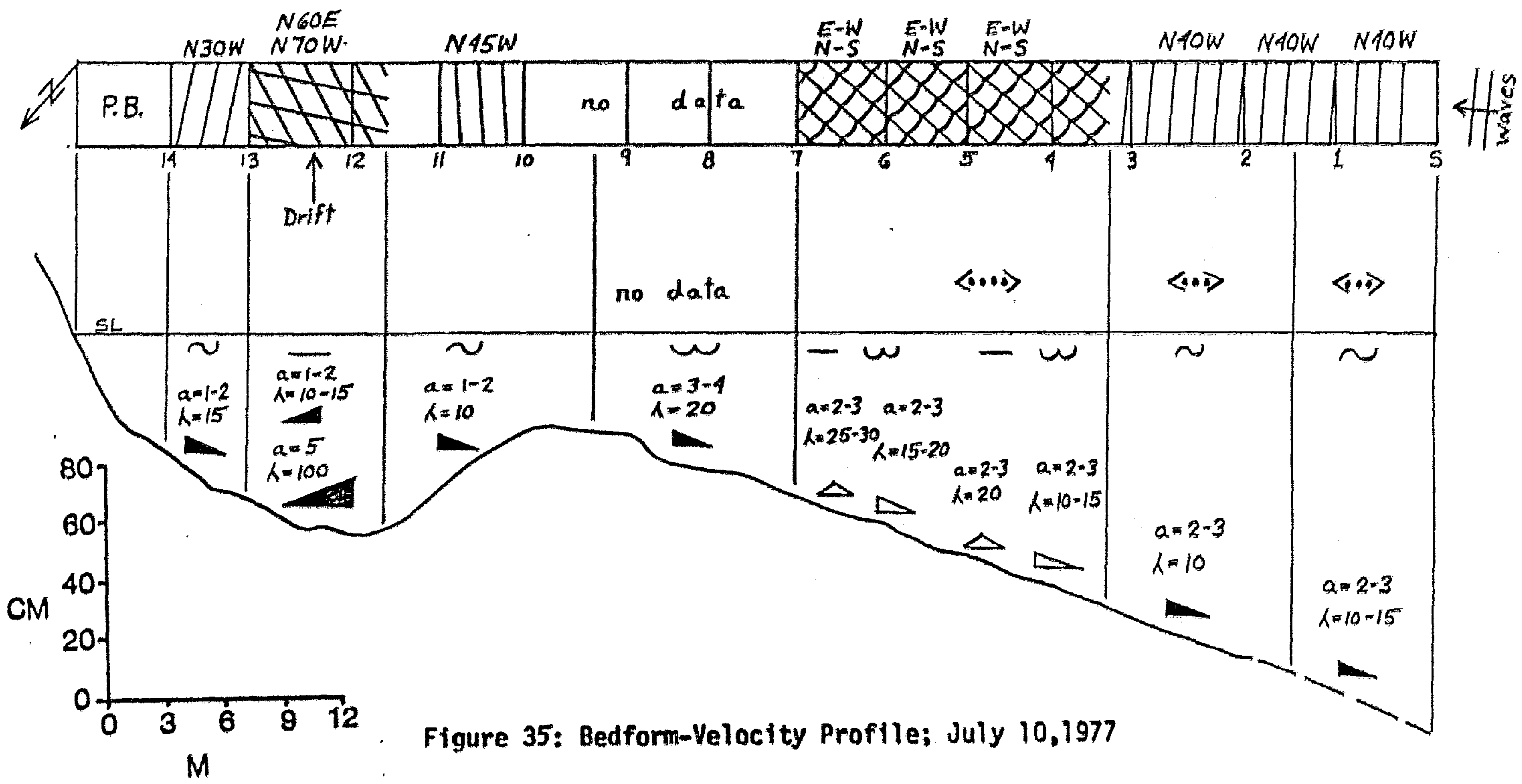

Figure 35: Bedform-Velocity Profile; July 10,1977

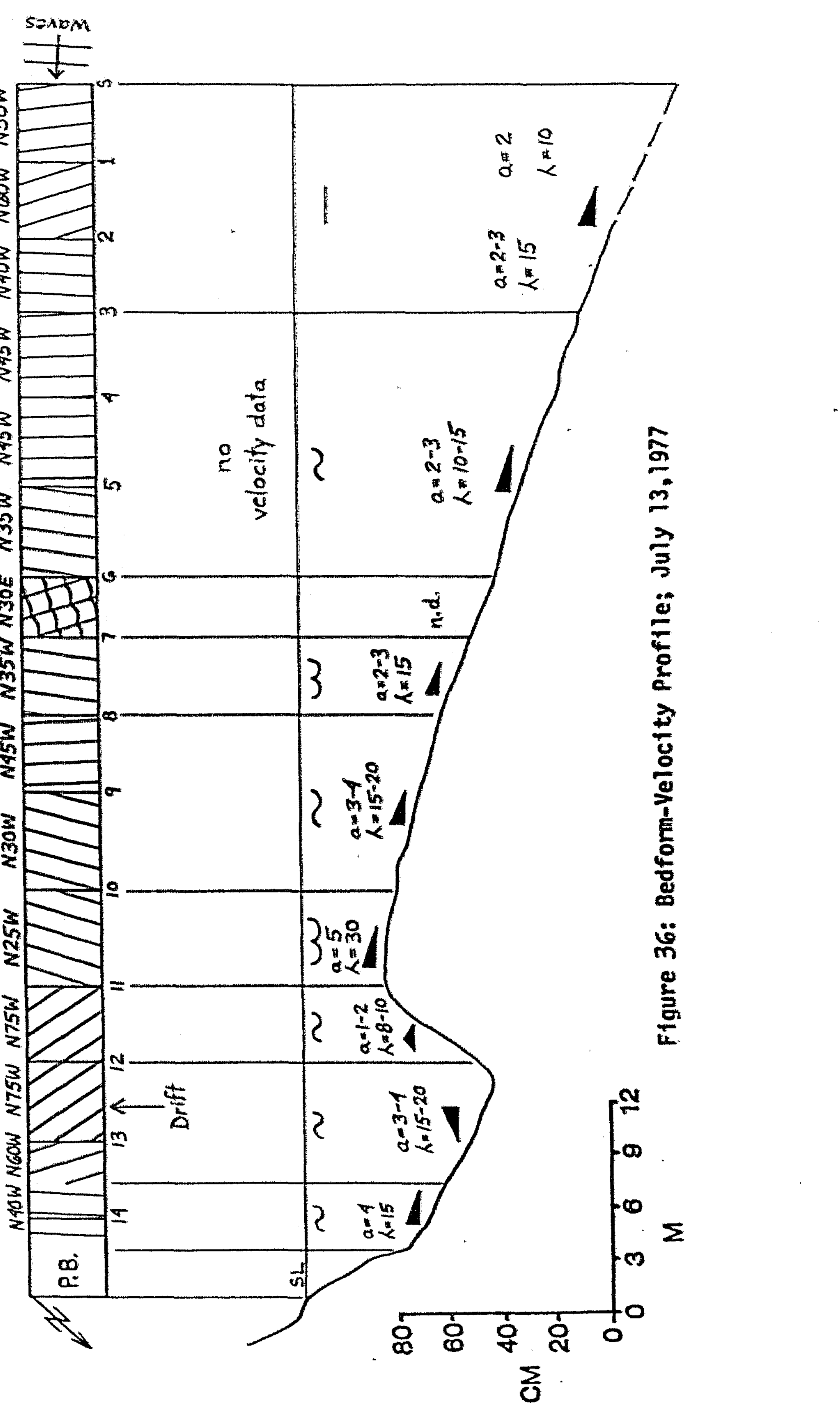

Figure 36: Bedform-Velocity Profile; July 13, 1977

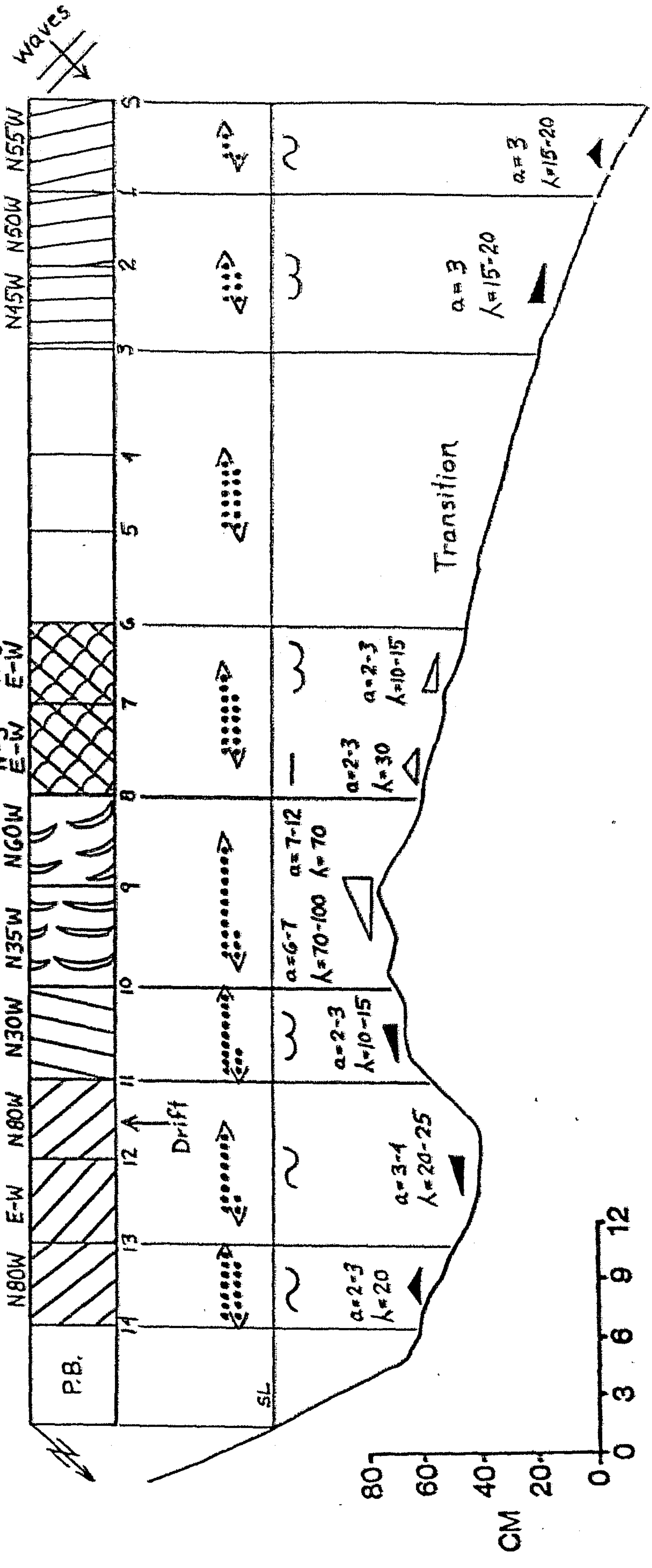

Figure 37: Bedform-Velocity Profile; July 15,1977

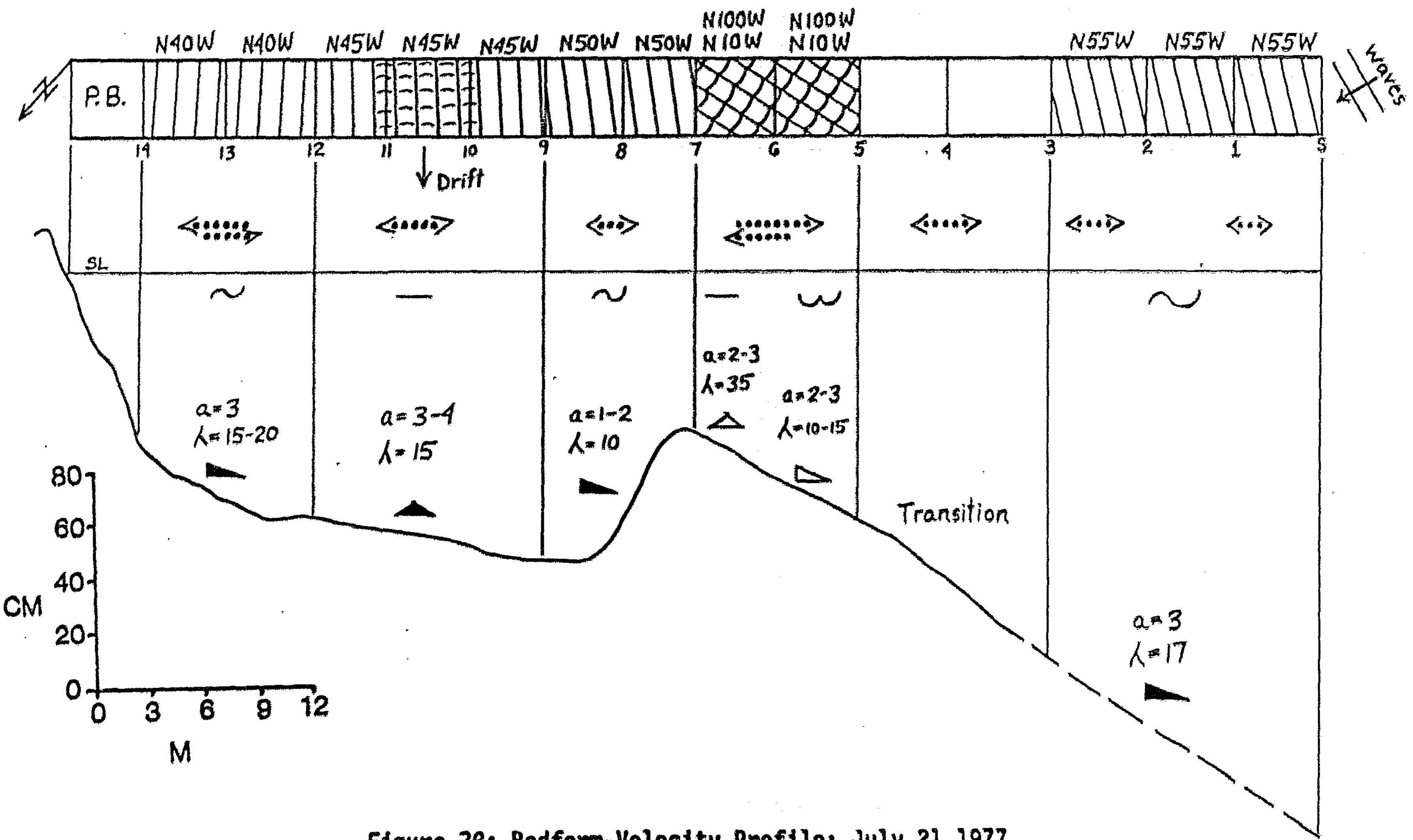

Figure 38: Bedform-Velocity Profile; July 21, 1977

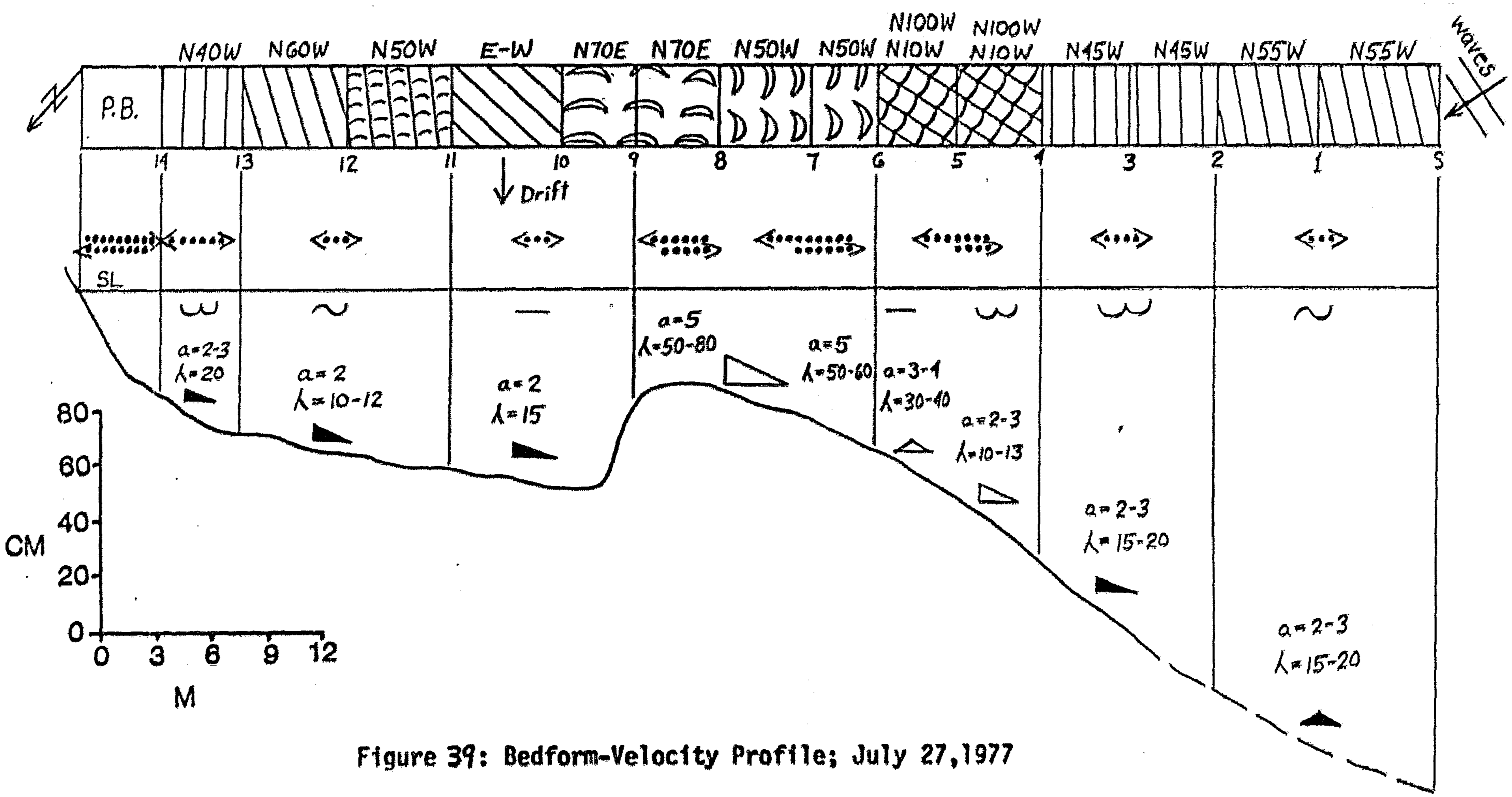

Figure 39: Bedform-Velocity Profile; July 27,1977

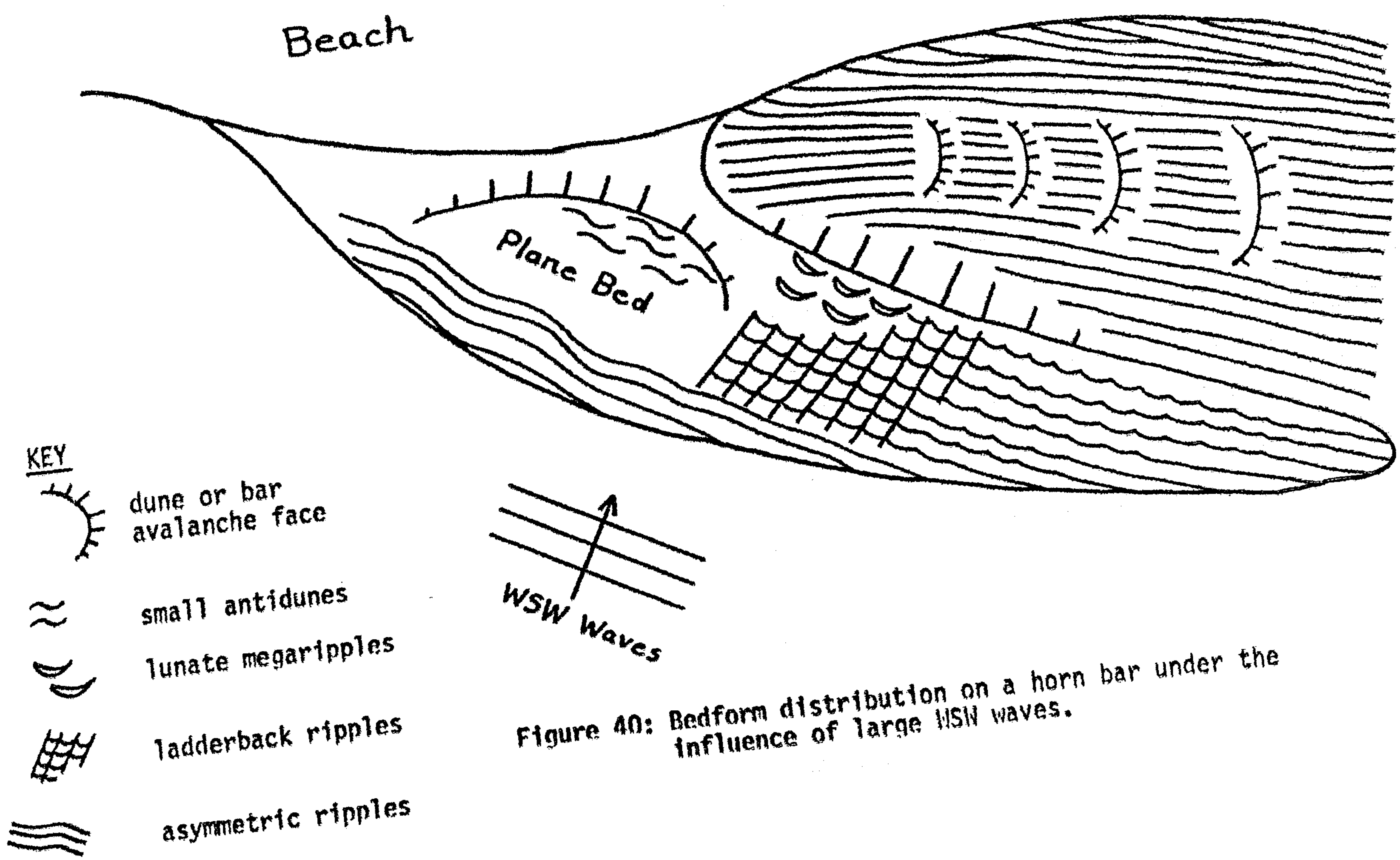

Figure 40: Bedform distribution on a horn bar under the influence of large WSW waves.

Plan View

Bedform Maps

Horn Bar

The horn bar pattern existed from June 29 through July 15, 1977. The bedform profiles for this period will be summarized and integrated with alongshore information on the plan view bedform maps shown in Figures 40 and 43-49. These sketch maps do not always represent specific dates but they do depict observed bedform patterns which were recorded during the existence of the horn bar configuration. Figure 40 portrays the nearshore bedforms on a day when the waves are larger than usual and approaching from the WSW. A small low-profile bar is shown on top of the larger horn bar close to its juncture with the beach. These small bars form in very shallow water ($\leq$30 cm) and migrate onshore. As they approach shore they acquire their own systems of bedforms which mimic those of the larger-scale bar topography. Figure 41a is a photograph of one of these small bars, migrating toward the beach on the left. The white scale in front of the avalanche face is 50 cm. Figure 41b is a close-up of the avalanche face and the small trough between it and the beach. Longshore flow in the trough is from right to left. These bedforms are more linguoid than those found in the large-scale trough. The trough ripples are also superimposed on the bar's active avalanche face as are the bedforms on the large-scale bar. Figure 41c shows a set of ladderback ripples as seen from the bar looking toward the beach. Longshore flow is from left to right and wave approach is from the lower left. These ladderbacks are unique in that the crests of the longshore forms are superimposed on the crests of the oscillation forms instead

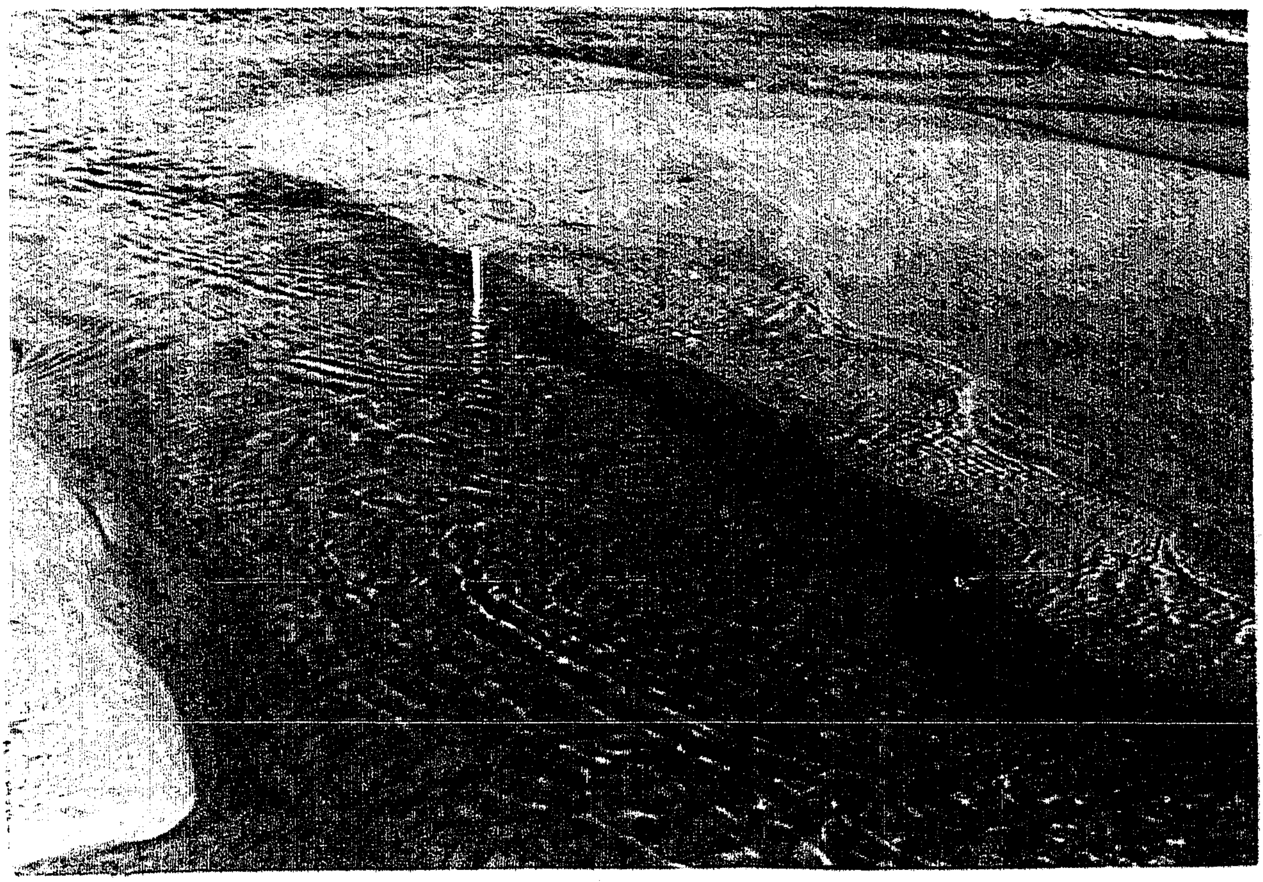

Figure 41A: Photograph of swash bar migrating onshore. Scale is 50 cm.

Figure 41B: Close-up of swash bar avalanche face showing current ripples perpendicular to the bar crest line. Scale is 50 cm.

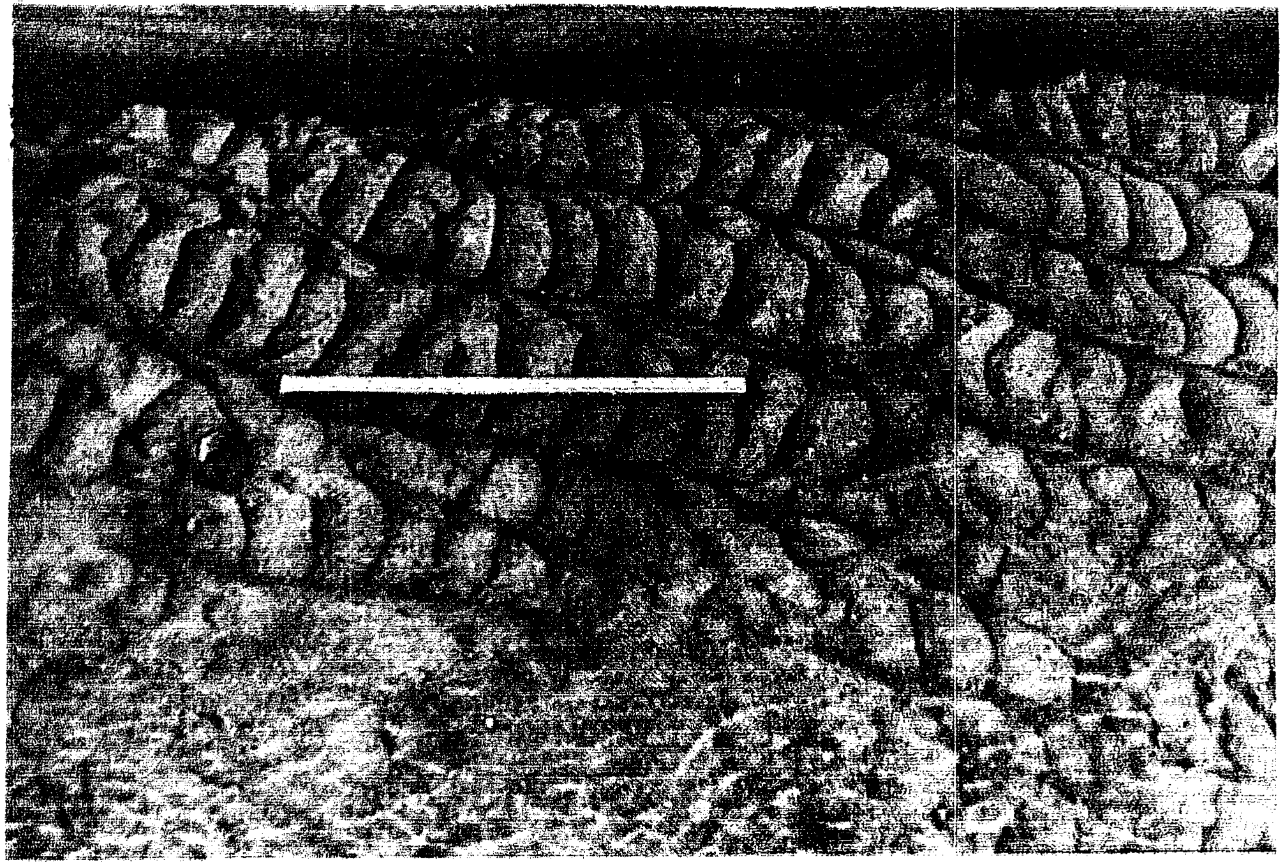

Figure 41C: Shoreward view of ladderback ripples in the trough between the swash bar and the beach. Scale is 50 cm.

of forming in the troughs. Again, the scale is 50 cm.

Bedforms on top of the small-scale bar include catenary-crested ripples, plane bed, and small antidune-like bedforms. Figure 42a shows the catenary-crested ripples in 10 cm-deep water with a 70 cm scale. Wave approach is from the upper right. Figure 42b is a photograph of the small-scale bar crest taken towards shore. The plane bed is on the left, the antiforms are central, and the bar avalanche face is on the right. Wave approach is from the left and the wavelength of the antiforms is about 10 to 15 cm.

Returning to Figure 40 it should be noted that the distribution of lunate megaripples and ladderbacks is confined to that part of the horn bar which has a steep avalanche face. Ladderbacks are found on the seaward slope behind the lunate megaripples and also aside of them along the bar crest. In both cases the ladderbacks pass into catenary-crested, asymmetric ripples in deeper water.

The trough bedforms in Figure 40 appear to conform to the overall shape of the trough and the direction of longshore drift. Wave influence upon ripple orientation is most obvious at the shoreward edge of the trough. Low-amplitude dunes or bars are found migrating down the trough, perpendicular to the longshore flow.

Figure 43 shows the inner trough bedforms in a different configuration. The waves are from the West-Southwest but the bedforms are not aligned with this direction. The trough is constricted by shoreward bar migration and a strong longshore current has produced ripples and dunes which are perpendicular to shore. Ripples in the shallow,

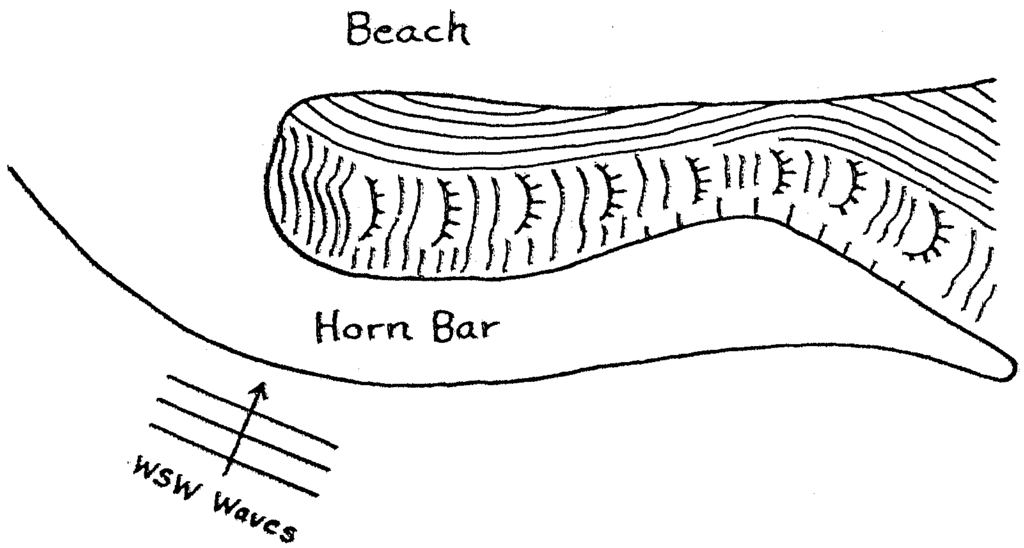

Figure 43: Inner trough bedforms dominated by longshore drift. Trough is constricted by onshore migration of the horn bar.

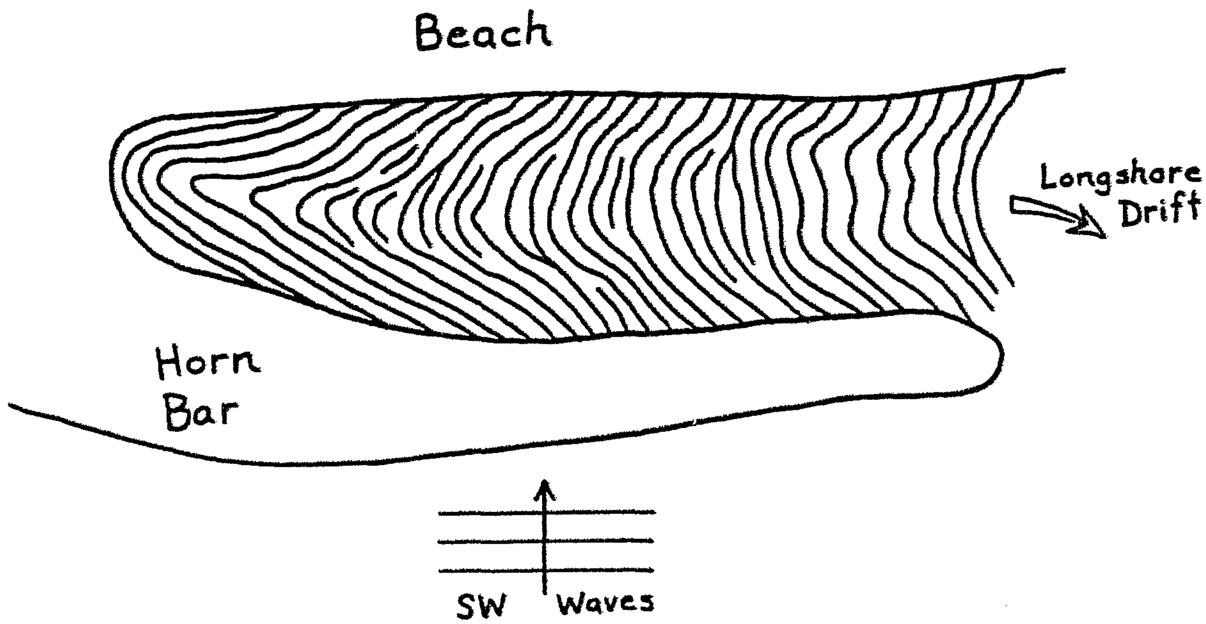

Figure 44: Inner trough bedforms produced by small waves and weak longshore flow guided by the horn bar topography.

shoreward edge of the trough seem to reflect the crestline of the horn bar.

Figure 44 shows the inner trough bedforms on a day when the wave height is small but a longshore drift is still operating. The crestlines of the ripples are roughly parallel to depth contours. Again the alignment of ripple crests with wave crest orientation is not pronounced.

Figure 45 portrays the bedforms on a day in mid-July when the horn bar has migrated in towards shore resulting in a long, narrow inner trough. The waves are small, from the South-Southeast and the longshore current is very strong. Lunate-crested, asymmetric-landward ripples cover most of the bar crest. They increase in wavelength towards the seaward end of the horn bar. Near the end of the horn where the avalanche face has a gentle slope, there are lunate megaripples which are asymmetric seaward. The lunate-crested ripples in the inner trough, landward of these megaripples, are also migrating seaward. Ladderback ripples on the seaward slope of the bar are asymmetric landward. Bedforms in the deeper portions of the inner trough are asymmetric in the direction of the longshore current. In the shallow, shoreward edge of the trough bedform asymmetry is landward. A field of interference ripples or ladderbacks exists in the shallow, closed end of the trough in the lower part of the diagram. The longshore current is very strong along the whole length of the trough but seems to be even stronger where it flows seaward across the bar as a rip current.

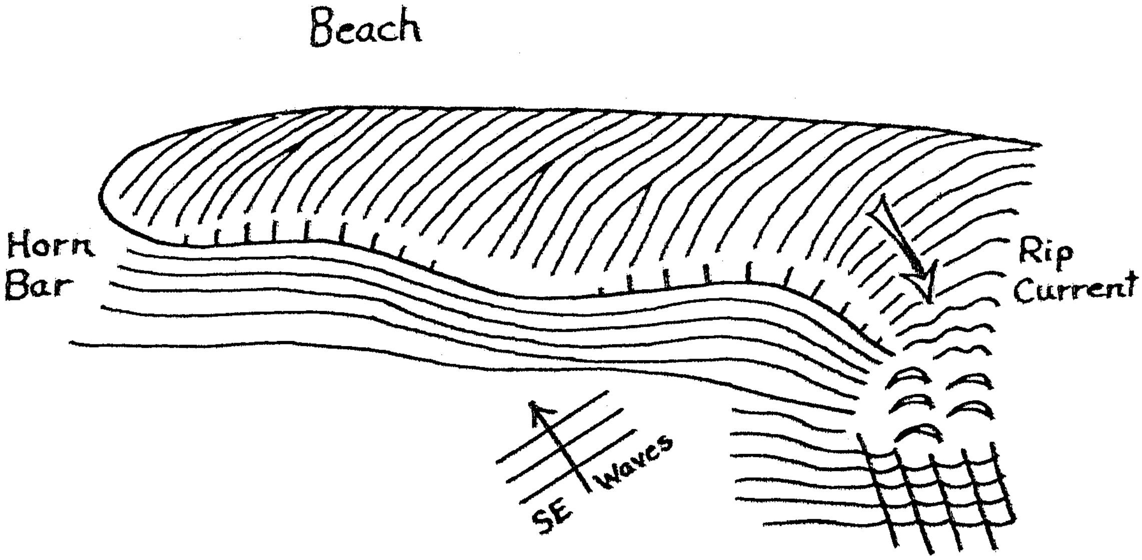

Figure 45: Nearshore bedforms occurring when the inner trough is constricted by shoreward bar migration. Rip current flow opposes SE wave approach.

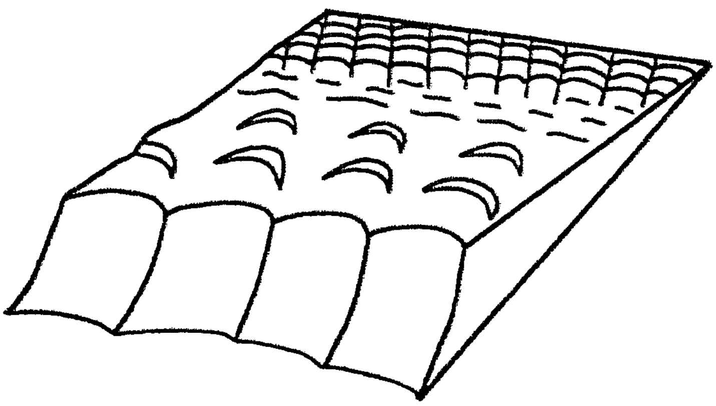

Figure 46: Schematic diagram of the scalloped avalanche face of the inner bar and its relationship to the bar crest bedforms.

Figure 46 is a schematic diagram showing the bar crest and avalanche face on a day when the bar front is actively migrating shoreward. The main feature here is the scalloped upper edge of the bar's avalanche face. The scallops were observed frequently and were usually aligned with lunate megaripples on the bar crest.

Shore-Parallel Bar

Bedform Profiles

Two bedform profiles were mapped subsequent to the three-day storm which created a shore-parallel bar. The bedforms are shown in Figures 38 and 39. Southerly wave approach on July 21 (Fig. 38) is reflected in the orientation of the ripples on the seaward slope of the inner bar. Ladderback ripples on the bar crest have straight-crested subsets which are essentially parallel to the wave crests. The orientation of the inner trough ripples exhibits some wave influence. Small, trough bedforms are migrating toward the west with the longshore drift. In general the ripple orientations become gradually more parallel to shore in the onshore direction. The bedforms mapped on July 27th (Fig. 39) display the same relationships and in addition there are lunate megaripples on the bar crest. The ripples at the base of avalanche face and the megaripples on the bar crest are oriented almost perpendicular to shore. The longshore current is flowing westward on both dates.

Plan View Maps

Three plan view sketch maps were made of bedforms associated with the shore-parallel longshore bar. Figure 47 shows the arrangement of bedforms on the linear bar a few days after it was formed by storm waves. The waves are still arriving from the South-Southeast and the longshore current flows westerly. Lunate megaripples and ladderback ripples occur all along the length of the bar. The bar avalanche face maintains a slope of 20 to 30 degrees along the 100 meter stretch which was surveyed. Inner trough ripple orientations appear to be influenced by the wave crest orientation.

With time the shore-parallel bar develops minor cusps as portions of the bar migrate shoreward. Breaking waves occur only at these cusps instead of all along the bar. Therefore the larger bedforms are confined to the cusps and are no longer continuous in their distribution alongshore. This situation is portrayed in Figure 48. The inner trough is fairly broad and ripples are eigher parallel to shore or to the incoming waves. The same cuspate bar is shown in Figure 49 on a morning when the waves are small ($\leq$30 cm). The waves are arriving parallel to shore and most of them do not break until they reach the swash zone. A weak circulation cell current exists here. The only bedforms present are sinuous to catenary-crested, asymmetric ripples. The crests become more lunate and discontinuous on the crest of the bar cusp. The largest ripples are located on the bar crest and on the seaward edge of the swash zone. Ripple orientations appear to be related to the bar topography in that they are symmetrical with respect to the bar form.

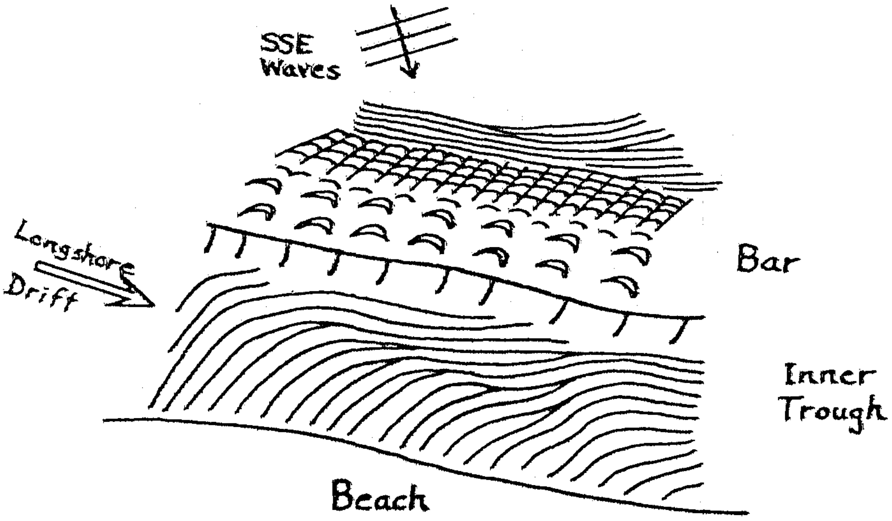

Figure 47: Bedform distribution on a shore-parallel inner bar under the influence of SSE waves.

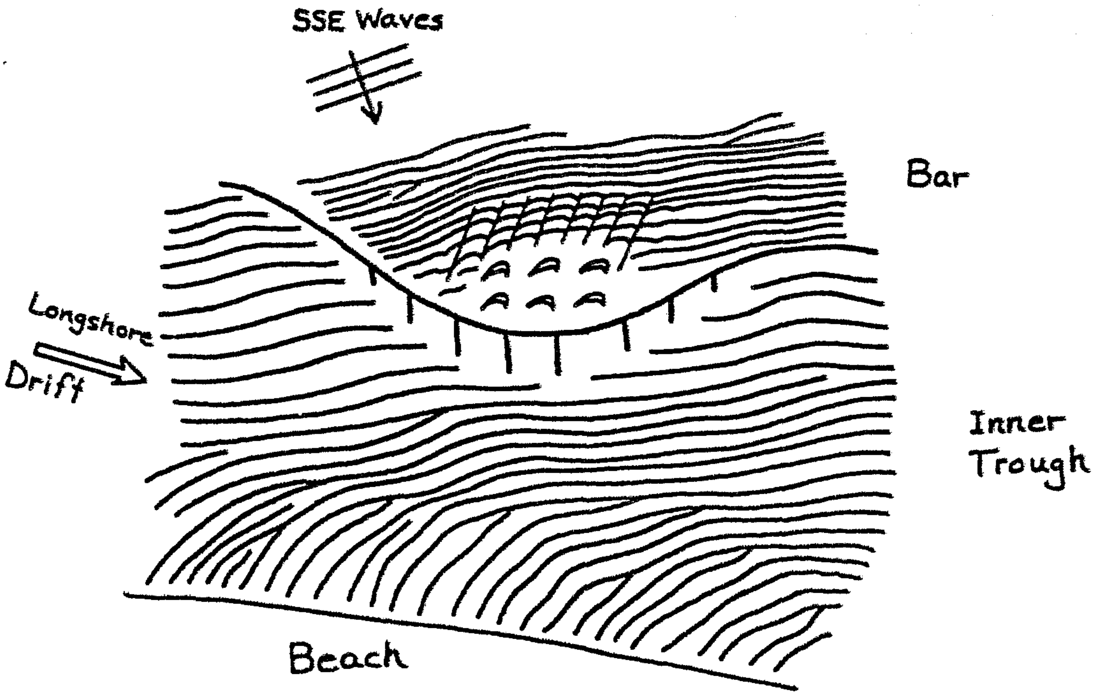

Figure 48: Bedform pattern on a cuspate portion of the shore-parallel bar. Breakers and high regime bedforms are confined to the cusp.

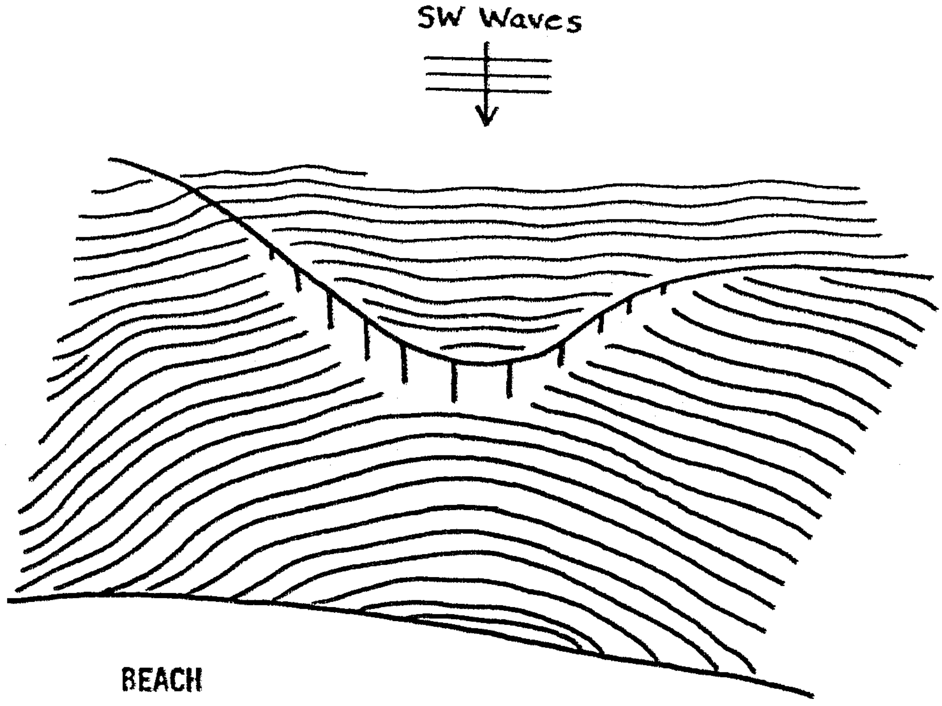

Figure 49: Bedform pattern on a shore-parallel, cuspate bar during small waves whose crests are shore-parallel. Longshore current is weak and disorganized.

Outer Bar and Trough Bedforms

Bedforms in these two environments were examined infrequently because of logistical difficulties and because of the minimal amount of physical reworking at these water depths. Changes in the depth over the outer bar crest was observed over the three year period of the study. It varied from 2 meters in August, 1975 to 3.3 meters in 1976 to 2.5 meters in 1977. The surface features of the outer bar were observed two or three times in the course of each field season. Each time there were sinuous-crested asymmetric ripples present with numerous burrow structures in the ripple troughs. The ripples were oriented parallel to the bar and to the shoreline at about N45°W. Ripple amplitudes varied from 1 to 4 cm and wavelengths varied from 10 to 17 cm. Bottom velocities were never more than 30 cm/sec.

The outer bar's avalanche face was a smooth, gentle slope deepening gradually into the outer trough. The outer trough was 4 to 5 meters deep over most of its width (Fig. 2). The bottom of the outer trough was dominated by conical burrow mounds, 3 to 4 cm in height. Ripples were usually inactive and poorly formed. On July 27, 1976 there were some continuous, straight to sinuous-crested, symmetric ripples in the outer trough. Their amplitude was 3 cm, the wavelength was 20 cm and their orientation was N50°W. The sediment was colored black with reduced material and fecal pellets were locally abundant in the depressions.

Box Core Peels

Box cores were obtained with their long axis perpendicular to the shoreline in the various sub-environments along the topographic profiles. A total of 29 core peels were made and they will be described and summarized in this section. The core locations are shown in Figure 50.

Swash

Two cores were collected from the swash zone at Panama City Beach. Core 2A (Fig. 51) has four distinct layers of alternating coarser and finer material. The top layer is 9 cm thick and contains medium sand, abundant shell fragments, and low-angle, seaward-inclined laminae. The second layer from the top is 7 cm-thick and is composed of fine sand devoid of shell fragments with no apparent internal structure. The bottom two layers are 5 and 6 cm-thick respectively and they repeat the sequence described above. The other core peel from the swash, core 7B, contains a 6 cm layer of landward-inclined, ripple cross-bedding at the top and gently-dipping, seaward-inclined laminae throughout the rest of the peel. Core 7B also has abundant shell fragments and medium sand.

Inner Trough

Seven cores were collected from the inner trough environment. Core 13A (Fig. 52) was taken at the shoreward edge of the trough, near the swash. It displays an abundance of physical sedimentary structures and a possible organic structure. The ripple cross-bedding in the upper half of the peel is primarily seaward-inclined. Most of the peel is

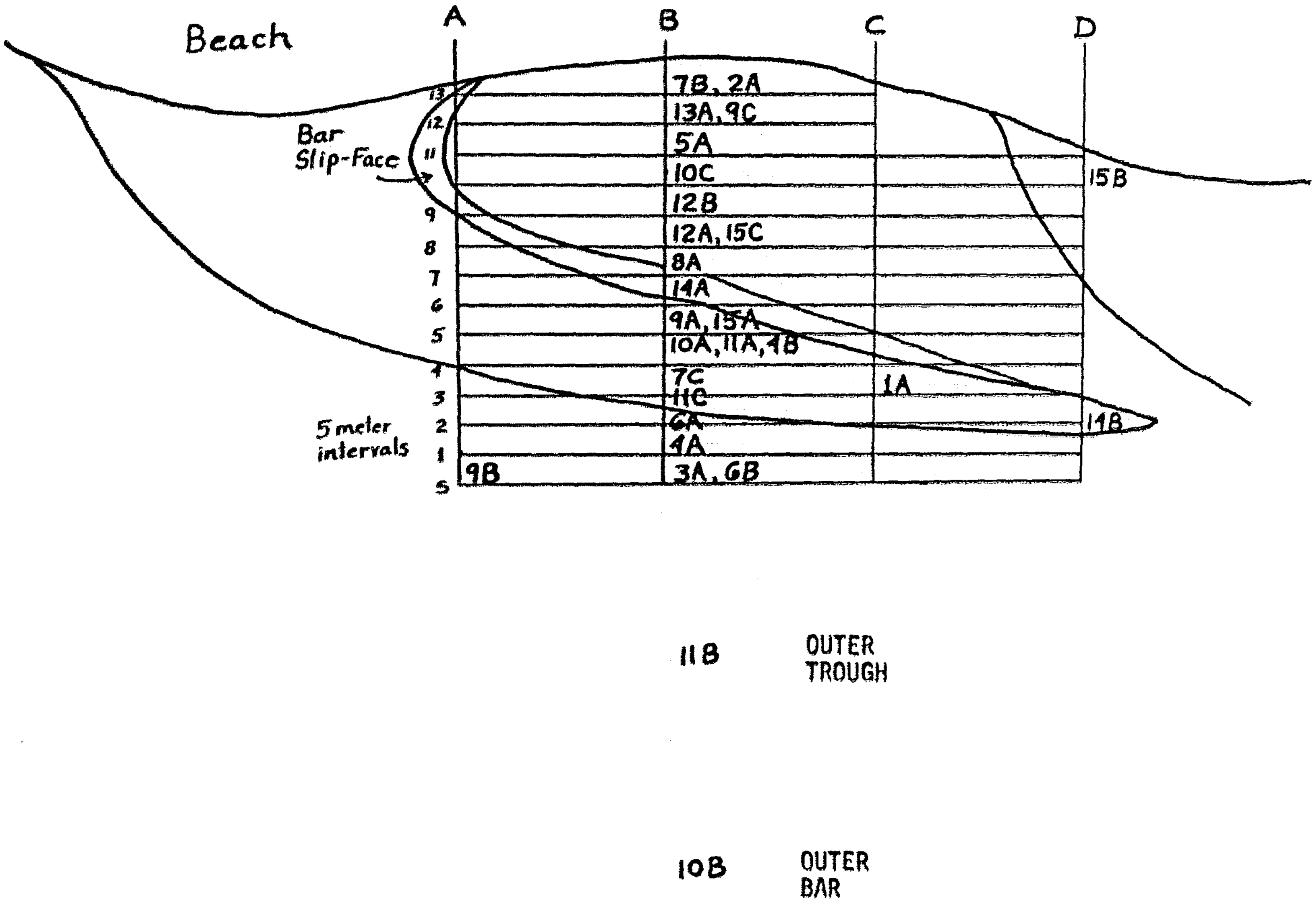

Figure 50: Box core location map. A,B,C, and D are the profile localities.

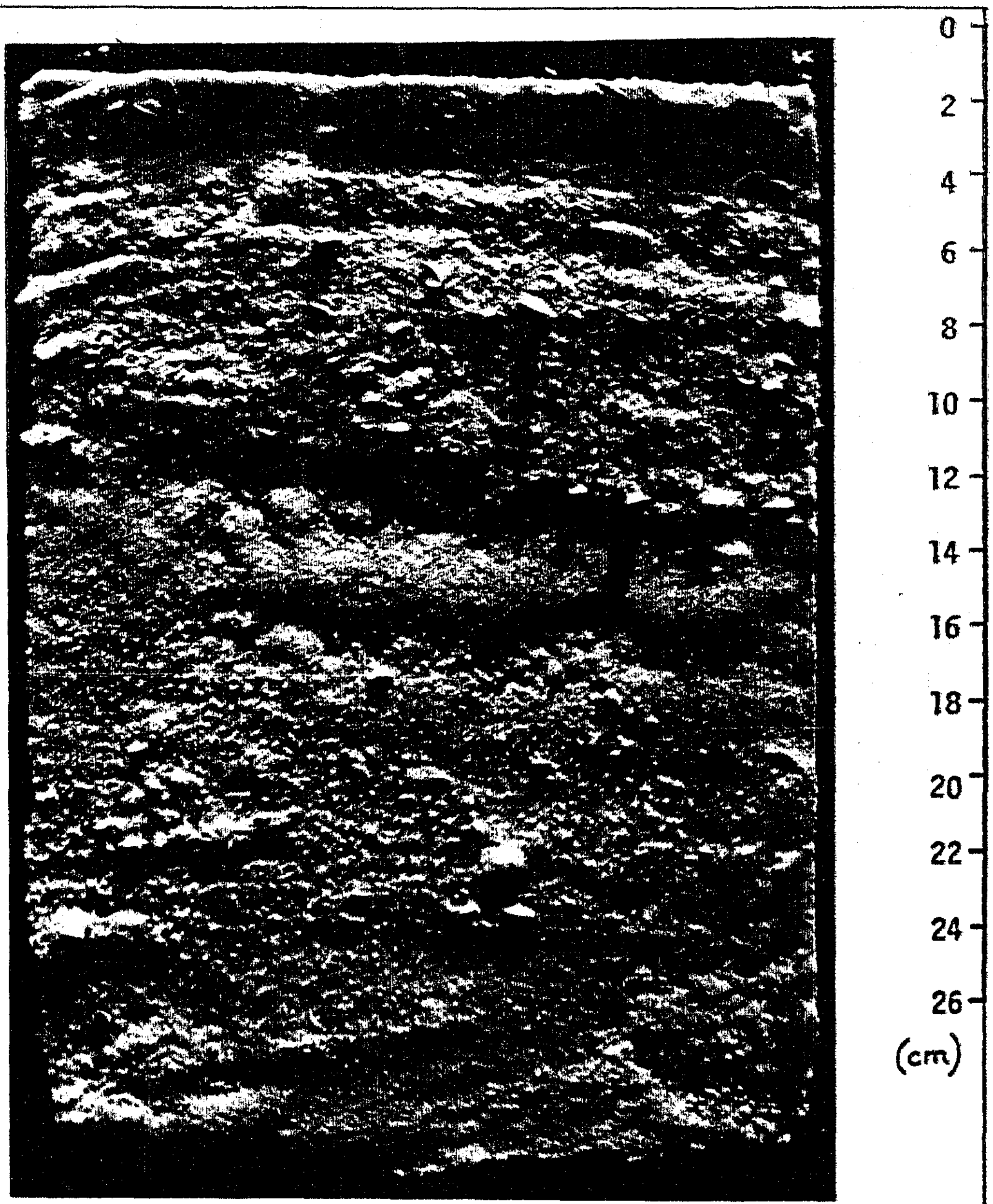

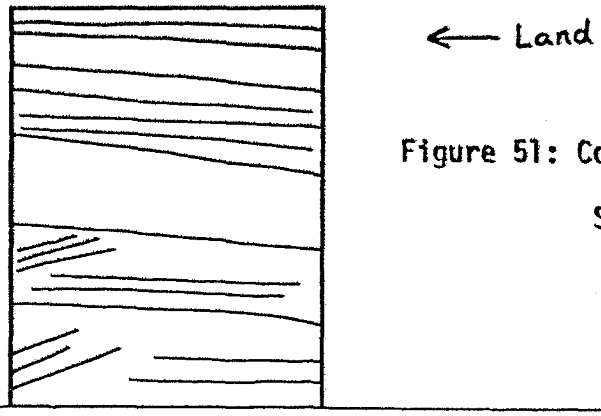

Figure 51: Core peel 2A;

Swash

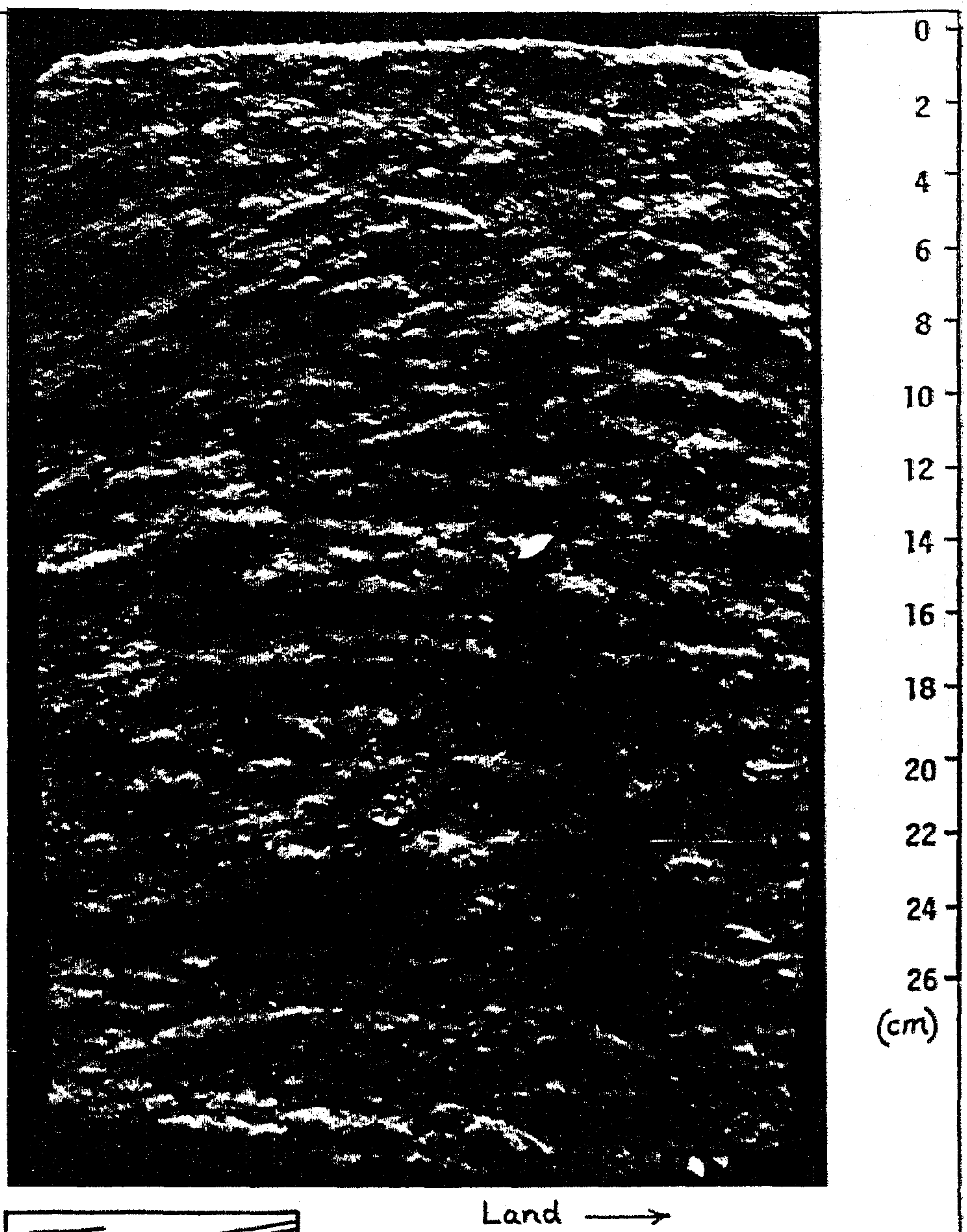

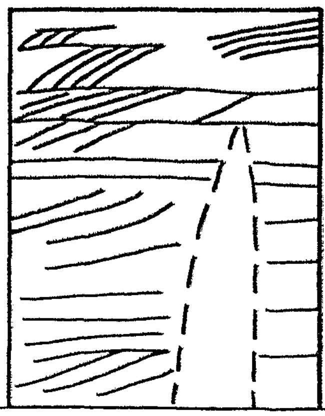

Figure 52: Core peel 13A;
Inner trough near
the swash.

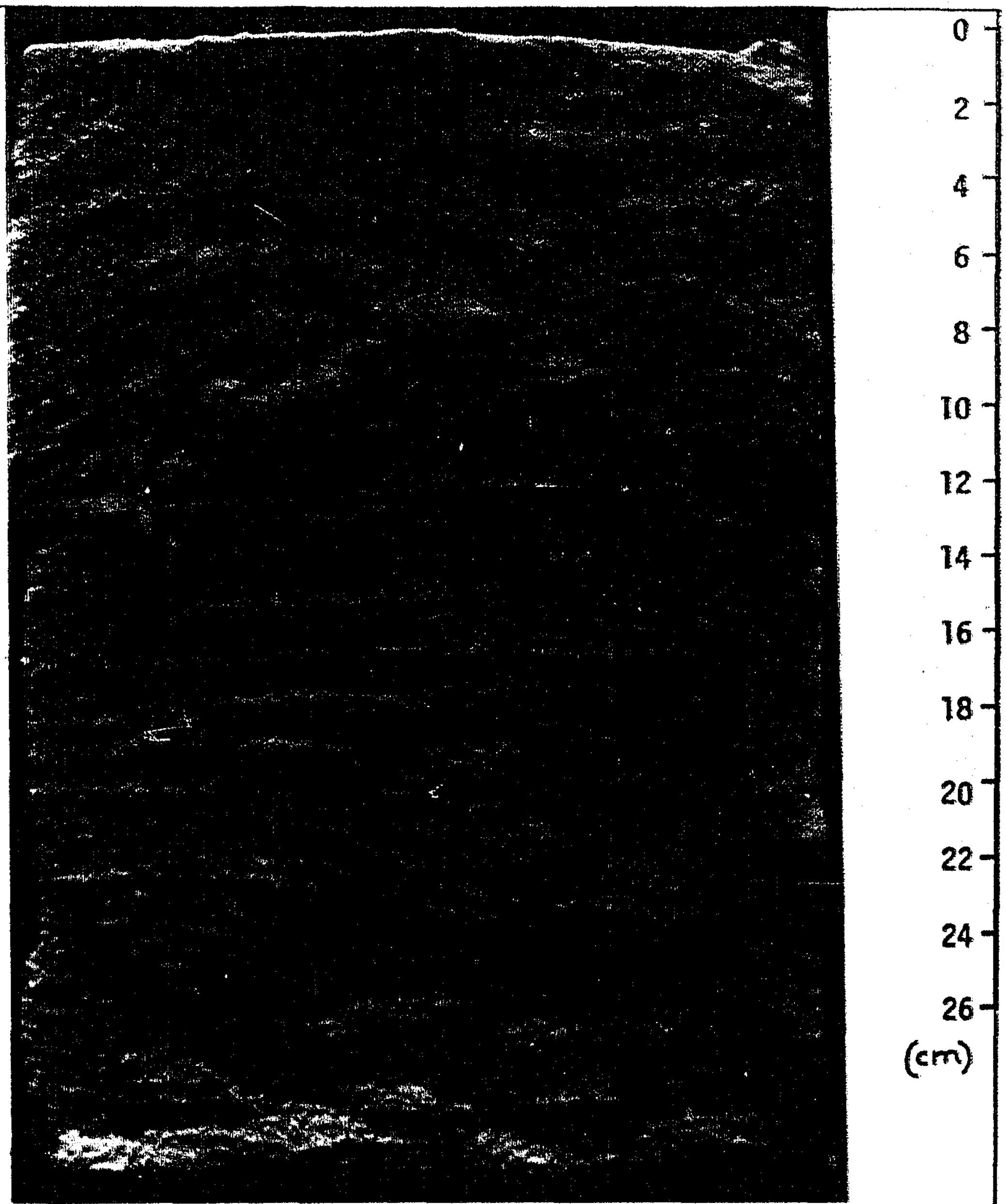

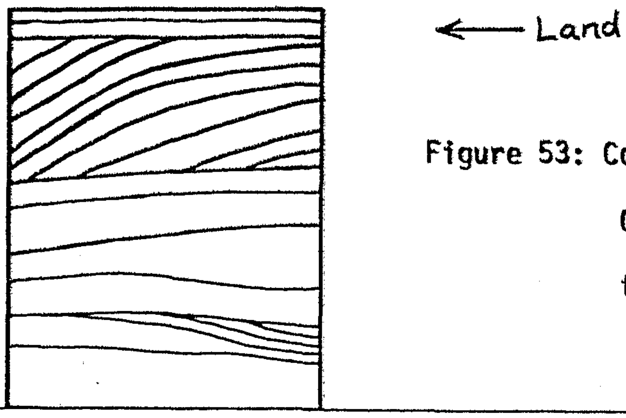

Figure 53: Core peel 10C; Center of the inner trough.

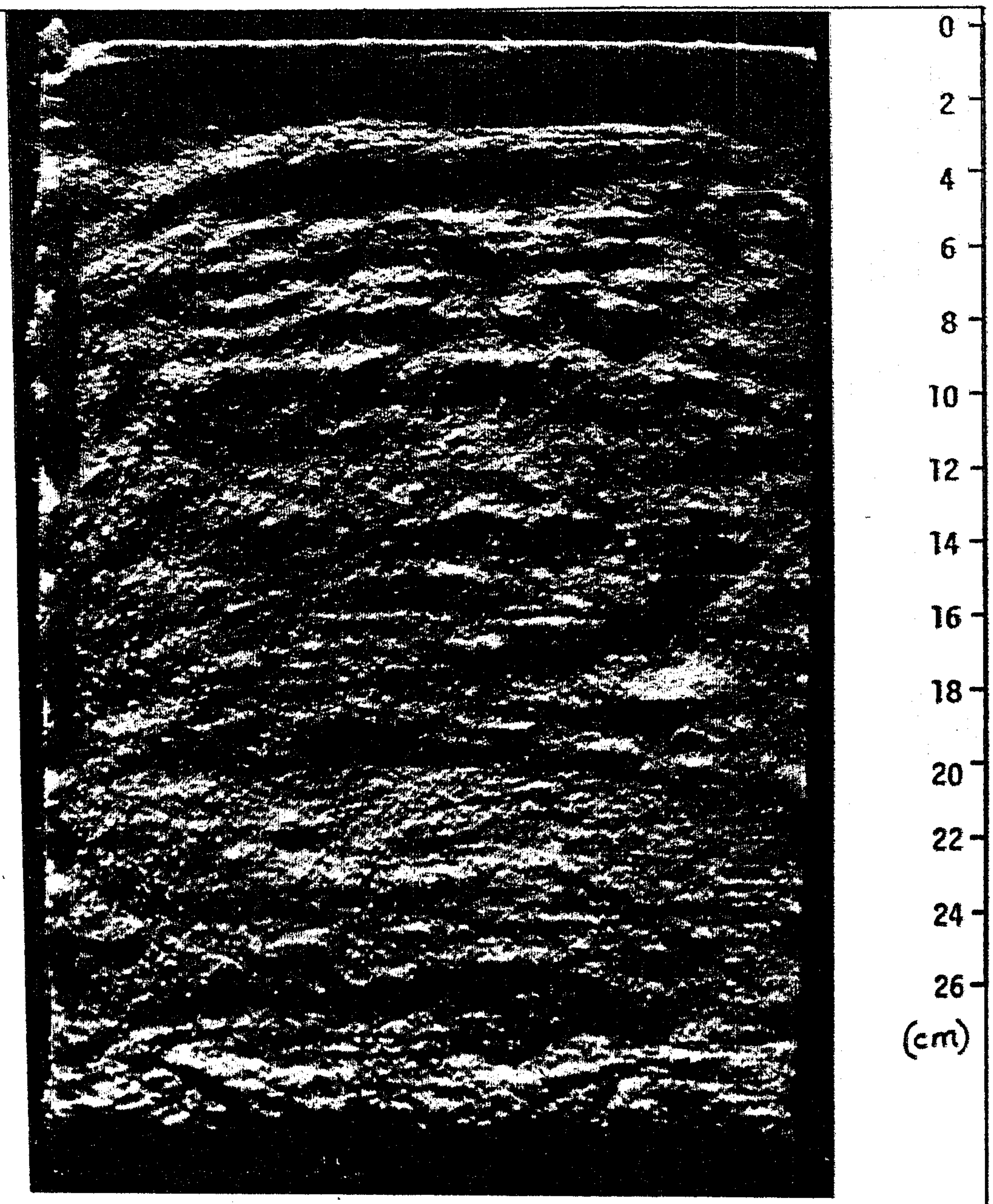

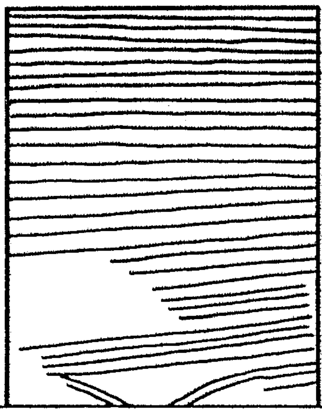

Figure 54: Core peel 15C; Inner trough at the base of the bar slip-face.

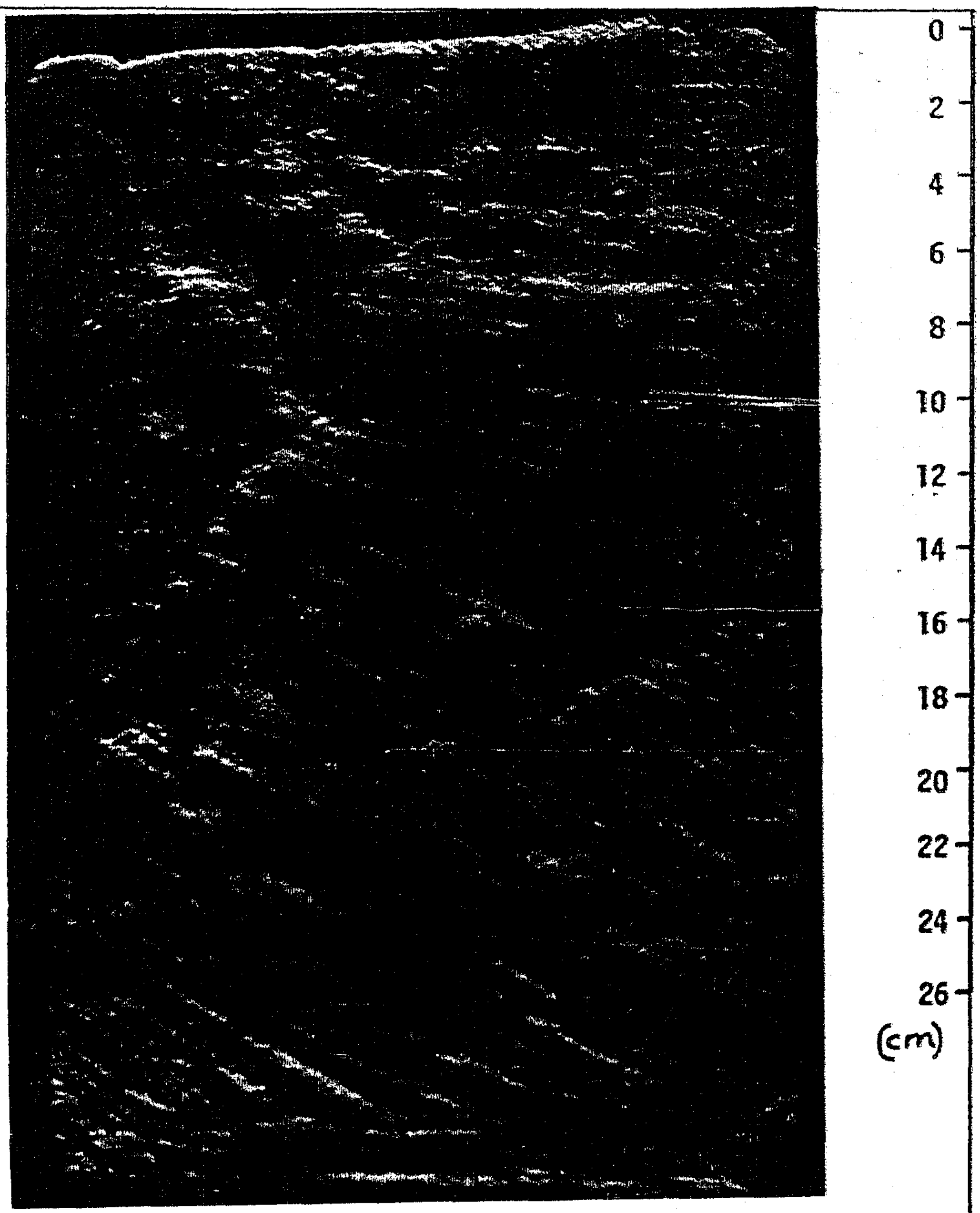

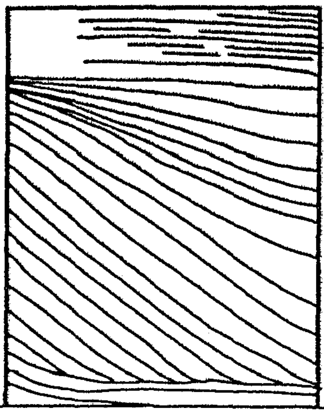

Land →

Figure 55: Core peel 8A;

Bar avalanche face.

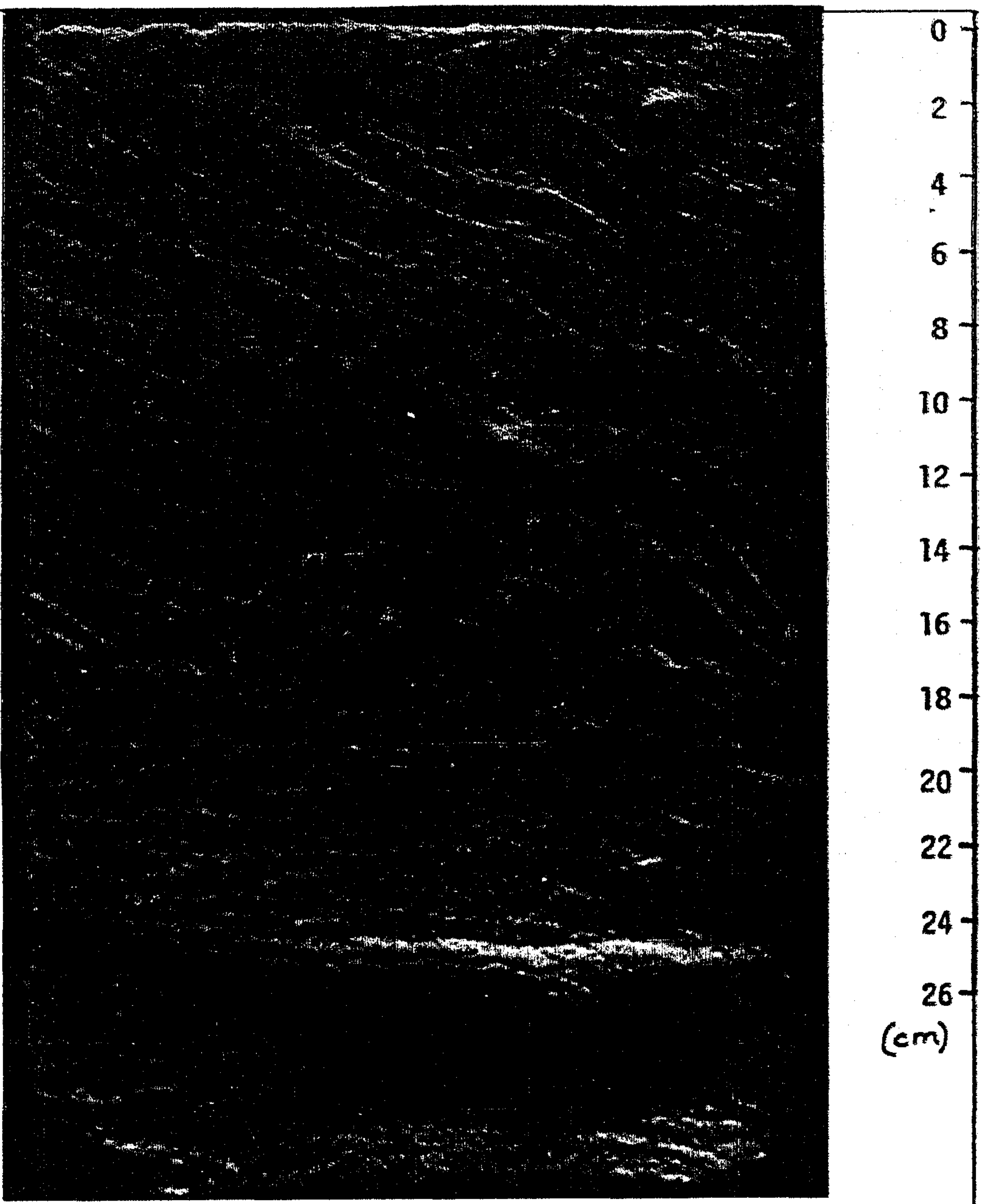

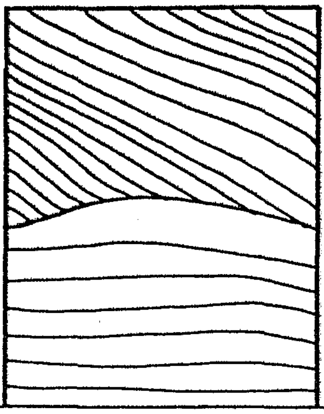

Figure 56: Core peel 14A;

Upper bar avalanche

face.

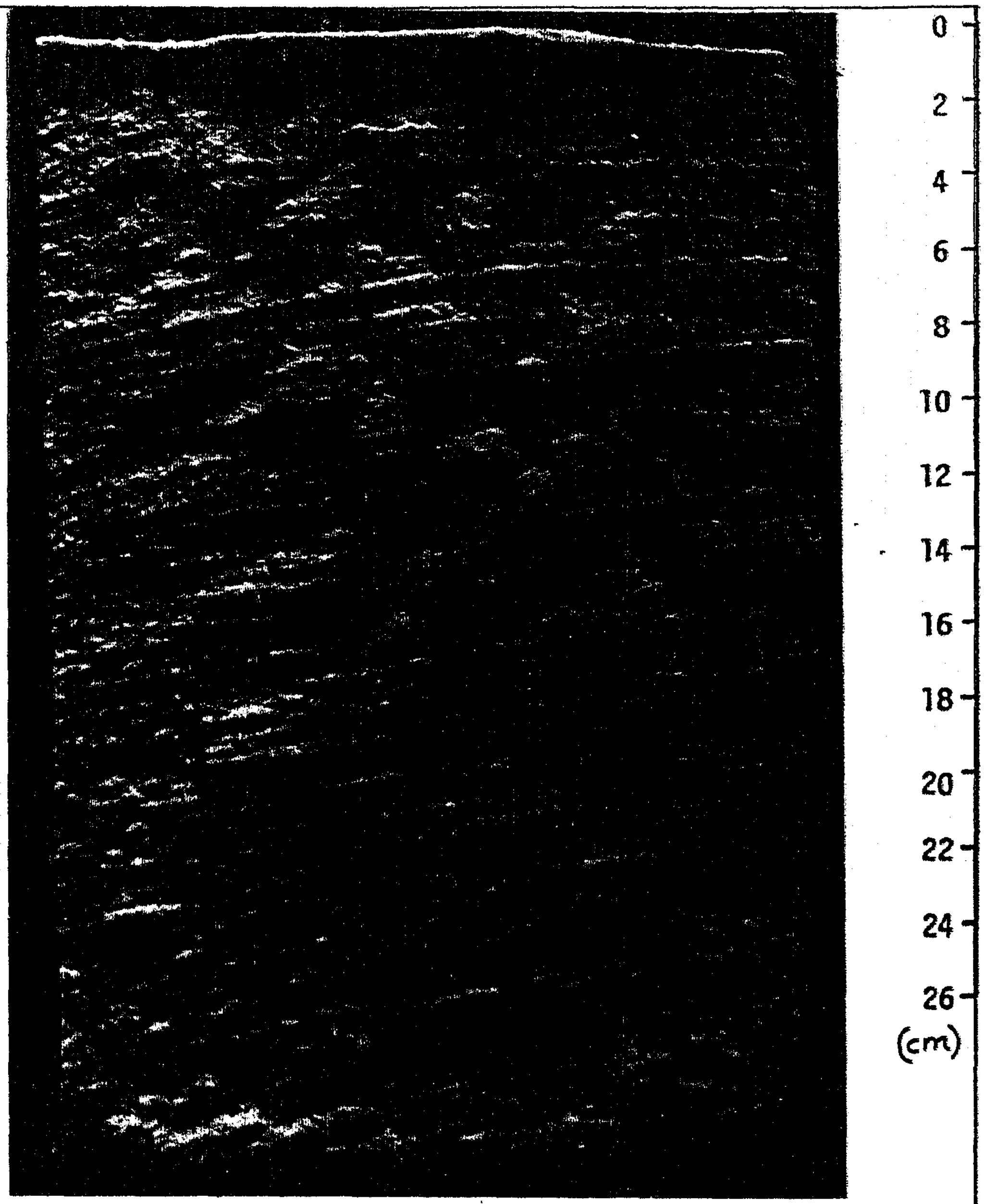

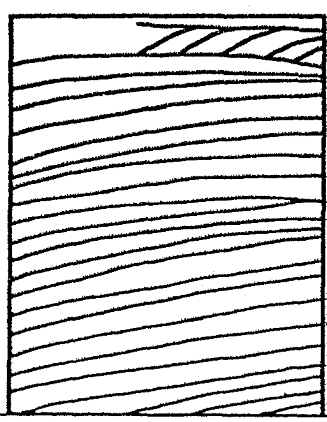

Figure 57: Core peel 11A;

Bar crest.

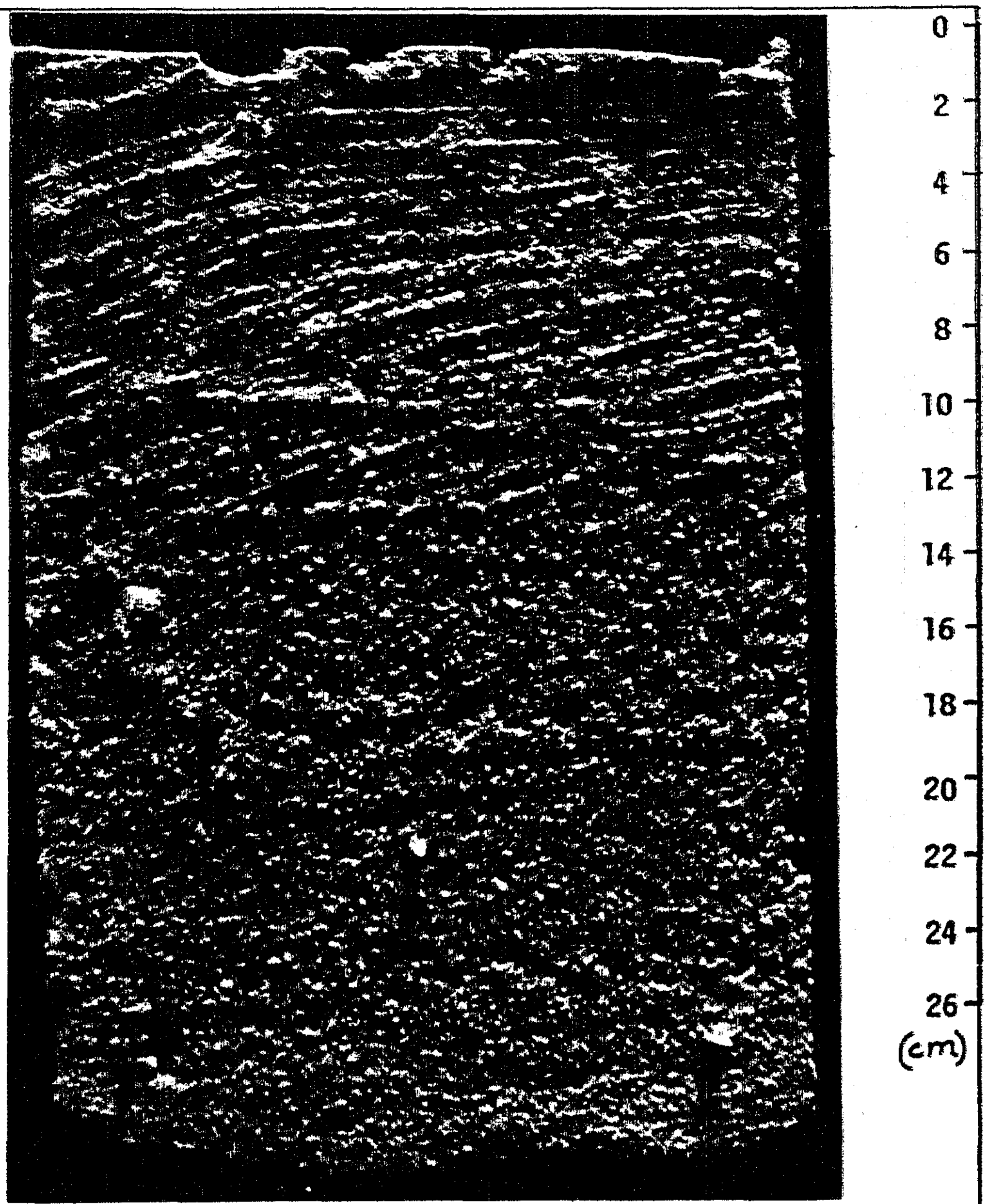

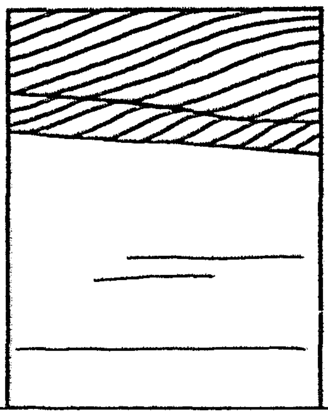

Figure 58: Core peel 10A; From a field of lunate megaripples on the bar crest.

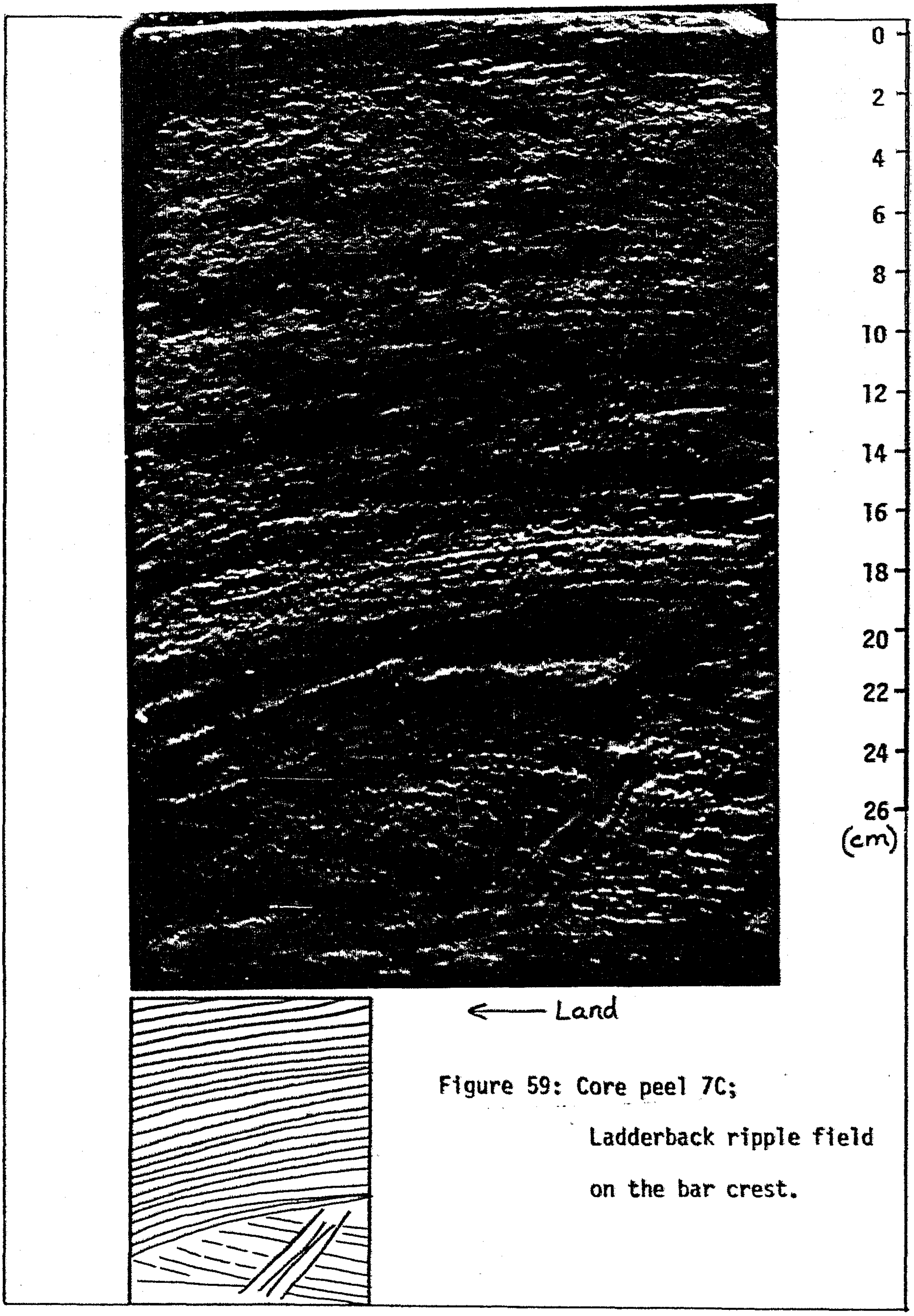

Figure 59: Core peel 7C; Ladderback ripple field on the bar crest.

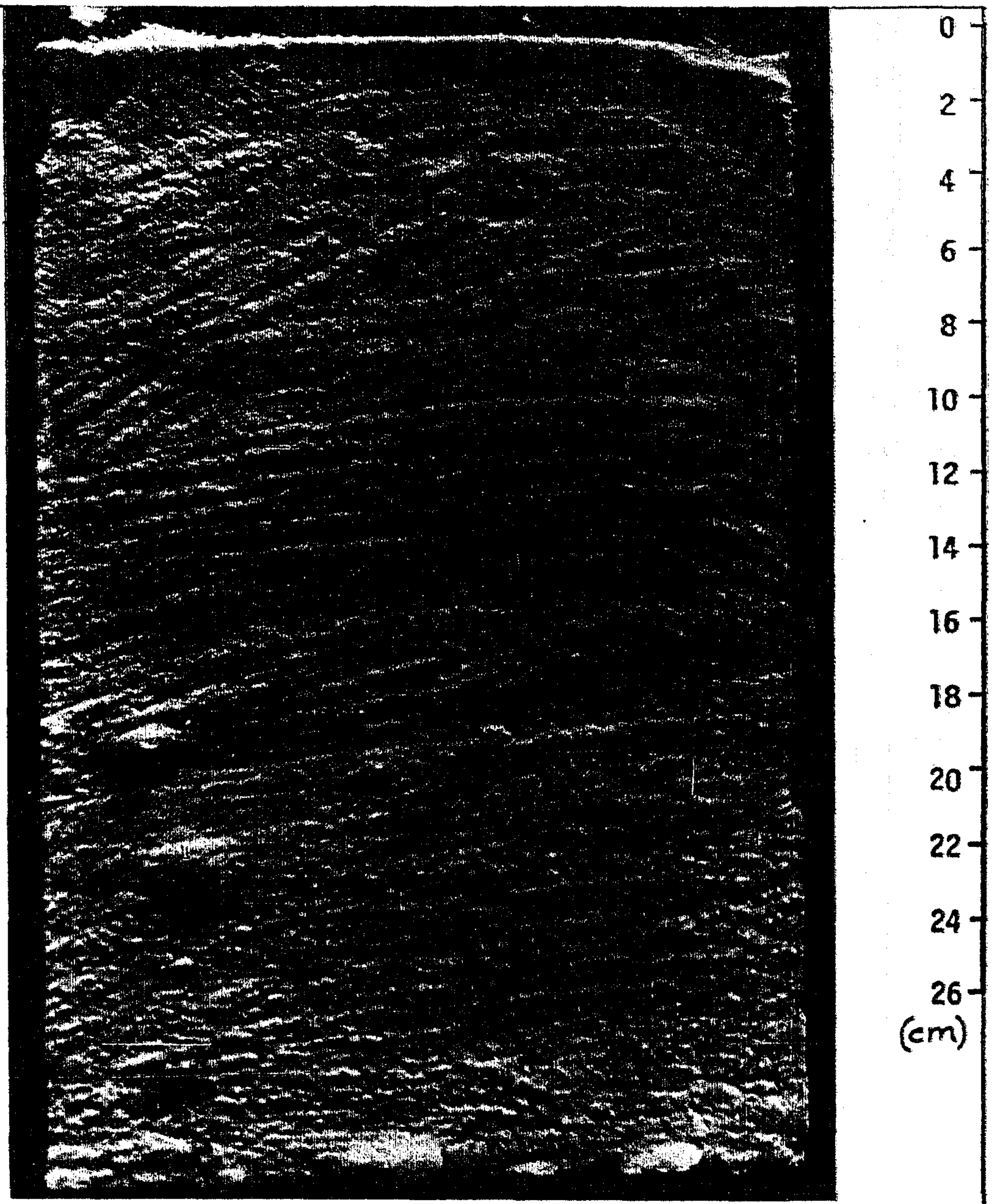

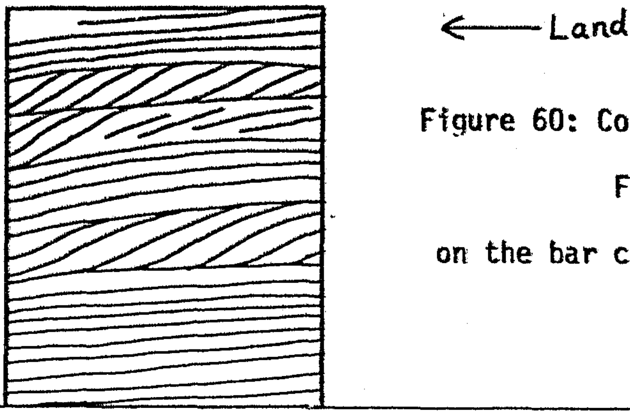

Figure 60: Core peel 4B;
From a ripple field
on the bar crest after a storm.

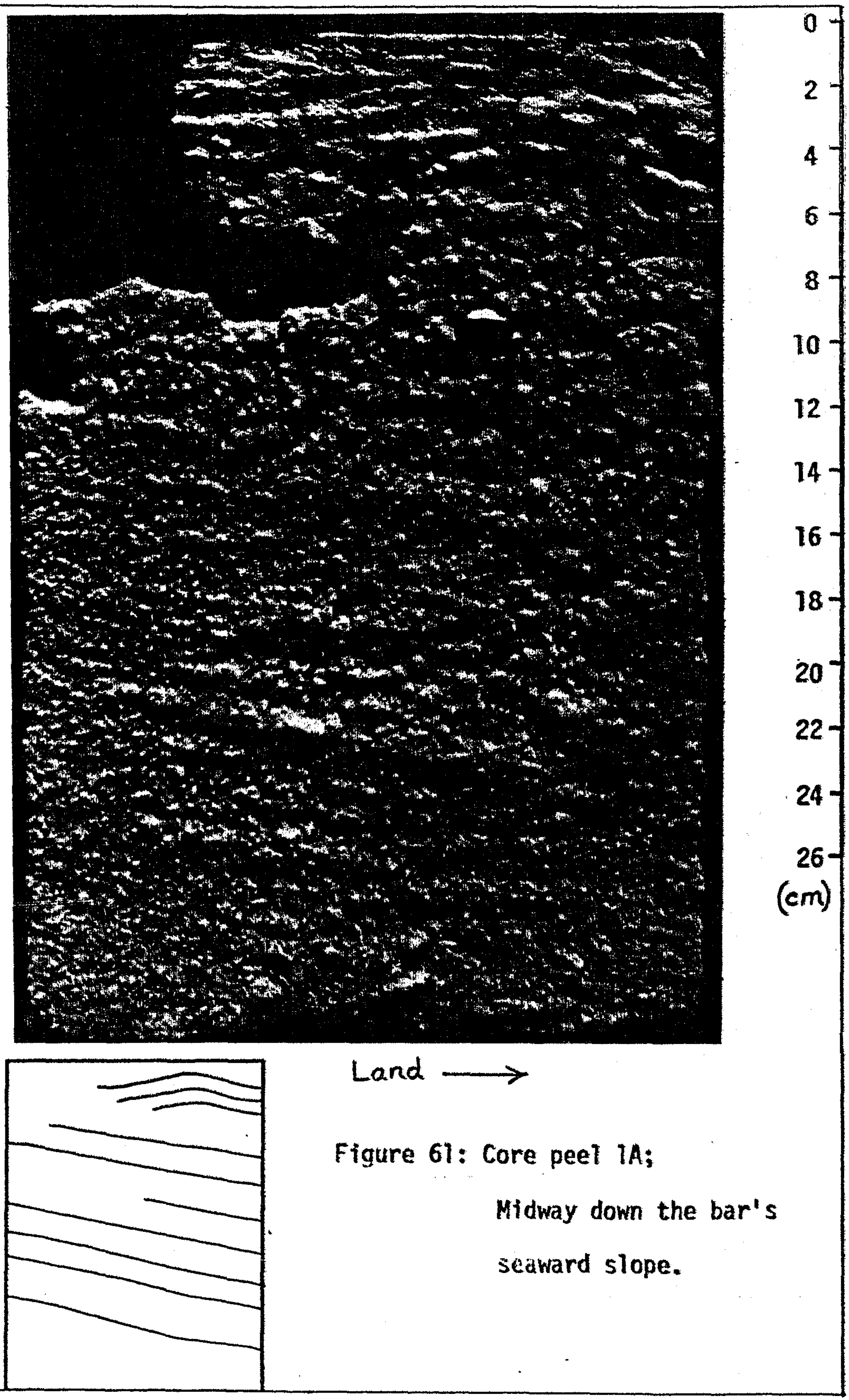

Figure 61: Core peel 1A;
Midway down the bar's
seaward slope.

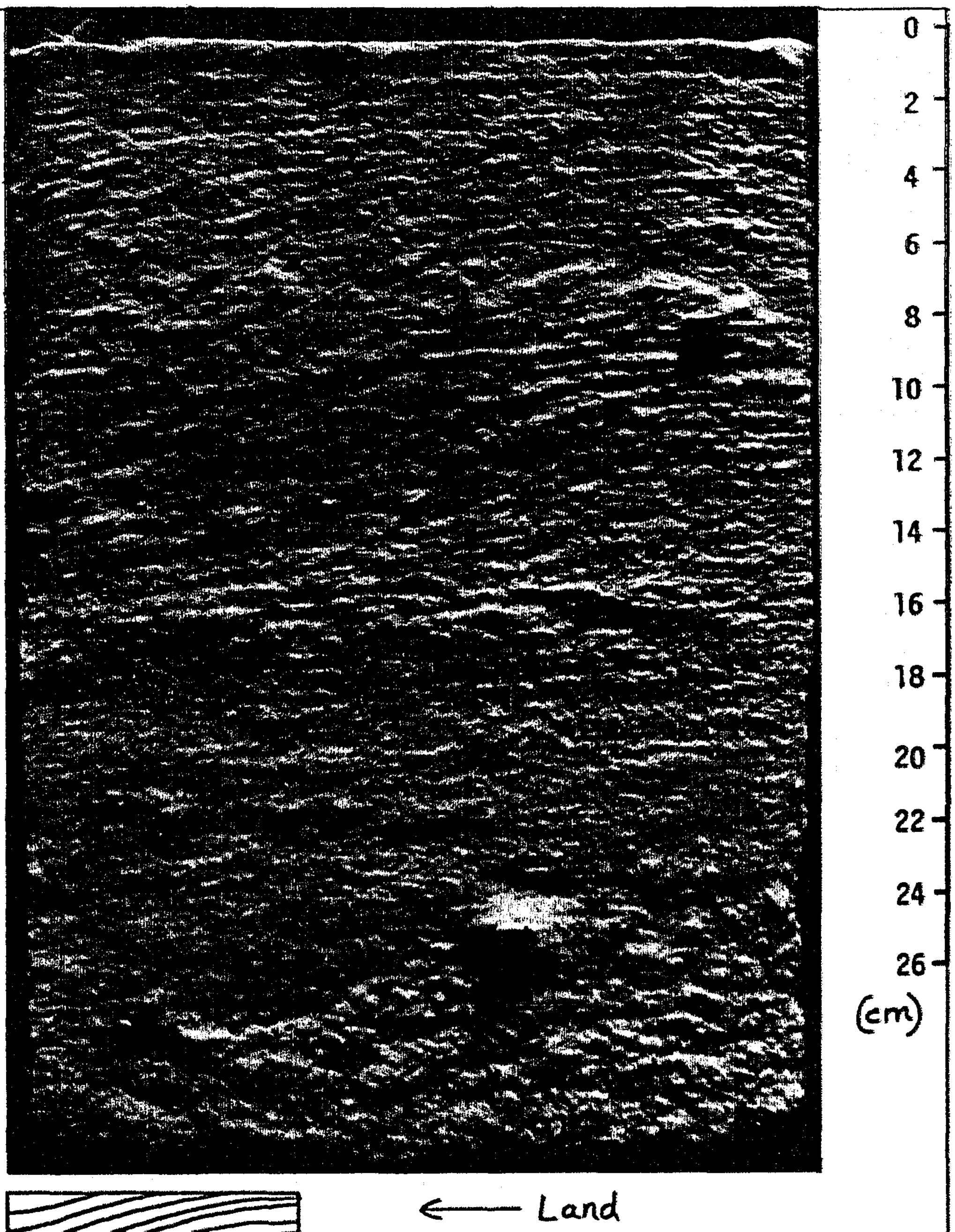

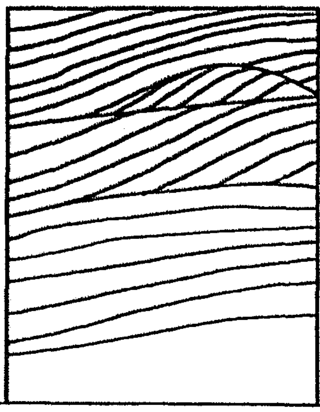

Figure 62: Core peel 11C; Midway down the bar's seaward slope.

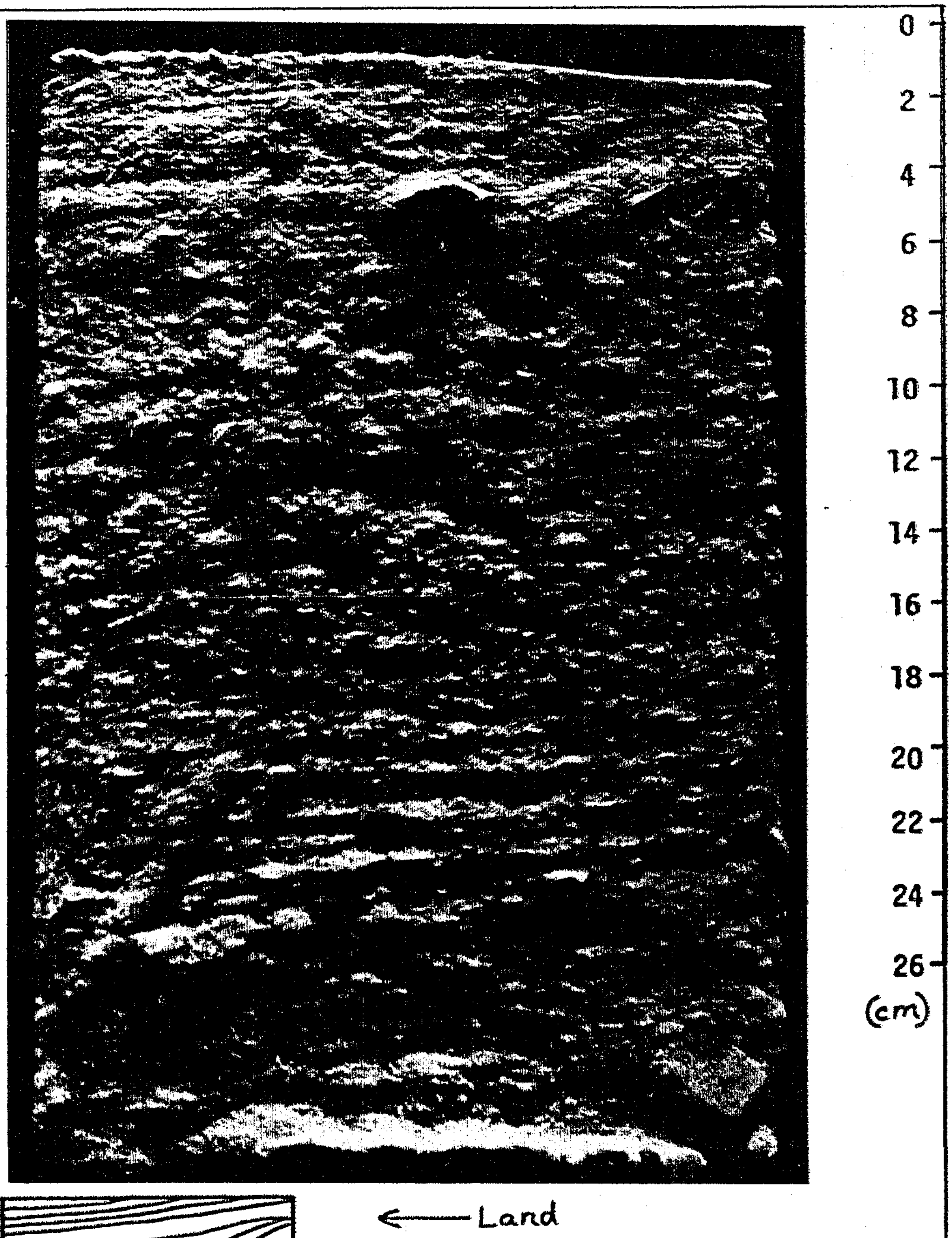

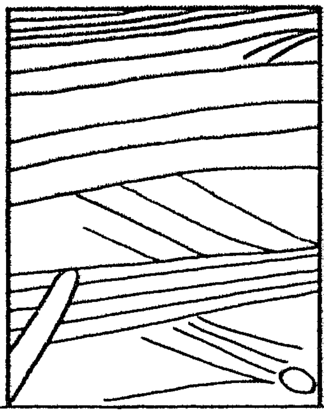

Figure 63a: Core peel 4A;
From interval 1 on
the bar's seaward slope.

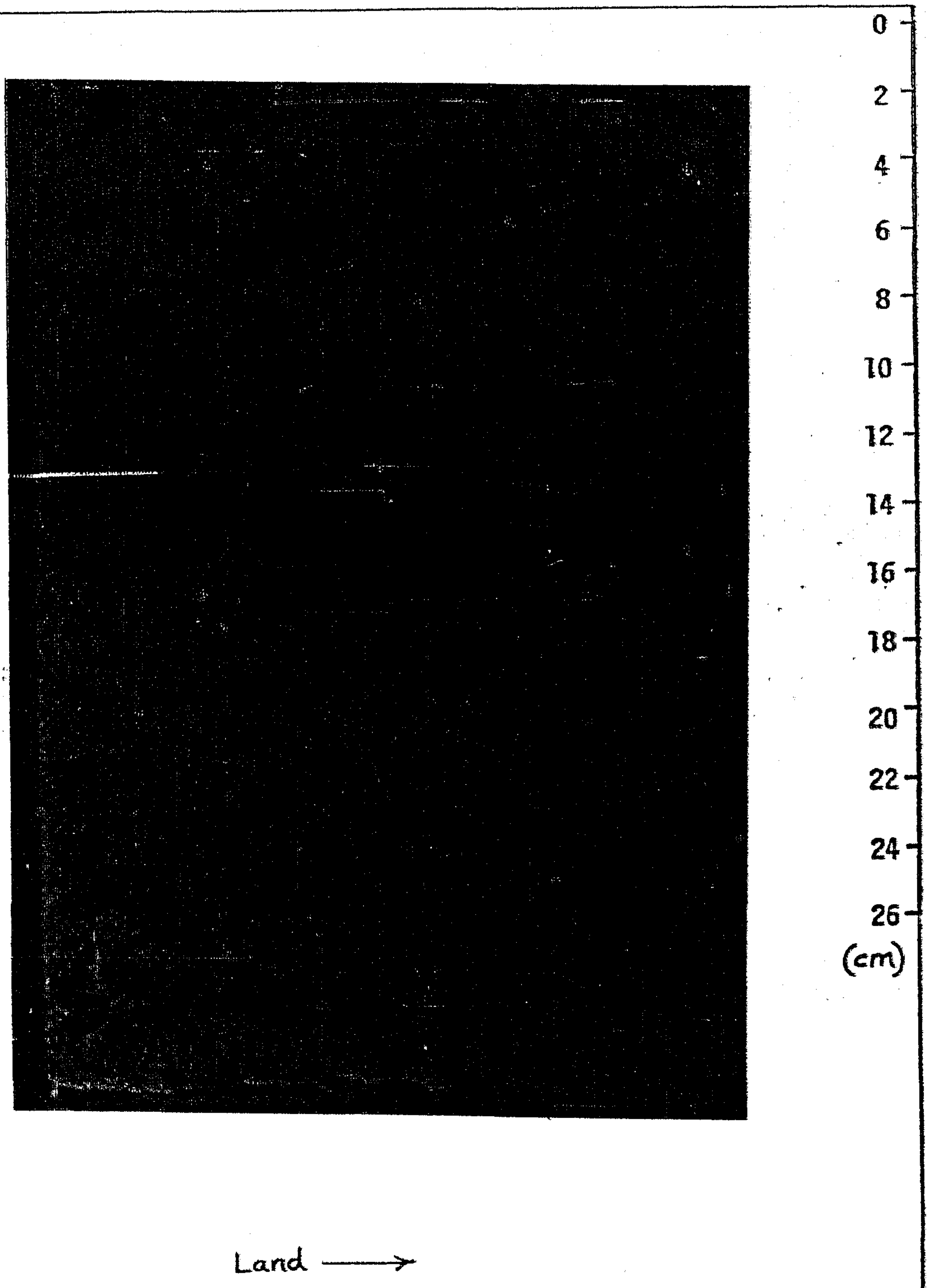

Figure 63b: Wet core slice of 4A showing an unconformity not seen on the epoxy peel.

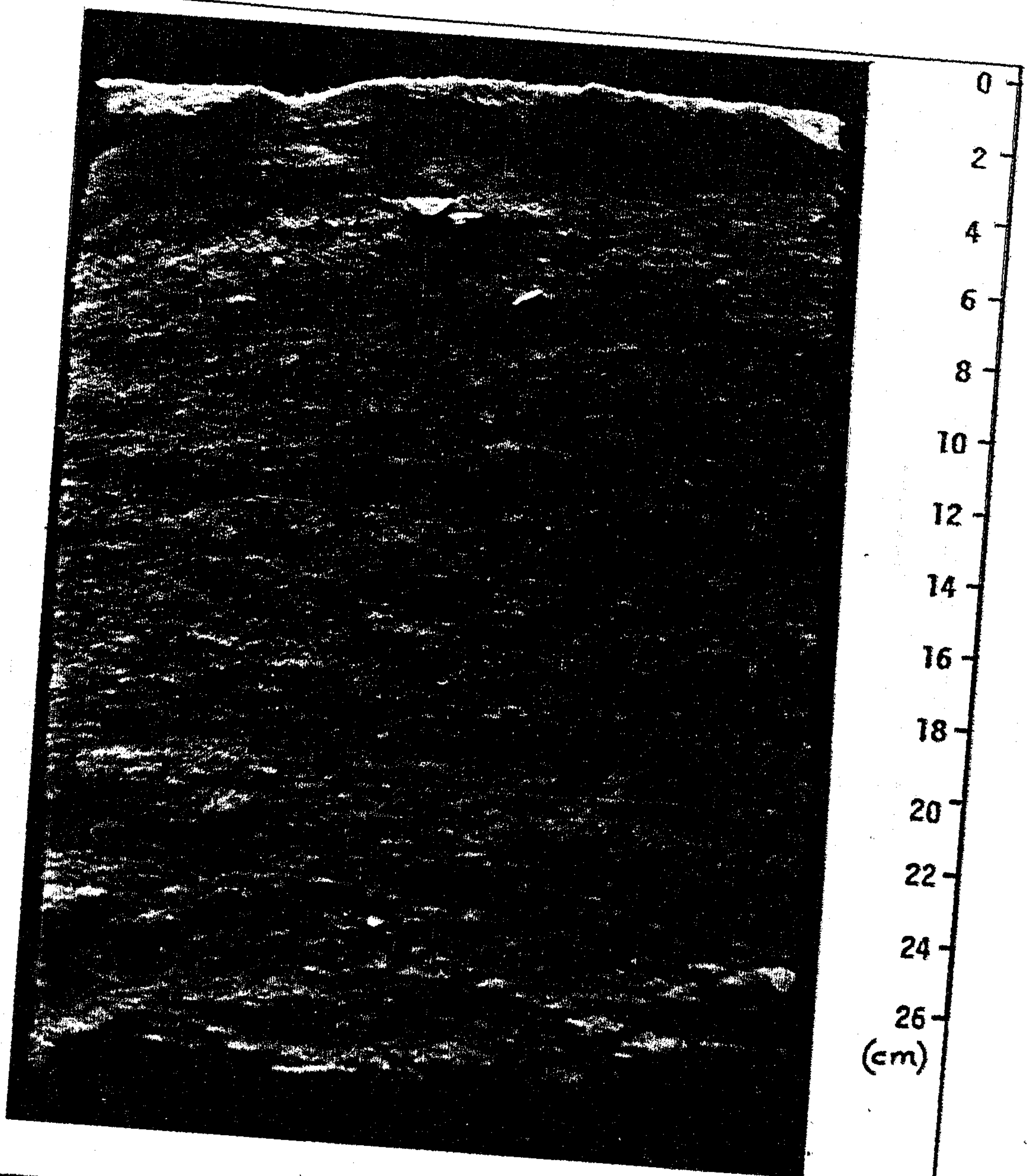

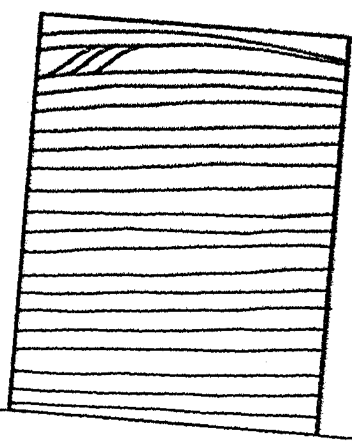

← Land

Figure 64: Core peel 8B;

From the end of the profile on the bar's seaward slope.

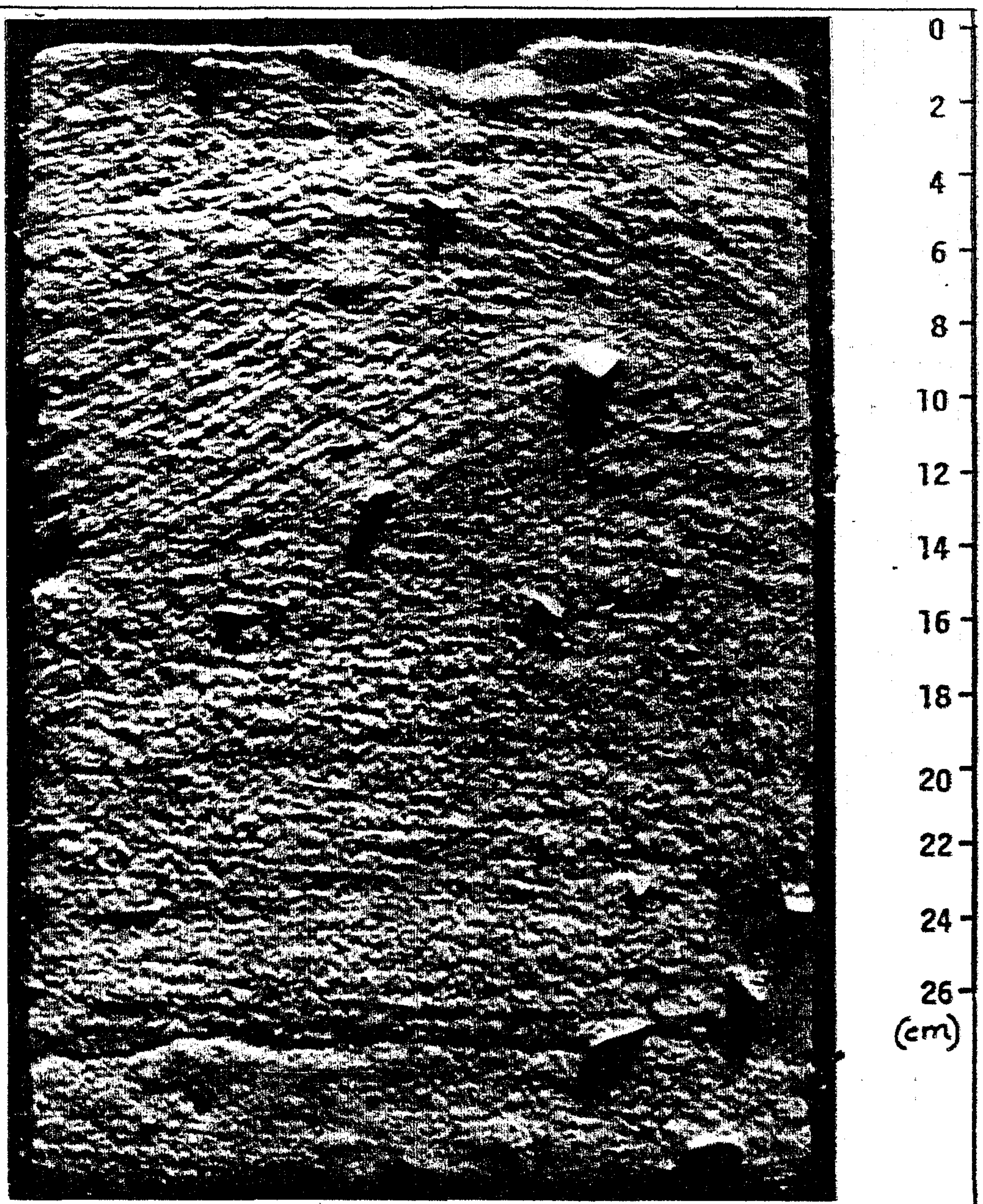

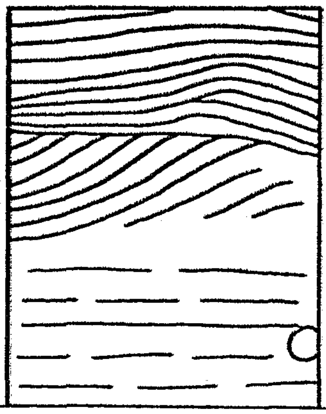

Figure 65: Core peel 6B;

From the end of the profile on the bar's seaward slope.

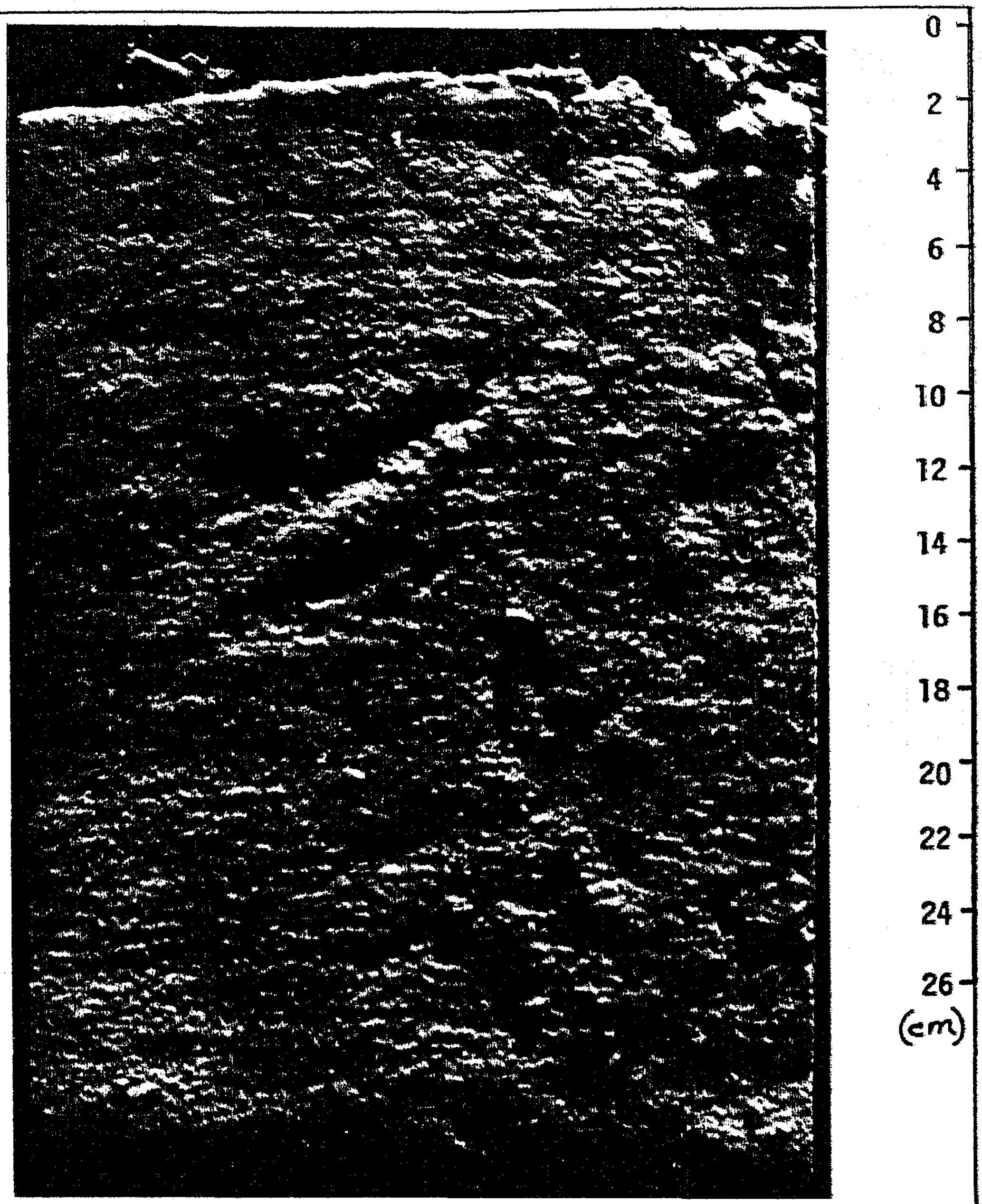

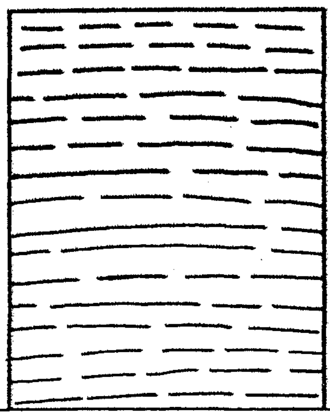

Figure 66: Core peel 11B;

Outer trough.

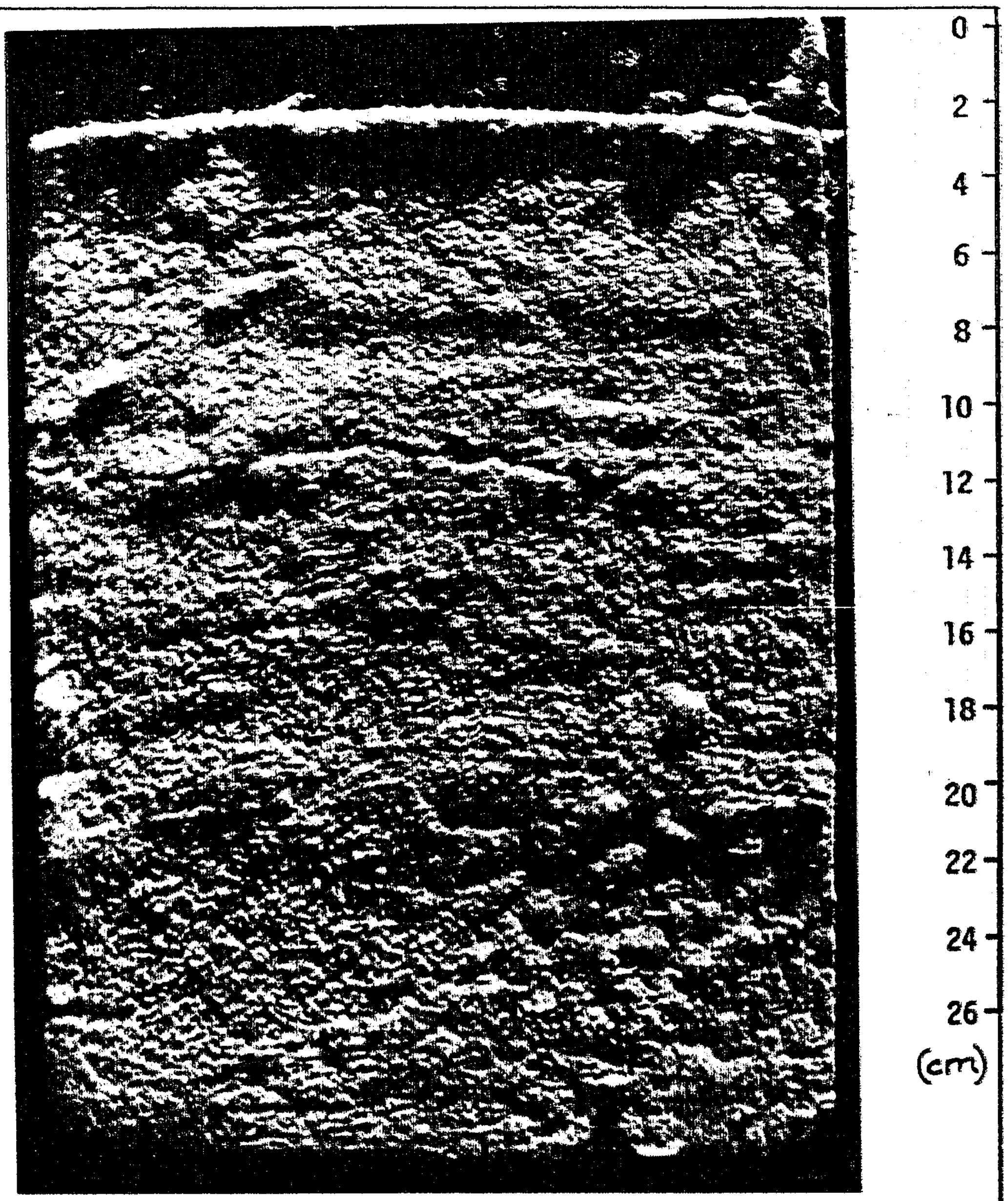

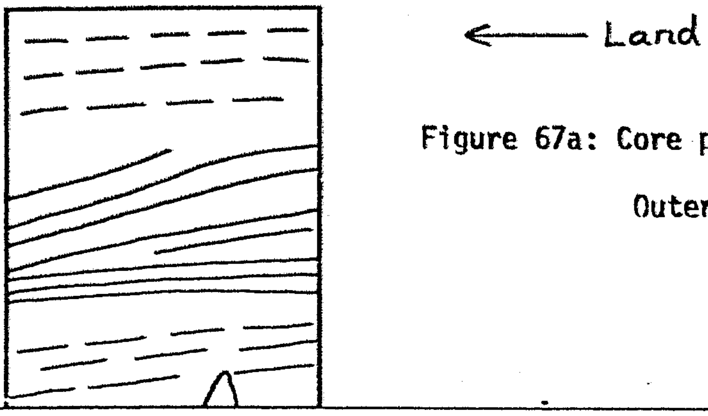

Figure 67a: Core peel 10B;

Outer bar crest.

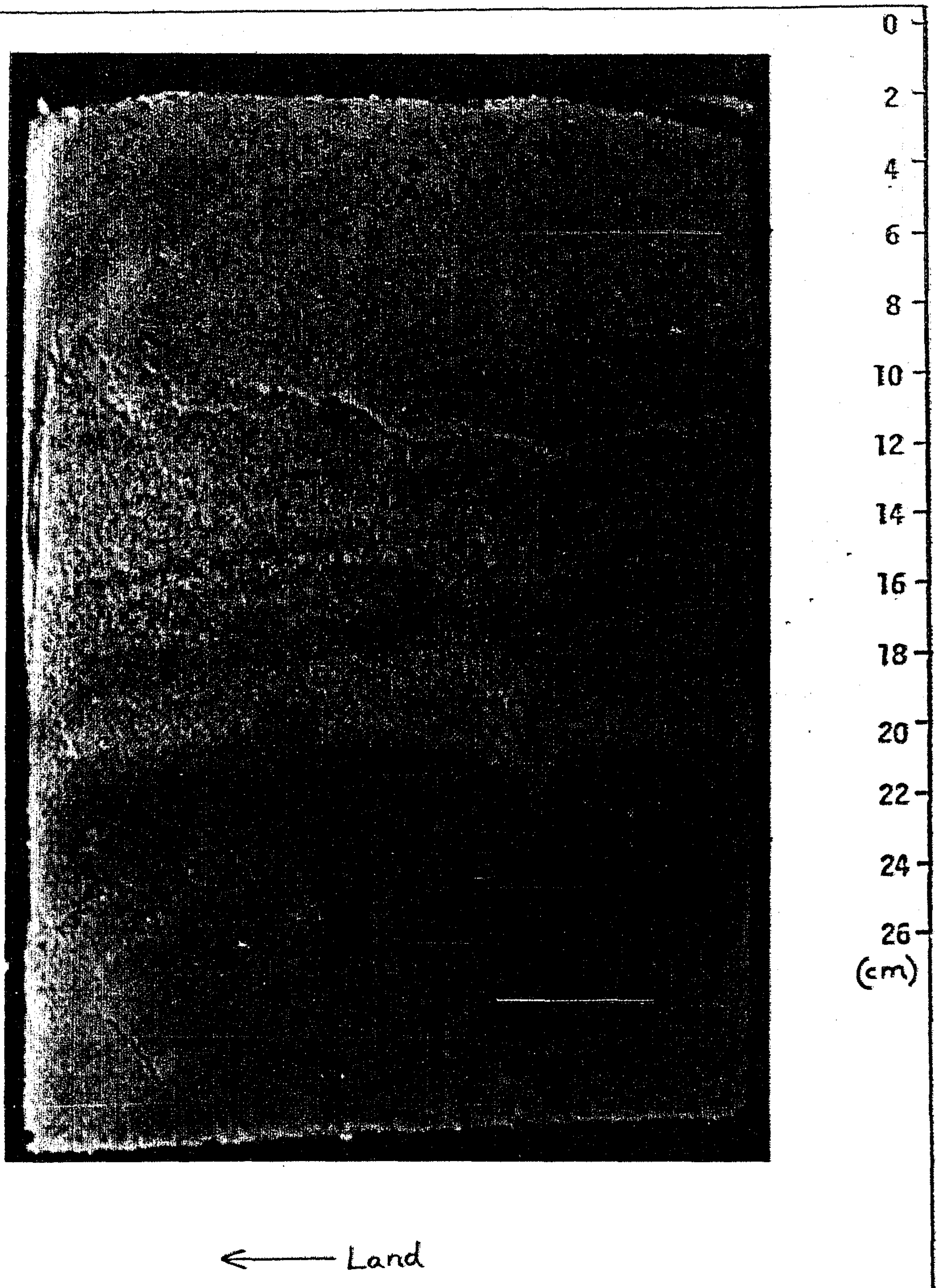

Figure 67b: Wet core slice of 10B showing the heavy mineral layer intersected by a fecal pellet-lined Callianassa shrimp burrow.

characterized by low-angle laminae, both landward and seaward-inclined. The lower half of the peel has abundant shell fragments, some of them concentrated in layers. There is a large area of discolored sand and disturbed bedding in the lower right-hand corner of the core which appears to be a burrow structure.

Cores 9C and 5A were also obtained from the shoreward edge of the inner trough. X-rays of core 5A show a few low-angle landward and seaward-inclined laminae. There is a lot of coarse shell included in this core peel. A mole crab and a marine worm were also found in core 5A. The upper half of core 9C displays ripple cross-bedding which is landward-inclined and the bottom half has horizontal laminae with shell fragments. This core was collected after the three-day storm.

Core 10C (Fig. 53) came from the center of the inner trough and was also obtained after the storm. The upper half of core 10C is cross-bedded with landward inclination. The lower half of this peel contains parallel laminae whose orientation changes from horizontal to seaward-inclined with depth. Very few shell fragments are present in this sample. Core 12A was a pre-storm specimen from the central inner trough. It has some faint horizontal laminae in an otherwise structureless core.

Core 15C (Fig. 54) is from the inner trough at the base of the bar's avalanche face. It is dominated by horizontal parallel laminae. X-rays show a layer of coarser sand and shell fragments at the base of the core peel which has ripple cross-beds inclined in both directions. Core 12B is another trough core from the base of the bar. Its upper half is featureless but the lower half is cross-bedded with landward inclination. There is a horizontal, 3 cm-thick, layer of coarser sand and shell fragments at the bottom of core peel 12B. A marine worm was found in this core.

Bar Avalanche Face

Four cores were obtained from the bar's avalanche face. Cores 15B, 9A, 14A, and 8A all display large-scale cross-bedding inclined in the landward direction. The angle of the cross-beds varies from 20 to 30 degrees. None of these cores contains a significant amount of shell material. Core 8A (Fig. 55) displays topset and bottomset beds in association with the bar foreset beds. Core 14A (Fig. 56) shows bar foreset beds on top of an erosional unconformity. Beneath the unconformity one can see horizontal to undulatory parallel laminae. The prominent ridge of sand in the lower part of the peel is an epoxy-filled crack in the core. Core 15B exhibits a marked alternation of coarser and finer sand laminae in the bar foreset beds.

Bar Crest

Cores 15A, 11A, 10A, 7C, and 4B were taken from the bar crest. Core peel 15A contains gently landward-inclined laminae which are 10 to 20 degrees from the horizontal. Between some of these laminae in the upper half of the core there appear to be vague sets of ripple cross-beds. Core 11A (Fig. 57) exhibits gently landward-inclined laminae which steepen with depth. There is some poorly defined, landward, ripple cross-bedding in the uppermost layer of this core peel. Two mole crabs were discovered in this core. Core 10A (Fig. 58) comes from a field of lunate megaripples on the bar crest. The upper portion of this peel has two layers of well-defined, landward-inclined cross-bedding. The two sets are separated by a seaward-sloping unconformity. The bottom half of core peel 10A is almost structureless except for a few vague parallel laminations which appear on the x-rays.

Cores 7C and 4B were removed from the bar crest following the three-day storm of July, 1977. Core 7C (Fig. 59) is from a field of ladderback ripples. The sample was taken on top of one of the straight-crested ripples with the long dimension of the core box parallel to the ripple crest. The upper two-thirds of core peel 7C is composed of very low-angle, landward-inclined, fine, parallel laminae. The lower third of the peel contains seaward-inclined laminae interrupted by a probable burrow structure, oriented at 90 degrees to the surrounding laminae. The angular unconformity between the upper and lower bedding sets is visible but not obvious. Core 4B (Fig. 60) was obtained from a ripple field on the bar crest, the day after the storm waves subsided (July 21, 1977). This peel has a variety of cross-bedding styles which are all landward-inclined at different angles. Near the top of the core there are two sets of 2 to 3 cm-thick, ripple cross-beds. Below these there is a 5 and a 3.5 cm-thick layer of lower-angle cross-beds. The bottom third of core peel 4B appears to be a single unit of low angle, landward-inclined, parallel laminae. Two small marine worms were found in vertical burrows during the processing of this core. Shell material is rare in all of the bar crest peels compared to the other environments.

Seaward Slope

Cores 14B, 1A, 11C, 6A, and 4A were recovered from the seaward slope of the longshore bar. Core 14B is dominated by fine, horizontal, parallel laminae with scattered shell fragments. In the middle upper half of the peel there is a 4 cm-thick layer of landward, ripple cross-beds with locally abundant shell hash. Most of core peel 1A, shown in Figure 61 is covered with parallel laminae dipping landward at about 10 degrees. In the fragmented top portion of the peel one can see a 3 cm-thick layer of landward ripple cross-bedding. Core peel 11C (Fig. 62) is a post-storm sample from the back of the bar. The most interesting feature in this core is the ripple lens preserved in the middle upper half of the peel. The ripple cross-bedding in this lens is landward-inclined as is the rest of the cross-bedding in core 11C. The lens is overlain by a layer of gently-dipping cross-beds which are devoid of shell material. Beneath the ripple lens are two, 6 cm-thick, units which contain laminae composed of coarser sand and shell fragments. The upper layer is cross-bedded at a 20 degree angle and the lower has horizontal, parallel laminae. The bottom most layer in core 11C contains no discernible structure.

Core 6A is uniform in texture and appears to have faint, horizontal, parallel lamination. Shell fragments and fecal pellets are scattered throughout this core peel. Core 4A (Fig. 63a) displays four layers of bidirectional cross-bedding and a burrow structure. A photograph of the wet core slice (Fig. 63b) shows the erosional unconformity between the first two layers in the top of the core. Shell fragments are abundant in core 4A, especially in the ripple cross-beds. A large echinoderm fragment is located in the lower right-hand corner. Several marine worms were encountered in this core also.

Cores 3A, 6B, 8B, and 9B were obtained from the deepest part of the seaward bar slope, where the outer trough environment begins. The water depth at this point is approximately two meters. The cores were taken at the seaward end of the topographic profiles. The x-ray of core peel 3A shows physical sedimentary structures only in the upper third of the core. At the top of 3A there is a layer of landward-inclined ripple cross-bedding. Below that there are two gently seaward-sloping (∿10 degrees) laminae of coarser sand and shell. This core contains an abundance of fecal material and a burrow which is not preserved in the final peel. Core 8B (Fig. 64) is primarily composed of fine, horizontal, parallel laminae. A 2 cm-thick lens of landward, ripple cross-bedding is located in the upper left-hand corner of the peel. The ripple laminae contain shell fragments and sand which is coarser than the rest of the sediment in the core. A mole crab and a worm were found in core 8B. Several worms were found in their burrows in core 9B. The only visible sedimentary structure in core 9B is a wedge of landward-dipping, ripple cross-bedding in the middle of the peel. The cross-bedding is composed of coarse layers containing shell fragments. Core 6B (Fig. 65) was removed from the back of the bar two days after the three-day storm. It contains many large shell fragments and good physical sedimentary structures. There is a 7 cm-thick layer of landward-dipping cross-bedding near the top of core 6B. This layer is overlain by a small set of seaward-dipping, ripple cross-beds in the upper right-hand corner. The bottom half of this peel contains indistinct, horizontal, parallel laminae. In the lower right-hand corner there is a burrow structure filled with fecal material.

Outer Trough

Core peel 11B is from the outer trough and can be seen in Figure 66. The entire core is composed of fine laminae which are horizontal and parallel to each other. Very small shell fragments are present and they have their long axes aligned with the bedding. There were no organized ripples at the locality where this core was taken.

Outer Bar

Core 10B (Fig. 67a) was removed from the outer sand bar at Panama City Beach. At this locality the water depth was 2.2 meters and the bed was covered with 3 cm-high, sinuous-crested, asymmetric ripples. The only obvious physical structure in the core is a 3 cm-thick layer of horizontal, parallel laminae just below the middle of the peel. There is a heavy mineral layer at the base of this unit. Figure 67b is a photograph of a slice through core 10B showing a few gently shoreward-inclined laminae above the horizontal heavy mineral layer. Also, there is a well developed burrow structure outlined by fecal material. Small fragments of shell are abundant in the horizontal laminae.

Grain Size Analysis

Sediment samples were collected all along the measured topographic profiles, at the bed level and at shallow depths ($\leq$ 20 cm) within the sediment. Six profiles were sampled in 1976 and two in 1977. One representative profile from each year is shown in Figure 68. The mean grain size was quite uniform in time and space on Panama City Beach. Samples from some layers at depth are slightly coarser than the average surface sediment sample. Sediment from the swash zone is usually slightly coarser also. One sample from the outer bar is slightly finer than the average. The mean grain size for all the samples is 0.25 mm. Therefore the sands straddle the boundary between medium and fine sand.

The sorting of the sediment samples is also fairly uniform in all respects. The average sorting value for all samples is 0.28 phi, which means these sands are very well sorted. some swash samples are less well sorted than the average.

Burrow Data

Burrow counts were made along the measured profiles to obtain a crude measure of the degree of bioturbation. Nine burrow profiles from 1976 are displayed in Figures 69a and 69b. Nine burrow profiles from 1977 are shown in Figures 70a and 70b. These figures show the number of burrows per square meter plotted against distance from shore. The most noteworthy trend is an increase in burrow density toward the seaward end of the profile. No burrow counts were made in the outer trough or on the outer bar but visual observations confirm this trend of increased burrowing offshore. There is also a small peak in the number of burrows in the inner trough. The swash zone and inner bar crest are lacking in burrows. The plot from July 21, 1977 is conspicuous because of the uniform number of burrows along most of the profile. This burrow count was made on the day after the storm in mid-July.

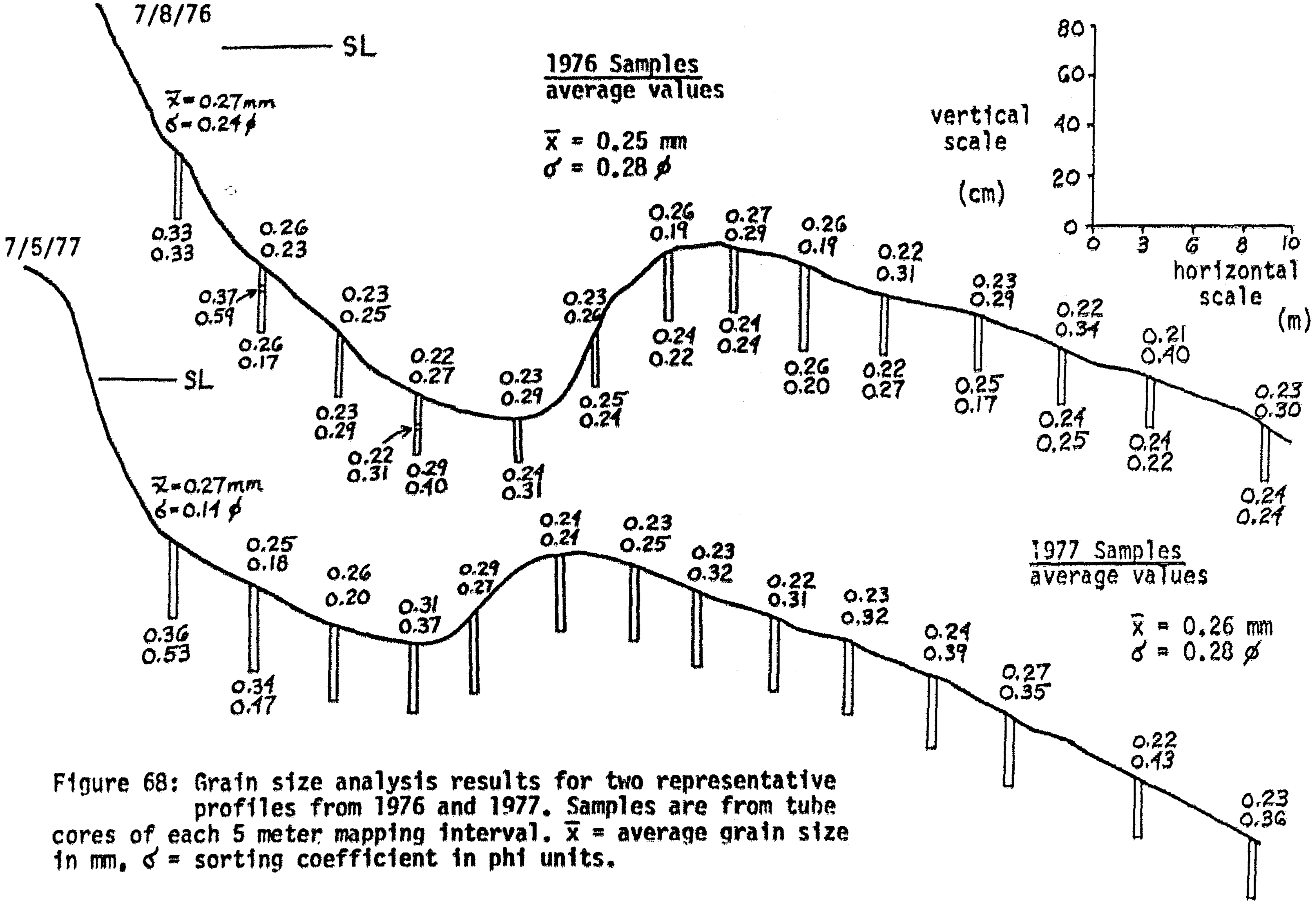

Figure 68: Grain size analysis results for two representative profiles from 1976 and 1977. Samples are from tube cores of each 5 meter mapping interval. $\bar{x}$ = average grain size in mm, σ = sorting coefficient in phi units.

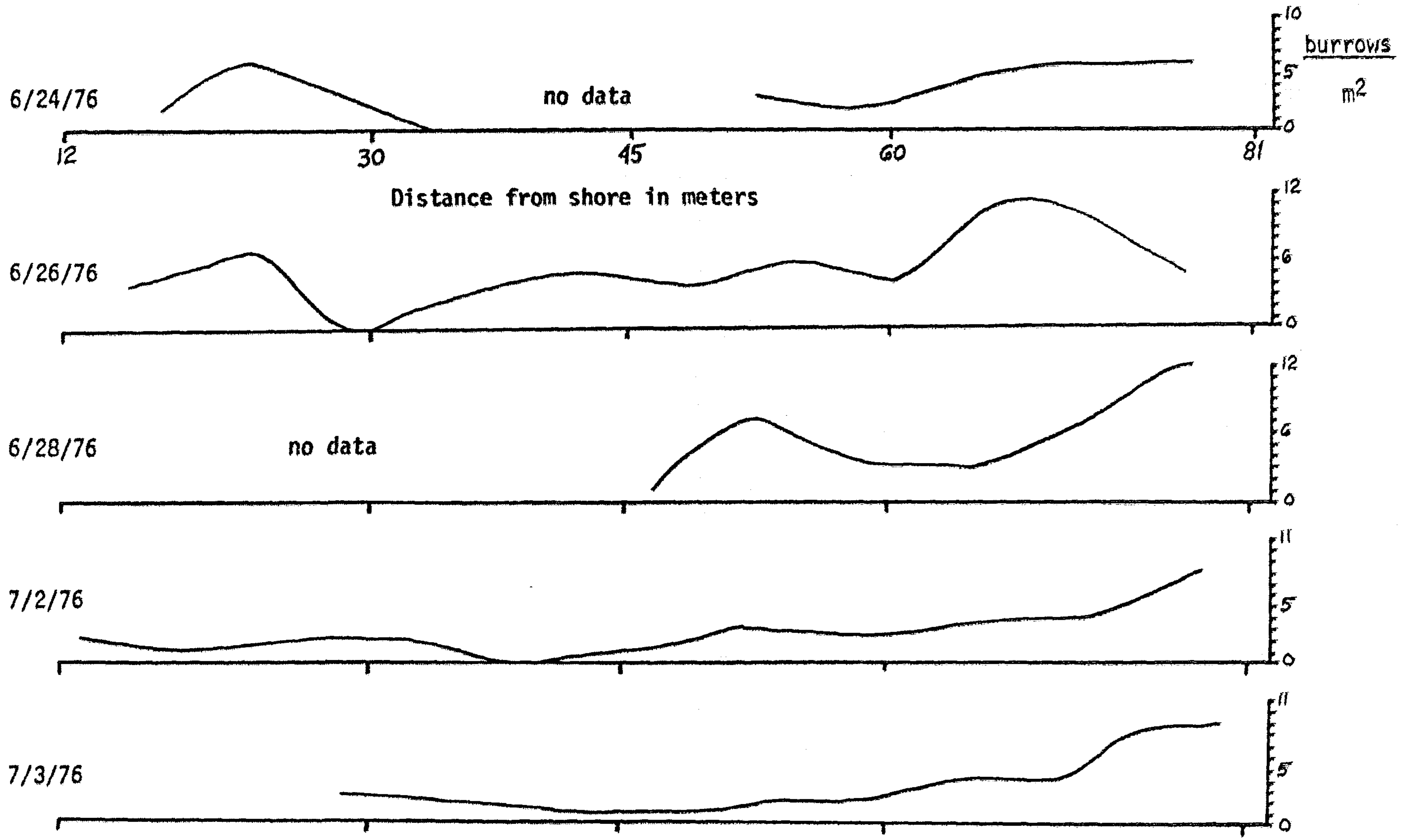

Figure 69A: 1976 burrow profiles

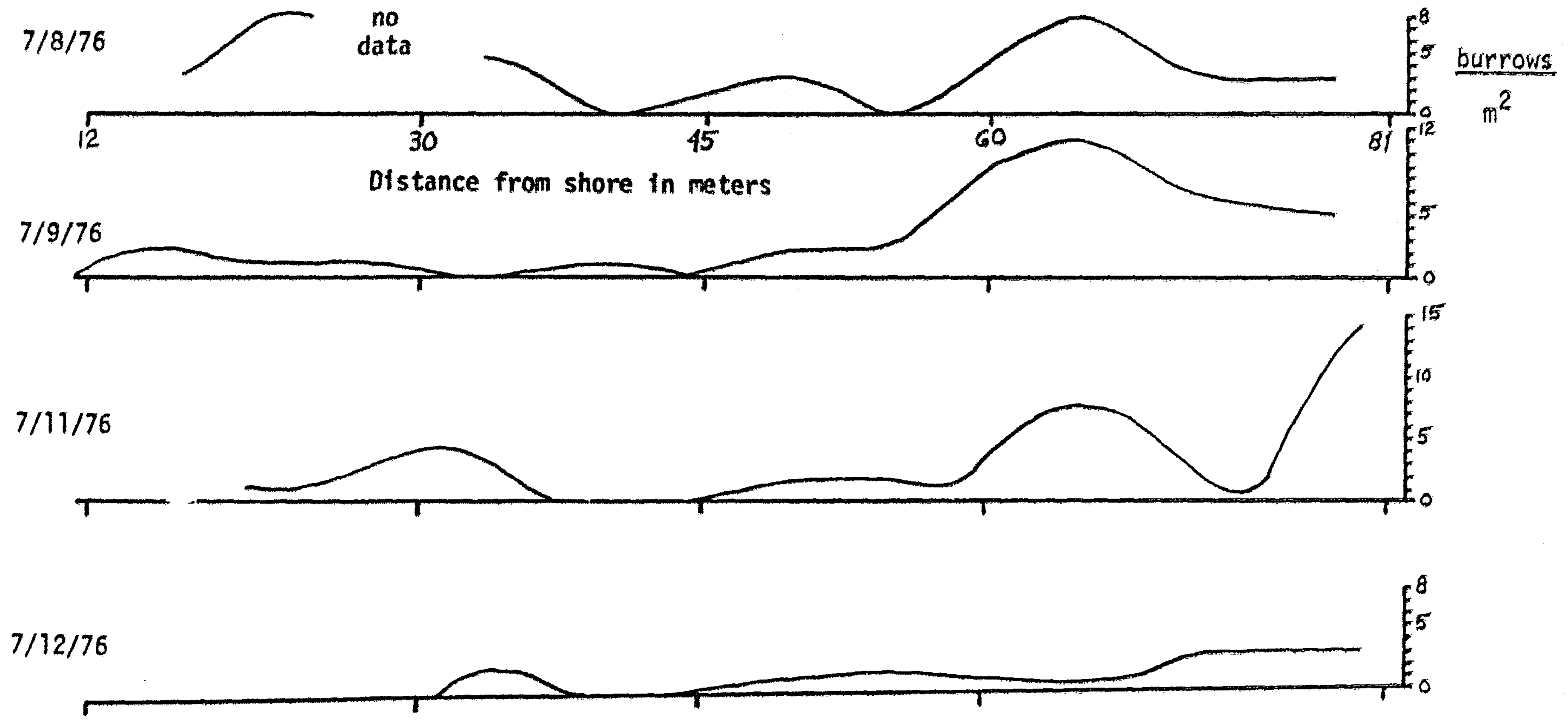

Figure 69B: 1976 burrow profiles

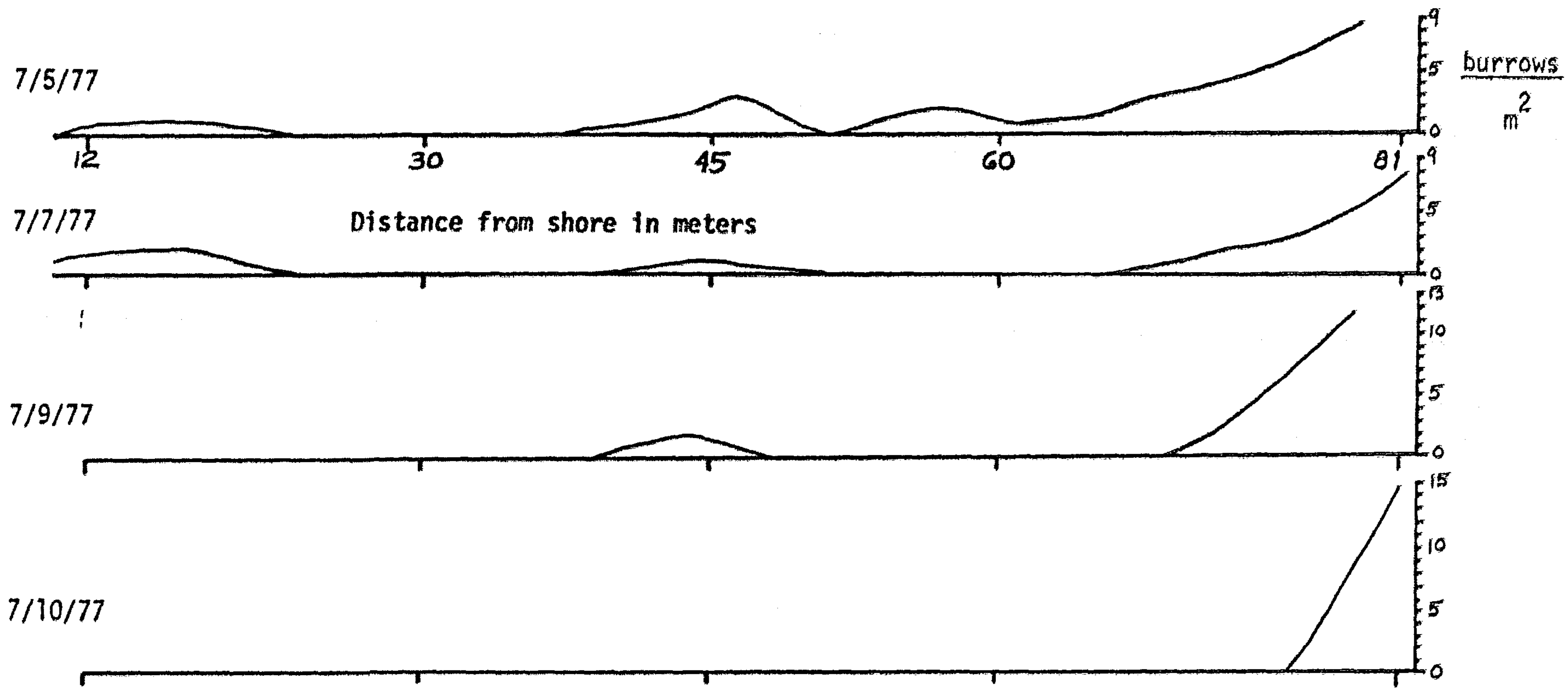

Figure 70A: 1977 burrow profiles

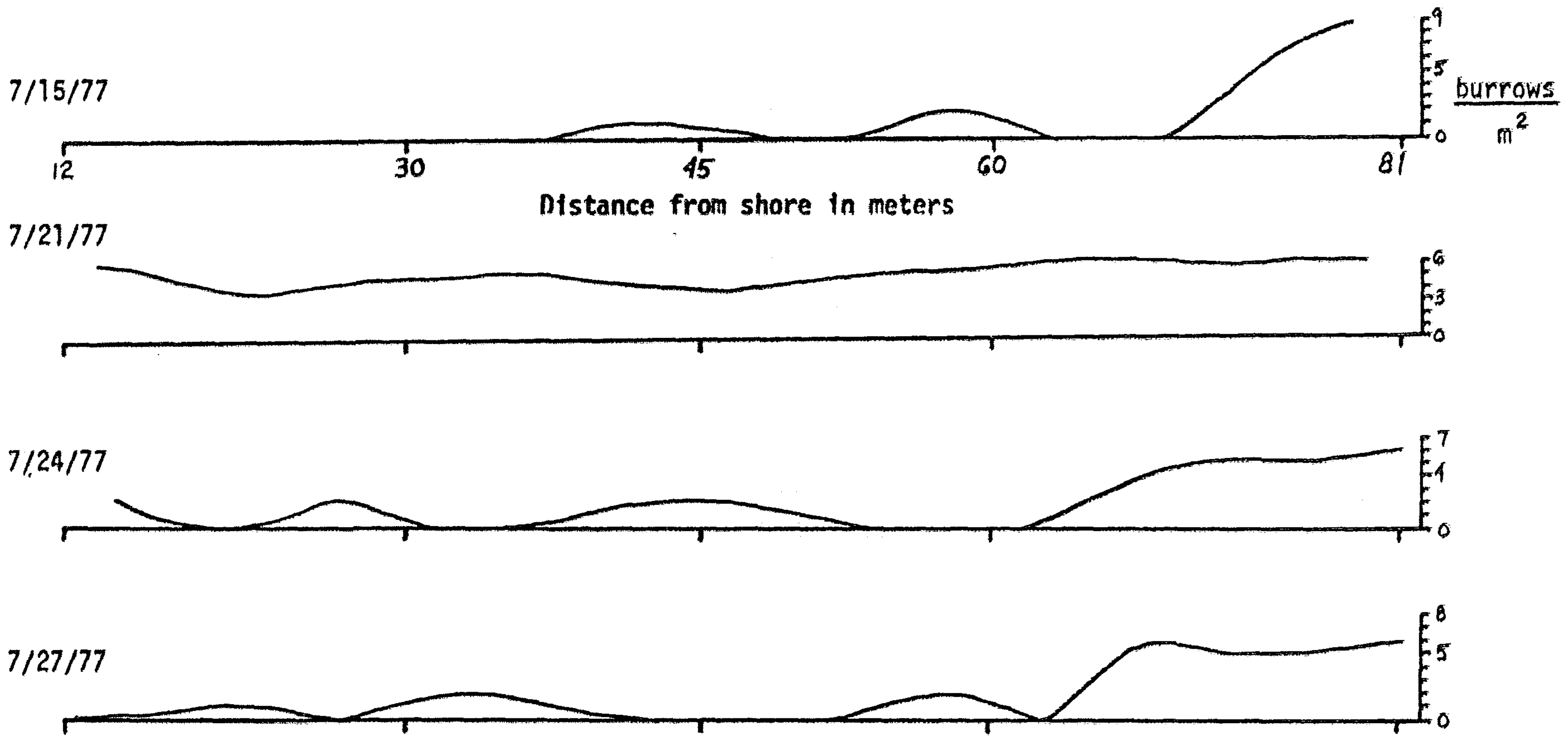

Figure 70b: 1977 burrow profiles

DISCUSSION

Wind, Waves and Bar Topography

The Sea Breeze Cycle

Sonu, et al. (1973) describes and documents the control of coastal wind systems over nearshore processes on the northern Gulf coast. Sonu, et al. studied a beach 50 miles west of Panama City and found that the daily cycle of onshore-offshore winds correlates well with the cyclicity in wave, current, and nearshore topographic behavior. The sea breeze cycle of onshore winds during the daytime and offshore winds at night is driven by the different rates of heat loss of the land versus the ocean under the influence of solar heating. This cycle is widely recognized in coastal regions but along this coast of the Gulf of Mexico it controls all other processes. Sonu, et al. observes that the daytime, onshore breeze peaks in intensity at 1 to 2 PM and maintains a fetch of 50 km over the ocean. The nighttime, offshore breeze is much weaker and has a limited fetch. Onshore wind velocities range from 5 to 10 m/sec which approaches the intensity of storm winds. Wave records from Sonu, et al. indicate that the afternoon is dominated by high-frequency wind waves whose period, amplitude, and direction are controlled by the sea breeze with a one-half hour lag. Wave-induced, nearshore currents change from closed circulation in the morning to meandering currents in the afternoon to shore-parallel currents at night. In general the nearshore currents flow from the shoals (where breakers occur) to the depressions in the submarine topography. Changes in bar patterns, observed over a period of three weeks, were related to the direction and intensity of wind-driven waves. Ripples, megaripples and beach cusps were modified in a period of an hour or two.

The daily cycles of clockwise change in wind direction described from the Panama City Beach wind data confirm the conclusions of Sonu, et al. about this coast. The wind direction rotates clockwise in the northern hemisphere from the nighttime, offshore breeze to the daytime, onshore breeze because of Coriolis force. The occasional dominance of winds from the Southwest (perpendicular to this coast) at Panama City is probably an indication of the superior strength of the onshore wind effect. During periods of significant solar heating in mid-summer the onshore breeze was able to continue through the night although with decreased intensity. Figure 71 shows how the onshore breeze dominated over periods of several days as the average daily temperature gradually increased. In all three incidences shown in the figure the period of constant onshore winds was broken up by the development of thunderstorms and the attendant cooling of average daily air temperature. Like the sea breeze cycle, the thunderstorms are generated by solar heating of the atmosphere. The moist air at sealevel is heated until it rises and cools, losing its moisture as precipitation. Whether the constant onshore breeze is broken-up by the cooling of the air or the atmospheric convection currents is not known but it appears that the thunderstorms are the mechanism which reinstates the onshore-offshore breeze cycle. Therefore these local thunderstorms function like a thermostat in that

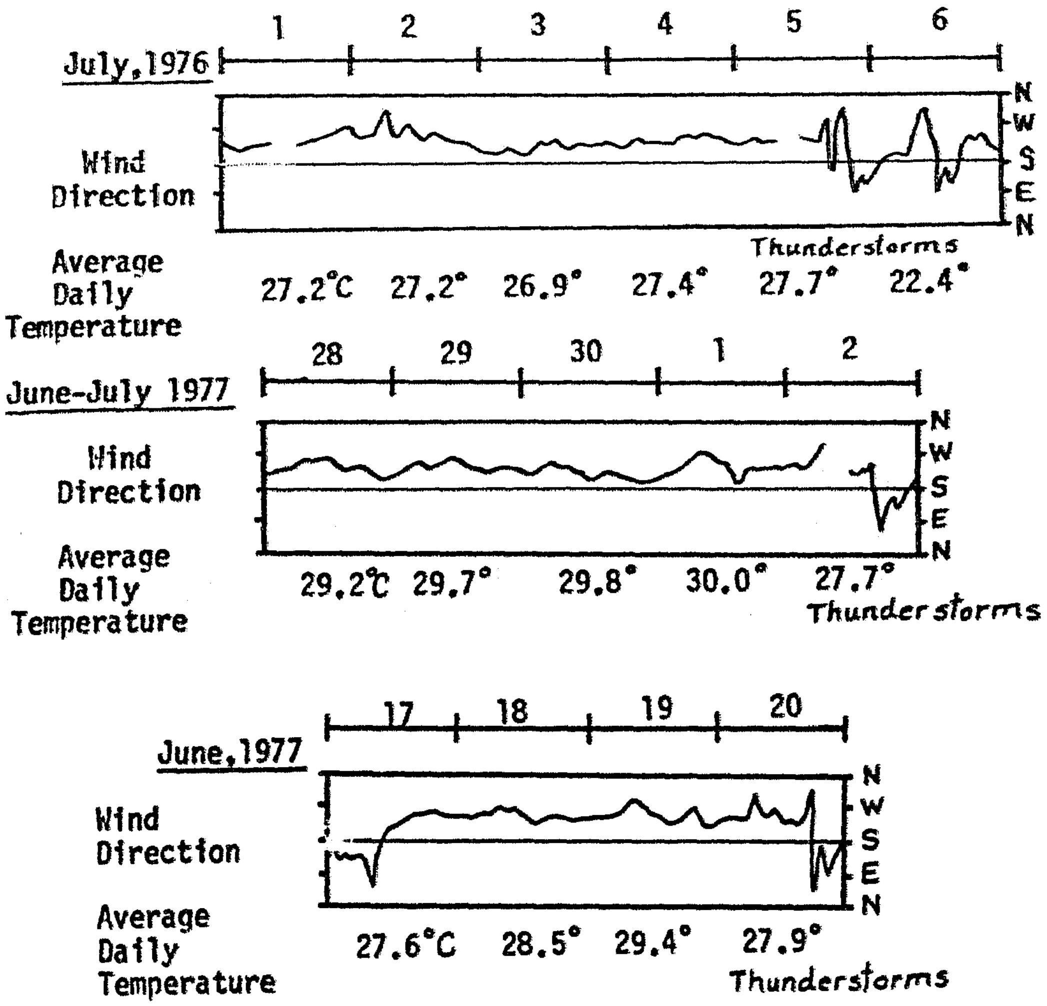

Figure 71: Periods of constant SW winds correlated with average daily temperature trends.

they form because of prolonged solar heating and by their formation they limit any further temperature increase.

Because of the strong relationship between the sea breeze cycle and the wave patterns, the recorded fluctuations in the latter become more meaningful. The wave period, amplitude, and direction are just as constant and predictable as the winds. Peaks in significant wave height correspond to the peak wind velocities in the afternoon or the wave height may build over a period of several days under the influence of constant onshore winds. Occasional frontal storms like the one from July 17-19, 1977 may temporarily disturb the sea breeze pattern but the onshore-offshore winds re-establish themselves immediately thereafter.

Bar Patterns

A comparison of the wind direction records from 1976 and 1977 field seasons shows a significant difference (Appendix A). The 1976 record shows many daily cycles resulting in variable onshore winds while in 1977 there were many periods of constant onshore winds. Sonu, et al. (1973) recognizes two distinct nearshore bar patterns which resulted from these two types of wind patterns. Wind waves which arrive parallel to shore produce a cuspate bar and those which arrive at some angle to the shoreline produce the horn bar pattern. At Panama City Beach the cuspate bar formed under the dominant influence of the sea breeze cycle with its variable onshore winds in 1976. In 1977 the horn bar formed under the dominant influence of nearly constant West-Southwest onshore winds.

A shore-parallel bar like the one observed at Panama City Beach following the frontal storm of July 17-19, 1977 is an entirely different problem. Although the waves from this storm arrived at an angle to shore they did not produce a horn bar. Perhaps the large wave amplitude (2m) and slightly longer wave period influenced the formation of a shore-parallel bar. Hom-ma and Sonu (1963) state that during intense long-shore drift the bar form is smoothed and straightened. King and Williams (1949) found that steep storm waves cause seaward sand transport in the swash and landward sand transport from offshore. The net effect is a steep-profile, longshore bar at an intermediate distance from shore. The exact location of the bar is determined by the location of the breaker zone which is in turn controlled by wave height (Keulegan, 1948). In general, a wave will break when it reaches a depth which is equal to half of its amplitude.

The post-storm modification of the shore-parallel bar indicates a return to the onshore-dominated water motion along the bed of the entire profile. The storm bar profile became flattened and portions of it began to migrate shoreward. The inception of a regularly-spaced cusp system can be seen on aerial photography from July 27, 1977 (Fig. 8) just eight days after the storm. Sonu, et al. (1973) cite the rapid recovery of nearshore topography following hurricanes as proof of the strength of the sea breeze system.

Rhythmic Topography

The origin of rhythmic nearshore topography is a contested issue which has not been satisfactorily resolved. Sonu, et al. (1973) reports the field conditions in which beach cusps and associated rhythmic submarine topography occur. Dolan and Ferm (1968) discuss rhythmic bar topography as part of a heirarchial grouping of rhythmic shoreline features ranging in size from one meter to one million meters. Dalrymple (1976) suggests that beach cusps are caused by the intersection of two separate wave trains. Bowen and Inman (1971) proposed that the rhythmic features are caused by edge waves, a theoretical mechanism which cannot be substantiated by field measurements. Komar (1971) also advocates the edge wave mechanism but emphasizes its indirect influence upon topography through its modification of the breaker height alongshore. Sonu (1972) refutes the edge wave theory on the basis of its inability to generate the necessary velocities for sand transport. One of the more imaginative theories was presented by Preston Cloud (1966) and invoked the principle of Plateau's Rule. The rule states that a liquid cylinder becomes unstable when its length exceeds $2\Pi r$ and breaks up into subequal portions whose lengths are proportional to the diameter of the cylinder. The water motion inside an ocean wave approximates a liquid cylinder and Cloud thinks that during wave collapse the segmentation of the wave front could produce rhythmic topography.

The form of nearshore topography is of interest to this study only in terms of how it controls water depth, wave breakage, and the resultant currents. It should be recognized that the bar topography is shaped by the average wave climate and that it, in turn, provides feedback to the nearshore hydraulics (Sonu, et al., 1966).

Nearshore Hydraulics

Research on the velocity fields in nearshore areas has been complicated by the complexity of the water motion there. The combination of oscillatory water motion of variable asymmetry and unidirectional current flow all in one locality makes description difficult. In addition, the oscillatory motion is short-lived and the hydraulics vary continuously with changing wave characteristics. The latter variable was considered to be constant at Panama City Beach because of the uniform wave character. The brief duration of oscillatory water motion was measurable with the swing-surge velocity meter used in this study.

Clifton, et al. (1971) described the general velocity field and resulting bedforms of a non-barred, high-energy nearshore region on the Oregon coast. He concluded that there was a gradual transition in the onshore direction from symmetric oscillation offshore to increasingly asymmetric oscillation in the surf zone. He allowed that the velocity field was more complicated shoreward of the breakers because of longshore drift, broken waves traveling landward as bores, and seaward return flow from the swash.

Breaking Waves

Miller (1964) was the first to unravel the internal velocity field of a breaking wave. He demonstrated the differences between the velocity fields of spilling and plunging breakers using field measurements. The velocity vectors in a spilling breaker are very asymmetric landward in comparison to those of a plunging breaker. As a result of this difference the reversal from seaward to landward oscillation along the sediment bed during the passage of the wave is sudden and violent. In a later paper (Miller, 1976) Miller used a laboratory flume to demonstrate the presence of vortices within breaking waves. Again he distinguished plunging breakers from spilling breakers, this time on the basis of the number and size of their vortices. Plunging breakers exhibited one or more large vortices of great strength. The spilling breakers generated much smaller vortices which remained near the water surface.

Miller's theory of breaker vortices (Miller, 1976) cannot be argued effectively using the Panama City Beach data because of the predominance of spilling breakers and their weak vortices. My near-surface vertical velocity measurements were larger than those on the bottom but they were still quite small in comparison to horizontal bottom velocities. This fact casts doubt upon the importance of the vortex mechanism in generating bedforms but does not deny their existence within breaking waves.

Roller Vortices

Robert Folk (1976) advocates a vortical theory of water motion for the formation of all bedforms regardless of whether they evolve under current flow or oscillatory flow. The theory is not supported by numerical data and is an elaboration on an idea suggested by G. K. Gilbert in his 1914 flume study. Folk suggests that well-organized, continuous, cylindrical vortices occupy the troughs of ripple fields. The ripple crests supposedly result from the heaping-up of sediment between the rows of roller vortices. The vortices are confined to the boundary layer and are initiated by shear from overlying water layers. In the past it was generally thought that bedforms were a product of shear between the boundary layer and the sediment interface. If Folk's vortices exist then there should be measurable tangential velocity components in the vertical direction as well as the horizontal. Vertical velocities measured within the boundary layer at Panama City Beach are far too weak to suspend the sediment or even maintain its suspension. If vortices exist at all, they form in the lee of ripple crests as weak, disorganized eddies which are a result of the ripple form and not the cause thereof. Tunstall and Inman (1975, p. 3483) found that vortices generated by flow over ripples dissipate only seven percent of the total energy expended on the bottom.

Vertical velocities measured near the water surface in the breaker zone are sufficient to maintain suspension of sand grains. However the sand must be picked up off the bottom by some other mechanism. The mechanism is probably horizontal shear of the water over the sand bed.

Velocity Asymmetry

Clifton's model for the increasing asymmetry of bottom velocities in the onshore direction constitutes an ideal situation which was seldom seen in the field. Although this generalization can be applied to the seaward slope of the inner bar at Panama City Beach, there were many exceptions. The common situation on the back of the bar was one of symmetric oscillation along the bottom, right up to the breaker zone where asymmetric bottom velocities first appeared. The few profiles which do conform to Clifton's model (Fig. 18, July 3, 1976, and Fig. 19, July 5, 1976) coincide with periods of large waves. In view of the fact that larger waves begin to "feel bottom" in deeper water than smaller waves do, this relationship makes sense. Apparently the typical low amplitude, high steepness, wind waves of Panama City Beach did not exert any significant influence on bottom velocities until the waves broke on the bar crest. Bedforms with asymmetric profiles did occur in these zones of symmetric oscillation but their asymmetry was probably preserved by either an occasional large wave or a very slight velocity asymmetry, not measurable with the swing-surge velocity meter.

Longshore and Seaward Flow

Some other exceptions to Clifton's model involve the seaward velocity asymmetries observed on the bar crest and seaward slope. In a few cases these seaward asymmetries result from the presence of a rip current. The velocity profiles from July 11, 1976 (Fig. 22), June 23, 1977 (Fig. 28), and July 15, 1977 (Fig. 37) were probably influenced by rip currents. Their flattened bar profiles and the seaward velocity asymmetry across most of the profile suggests an organized seaward flow. Some other profiles with seaward velocity asymmetry over the bar crest can be explained by other mechanisms. The July 1, 1976 profile (Fig. 16) was influenced by plunging breakers which are known to produce seaward return flow along the bottom. The July 12, 1976 profile (Fig. 23) involved a steep bar form, very close to shore. The seaward flow across this bar crest probably resulted from the large waves which piled up water in the constricted inner trough. In such a case, a general seaward bottom flow would occur all along the bar front instead of being restricted to a narrow channel.

Sonu, et al. (1973) notes that coastlines with rhythmic topography are more subject to general seaward flow than to rip currents. Sonu observed relatively slow, pulsating flows which originated on the bar cusp shoals and then deflected off of the shoreline to flow seaward across intercusp low points in the bar topography (Fig. 72a). This type of nearshore current pattern is called a "circulation cell". It differs from the classical idea of longshore drift because of the opposing flow directions of currents in adjacent cells.

The presence of a horn bar configuration creates a situation where unidirectional longshore currents are well developed and submarine topography exercises complete control over nearshore circulation. The horn bar topography is characterized by discontinuous reaches of the inner trough which slant seaward, away from the shoreline (Fig. 72b). These channels drain the excess water from the nearshore and often produce well-defined rip currents which can operate regardless of the direction of wave approach. The velocity profile from July 9, 1977 (Fig. 34) illustrates the persistence of topographic influence on nearshore currents in the face of opposing waves. On this date the incidence of southeast waves on horn bar topography caused a westerly longshore drift on the seaward side of the bar while a strong easterly drift maintained itself on the landward side of the bar.

The presence of a straight, shore-parallel bar allows bidirectional

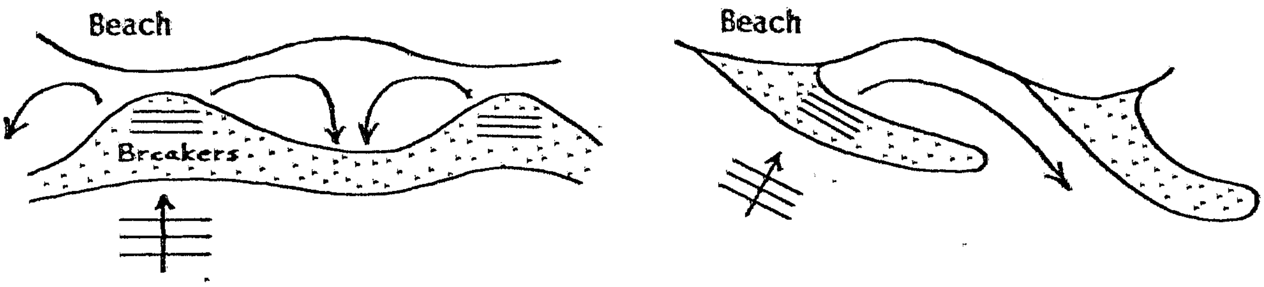

a: Normal wave incidence (circulation cells)

b: Oblique wave incidence (rip currents)

Figure 72a and b: Nearshore circulation patterns.

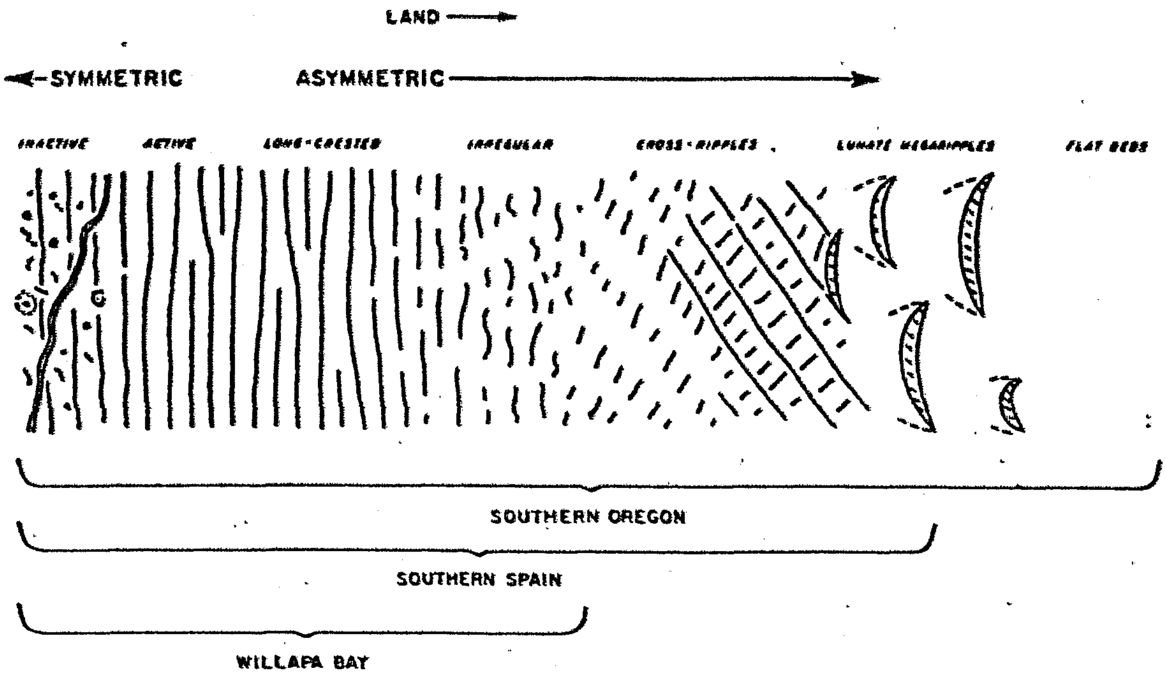

FIGURE 73—Sequence of structures commonly observed off the coast of southern Oregon, southeastern Spain, and Willapa Bay, Washington. Brackets below diagram indicate the range of structures observed in each environment. FROM CLIFTON, 1976, P. 136

longshore currents to form, responding to the direction of wave approach. Cuspate bars such as the one observed in 1976 exhibited longshore drift directions which responded to wave approach direction but were also influenced by topography. A perusal of the bedform plan view maps from 1976 (Figs. 12-23) shows how wave direction and drift direction were in agreement for most but not all dates. The shore-welded cuspate topography observed in 1975 is the classical crescent bar pattern to which Sonu, et al. (1966) attributed the "circulation cell" configuration. The cusps are welded to the shoreline, creating a series of isolated bays, preventing any continuous, alongshore, current flow.

Longshore current velocity measurements were made for several profiles in 1977. The data are too sparse to make any specific statements about trends in velocity magnitude. Results from four profiles show that the maximum, longshore bottom velocity vector was located in the shallow, landward half of the inner trough. Therefore the maximum velocity is not coincident with the thalweg of the inner trough. In open channel flow the maximum velocity vector lies in the thalweg of the stream channel. The measured bottom velocities ranged in magnitude from zero to 55 cm/sec. An Army Corps of Engineers study found that the average annual longshore current rate along this coast was 9.4 to 12.2 cm/sec and the maximum was about 123 cm/sec (Balsillie, 1975, p. 28). Longshore current measurements at the water surface in the inner trough ranged from 20 to 37 cm/sec on July 27 and 28, 1977 according to my data.

Inner Trough Velocity Trends

Oscillatory velocity trends in the inner trough were either symmetric or landwardly asymmetric with the exception of a few velocity profiles across rip channels and zones of seaward flow. The seaward-dominated velocity profiles usually occurred on low profile bars or portions of the bar which were distant from shore. All other profiles demonstrated a variety of velocity trends in the inner trough. Sometimes the trend alternated between landward asymmetry, seaward asymmetry, and symmetric oscillation on a single profile. On other days the inner trough displayed an orderly increase in landward velocity asymmetry between the bar and the swash zone. A single, five meter interval of seaward velocity asymmetry was often measured at the seaward edge of the swash. This repeated occurrence was attributed to the gravity return flow of water from the swash zone.

Swash Velocities

Some of the highest measured velocities ($\geq$92 cm/sec) occur in the swash zone. The landward and seaward components of the swash velocities are often of equal magnitude. This results in symmetric or nearly symmetric oscillation of great intensity. The extremely shallow depths and high velocities in the swash zone cause the most sediment suspension (Brenninkmeyer, 1976) and make this the most competent portion of the nearshore profile.

Bedform Orientation

In the past it was assumed that nearshore ripple crests were oriented parallel to shore. The results of this study show that this is true in a general sense but there are several exceptions. Bedform crestline orientation on the seaward slope of the inner bar is invariably controlled by wave crest orientation. The refraction of wave fronts during shoaling on the bar is duplicated on the bottom in the increasingly shore-parallel orientation of ripple crests in the shoreward direction. Although the ripple crests do not vary more than twenty degrees from the shoreline orientation (with the exception of ladderback ripples) they consistently respond to changes in wave direction. Bedforms on the bar crest are either parallel to shore, parallel to the bar avalanche face or they show influence from longshore currents. A strong longshore current can produce bar crest ripples with orientations perpendicular to shore.

Inner Trough

Bedform orientation in the inner trough is highly variable depending upon wave conditions, strength of nearshore currents, and topography. On most of the dates surveyed the ripple crests in the inner trough were essentially shore-parallel, especially in the shallower, shoreward edge of the trough. When wave energy is low and nearshore currents are weak (which is often the case in the morning) the ripple crests are oriented in patterns which reflect the symmetry of the submarine topography. This pattern (Fig. 49) is probably the result of refraction of low amplitude shore-parallel waves across the inner bar. When a weak longshore current is present, small-amplitude ripples (one cm high) form in the troughs of the shore-parallel bedforms. These trough forms are perpendicular to the larger forms. On days when the longshore current is strong the inner trough bedforms graduate to a full-fledge ladderback ripple system with oscillation forms parallel to wave crests and current forms perpendicular to the longshore current direction. When the longshore current is very strong, sinuous dunes form perpendicular to the current direction in the center of the trough.

Ladderback Ripples

The orientation of ladderback ripple sets in the inner trough is easier to explain than are the ladderbacks on the seaward slope of the inner bar. The ladderbacks in the inner trough have catenary ripple subsets whose asymmetry is always consistent with the direction of longshore current flow. The straight-crested ripple subset is called "the oscillation ripple set" by Komar (1976) and its formation is attributed to wave oscillation. The orientation of the ladderback oscillation ripples in the inner trough at Panama City is generally conformable with wave crest orientation. However the ladderback ripples on the inner bar are not that simple. Although their catenary ripple subset is usually consistent with the general direction of longshore drift, the oscillation (or straight-crested) ripple subset is not parallel to the wave crest orientation. Clifton (1976) noted that the direction of wave approach commonly bisects the angle between the two ripple subsets of the ladderback ripples. Clifton also observed that both ripple sets migrate during a landward oscillation pulse. Both of these observations are true of the ladderback ripples at Panama City Beach.

The transition ripples which often occur in association with ladderbacks do not display any organization or consistent orientation.

Clifton (1976) described these forms as being arranged in an echelon pattern similar to the diagonal pattern of the ladderbacks. It is possible that in a higher energy environment such as the Oregon coast the transition ripples display more regularity.

Bedform Symmetry

The asymmetry of bedforms on the seaward slope of the bar is always landward despite the seaward velocity asymmetry which is occasionally observed there. Bar crest bedforms are also asymmetric-landward with the exception of rip channel bedforms which are sometimes found on the bar crest. Inner trough bedforms are quite variable in asymmetry. The deeper portions of the inner trough display bedforms with landward or longshore asymmetry and the shallower portions display bedforms with landward, seaward, and longshore asymmetry. Symmetric bedforms occur in deep water on the seaward slope of the inner bar and occasionally in the deeper parts of the inner trough.

Bedform Sequence

The persistence of a recognizable sequence of bedforms on the seaward slope of the inner bar, in the zone of shoaling waves, lends itself well to a study of marine bedforms. The surf zone sequence of bedform types observed at Panama City Beach is identical to that observed by Clifton, et al. (1971) on a plane-sloping beach in Oregon (Fig. 73). The only difference being that the average waves on the Gulf Coast are not large enough to produce the complete sequence of bedforms all the way up to plane bed. Clifton, et al. (1971) hypothesized that nearshore marine bedforms are similar to unidirectional current forms in their response to increasing flow intensity. Using various wave theories Clifton, et al. predicted that as waves shoal, the maximum bottom velocity (U_m) and the velocity asymmetry (ΔU_m) both increase onshore. Velocity asymmetry is defined as the difference between the landward and the seaward maximum bottom velocity vector.

The observed sequence of marine bedforms which exists in the zone of gradually-increasing flow intensity is comparable to that observed by Simons, et al. (1965) for stream bedforms. Simons, et al. (1965) found that for a particular size of sediment the following sequence of current bedforms evolves with increasing flow intensity: ripples → dunes → plane bed → antidunes. Clifton, et al. (1971) observed the following sequence in the nearshore: symmetric ripples → asymmetric ripples → ladderback ripples → lunate megaripples → plane bed. Davidson-Arnott, et al. (1976) observed a slightly different bedform progression on a barred beach: symmetric ripples → asymmetric ripples → plane bed → lunate megaripples → plane bed. This sequence was found on the seaward slope of the inner bar and then again in the inner trough.

Factors Controlling Bedform Sequence

Clifton (1976) states that the nature of marine bedforms is controlled by the interaction of many independent variables, including fluid factors (density and viscosity), flow factors (unidirectional currents), wave factors (height, period, direction, and variability), bottom configuration (depth, local and overall slope), and sediment factors (grain diameter, sorting, density, and shape). He assumes constant values for fluid, wave, and sediment factors. He also assumes a uniformly-sloping foreshore and no unidirectional currents. The problem of characterizing the bedforms according to the variables which directly influence the forms then narrows to: U_m, maximum bottom velocity just above the boundary layer; d_o, the diameter of the oscillatory orbit near the bottom; and ΔU_m, the velocity asymmetry.

Velocity Asymmetry

Clifton (1976) contains a series of plots of U_m versus ΔU_m for various ranges of wave period and sediment size. The wave period is used to represent orbital diameter because the orbitals are difficult to measure directly. The plots are based upon shore-based wave observational data and measured water depths from which values for U_m and ΔU_m are calculated using Stokes second-order equation (U.S. Army Coastal Engineering Research Center, 1973). Clifton consulted field data from Inman (1957) and Tanner (1971) to support the validity of his plots. However he states that "virtually no systematic measurements of current velocities exist that can be related to bedform developments and no full-scale experiments have been devised that approach the flow intensities of asymmetric oceanic oscillatory currents" (Clifton, 1976, p. 136).

Figure 74 is a plot of U_m versus ΔU_m similar to that of Clifton (1976) and utilizing data from Panama City Beach. The bedform field boundaries are modeled after Clifton's plot for waves with a five sec-

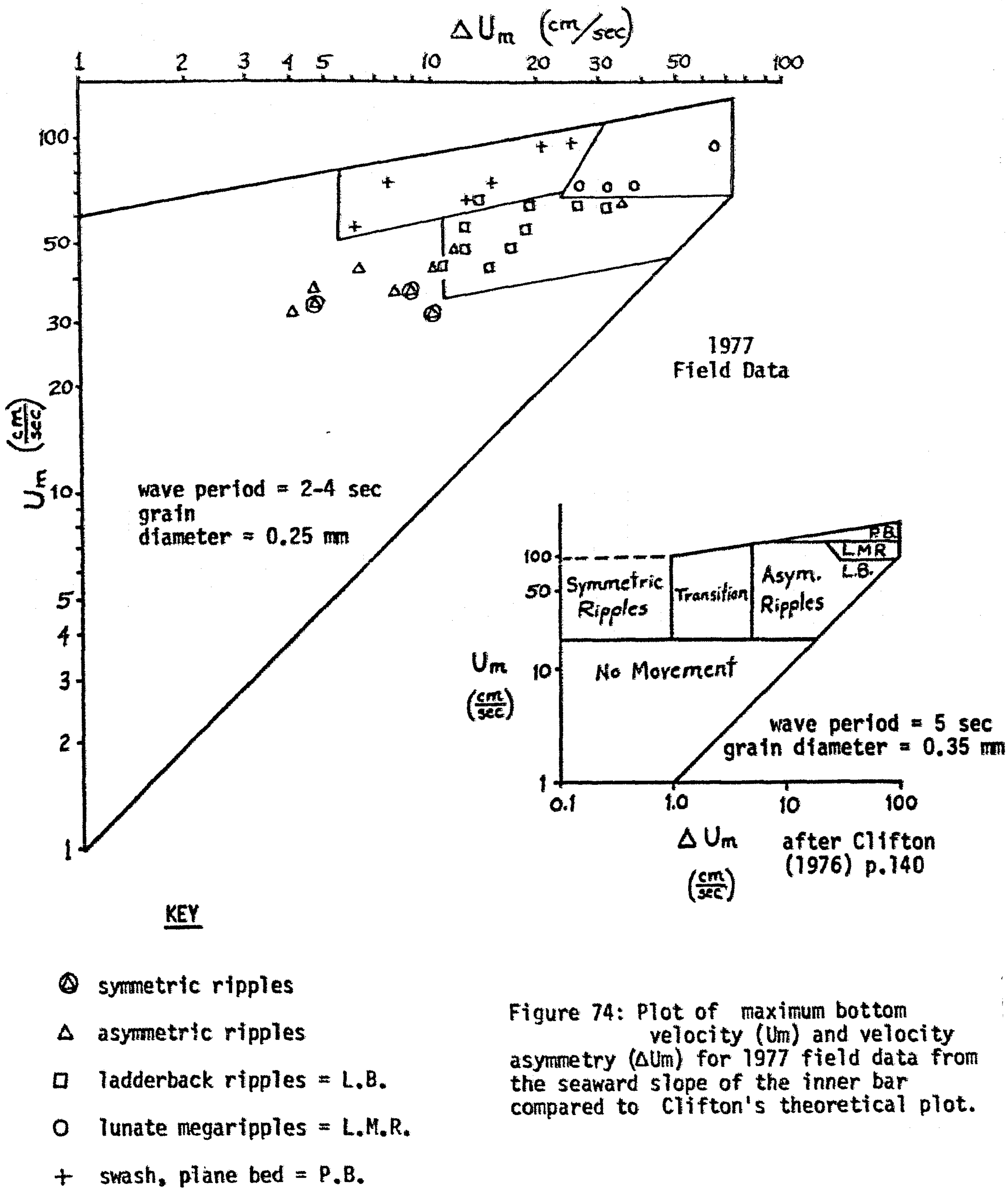

Figure 74: Plot of maximum bottom velocity (Um) and velocity asymmetry (ΔUm) for 1977 field data from the seaward slope of the inner bar compared to Clifton's theoretical plot.

ond period and a sediment diameter of 0.354 mm. The average values for Panama City Beach were two to four second waves and 0.25 mm sand. The field data fits into Clifton's theoretical model fairly well. There is a lack of separation between asymmetric and symmetric ripples that might be accounted for by the difficulty in distinguishing the two underwater. Harms, et al. (1975) states that asymmetric ripples can be formed by a very small amount of velocity asymmetry.

The ladderback and lunate megaripple fields are conformable with those in Clifton's model. Swash plane bed measurements are included in the absence of plane bed data from the bar crest. Although Clifton did not intend that his model be applied to bedforms shoreward of the breaker zone the inclusion of the swash data illustrates a difference between the two types of plane bed. The velocity asymmetry and the absolute magnitude of the measured velocities in the swash zone are significantly lower than the theoretical values proposed for the plane bed formed on the bar crest. There has to be another important variable which affects the bedform and is not considered in this type of plot. The obvious variable is depth.

Depth and Bottom Velocity

A plot of depth and U_m was devised, similar to that used by Southard (1971) for stream bedforms. The resulting plot, using field data from 1977, is shown in Figure 75. The separation of the data points for various bedform types is encouraging. Higher regime marine bedforms occur at shallower depths and higher velocities as do stream bedforms. Southard's stream bedform fields are superimposed on this

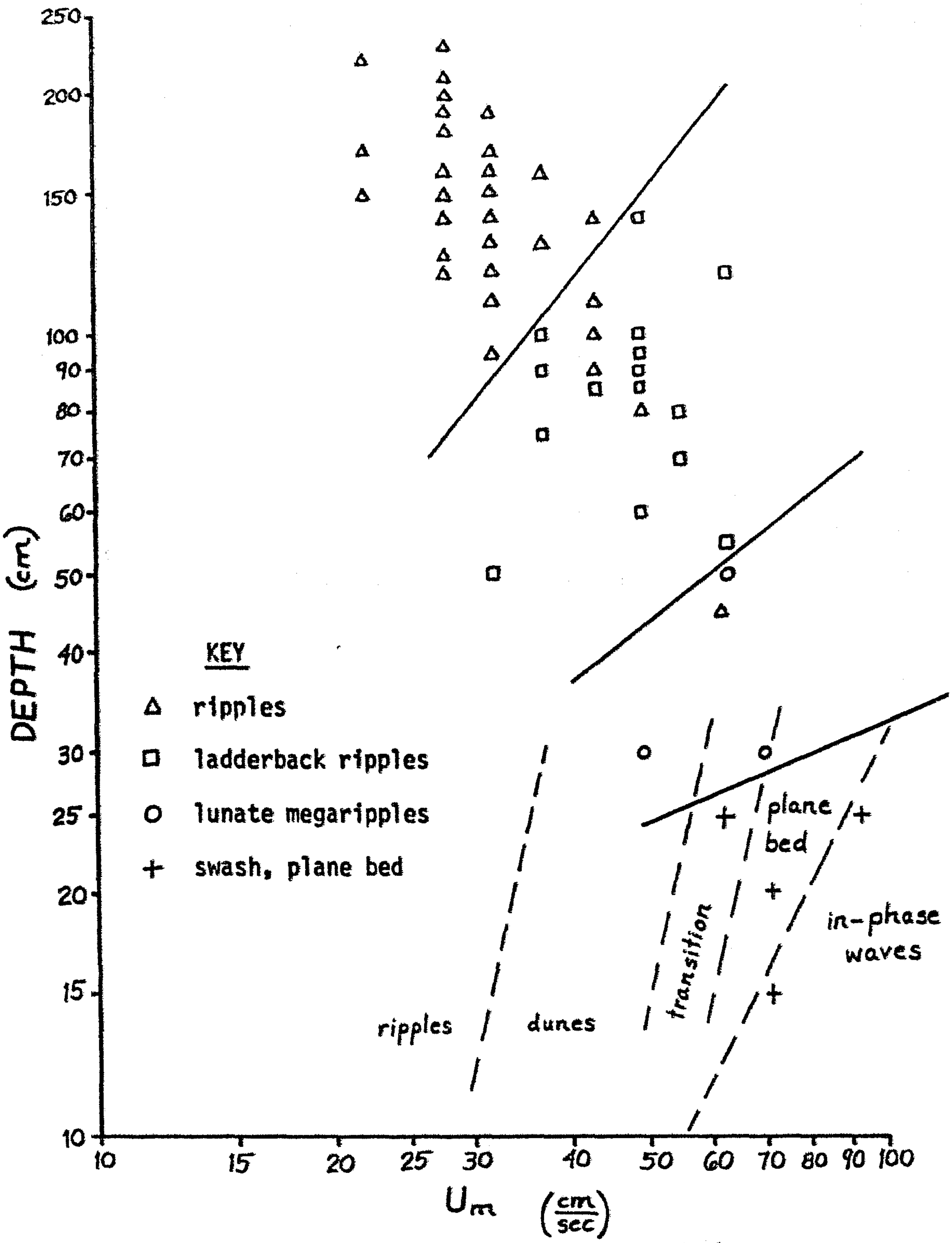

Figure 75: Plot of depth and maximum bottom velocity ; 1977 field data from the seaward slope of the inner bar.

plot for the sake of comparison. One important difference is that Southard's data were originally plotted on a depth and average velocity graph. Here his data are compared to depth and maximum bottom velocity data. Southard's data plots at shallower depths because of the limitations of flume size. His bedform field boundaries have a much steeper slope that those shown for marine bedforms. The slope of his boundaries suggests that stream bedforms might be more dependent upon depth than velocity. The diagonal slope of the marine bedform boundaries suggests an equal dependence upon depth and velocity. The fact that Southard's data were obtained in a laboratory flume with perfectly uniform sediment in fresh water prevents any detailed comparison. Another difference is that the velocity used to characterize the fluvial bedforms is an average value for the entire water column overlying the bed. However the dependence of both marine and fluvial bedforms upon depth and velocity seems clear.

A depth versus bottom velocity plot of 1976 field data failed to discriminate between all of the various bedform classes (Fig. 76). This plot shows many higher regime forms located in lower regime positions among the asymmetric ripples. It would appear that these higher regime forms were measured during waning flow conditions and were therefore out of equilibrium. The dominance of the sea breeze cycle during the 1976 field season might explain the nonequilibrated bedforms. Continuous variability of wind direction would keep the bedforms from reaching equilibrium. Wave conditions during 1976 varied significantly in height and direction relative to the 1977 season. It is extremely

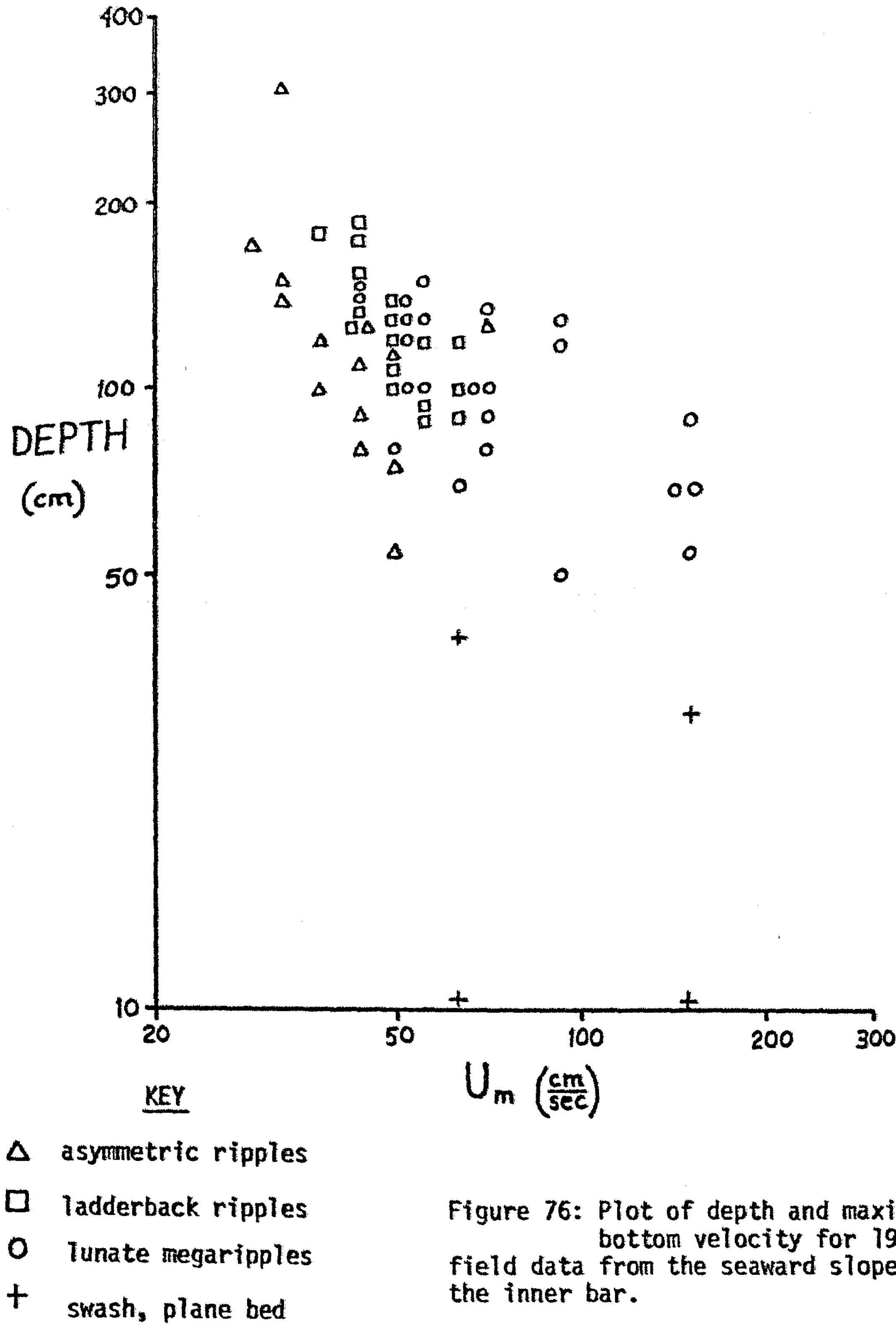

Figure 76: Plot of depth and maximum bottom velocity for 1976 field data from the seaward slope of the inner bar.

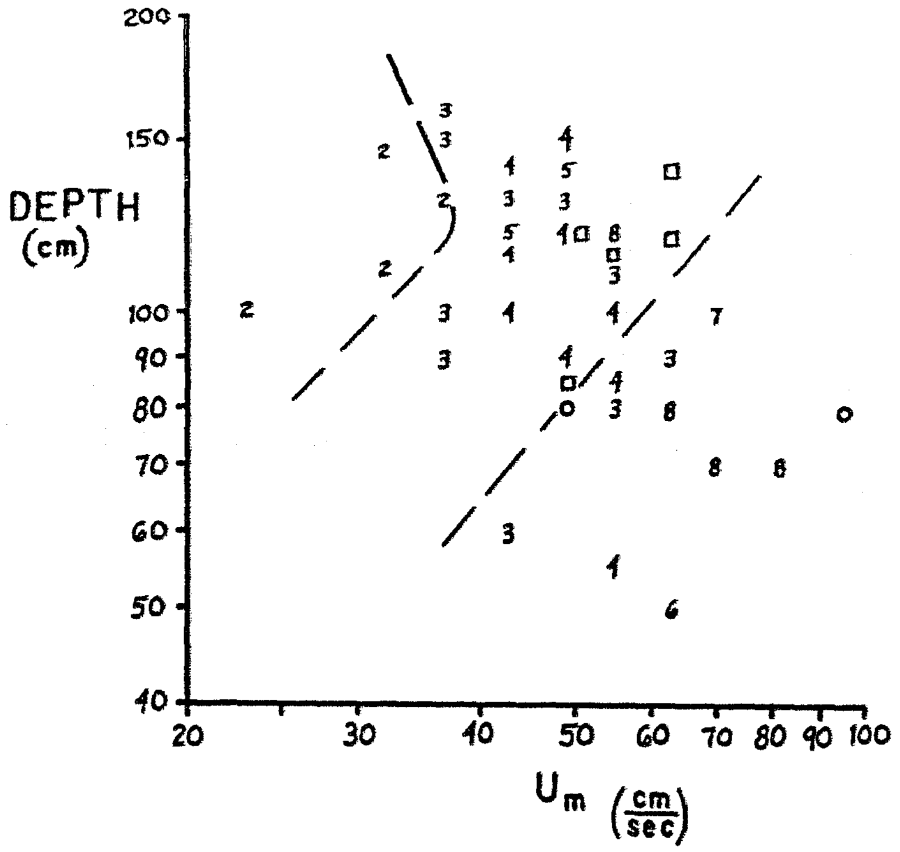

KEY

"3" = asymmetric ripples of 3 cm amplitude

□ = ladderback ripples

O = dunes

Figure 77: Depth vs. maximum bottom velocity for 1976 inner trough bedforms.

difficult to find nearshore marine bedforms in an equilibrium situation.

Inner trough bedform data from 1976 were also plotted in the depth and bottom velocity format (Fig. 77). The bedform fields are not as well defined as the 1977 seaward slope data plot but the same trends are shown. Asymmetric ripple height increases towards the lower right and the higher regime bedforms which are present exhibit the same trend. The inner trough bedforms from 1977 were limited to asymmetric ripples. A depth-velocity plot of this data exhibited no clear-cut trends in ripple heights.

Origin of Ladderback Ripples

The presence of ladderback ripples in a persistent sequence of bedforms on the seaward slope of the inner bar suggests that they represent a distinct stage in the evolution of bedforms with increasing flow strength. Komar (1976) states that ladderbacks are formed by a combination of oscillatory and longshore currents. However the orientations of the two ripple sets comprising the ladderbacks are not perfectly conformable with the orientations of the longshore and oscillatory water motion although they do agree in a general sense. Ripple orientations have been observed to change with wave direction during the course of a day. Given the complexity of water motion in a breaking wave it is possible that there is a stage where the oscillatory and current flow characteristics become equal in strength. Consider the fact that oscillatory motion dominates seaward of the ladderback ripple fields and unidirectional current flow dominates in the landward direction. Ladderback ripples occupy the transition zone. The lunate megaripples which occur landward of the ladderbacks are very similar to the dunes found in current flows. Clifton (1976) observed that lunate megaripples did not form on days when the ocean surface was confused by several directions of wave approach. The need for further research on breaking wave flow transformations is obvious but it appears that ladderback ripples represent a stage in this transition.

Lunate Megaripples

Lunate megaripples are the largest bedforms found in the nearshore (excluding sandbars). The megaripples found in the inner trough have a continuous crestline and smaller dimensions than those on the bar crest. The largest lunate megaripples occur at the seaward edge of the breaker zone and diminish in amplitude and wavelength in both landward and seaward directions. The highest bottom velocities do not occur over the largest bedforms but are instead located over rippled-back lunate megaripples of smaller dimensions on the bar crest. This trend emphasizes the importance of water depth in controlling bedform character. There were a few occurrences of lunate megaripples with amplitudes as low as four centimeters. These bedforms were either being transformed into lower regime structures or being washed-out by higher regime flow, transitional to a plane bed.

Summary of Bedform Parameters

Table 2 summarizes the dimensions of the bedforms on the seaward slope of the inner bar and the values of the flow factors affecting

BEDFORM	AVERAGE AMPLITUDE	WAVELENGTH	U_m	ΔU_m	DEPTH
Symmetric Ripples	$\bar{x}$ = 3 cm range = 2-4 cm	$\bar{x}$ = 15 cm range = 10-20 cm	28-36.6 $\frac{cm}{sec}$	0-10 $\frac{cm}{sec}$	1.4 - 1.8 m+
Asymmetric Ripples	$\bar{x}$ = 2-3 cm range = 1-4 cm	$\bar{x}$ = 10-20 cm range = 10-40 cm	22-45 $\frac{cm}{sec}$	4-6 $\frac{cm}{sec}$	0.8 - 2.0 m
Ladderback Ripples	straight-crested $\bar{x}$ = 2-4 cm range = 2-7 cm catenary-crested $\bar{x}$ = 2-3 cm range = 1-4 cm	straight-crested $\bar{x}$ = 30-50 cm range = 20-70 cm catenary-crested $\bar{x}$ = 10-20 cm range = 8-30 cm	32-62 $\frac{cm}{sec}$	10-32 $\frac{cm}{sec}$	0.5 - 1.4 m
Lunate Megaripples	$\bar{x}$ = 10-15 cm range = 9-26 cm	$\bar{x}$ = 1-2 m range = 0.5-3.0 m	50-92 + $\frac{cm}{sec}$	25-60 $\frac{cm}{sec}$	0.3 - 0.8 m

Table 2: Summary of average bedform parameters from field data. Note- "+" indicates that the magnitude may exceed the range of values given.

them. The values in this table reiterate the trends already displayed in graphical form in Figures 75, 76 and 77. One interesting and new aspect is the range in ladderback ripple amplitudes. In the past the distinction between ripples and dunes has been the large gap between their characteristic amplitudes (ripples are $\leq$4 cm and dunes are $\geq$9 cm (Harms, et al., 1975)). Ladderback ripple amplitudes fill this gap and provide a continuum of values through the range of ripples, ladderbacks, and lunate megaripples. Therefore the distinction between ripples and dunes is more marked for current bedforms than it is for marine bedforms.

Dependence on Nearshore Topography

In the previous discussion of marine bedforms and their evolution with increasing flow strength, very little attention was given to the overall bedform patterns. The bedforms dealt with in the plots were primarily those occupying the seaward slope of the inner sand bar. That is because this portion of the nearshore is the easiest to interpret in terms of hydraulics. The inner trough forms are subject to more variability in terms of oscillatory and unidirectional currents and topographic influence. A model for bedform development in the inner trough was not attempted here because of a lack of field time. Details of the longshore current structure and the inner trough topography would be required to accurately describe the controlling factors for these bedforms. The form of the inner bar plays a large role in controlling the processes which in trurn control the bedforms. The bedform distribution, types, dimensions, and orientations all exhibit a strong relationship to nearshore topography. This dependence on submarine topography is probably not as marked on plane-sloping beaches such as the one Clifton, et al. (1971) studied. With such a simple bottom configuration the most significant effects on bedforms are probably wave variability and tidal control of water depth. Shorelines exhibiting rhythmic topography such as the Gulf Coast are more common than plane-sloping beaches in the modern environment (Komar, 1976). Therefore my study has wide applicability.

Internal Structure

Figure 78 is an idealized cross section of the nearshore, summarizing the sedimentary structures discovered by box coring. There is nothing revolutionary in this depiction of the internal structures. The nearshore facies described from a double-barred nearshore in New Brunswick, Canada by Davidson-Arnott, et al. (1976) are essentially the same. The main difference is the better preservation of cross-bedding in the New Brunswick beach.

Physical structures dominate the swash zone and the bar avalanche face. The internal structure of the swash zone is characterized by well-defined coarse and fine layers of sand and shell. The layers dip seaward at angles of less than ten degrees. The bar avalanche face produces large-scale, tangential cross-bedding which is the largest feature found here. An unconformity within the inner bar spearates an earlier and lower-profile bar from the overrriding cross-bedding of a

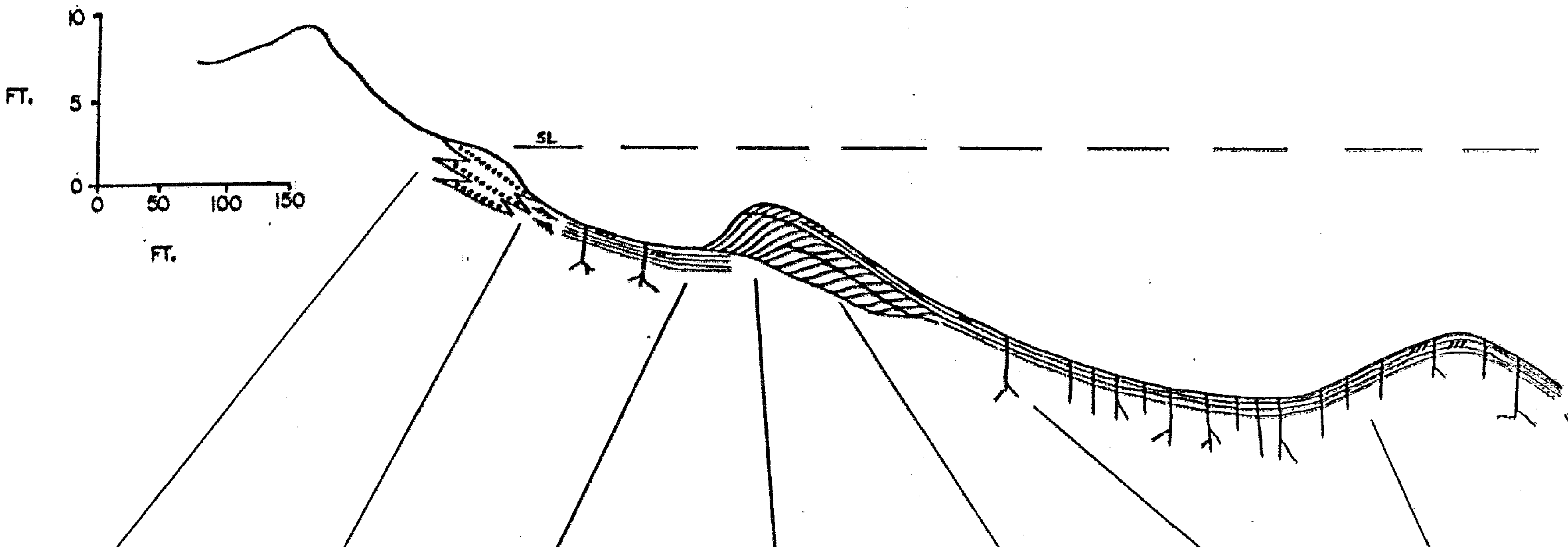

SWASH	INNER TROUGH	AVALANCHE FACE	BAR CREST	SEAWARD SLOPE	OUTER TROUGH	OUTER BAR
coarse, shelly, seaward-inclined layers	ripple cross-beds and horizontal laminae; some shell and burrows	large-scale cross-beds; no shell	medium and small-scale cross-beds; horizontal to seaward-inclined laminae; no shell	small-scale cross-beds dip landward and seaward; parallel laminae dip seaward	vague parallel laminae; bioturbation dominates	landward ripple cross-beds; parallel laminae and bioturbation

Figure 82: Summary of nearshore internal sedimentary structures.

more recent bar.

The inner bar crest and seaward slope contain a lot of fine, parallel laminae which dip gently seaward, parallel to the surface slope. The internal structure of the bar crest includes occasional examples of medium and small-scale cross-bedding. The medium-scale cross-beds are produced by lunate megaripple migration and they dip landward. Ripple cross-bedding is present but does not reflect the abundance of rippling at the surface of the sediment bed. Further down the seaward slope of the inner bar the occasional lenses of ripple cross-bedding dip both landward and seaward.

The inner trough sediments are parallel-laminated with occasional ripple cross-bedding and burrow structures. Layers of abundant shell debris from periods of weak longshore current flow alternate with clean sands from periods of strong longshore current. The dip of ripple cross-beds is dominantly landward but seaward dips are abundant near the swash zone.

The outer trough and outer bar have the least distincitive internal structure except for the abundant burrow structures. Physical sedimentary structures are limited to the ever-present fine parallel laminae and some landward-dipping ripple foresets on the outer bar crest. It is surprising to find any preservation of physical structures in the bioturbated outer trough. Fine parallel laminae are the most often observed structure in the twenty-nine box cores of the nearshore. Newton (1968) observed that this type of planar bedding can result from migration of long-crested ripples under conditions of slow sediment accumulation. The other possible origin for planar bedding is upper regime flow. At Panama City Beach, upper regime flow is confined to the swash and probably the inner bar crest during large (storm) waves.

Preservation

The preservation of nearshore sand deposits is usually limited to storm deposits (Harms, et al., 1975). The depth of scour induced by typical, daily, wave conditions is sufficient to remove sand accumulations to at least a depth of one half meter. The daily changes in measured topographic profiles shown in this paper support this fact. The removal of sand to the offshore by storm waves is a more likely way to preserve the nearshore sands in the geologic record. If the Panama City Beach nearshore were to experience a rise in sealevel then the burrowing organisms offshore would migrate landward and obliterate all physical structure. However, the coarser sand layers in the swash might retain enough of their identity to allow recognition of the nearshore sand body in the rock record. Sea level drop would expose the beach sands to wind erosion and chemical alteration resulting in poor preservation.

Figure 79 shows an idealized nearshore stratigraphic sequence for a regressive shoreline. Under conditions of abundant sediment supply a prograding shoreline on the Panama City Beach could produce a deposit similar to this. The sequence of bedding types would be the most important characteristic used to recognize the nearshore origin of these sands. The transition from bioturbated offshore sands to shoreward-dipping, bar avalanche face cross-beds to low-angle, seaward-dip-

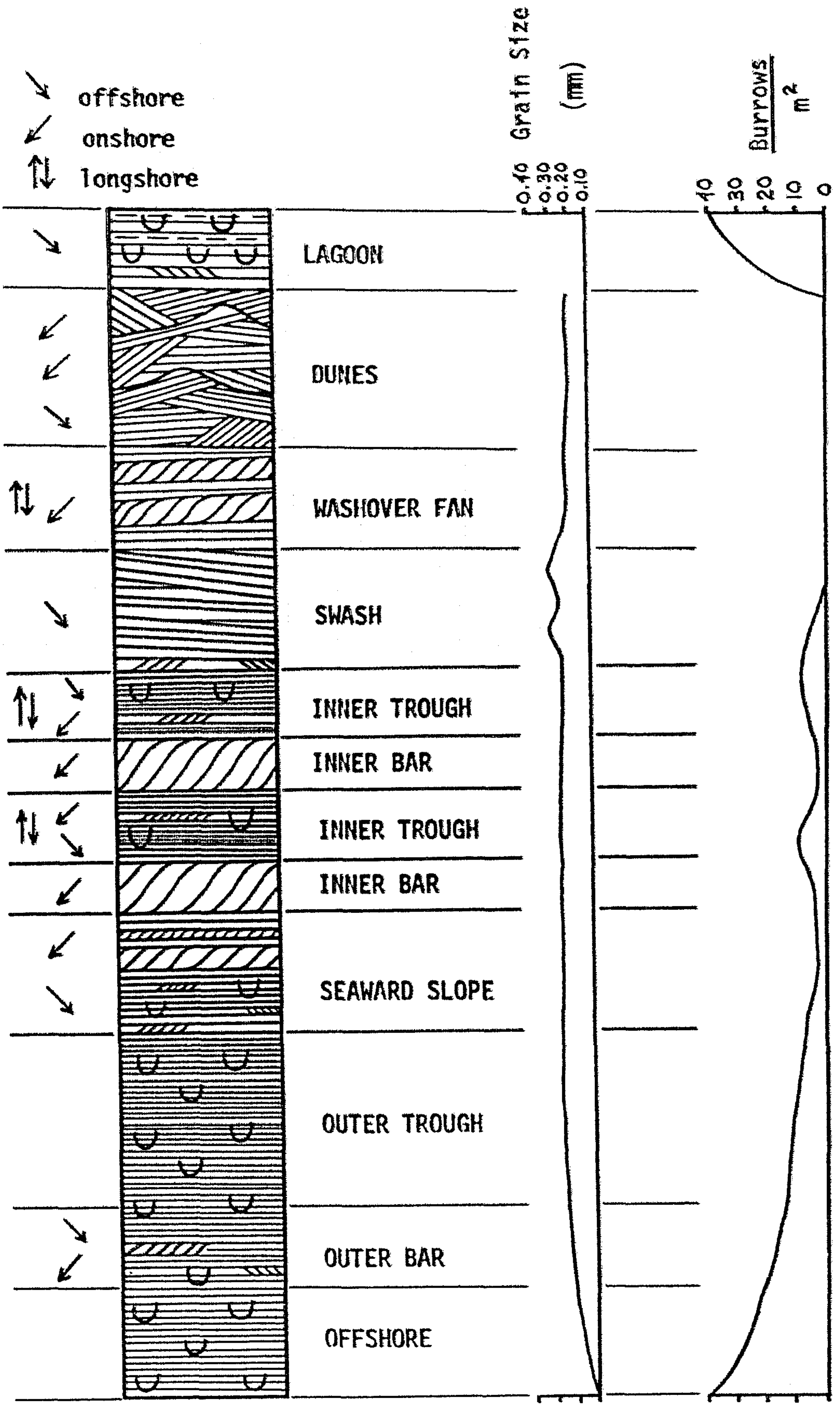

Figure 79: Model of nearshore stratigraphic sequence.compiled from Panama City Beach data.

ping swash layers is most distinctive.

Other distinctive characteristics of the nearshore sedimentary deposits include the variability of bedding dip direction. Most bedding dips landward but seaward and alongshore dips are also quite abundant. The grain size and sorting are most uniform throughout these sands. Bioturbation is most abundant in quiet water areas such as the lagoon and offshore (Frey, Howard, and Pryor, 1978). Bioturbation in the subaerial beach is largely confined to crab burrows for which there is no data on abundance.

Biota

Carl Saloman (1976) conducted a detailed survey of the biota of the Panama City Beach nearshore during 1975. His results are of interest to this study in terms of the effect of burrowing organisms on the preservation of physical bedding texture.

Saloman (1976, p. 2) found that the most abundant taxa in the Panama City nearshore is 69 species of polychaetes. Fourteen of the species of polychaetes made up 80 percent of the individuals recovered. Amphipods (sand fleas), Donax (surf clams), and polychaetes (worms) are the most abundant infauna distributed across the nearshore. Less abundant, but more significant in terms of burrow size is the presence of Callianassa shrimp and heart urchins. Both organisms inhabit the inner trough, the seaward slope of the inner bar and the outer trough and bar.

Saloman (1976) discovered that the number of species and the diversity index is lowest in the swash and both parameters increase steadily offshore. Surveys were made on a daily basis before and after Hurricane Eloise on September 23, 1975 with surprising results. The number of species and individuals increased rapidly on the day after the hurricane and remained high for six days! Thereafter it dropped until the last sampling date. This fact would make it difficult to preserve even storm deposits if it were not for the fact that 75 percent of the individuals were found in the first ten centimeters of the sediment (Saloman, 1976). Thicker, rapidly-deposited, sand deposits have some chance for preservation.

CONCLUSIONS

1. The regularity of the nearshore processes at Panama City Beach under the influence of the sea breeze system allows controlled experiments on bedform behavior.
   a. Wave character is a direct function of daily wind patterns.
   b. Wave approach direction is variable on days when the sea breeze cycle is operating and is from the Southwest to West on days when the onshore winds dominate.
   c. Nearshore topography is normally controlled by the direction of wave approach and sometimes by wave size during prolonged storm conditions (more than a day in duration).
2. Submarine topography plays a dominant role in the breaking wave hydraulics, the wave-induced nearshore currents, and the nearshore bedforms.
   a. Topography is involved in a dynamic relationship with wave character such that each parameter modifies the other in a constant quest for equilibrium.
   b. Topography appears to be the dominant control over bedform type and distribution on coasts with rhythmic topography.
   c. The "horn" bar pattern exercises complete control over nearshore current direction and some influence upon its intensity.
3. The presentations in this study, of coordinated bedform and

velocity data for nearshore bedforms represents a first step in the interpretation of the flow regime of structures preserved in the geologic record.

4. Nearshore marine bedforms can be successfully discriminated on a depth-velocity plot like that used by Southard (1971) for unidirectional flow bedforms.
   a. Bedforms on the seaward slope of the inner bar, in the zone of shoaling waves, are best discriminated on such a plot.
   b. Inner trough bedforms are subject to highly variable flow conditions and therefore cannot be discriminated as well on a depth-velocity plot.
   c. Field data from this study conforms fairly well with a theoretical plot involving maximum bottom velocity (U_m) and velocity asymmetry (ΔU_m).

5. Ladderback ripples are unique bedforms which probably reflect the transformation from oscillatory motion to unidirectional flow in the surf zone.
   a. Lunate megaripples may be the closest thing to a unidirectional flow bedform found in the nearshore.
   b. In the swash, a plane bed results from near-symmetric oscillation of high intensity. This situation contrasts sharply with the unidirectional flow attributed to plane beds formed under breaking waves (Clifton, 1976).
   c. The vortical theory of ripple formation (Folk, 1976) is not

supported by velocity data gathered at Panama City Beach.

6. Internal structure in the Panama City Beach nearshore sands is dominantly fine, plane, parallel lamination. The bar avalanche face produces large-scale cross-beds which are the most prominent feature observed.
   a. Physical sedimentary structures are not well preserved in the Panama City Beach sands because of the uniform nature of the sediment, daily reworking of the deposits, and bioturbation.
   b. Storms provide the most promising mechanism for preservation of nearshore sedimentary structures.
7. Recommendations for future work on nearshore marine bedforms include:
   a. Fuller instrumentation of the nearshore than was possible in this study to detail the continuous fluctuations in longshore current, wave character, and bottom velocity.
   b. The gathering of bedform and velocity data associated with storm wave conditions, which are the most important in terms of the geologic record.
   c. Laboratory studies of the transformation from oscillatory to unidirectional flow associated with breaking waves.

Bibliography

Allen, John R. L., 1968, Current Ripples. Ansterdam: North-Holland Pub. Co., 433 p.

Balsillie, J. H., 1975, Analysis and interpretation of littoral environment observation (LEO) and profile data along the western panhandle coast of Florida: Fort Belvoir, Va., U.S. Coastal Engineering Res. Center, Tech. Memo No. 49, 104 p.

Bowen, A. J., and Inman, D. L., 1971, Edge waves and crescentic bars: Jour. Geophys. Res., v. 76, no. 36, p. 8662-8671.

Breeding, J. Ernest, 1972, Refraction of gravity water waves: NCRL Rept. 124-72, 161 p.

Brenninkmeyer, B. M., 1976, Sand fountains in the surf zone: in Davis and Ethington, eds., Beach and Nearshore Sedimentation: Soc. Econ. Paleontologists and Mineralogists Spec. Publ. no. 24, 187 p.

Clifton, H. E., Hunter, R. E., Phillips, R. L., 1971, Depositional structures and processes in the non-barred high energy nearshore: Jour. Sed. Pet., v. 41, no. 3, p. 651-670.

Clifton, H. Edward, 1976, Wave-formed sedimentary structures - a conceptual model: in Davis and Ethington, eds., Beach and Nearshore Sedimentation: Soc. Econ. Paleontologist and Mineralogists Spec. Publ. no. 24, 187 p.

Cloud, Preston, 1966, Beach cusps: response to Plateau's rule: Science, v. 154, no. 3751, p. 890-891.

Dalrymple, R. A., and Lanan, G. A., 1976, Beach cusps formed by intersecting waves: Geol. Soc. America Bull., v. 87, p. 57-60.

Davidson-Arnott, Robin G. D., and Greenwood, Brian, 1974, Bedforms and structures associated with bar topography in the shallow water wave environment, Kouchibouguac Bay, New Brunswick, Canada: Jour. Sed. Pet., v. 44, no. 3, p. 698-704.

Davidson-Arnott, R. G. D., and Greenwood, Brian, 1976, Facies relationships on a barred coast. Louchibouguac Bay, New Brunswick, Canada: in Davis and Ethington, eds., Beach and Nearshore Sedimentation: Soc. Econ. Paleontologists and Mineralogists Spec. Pub. no. 24, p. 419-168.

Dolan, Robert, and Ferm, J. C., 1968, Crescentic landforms along the Atlantic Coast of the United States: Science, v. 159, p. 627-629.

Draper, L., 1966, The analysis and presentation of wave data - a plea for uniformity: Proc. of 10th Coastal Engineering Conf., Chap. 1, p. 1-11.

Folk, Robert L., 1976, Rollers and ripples in sand, streams, and sky: rhythmic alteration of transverse and longitudinal vortices in three orders: Sedimentology, v. 23, p. 548-669.

Frey, R. W., Howard, J. D., and Pryor, W. A., 1978, Ophiomorpha: its morphologic, taxonomic and environmental significance: Palaeogeography, Palaeoclimatology, Palaeoecology, v. 23, p. 199-229.

Gilbert, G. K., 1914, Transportation of debris by running water: U.S.G.S. Prof. Paper no. 86, 263 p.

Harms, J. C., and Fahnestock, R. K., 1965, Stratification bedforms, and flow phenomena: in G. V. Middleton, ed., Sedimentary processes: hydraulic interpretation of primary sedimentary structures: Soc. Econ. Paleontologists and Mineralogists, Reprint Series no. 3, p. 95-127.

Harms, J. C., Southard, J. B., Spearing, D. R., and Walker, R. G., 1975, Depositional environments as interpreted from primary sedimentary structures and stratification sequences: Soc. Econ. Paleontologists and Mineralogists, Short Course No. 2, 161 p.

Hom-ma, M., and Sonu, C. J., 1963, Rhythmic patterns of longshore bars related to sediment characteristics: Proc. 8th Conf. on Coastal Engineering, p. 248-278.

Inman, D. L., 1957, Wave generated ripples in nearshore sands: U. S. Beach Erosion Board Tech. Memo no. 82, 30 p.

Keulegan, Garbis, H., 1948, An experimental study of submarine sand bars: Beach Erosion Board Tech. Rept. no. 3, 40 p.

King, C. A. M., and Williams, W. W., 1949, The formation of movement of sand bars by wave action: Geog. Jour., v. 107, p. 70-84.

Kirst, A., Jr., and Gaul, R. D., 1964, Summary of automated environmental data collected off Panama City, Florida: (unpublished) Texas A & M Univ., Dept. of Oceanography and Meteorology, Ref. 65-2T.

Kofoed, J. W., and Gorsline, D. S., 1963, Sedimentary environments in Applachicola Bay and vicinity, Florida: Jour. Sed. Pet., v. 33, no. 1, p. 205-223.

Komar, Paul D., 1971, Nearshore cell circulation and the formation of giant cusps: Geol. Soc. America Bull., v. 82, p. 2643-2650.

Komar, Paul D., 1973, An occurrence of "Brick Pattern" oscillatory ripple marks at Mono Lake, California: Jour. Sed. Pet., v. 43, no. 4, p. 1111-1113.

Komar, P. D., 1976, Beach Processes and Sedimentation. Englewood Cliffs, N. J.: Prentice-Hall, 429 p.

Kumar, Naresh, and Sanders, J. E., 1976, Characteristics of shoreface storm deposits: modern and ancient examples: Jour. Sed. Pet., v. 46, no. 1, p. 145-162.

Manohar, Madhav, 1955, Mechanics of bottom sediment movement due to wave action: Beach Erosion Board Tech. Memo 75, 121 p.

Miller, R. L., 1976, Role of vortices in surf zone prediction: sedimentation and wave forces: in R. A. Davis and R. L. Ethington, eds., Beach and nearshore sedimentation: Soc. Econ. Paleontologists and Mineralogists, Spec. Pub. No. 24, 187 p.

Neumann, Gerhard and Willard Pierson, Jr., 1966, Principles of Physical Oceanography. Englewood Cliffs, N. J.: Prentice-Hall, Inc.

Newton, Robert S., 1968, Internal structure of wave-formed ripple marks in the nearshore zone: Sedimentology 11, p. 275-292.

Pryor, W. A., 1973, Permeability-porosity patterns and variations in some Holocene sand bodies: Amer. Assoc. Pet. Geol. Bull., v. 57, p. 162-189.

Saloman, Carl H., 1976, The benthic fauna and sediments of the nearshore zone off Panama City beach, Florida: U.S. Army Corps CERC, Misc. Rept. no. 76-10, 256 p.

Simons, D. B., Richardson, E. V., and Nordin, C. F., 1965, Sedimentary structures generated by flow in alluvial channels: in G. V. Middleton, ed., Primary sedimentary structures and their hydrodynamic interpreation: Soc. Econ. Paleontologists and Mineralogists, Spec. Pub. 12, p. 34-52.

Sonu, C. J., McCloy, J. M., and McArthur, D. S., 1966, Longshore currents and nearshore topographies: 10th Conf. of Coastal Engineering, v. 1, p. 525-549.

Sonu, Choule J., 1972, Comment on paper by "Bowen and Inman (1971) Edge Waves & Crescentic Bars": Jour. Geophys. Res., v. 77, no. 33, p. 6629-6631.

Sonu, Choule J., 1972, Field observation of nearshore circular and meandering currents: Jour. Geophys. Res., v. 77, no. 18, p. 3232-3247.

Sonu, C. J., Murray, S. P., Hsu, A. A., Suhayda, J. N., and Waddell, E., 1973, Sea breeze and coastal processes: EOS Trans., v. 54, no. 9, p. 922-933.

Southard, J. B., 1971, Representation of bed configurations in depth-velocity-size diagrams: Jour. Sed. Pet., v. 41, no. 4, p. 903-915.

Stapor, F. W., 1971, Sediment budgets on a compartmented low-to-moderate energy coast in NW Florida: Marine Geol., v. 10, no. 12, p. M1-M7.

Tanner, Wm. F., 1971, Numerical estimates of ancient waves, water depth and fetch: Sedimentology, v. 16, p. 71-88.

Tolbert, W. H., and Austin, G. B., 1956, Oceanographic data collected off Panama City beach, Florida during the period April 12, 1955 through December 28, 1955: USNMDL, Data Rept. no. 5602 (G-X-14).

Tolbert, W. H., and Austin, G. B., 1959, On the nearshore marine environment of Gulf of Mexico at Panama City, Florida, UNSMDL, Tech. Paper no. 161, 104 p.

Tunstall, E. B., and Inman, D. L., 1975, Vortex generation by oscillatory flow over rippled surfaces: Jour. Geophys. Res., v. 80, no. 24, p. 3475-3484.

U.S. Army Coastal Engineering Research Center, 1973, Shore Protection Manual: U. S. Army Coastal Eng. Res. Cent., 3 volumes.

U. S. Army Corps of Engrs., Mobile District, 1976, Beach Erosion Control and Hurricane Protection, Panama City, Florida, 85 p. + Appendices (2 vols.)

Walker, R. G., 1967, Turbidite sedimentary structures and their relationship to proximal and distal depositional environments: in G. V. Middleton, ed., Sedimentary processes: Hydraulic interpretation of primary sedimentary structures: Soc. Econ. Paleontologists and Mineralogists, Reprint Servies No. 3, p. 95-127.

APPENDIX A

This appendix contains Panama City Naval Coastal Research Lab plots of environmental data from the summers of 1975, 1976, and 1977. Appendix A also contains wind roses plotted on a weekly basis for the 1976 and 1977 field seasons. Wind rose data was derived from NOAA weather observations accumulated at Tyndall AFB, southeast of Panama City Beach.

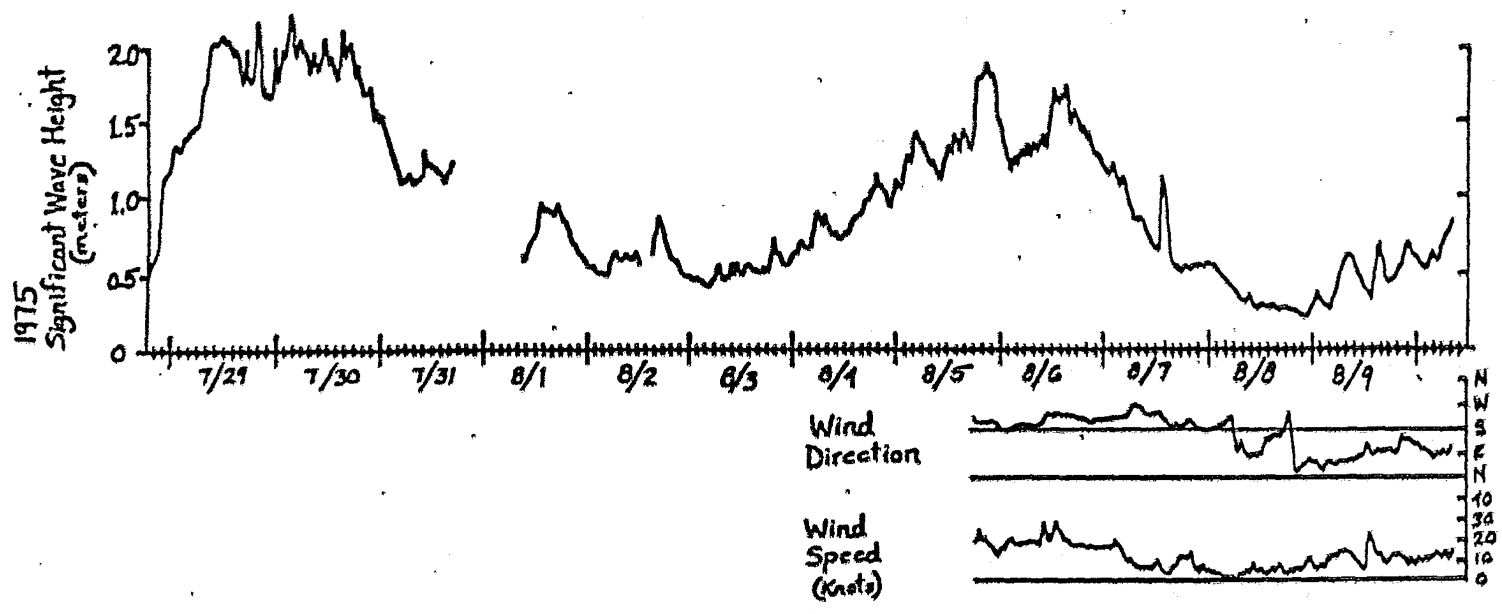

Figure A1: NCRL records of significant wave height, wind direction, and speed; 1975.

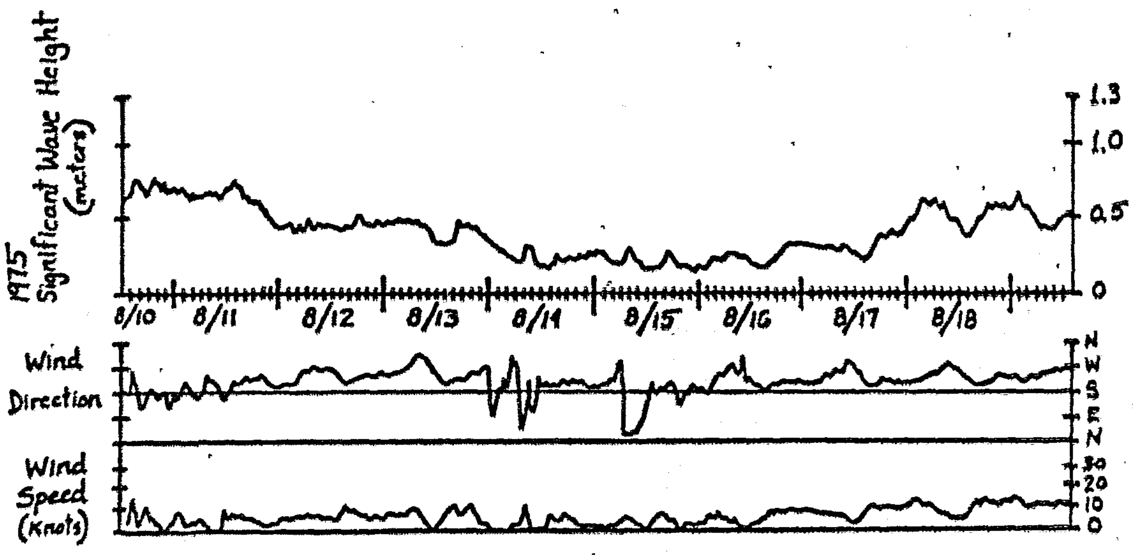

Figure A2: NCRL records of significant wave height, wind direction, and speed;1975.

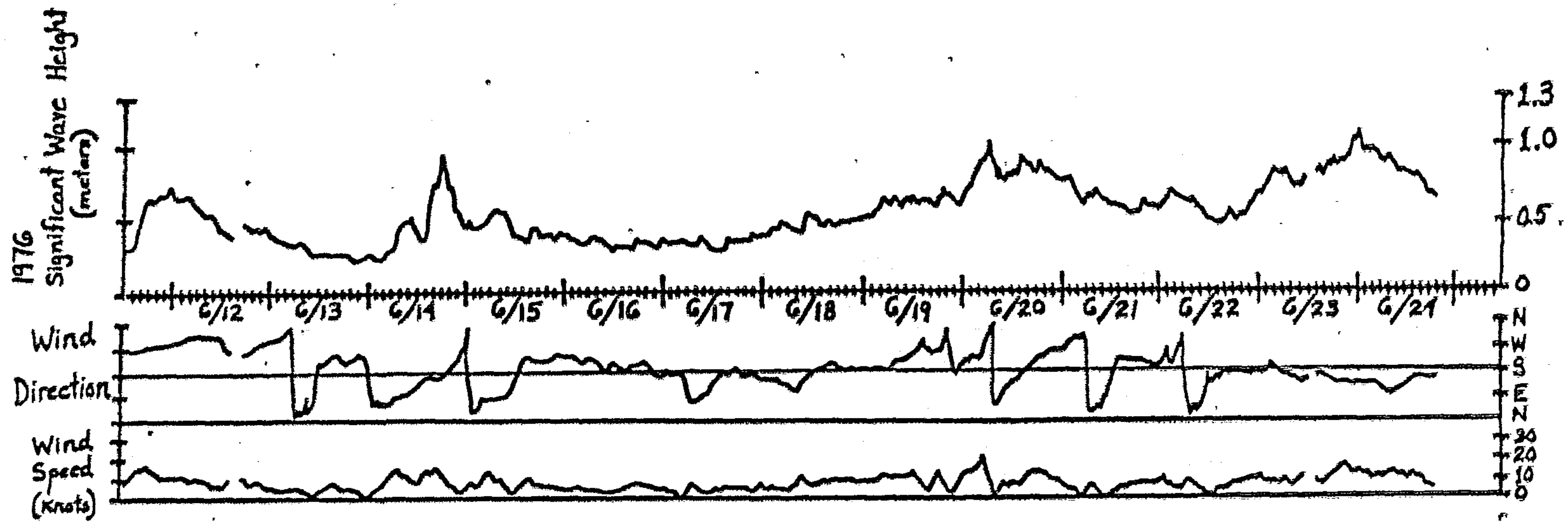

Figure A3: NCRL records of significant wave height, wind direction, and speed;1976.

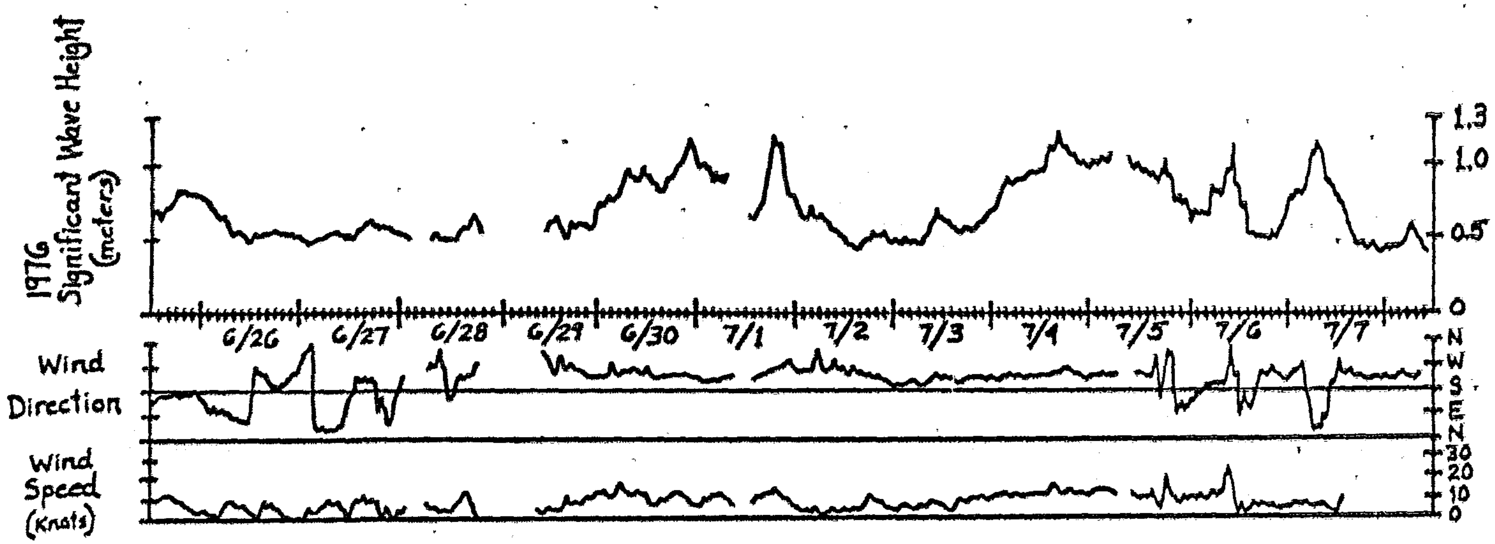

Figure A4: NCRL records of significant wave height, wind direction, and speed; 1976.

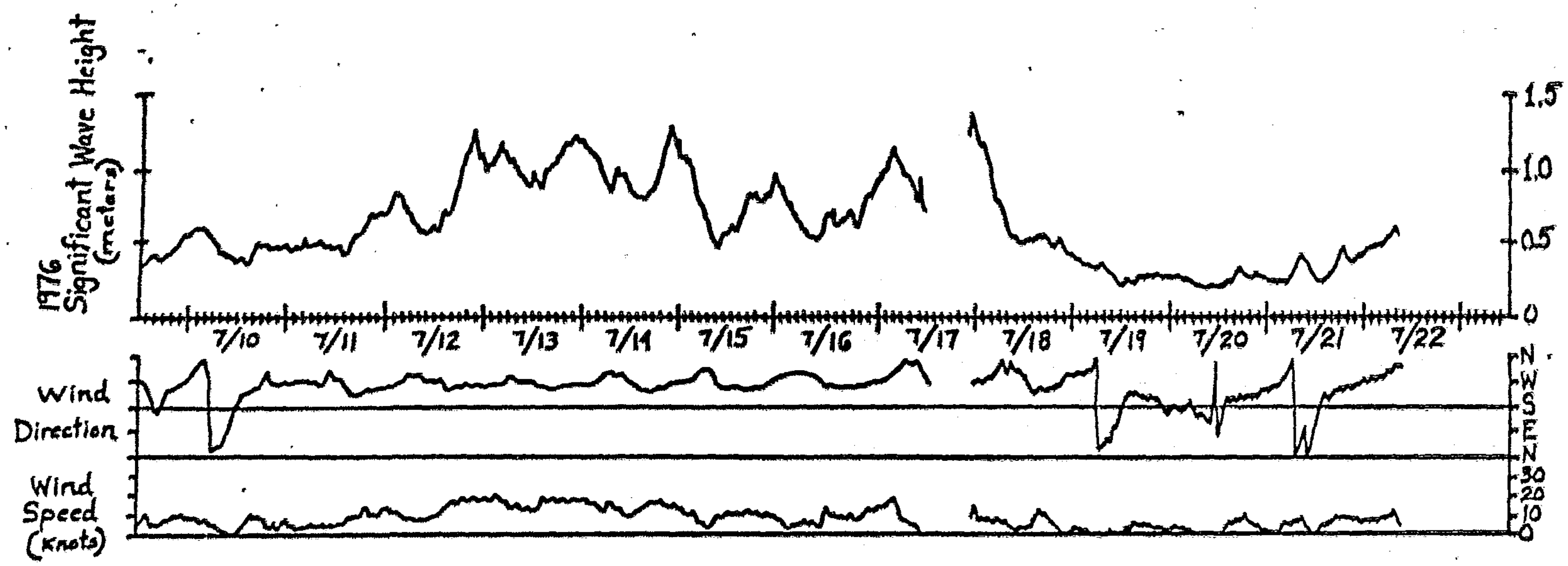

Figure A5: NCRL records of significant wave height, wind direction, and speed; 1976.

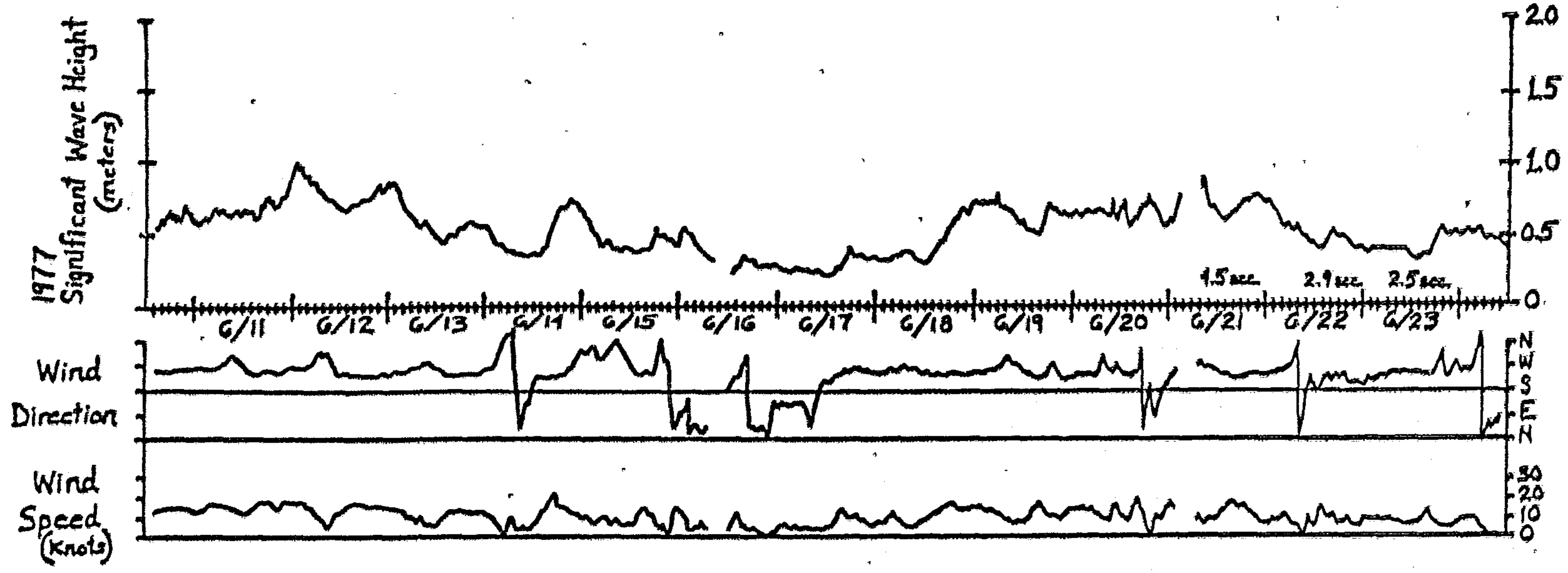

Figure A6: NCRL records of significant wave height, wind direction, and speed;1977.

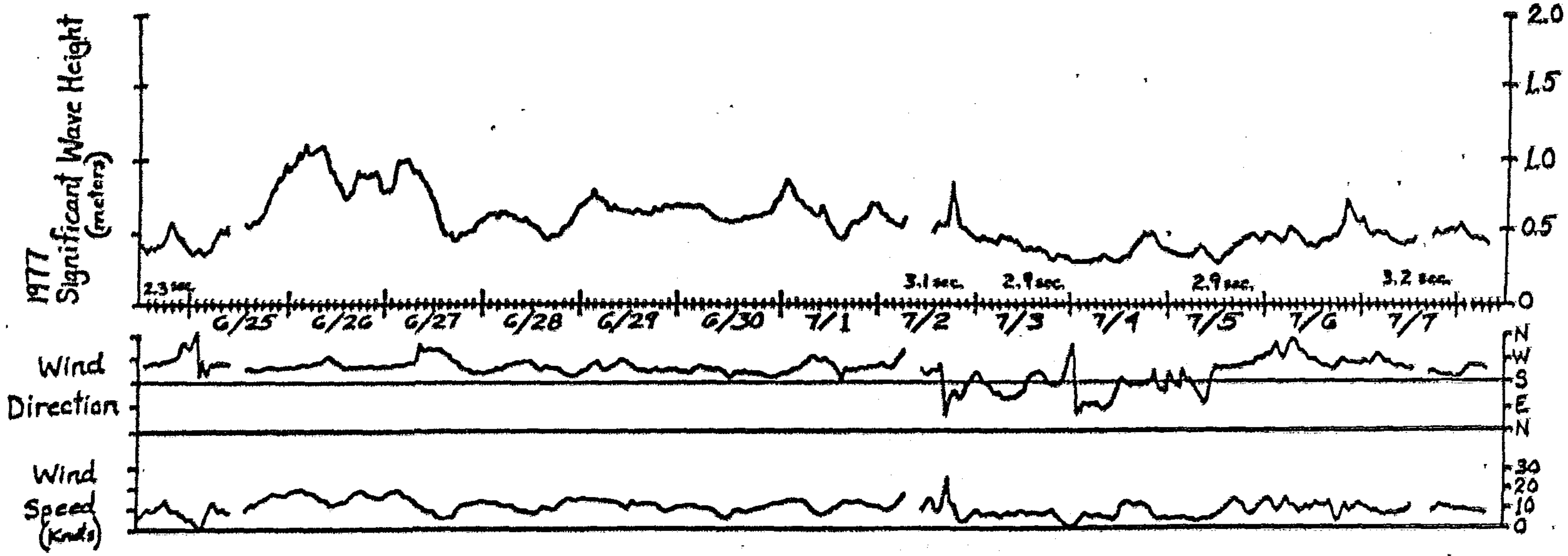

Figure A7: records of significant wave height, wind direction, and speed;1977.

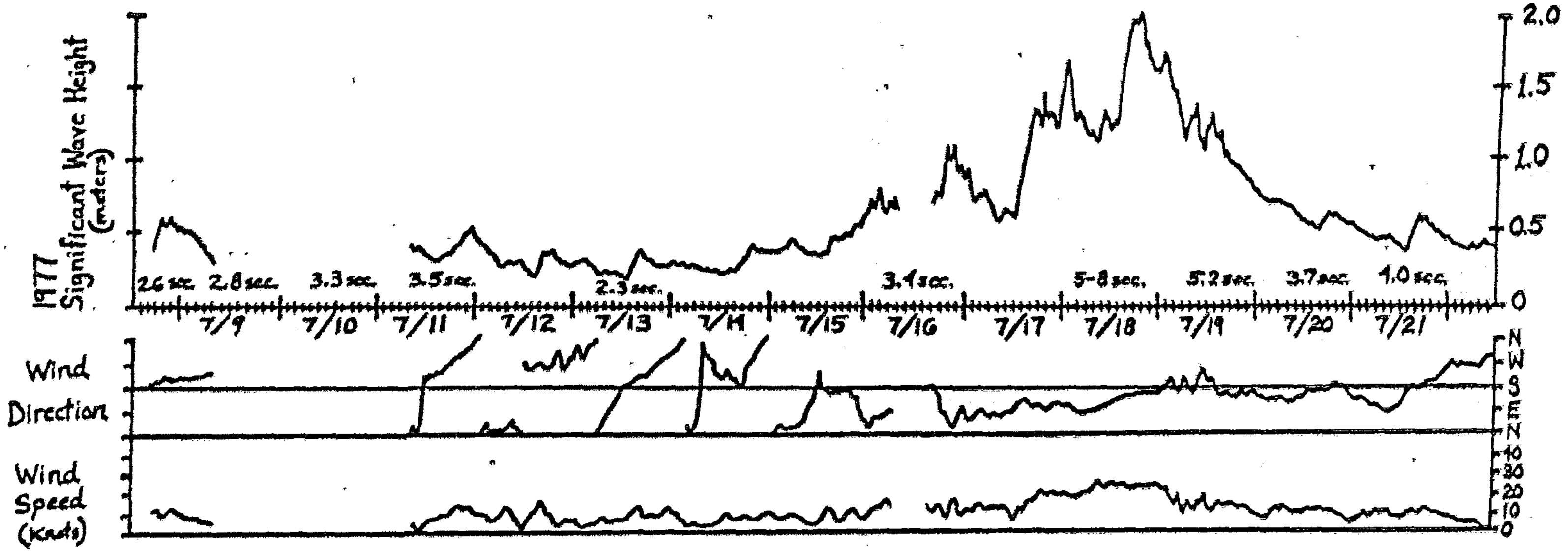

Figure A8: NCRL records of significant wave height, wind direction, and speed;1977.

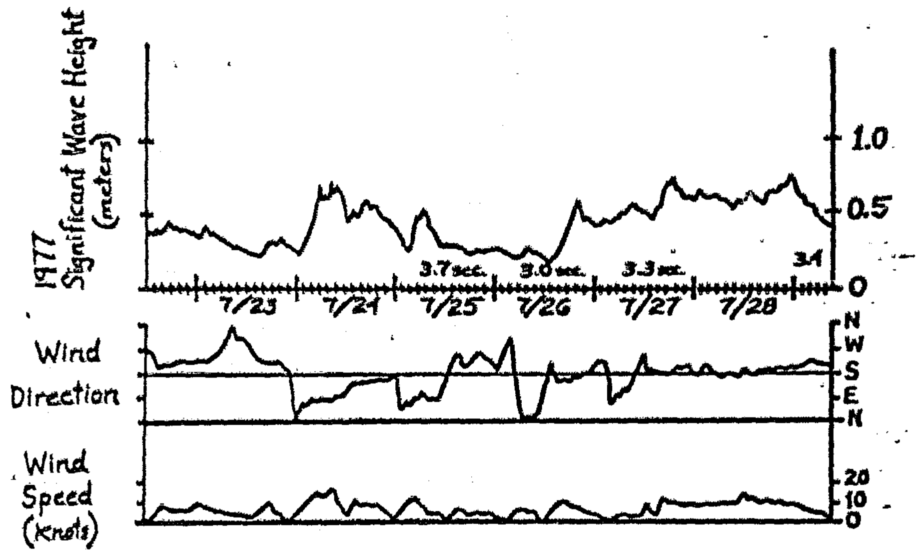

Figure A9: NCRL records of significant wave height, wind direction, and speed;1977.

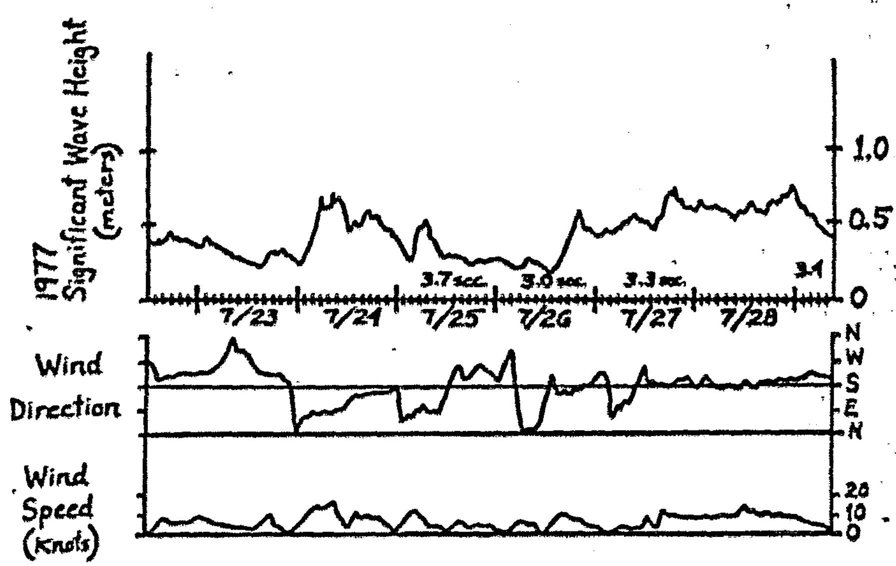

Figure A9: NCRL records of significant wave height, wind direction, and speed;1977.

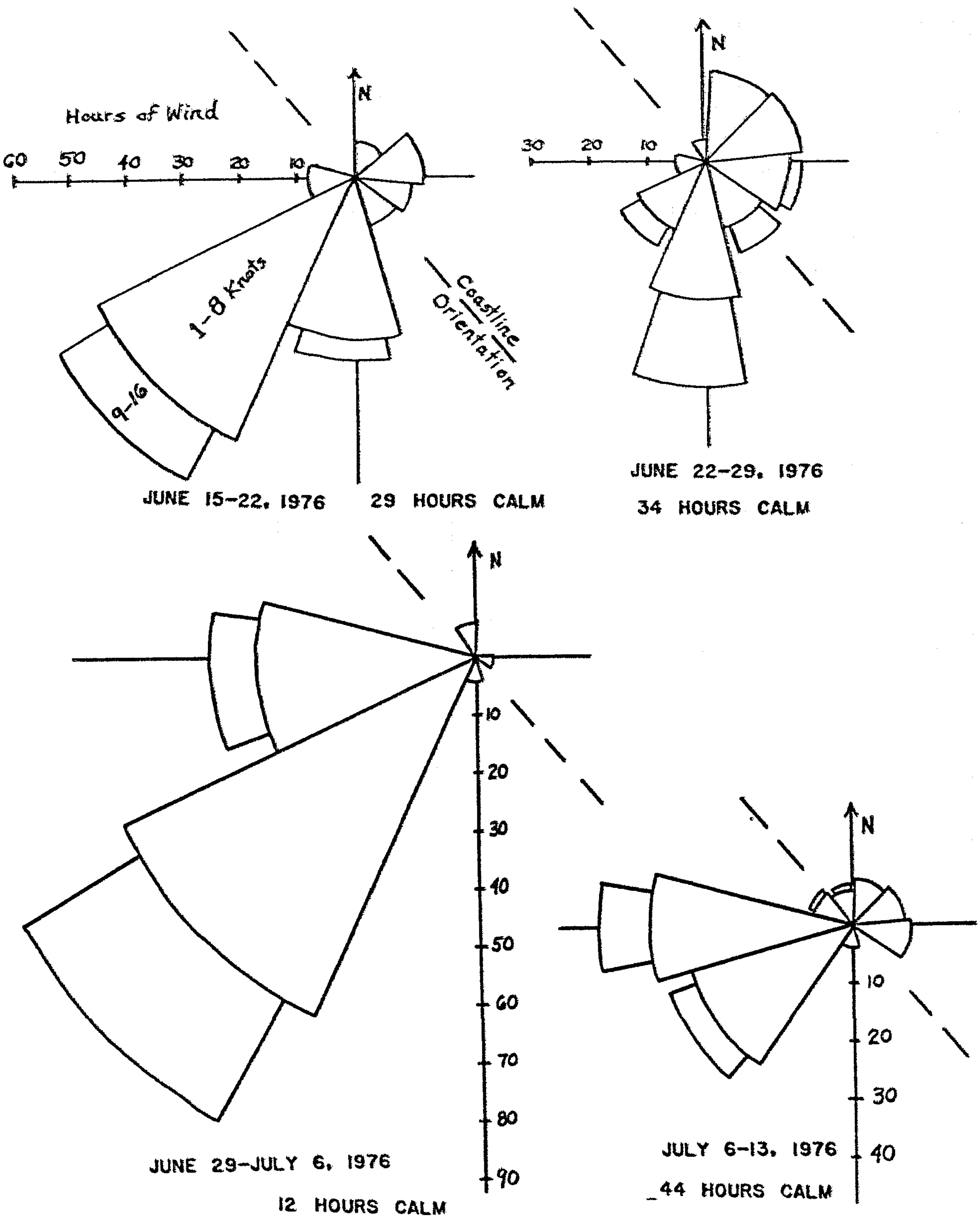

Figure A10: 1976 weekly wind roses from Tyndall AFB. Plots indicate the number of hours that winds blew from a particular direction and also the speed in knots.

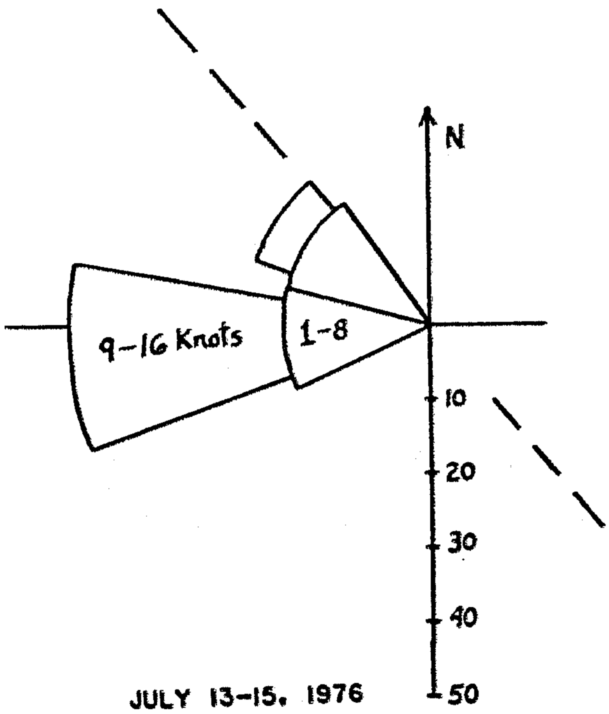

JULY 13–15, 1976

ZERO HOURS CALM

Figure A11: 1976 weekly wind roses (continued)

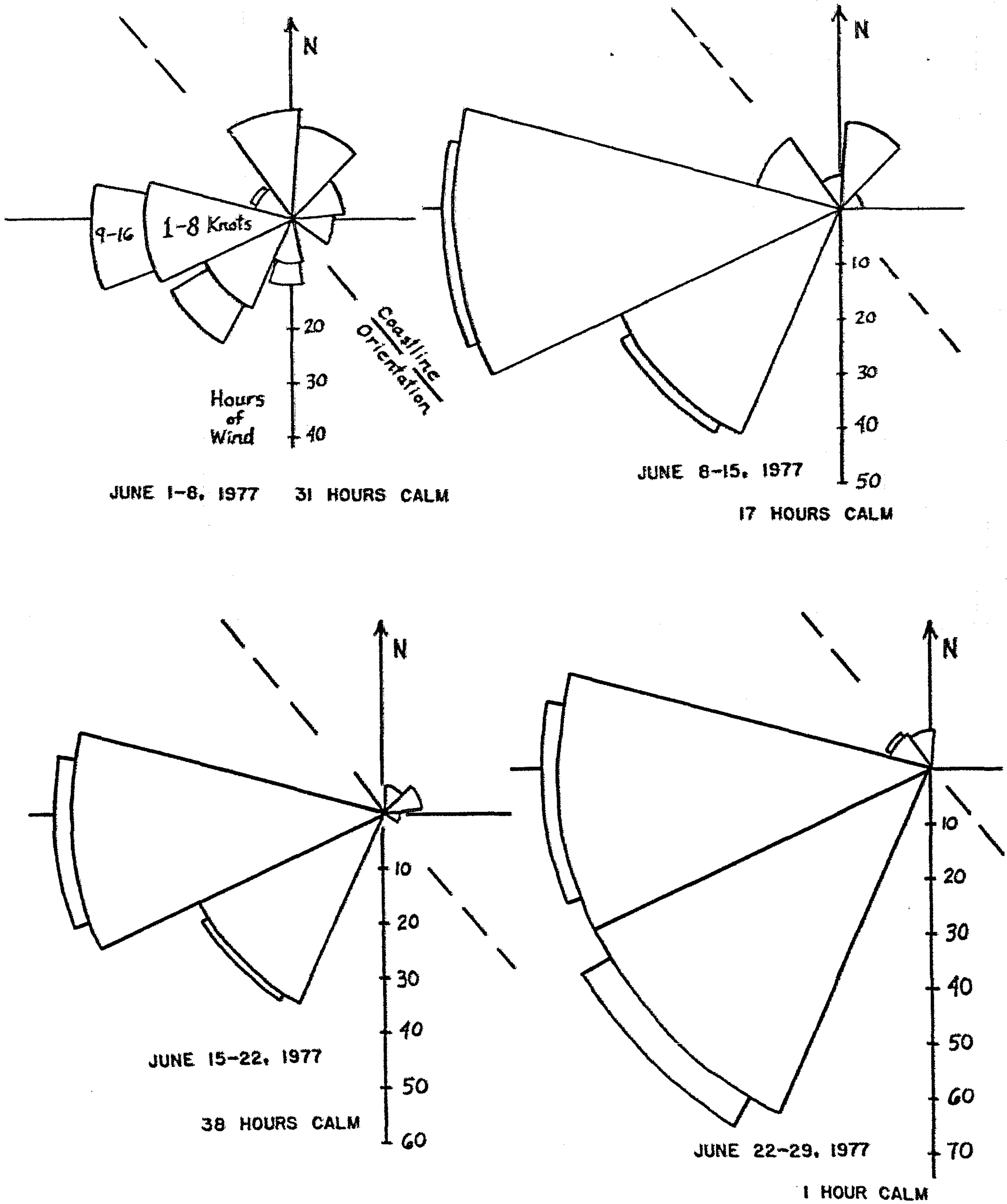

Figure A12: 1977 weekly wind roses from Tyndall AFB. Plots indicate the number of hours that winds blew from a particular sector and also the speed in knots.

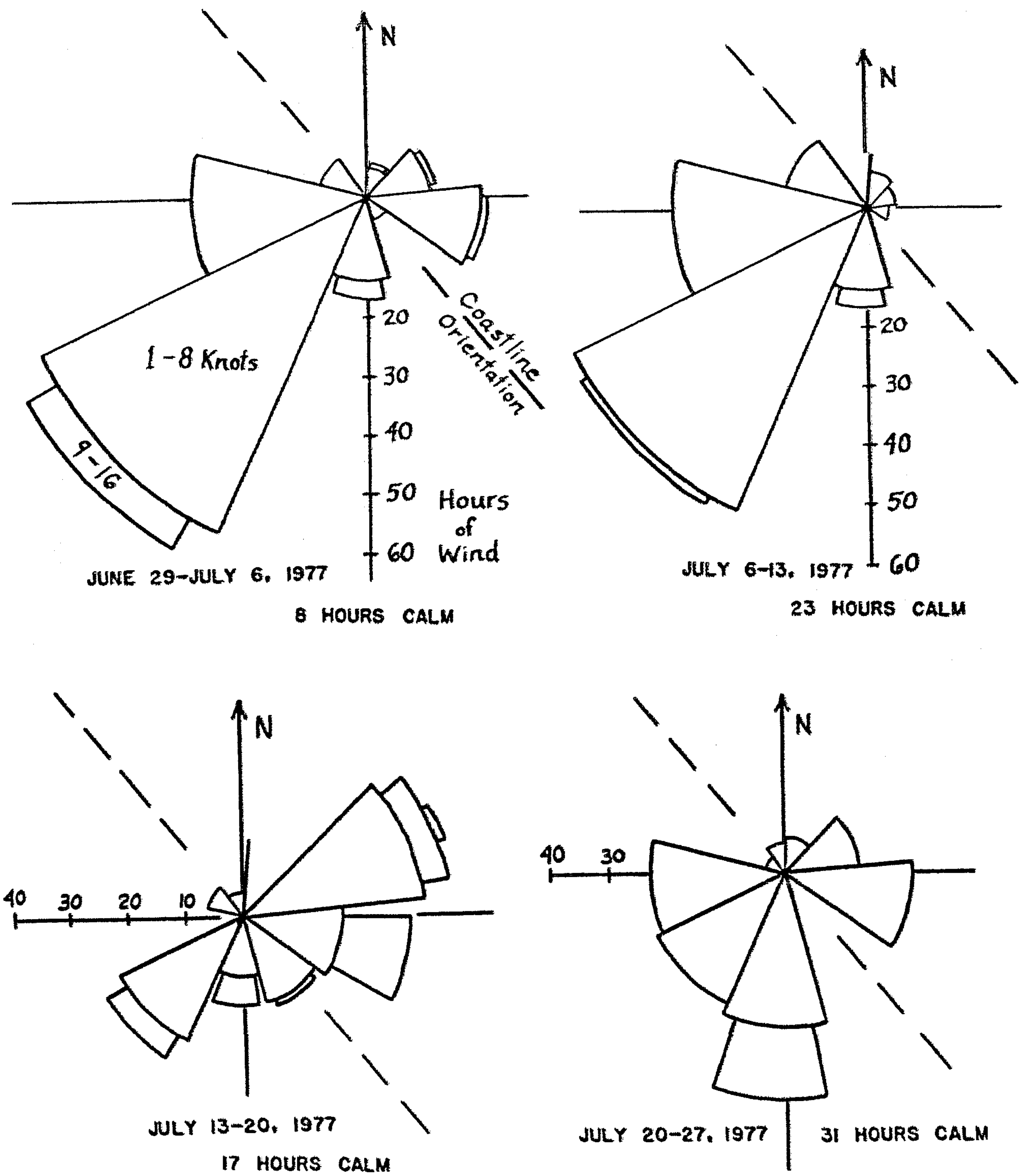

Figure A13: 1977 weekly wind roses (continued)

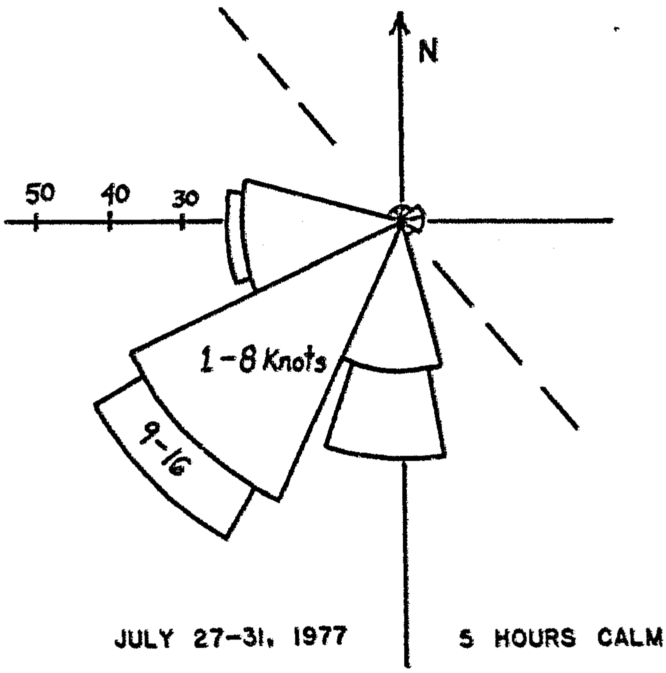

Figure A14: weekly wind roses (continued)

APPENDIX B

This appendix contains topographic profiles of the nearshore at Panama City Beach. Profiles from all three field seasons are included. All of the profiles were measured at one standard locality except for those profiles labeled A, B, C, or D. The locations of the lettered profiles are described in the "Bar Patterns" section of the results.

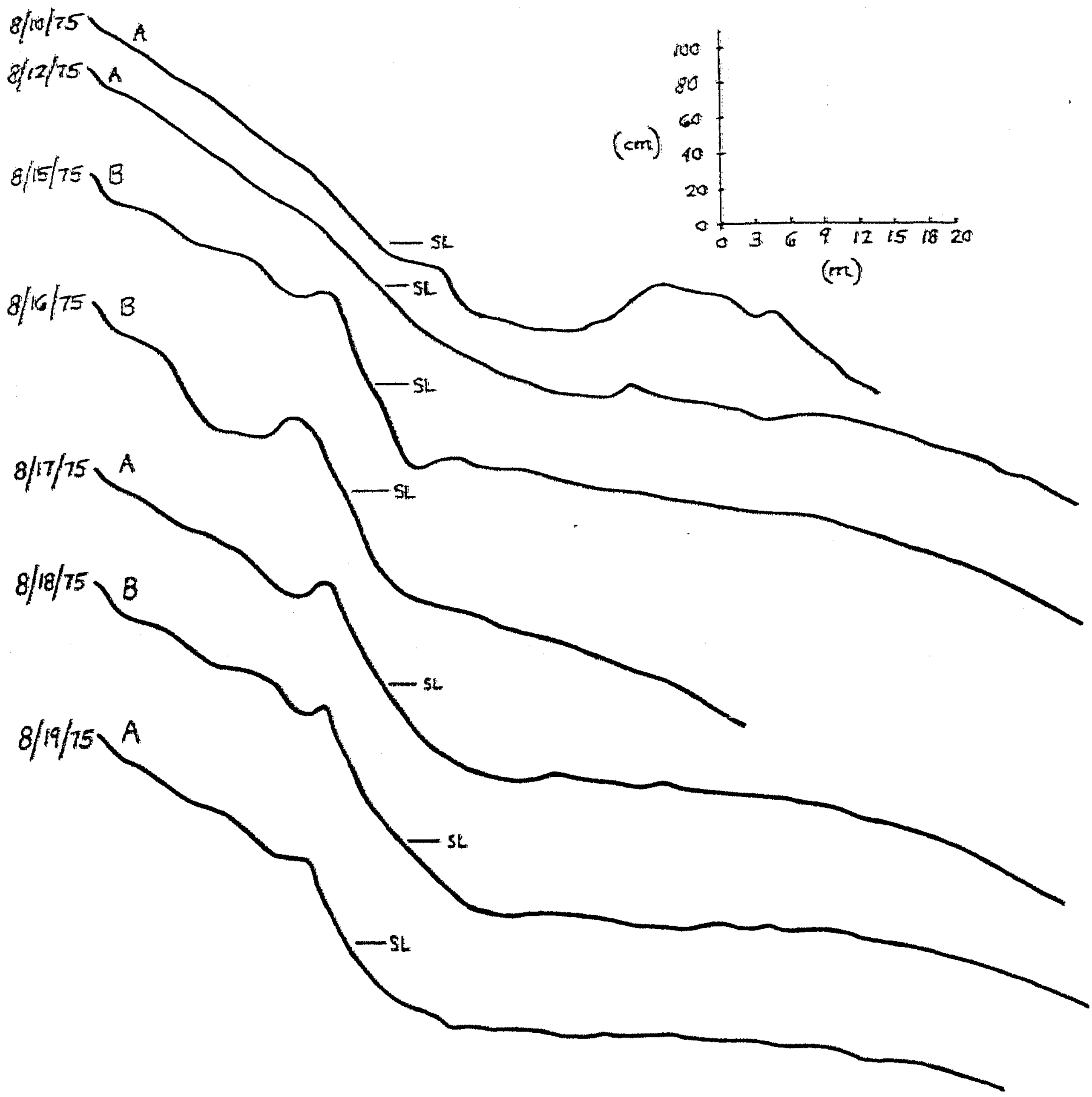

Figure B1: 1975 topographic profiles from two localities;

"A" is from a cusp and "B" is from a bay.

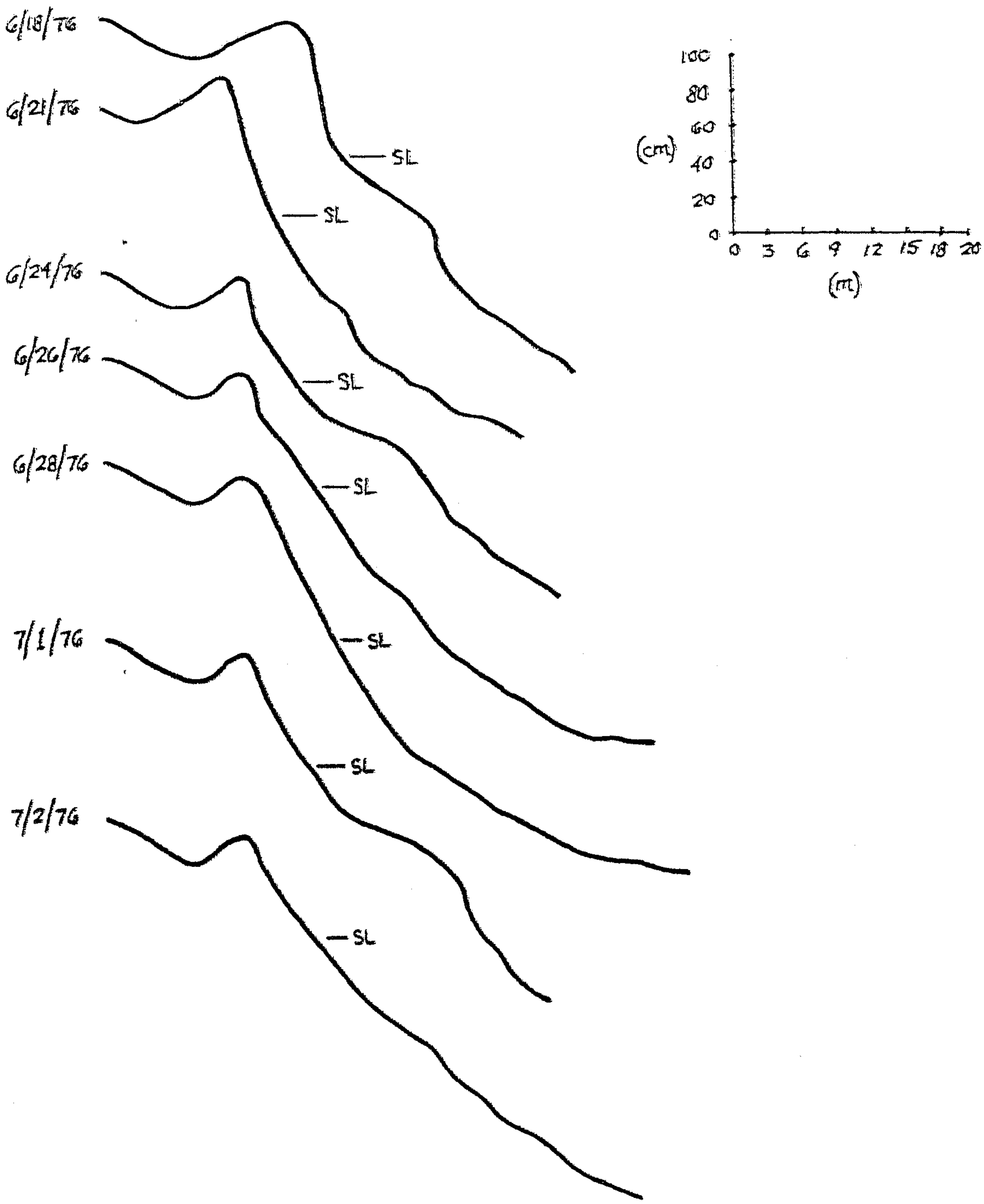

Figure B2: 1976 topographic profiles from the standard locality.

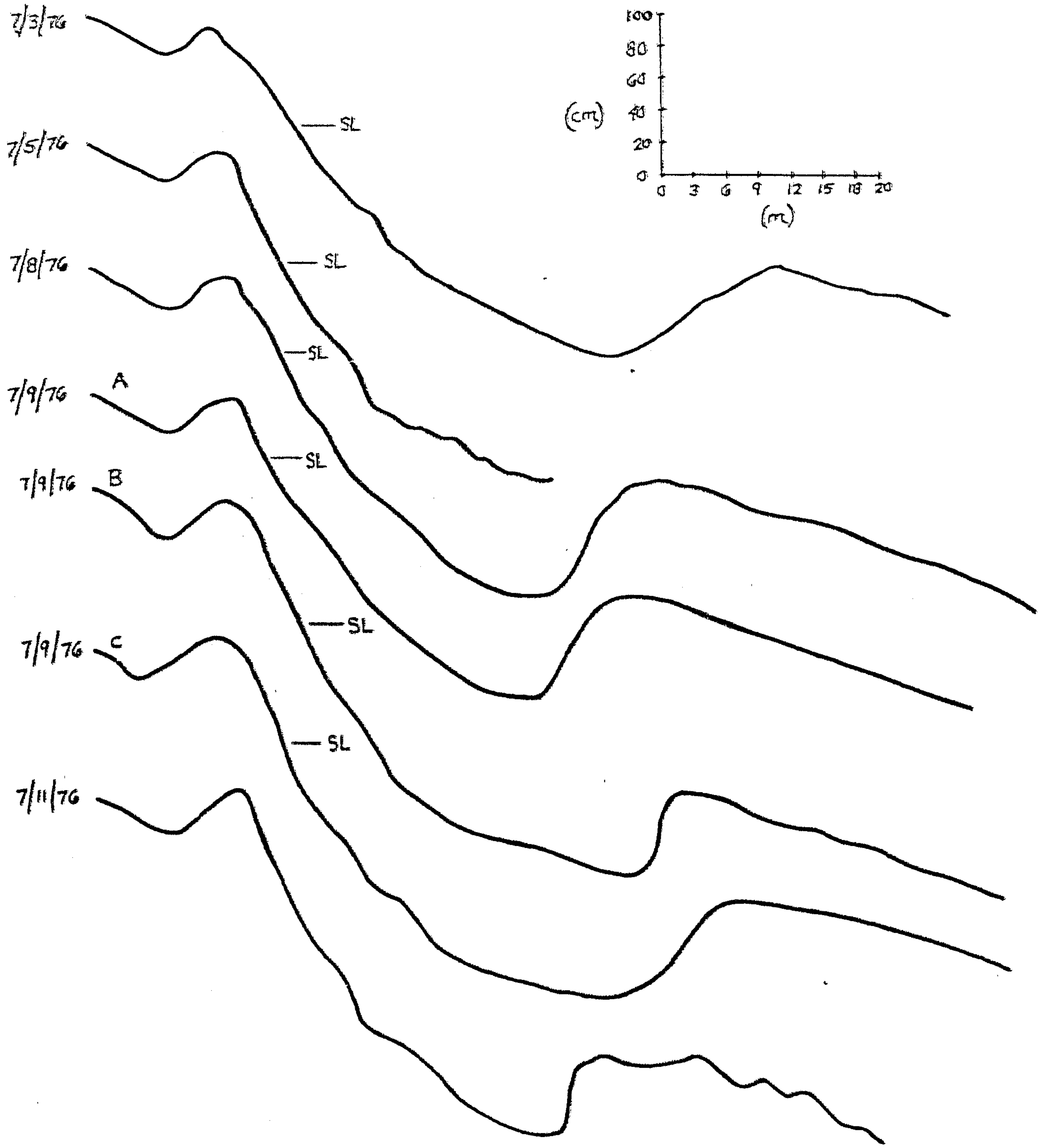

Figure B3: 1976 topographic profiles; all profiles including"A" are from the standard locality. "B" and "C" are from localities 13 and 26 m west of standard.

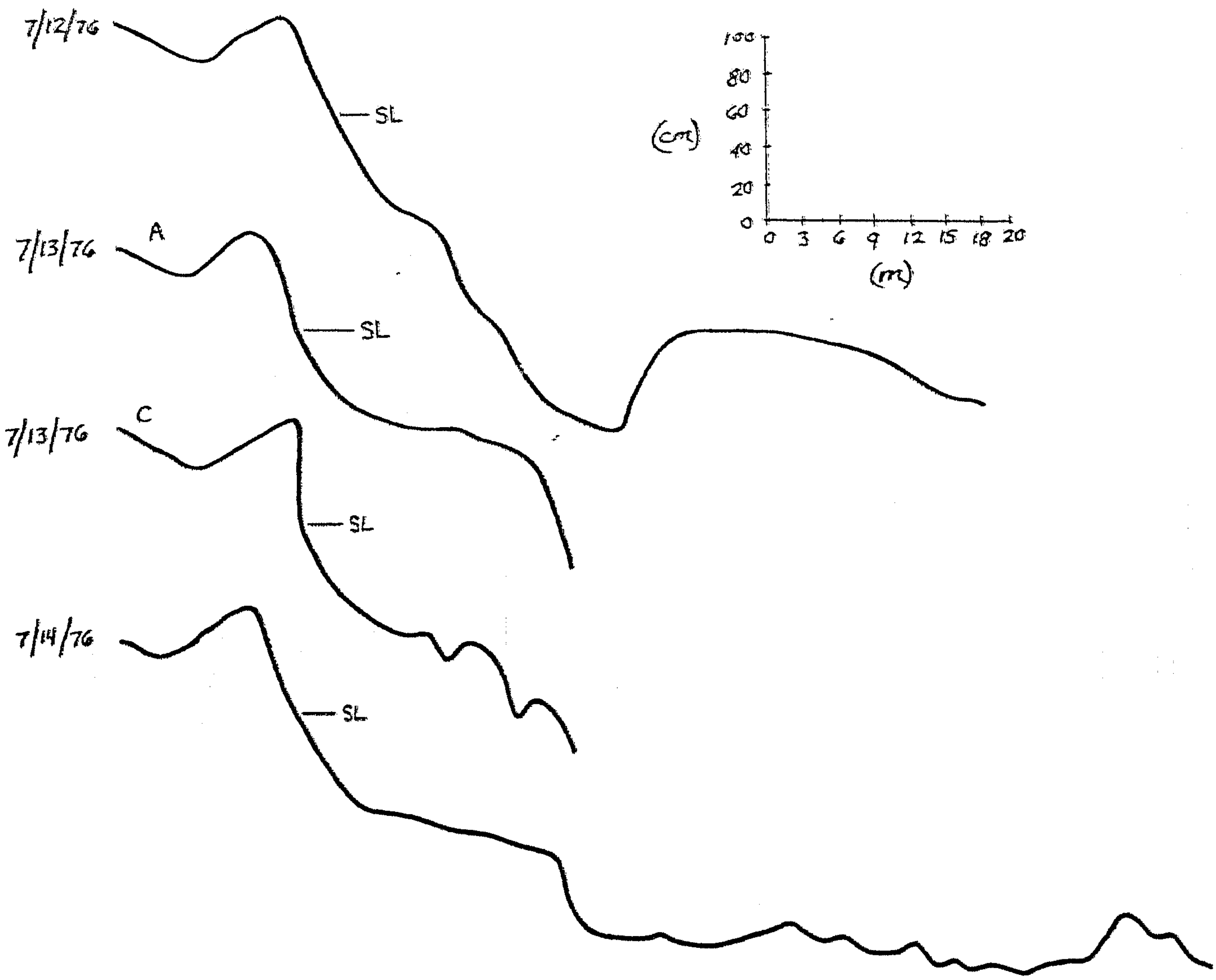

Figure B4: 1976 topographic profiles

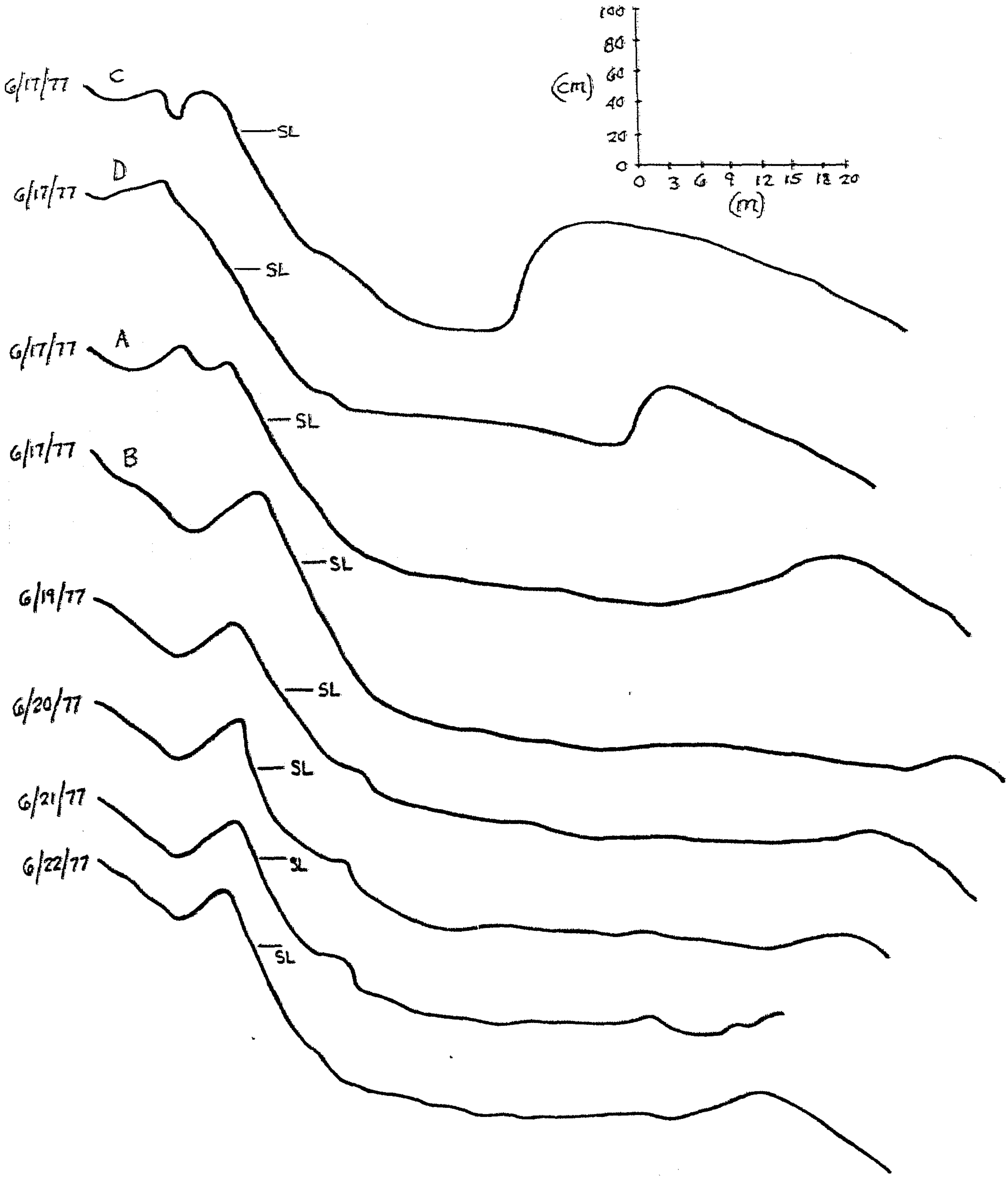

Figure B5: 1977 topographic profiles

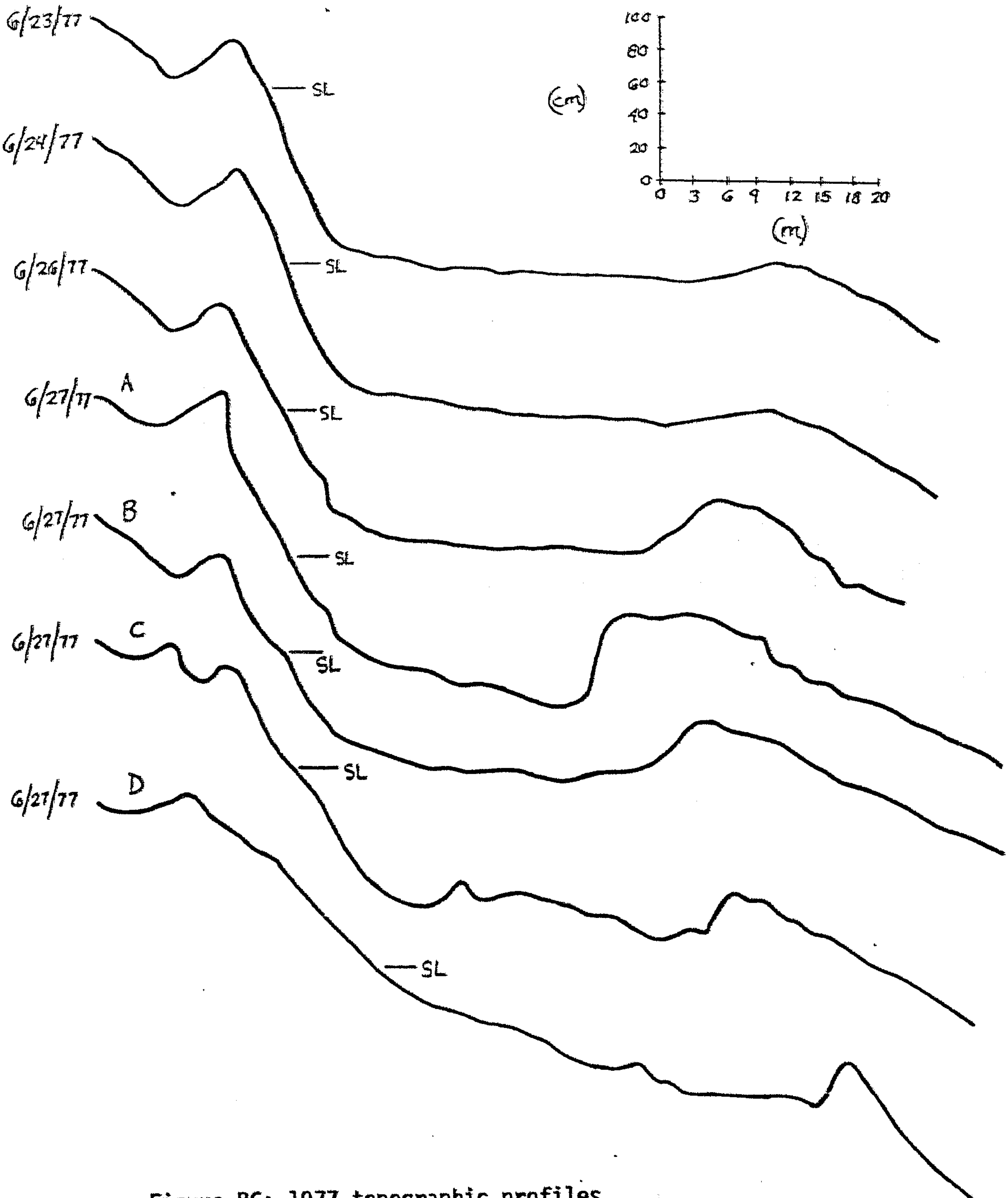

Figure B6: 1977 topographic profiles

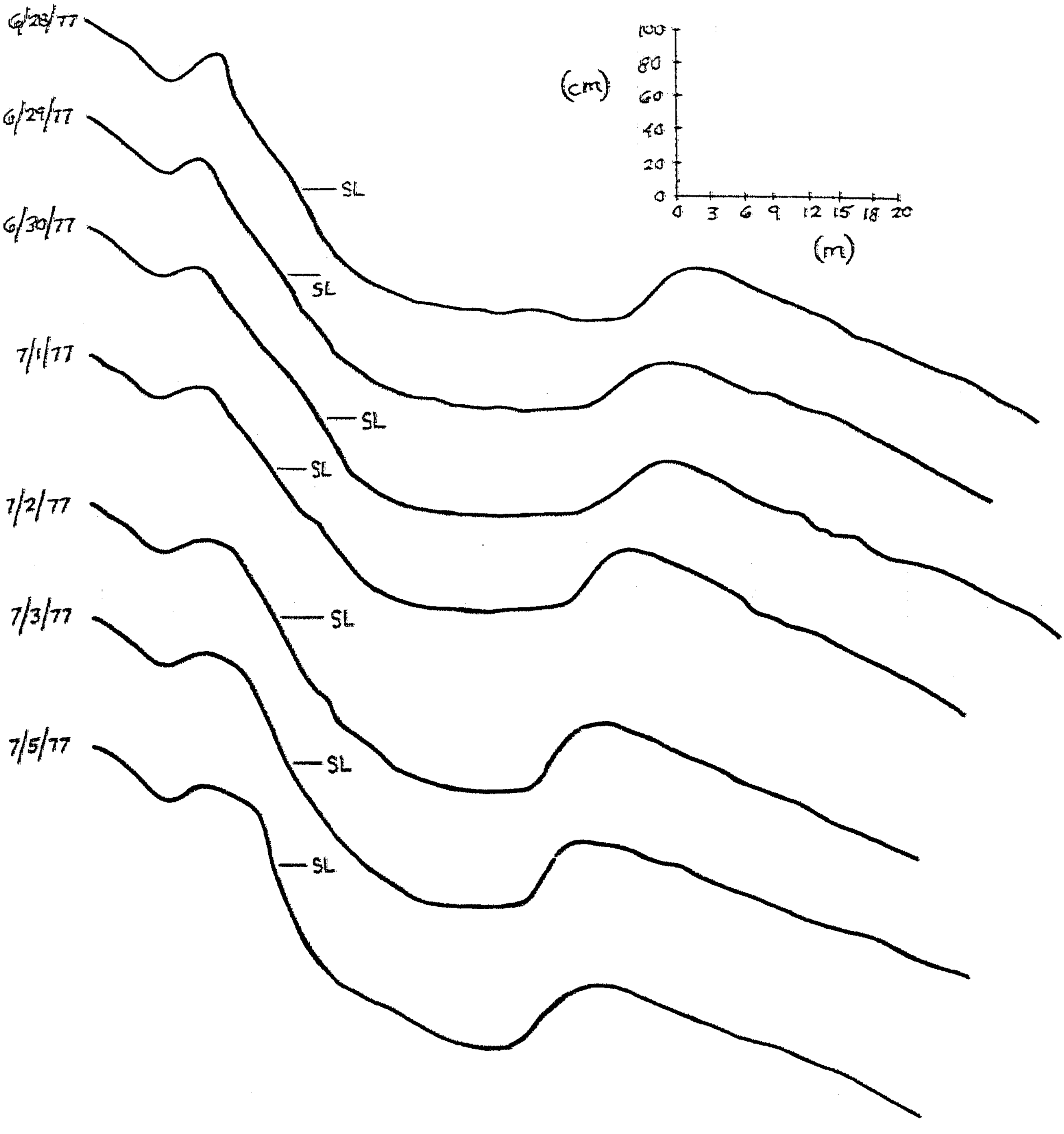

Figure B7: 1977 topographic profiles

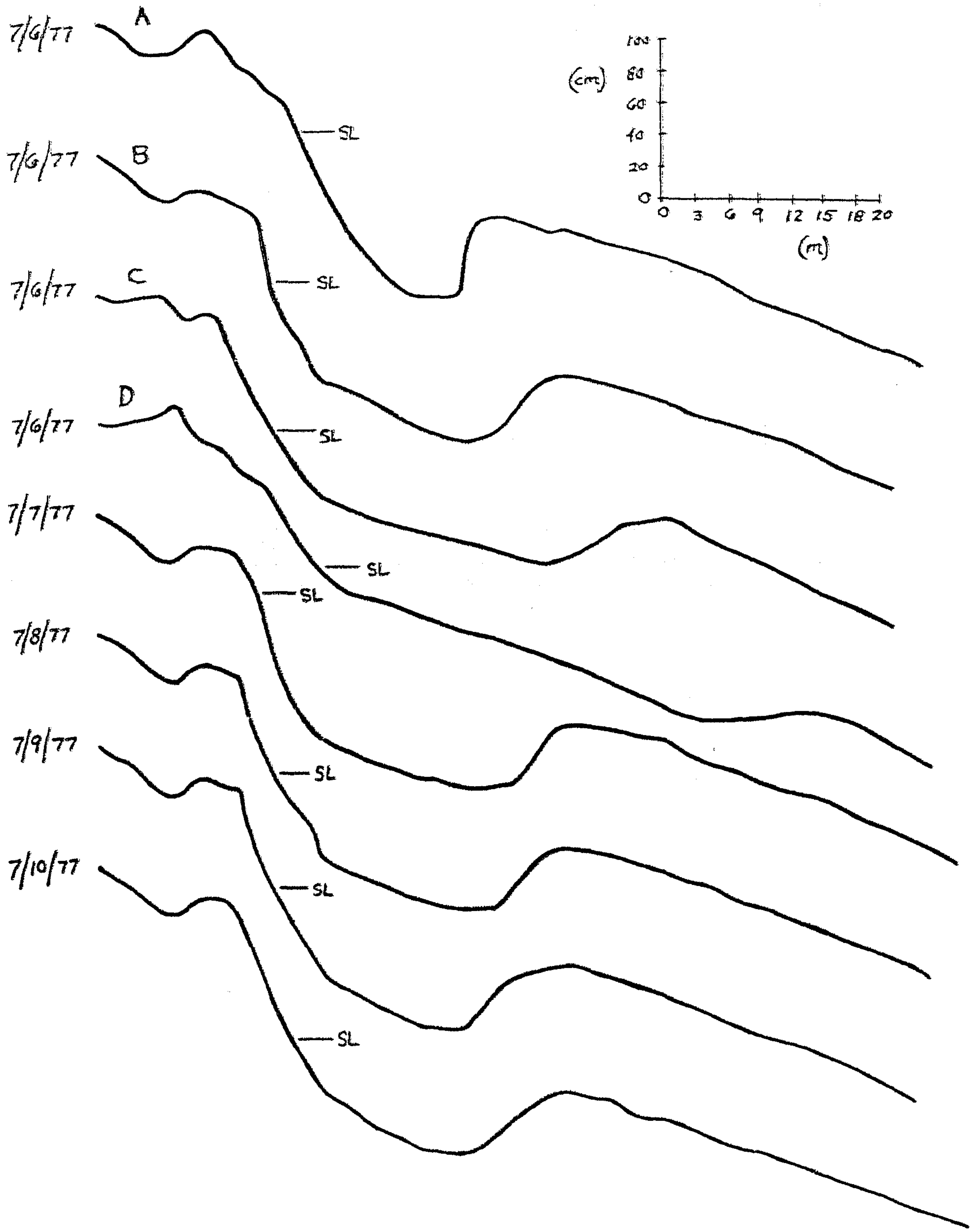

Figure B8: 1977 topographic profiles

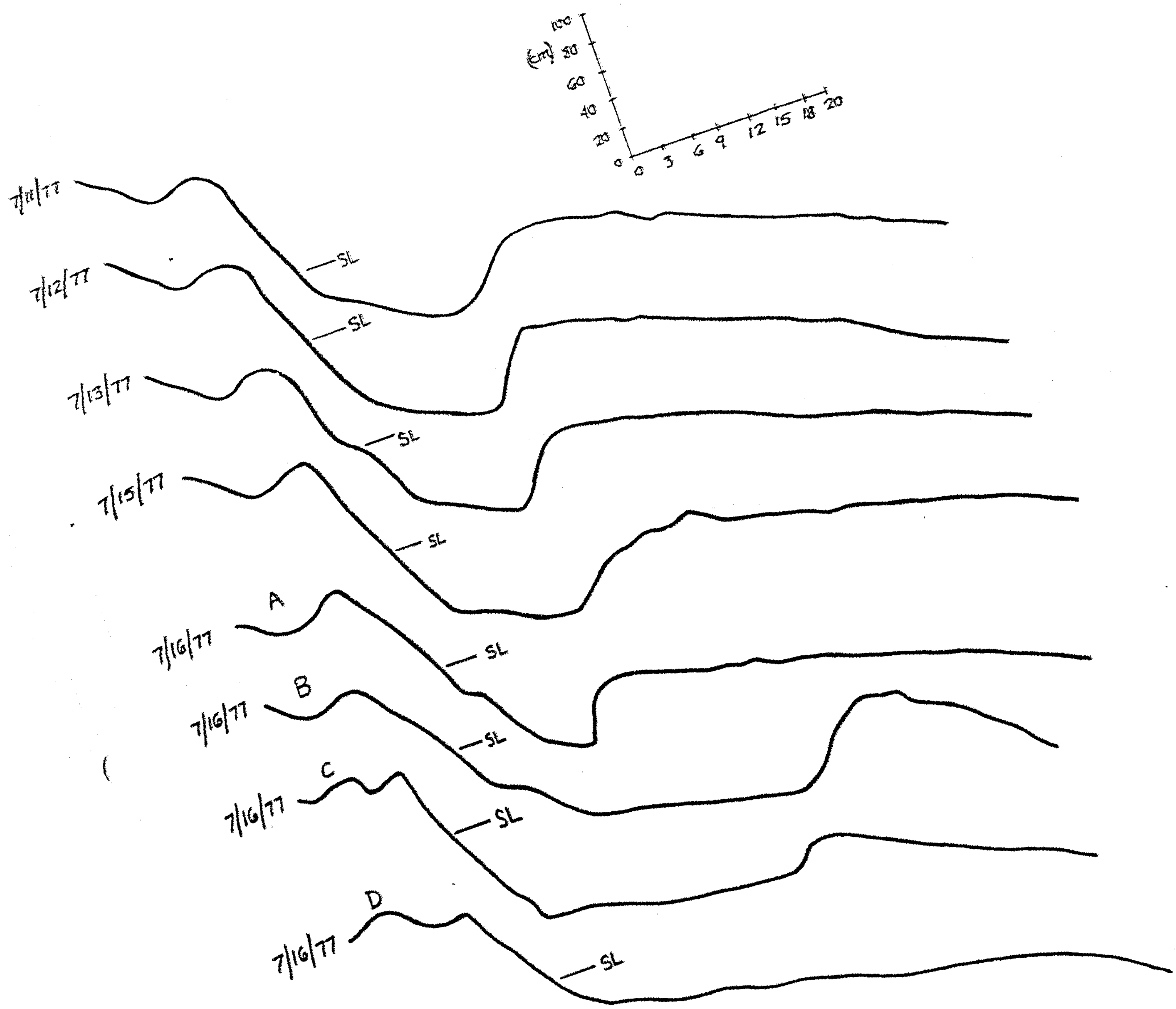

Figure B9: 1977 topographic profiles

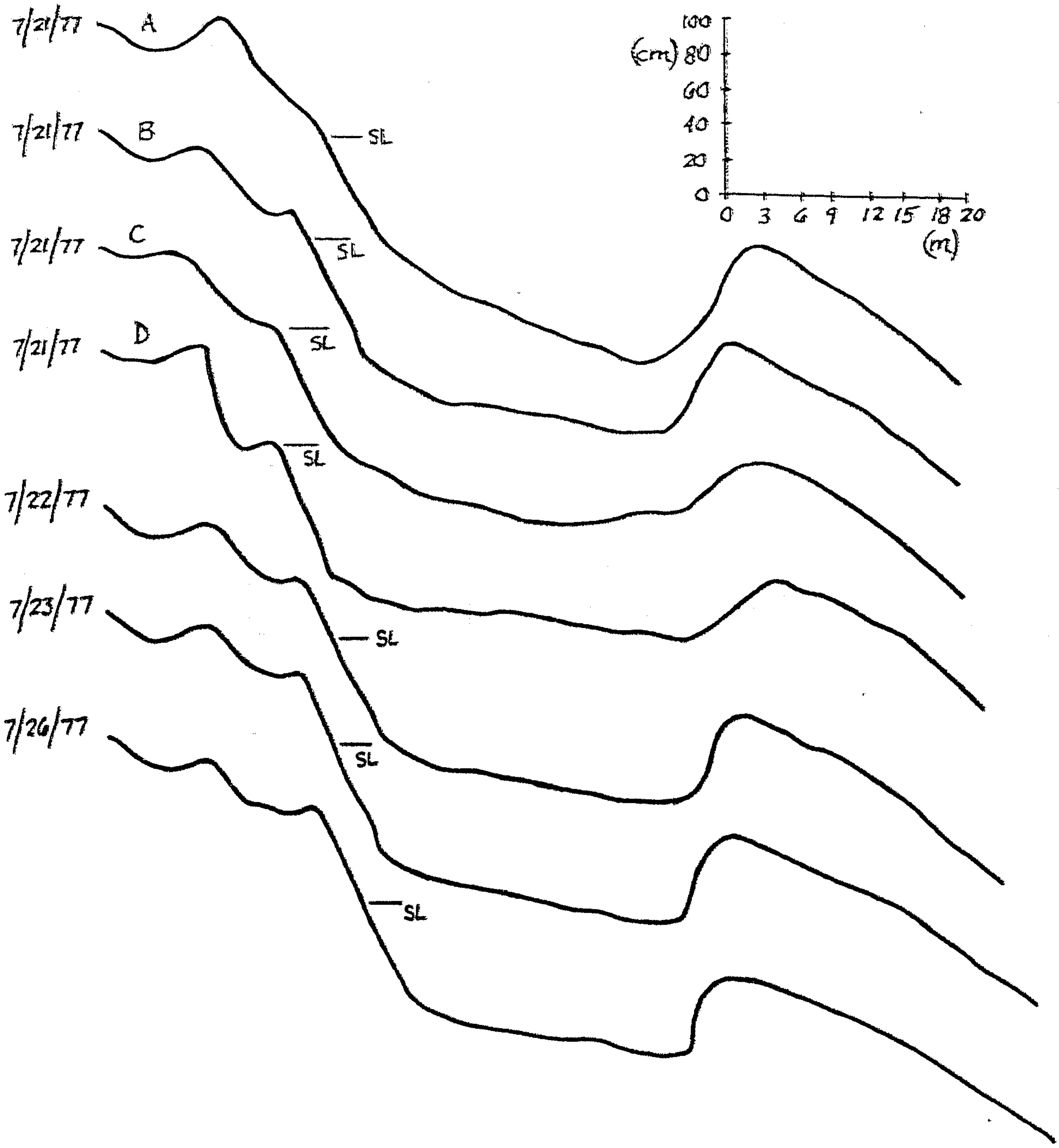

Figure B10: 1977 topographic profiles

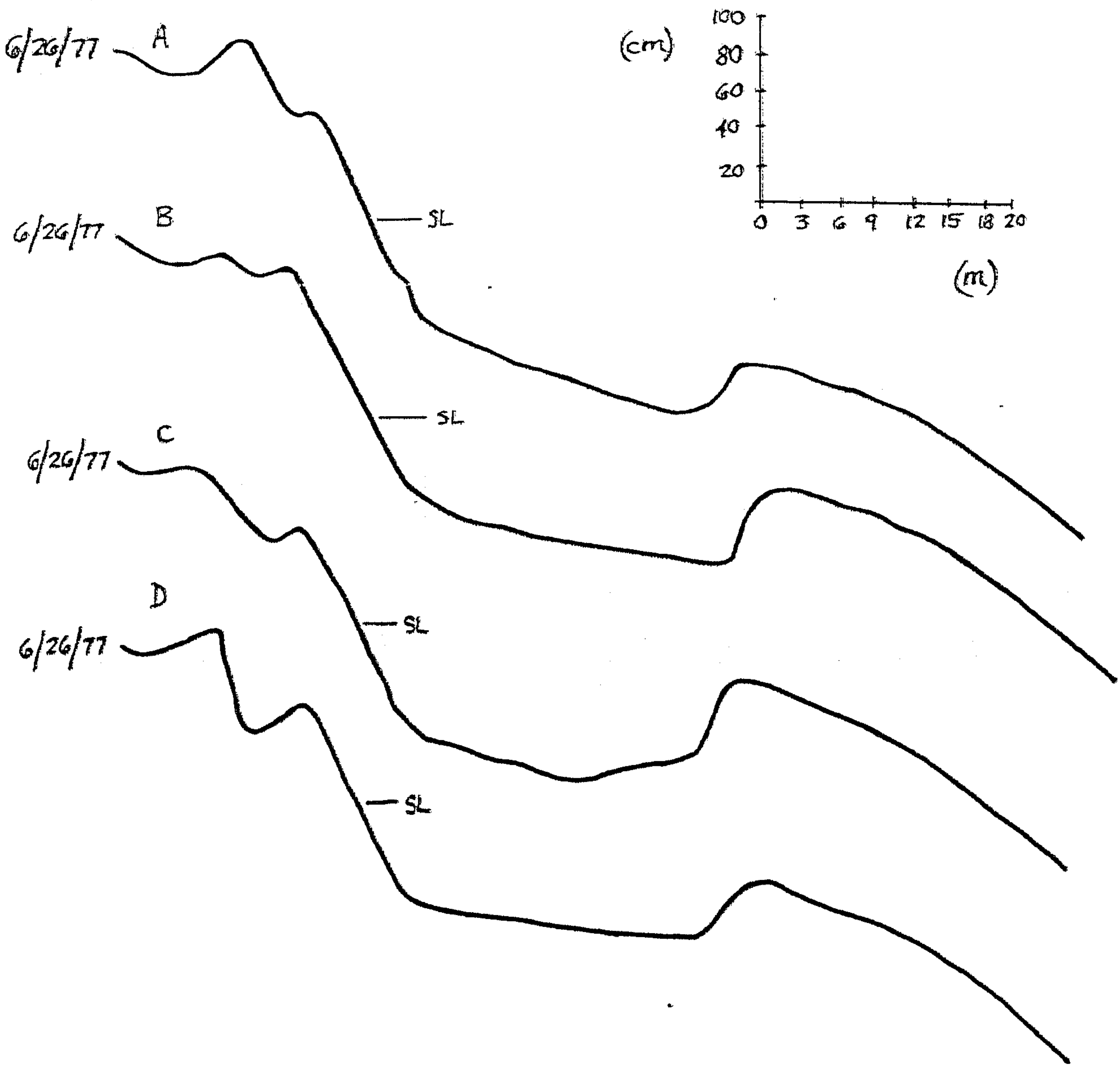

Figure B11: 1977 topographic profiles

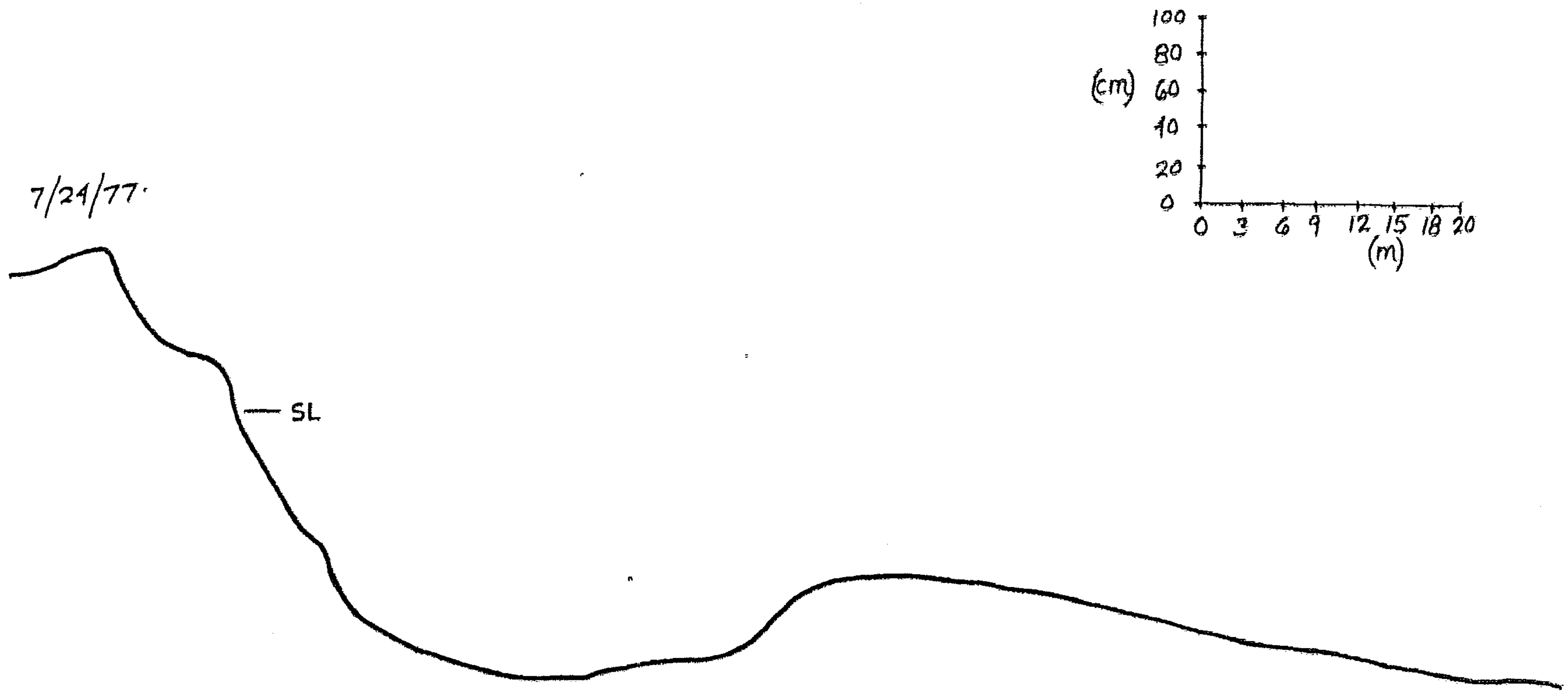

Figure B12: 1977 Shell Island nearshore topographic profile.

APPENDIX C

The swing current meter used in this study was calibrated in a flume belonging to the Engineering Department at the University of Cincinnati. Three different wiers were used to obtain the range of velocities which the swing meter was capable of recording. The three setups were: a low rectangular wier with normal slope, the high rectangular wier with normal slope, and no wier with reverse slope.

For each setup the procedure was to gradually increase the discharge or slope of the flume to produce a series of closely-spaced, incremental velocities. Each velocity was measured with both the swing meter and a Gurley Pygmy Current Meter. This is a commercially-obtained device which functions on the same principle as a water wheel. The wheel consists of a series of cups which are deflected by the current and the speed of the wheel's rotation determines the fluid velocity.

The Gurley meter readings were plotted against the swing meter's readings to obtain the plot shown in Figure C1. A semi-log plot (Fig. C2) was used to straighten the curve and provide a more accurate calibration. The shape of the plot indicates that there is a significant inertial effect involved in the initial deflection of the swing meter's weighted paddle. The remainder of the meter's velocity range (from 27 cm/sec to 92 cm/sec) is a straight-line relationship.

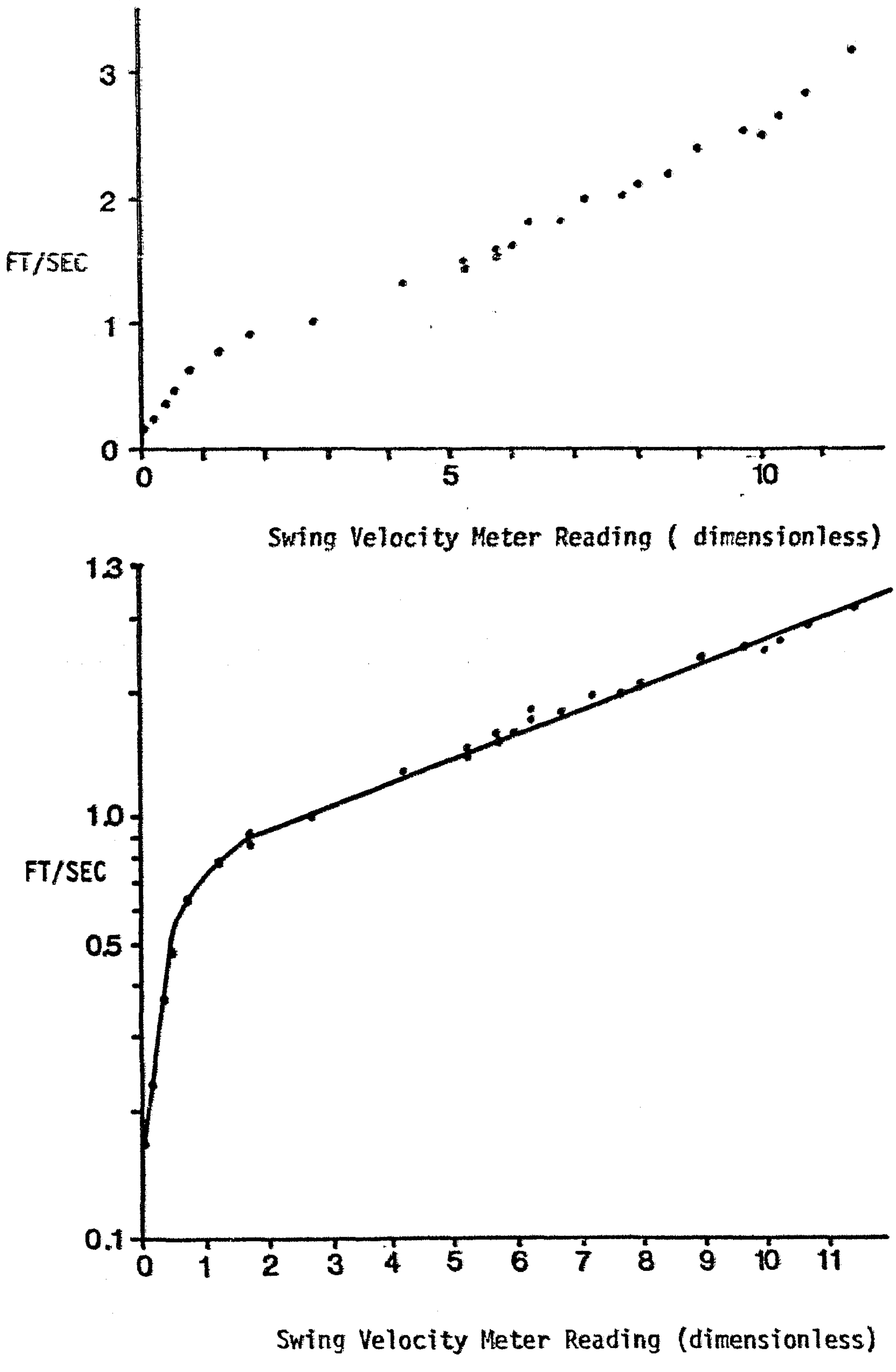

Figures C1 (top) and C2 (bottom): Calibration curves for swing velocity meter. The same data is shown in an arithmatic plot and a semi-logarithmic plot.